From the Department of Molecular Neurobiology, Clinic for Psychiatry and Psychotherapy,
Ludwig-Maximilians-Universität München

Dissertation

zum Erwerb des Doctor of Philosophy (Ph.D.) an der

Medizinischen Fakultät der

Ludwig-Maximilians-Universität zu München

The Role of Circadian Rhythms in Orexin Neurons of the Lateral Hypothalamus in the Regulation of Mood- and Anxiety-Related Behavior, and Metabolism in Mice

vorgelegt von:

Charlotte Maria Kling

aus:

Mainz, Deutschland

Jahr:

2023

Mit Genehmigung der Medizinischen Fakultät der

Ludwig-Maximilians-Universität zu München

First evaluator (1. TAC member): Dr. Dominic Landgraf

Second evaluator (2. TAC member): Prof. Dr. Charlotte Förster

Third evaluator: Prof. Dr. Maria del Sagrario Robles Martinez

Fourth evaluator: Prof. Dr. Jan Rémi

Dean: **Prof. Dr. med. Thomas Gudermann**

Datum der Verteidigung:

10.02.2023

_____

Table of Contents

Abstract

Mood and anxiety disorders are frequently associated with metabolic comorbidity. Therefore, the existence of a "metabolic mood syndrome" or "metabolic" depression has been discussed indicating common underlying biological causes. The orexin (ORX) and the circadian system both play a prominent role in the regulation of mood- and anxiety-related behavior, as well as metabolic processes. They are closely linked through the circadian gating of ORX neuron signaling, which restricts ORX neuron activity to the active phase. In this thesis, the impact of subordinate circadian clocks in ORX neurons of the lateral hypothalamus (LH) on mood- and anxiety-related behavior, as well as metabolic phenotypes in mice was investigated by genetically abolishing the expression of the circadian core clock gene *Bmal1* specifically in this neuronal population of the brain.

Cell-specific deletion of *Bmal1* was achieved using the Cre-loxP-system and the *Orx-Cre* driver line. The *Orx-Cre* transgene targets the whole population of ORX cells, which is characterized by the expression of the *prepro-orexin (Ppox)* gene. Since the entity of ORX cells in the mouse has not been fully characterized, a systematic screen for *Ppox* expression in peripheral and central tissues of the mouse was performed. Further, the presence of ORX peptides was immunohistochemically confirmed. *Ppox* expression in the periphery was considerably lower than in the LH and present in fewer tissues than expected based on previous publications. It was only consistently detectable in the testis and kidney. No ORX peptide was found in any peripheral organ, suggesting that *Ppox* expression in the testis and kidney is too low to be immunohistochemically detected. In addition, there was stable *Ppox* expression in extra-hypothalamic brain regions. Since ORX positive somas could only be visualized in the LH, it is unclear whether extra-hypothalamic *Ppox* expression in the brain is a correlate of ORX producing cells in these areas or of local translation in projections of ORX neurons residing in the LH.

In order to verify cell-specificity of the *Orx-Cre* transgene in ORX neurons of the LH, a lineage tracing experiment was performed to map expression of the *Orx-Cre* transgene. In the periphery, the *Orx-Cre* transgene was visualized in the pancreas and stomach and very few cells of the spleen. In the brain, *Orx-Cre* expression was mainly restricted to the LH, where it colocalized with the presence of ORX peptide. Very few single cells in the cortex, hippocampus and cerebellum expressed the *Orx-Cre* transgene but no ORX positive somas were found in these regions indicating random and ectopic expression of the *Orx-Cre* transgene, which frequently occurs in Cre lines. Due to the small amount of extra-hypothalamic cells expressing the *Orx-Cre* transgene in the brain, cell-specificity of

the *Orx-Cre* transgene in the brain was determined sufficient to continue with the generation of Orx-Bmal1$^{-/-}$, which lack the molecular oscillator in ORX neurons of the LH.

The disruption of the molecular clock in ORX neurons led to the loss of *Ppox* expression rhythms in the LH and to increased mean *Ppox* expression independent of circadian time point. This is the first time that it was demonstrated that rhythmic *Ppox* expression in the LH depends on subordinate clocks in ORX neurons. The loss of rhythmicity in ORX neurons was accompanied by lower anxiety- and reduced depression-like behavior. C57BL/6J mice have been previously shown to have comparatively low ORX levels in the brain, which are associated with increased depression-like behavior. Further, ORX-deficient mice behave more anxiously. It is possible, that the positive effect of the loss of ORX neuron rhythmicity on mood and anxiety in Orx-Bmal1$^{-/-}$ mice is due to the mean increase of *Ppox* expression, which might rescue the relatively lower *Ppox* expression in C57BL/6J mice. Investigation of the metabolic phenotype revealed no differences in body weight, food consumption or respiratory exchange rate (RER), indicating that the loss of ORX neuron rhythmicity in mice is not associated with drastic metabolic alterations.

List of Figures

List of Tables

List of Supplementary Tables

List of Abbreviations

AAV	Adeno-associated virus
ANOVA	Analysis of variance
BNST	Bed nucleus of the stria terminalis
BP	Bipolar disorder
bp	Base pair
CCG	Clock-controlled gene
CSF	Cerebrospinal fluid
DD	Dark dark / constant darkness
DF	Degrees of freedom
DIV	Day *in vitro*
EPM	Elevated plus maze
FR	Fixed ratio
HFD	High fat diet
LB	Lysogeny broth
LD	Light dark
LDT	Light dark test
LH	Lateral hypothalamus
LHP	Learned helplessness paradigm
MDD	Major depressive disorder
n.s.	Not significant
NAc	Nucleus accumbens
OFT	Open field test
ORX	Orexin
ORX-R1	Orexin receptor 1
ORX-R2	Orexin receptor 2
PBS	Phosphate-buffered saline
PCR	Polymerase chain reaction
PFA	Paraformaldehyde
Pmch	Promelanin-concentrating hormone
PPI	Prepulse inhibition
Ppox	Prepro-orexin
qPCR	Quantitative polymerase chain reaction
RER	Respiratory exchange rate
RT	Room temperature
SAD	Seasonal affective disorder
SCN	Suprachiasmatic Nucleus
SD	Standard deviation
SEM	Standard error of the mean
shRNA	Short hairpin sRNA
SPT	Sucrose preference test
TSSR	Tyrosine site-specific recombinase
TST	Tail suspension test
TTL	Transcriptional Translational Feedback Loop
VTA	Ventral tegmental area
Wt	Wildtype
ZT	*Zeitgeber* time

1. Introduction

1.1. Mood and Anxiety Disorders and Metabolic Comorbidity

The term mood disorders summarizes the group of psychiatric disorders including major depressive disorder (MDD), bipolar disorder (BP), manic depression and seasonal affective disorder (SAD). They are characterized by the experience of very strong positive or negative emotions or the complete lack of emotions of any kind (American Psychiatric Association, 2013). In contrast, pathological states of anxiety are referred to as anxiety disorders, including for example generalized anxiety disorder and panic disorder (American Psychiatric Association, 2013). Mood and anxiety disorders are frequently associated but occur also independent of each other.

In 2017, the World Health Organization estimated a global prevalence of 4.4 % for depressive disorders and 3.6 % for anxiety disorders (World Health Organization, 2017). The prevalence strongly depends on the investigated geographical region. A survey on depression in Europe in 2014/15 reported an overall prevalence of 6.6 % while the numbers in the individual countries ranged from 2.7 % (Czech Republic) to 10 % (Luxembourg) (Robert Koch-Institut, 2019). In case of depression, the prevalence is further influenced by sex and educational status, as women but also people with lower education are at higher risk (RKI, 2017). As a matter of concern, the numbers are increasing: in Germany, the prevalence of depression raised from 12.5 % in 2009 to 15.7 % in 2017 and considering the psychological burden of the corona pandemic which started in 2020, it can be further expected to grow (Karing, 2021; Steffen et al., 2020). In addition to the influence of psychosocial and socioeconomic factors, such as the accessibility to the mental health system, depression has a strong genetic component as twin studies indicate a heritability of 30 to 40 % (Sullivan et al., 2000).

Mood and anxiety disorders are frequently accompanied by other psychiatric and somatic comorbidities, thereby impacting different areas of the patients' life and reducing their overall quality of life (Saarni et al., 2007; Sinha et al., 2018). In particular the metabolic syndrome which describes a combination of symptoms associated with metabolic dysregulation such as obesity, high blood pressure, high blood sugar, high serum triglycerides and low high-density lipoprotein, has been linked to mood and anxiety disorders (Carroll et al., 2009; Vancampfort et al., 2015). In case of BD, the prevalence of metabolic syndrome among patients is nearly twice as high as in healthy controls (Moreira et al., 2017; Silarova et al., 2015). Although metabolic comorbidities have been attributed to antidepressant treatment, studies in drug naive patients support a drug independent effect of mood disorders on metabolic dysregulation (Guha et al., 2014; van Reedt Dortland et al.,

2010). Conversely, in patients primarily diagnosed with metabolic diseases such as diabetes, occurrence of comorbid depression is increased (Semenkovich et al., 2015). Due to the high degree of comorbidity between mood and metabolic disorders, the concept of a combined "metabolic-mood-syndrome" or a "metabolic depression" has been discussed (Mansur et al., 2015; Vogelzangs et al., 2011). In support of this hypothesis, subgroups within the two disease clusters share common underlying pathologies such as dysregulation of the hypothalamic-pituitary-adrenal axis and increased inflammation but also abnormalities in the circadian and the orexin (ORX) system (Adeghate et al., 2020; Hühne et al., 2018; James et al., 2017a; Li et al., 2012; Milaneschi et al., 2019). In the following work, the involvement of the circadian and the ORX system in the development of mood- and anxiety-related disorders with metabolic comorbidity is going to be explored.

1.2. The Circadian System

1.2.1. Hierarchy of the Circadian System

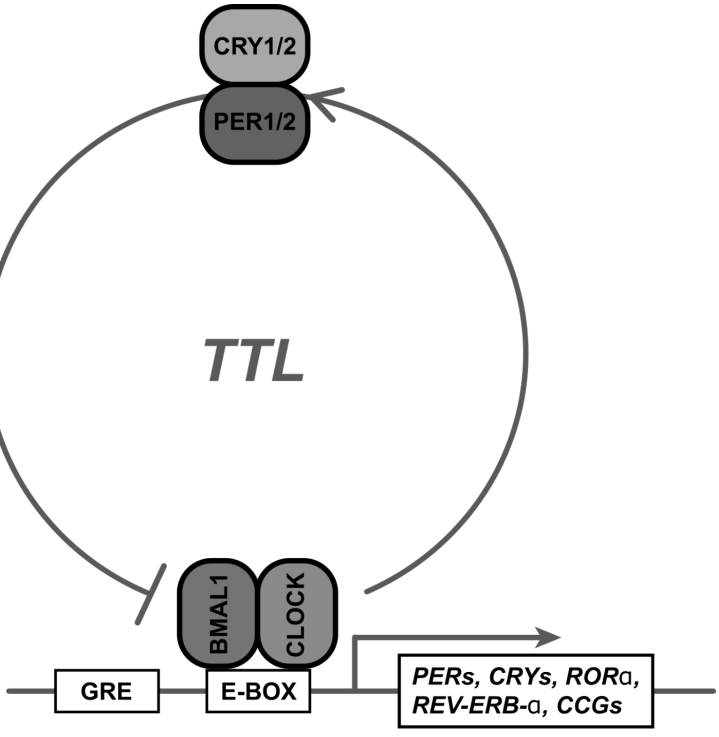

adapted from Kling and Landgraf, 2021

Figure 1 Transcriptional translational feedback loop (TTL). BMAL1 and CLOCK dimers induce the expression or *Per* and *Cry* genes as well as other clock controlled genes (CCGs). CRY and PER proteins form dimers that inhibit the BMAL1 and CLOCK complex and thus their own transcription.

One of the major challenges of living organisms is to maintain internal homeostasis in an ever-changing external environment. While some environmental events occur unpredictably in form of acute danger, there are additional predictable daily and seasonal fluctuations of resources such as food and water induced by the earth's position in the solar system. In particular the earth's rotation around its own axis causes drastic alternations in temperature and lightening recurring every 24 h. As a consequence, many organisms restrict their activity to a certain period of the day, which does not

only optimize energy expenditure but also increases survival by the establishment of distinct temporal niches. Since active and rest phase go along with different metabolic and behavioral needs, the circadian ("circa diem", lat. "about a day") system has evolved in order to enable organisms to anticipate these cyclic changes between day and night and to time physiological processes to the appropriate circadian phase. (Reviewed by Kling and Landgraf, 2021)

On the cellular level, the circadian system is based on molecular clocks ticking in every single cell of the body. They consist of a transcriptional translational feedback loop (TTL), in which the dimerizing clock proteins BMAL1 and CLOCK stimulate the transcription of the *Cry* and *Per* genes, whose proteins in turn dimerize and inhibit their own expression. As a result, abundancies of CRY and PER but also BMAL1 proteins fluctuate in the cytoplasm with a cycle length (period) of approximately 24 h. The TTL kinetics are insensitive towards temperature variations which allows poikilothermic organisms to keep a stable period independent of the environmental temperature. Robustness of this core TTL is increased by additional clock proteins such as REV-ERB-α and NPAS2. This endogenously generated rhythm is superimposed onto cellular signaling by the clock proteins ability to interact with other proteins but also to directly act as transcription factors for clock-controlled genes (CCGs). (Reviewed by Kling and Landgraf, 2021)

The presence of this many individual clocks of which the majority resides in organs incapable of sensing the external light-dark cycle, poses the difficulty of keeping these clocks in synchrony with the environment but also among each other. This is achieved by the master pacemaker, the suprachiasmatic nucleus (SCN) that is situated in the hypothalamus and receives direct input from the retina. It transmits the perceived external rhythm to subordinate clocks in other brain regions and peripheral tissues by direct neuronal connections, but also by the use of peripheral synchronizers such as glucocorticoids and core body temperature, whose circadian rhythms are directly controlled by the SCN. The process of synchronizing the circadian system to an external factor, a so-called "*Zeitgeber*" (German, "time giver") is called entrainment. Although light is the strongest known circadian *Zeitgeber*, there are also others such as food and exercise, of which some can directly entrain subordinate clocks. In line with the role of light as dominant *Zeitgeber*, circadian time points are based on the light-dark cycle and are referred to as *Zeitgeber* time (ZT), where ZT0 indicates the beginning of the light phase. (Reviewed by Kling and Landgraf, 2021)

1.2.2. Disruption of Circadian Clocks Using the Cre-LoxP-System

It has been of great interest for the circadian field to understand the relationship between the master pacemaker and its various subordinate clocks. For instance, one study showed, that internal synchrony as maintained by the SCN does not necessarily mean that all subordinate clocks are in the same phase (Yoo et al., 2004). Instead, internal circadian synchrony rather represents a state of stable phase relationships among clocks in different tissues (Yoo et al., 2004). This raises the question whether processes regulated by the circadian system are predominantly depending on the master pacemaker or on subordinate clocks in other tissues. A frequent approach to investigate the dependence of a certain process on the circadian clock is to study the process in a full body mutant of clock genes, in which the molecular clock is disrupted in all cells. While these experiments are capable of answering the question whether a certain process underlies circadian regulation in general, they cannot reveal whether its rhythmicity is induced by the master pacemaker or by any of its subordinate clocks. To overcome this limitation, the emergence of more advanced genetic tools has led to region and even cell-specific manipulations of subordinate circadian clocks in peripheral and central tissues.

One tool frequently used for this purpose is the Cre-loxP-system. Cre (Causes REcombination) belongs to the group of tyrosine site-specific recombinases (TSSRs), which are a widespread tool that allows precise genome editing without the risk of arbitrarily losing or gaining nucleotides. Apart from bacteriophages, in which they were first discovered, recombinases naturally occur in eubacteria, archaea and yeast where they cover a wide range of functions such as DNA integration and excision, plasmid copy number control or gene regulation (Meinke et al., 2016). Although they can be barely found in higher organisms, their unique properties enable usage in eukaryotic models (Meinke et al., 2016). Over the past few years TSSRs were used for various applications in life science, for example in the generation of disease models based on conditional knockout or lineage tracing systems (Meinke et al., 2016). There are more than 1300 different TSSRs known of which the Cre recombinase is the most popular one. Cre is a 343 amino acid protein that originated from the bacteriophage P1 and recognizes a 34 base pair (bp) long target site loxP (locus of crossing over P1) (Meinke et al., 2016). The genomic area of recombination is flanked by two loxP sites (floxed) each consisting of two 13 bp long palindromic sequences (half sites) that interact with the recombinase and an 8 bp spacer in between, where the DNA is recombined (Meinke et al., 2016). Depending on the relative orientation of the two loxP sites to each other, either insertion, excision, inversion or translocation can be performed (Meinke et al., 2016). In order to achieve a region or cell-specific knockout in mice, the Cre recombinase is expressed under the control of a specific

promoter in a so-called Cre driver line (Kim et al., 2018). The Cre driver line is then bred with another mouse line carrying two alleles of the floxed version of the gene, whose knockout is desired (Kim et al., 2018). In the progeny of these mice, in all cells expressing the promoter along with the *Cre* gene, the floxed gene is going to be excised (Kim et al., 2018). In circadian experiments the floxed gene is usually one of the core clock genes whose excision disrupts the functionality of the TTL and hence abolishes the molecular clock. There is a high degree of functional redundancy among the clock genes in the TTL which is why for many clock genes, deletion of only one clock gene is not sufficient to eliminate the molecular oscillator (Partch et al., 2014). In contrast, loss of *Bmal1* cannot be substituted and the single knockout of *Bmal1* abrogates clock function (Partch et al., 2014).

Despite the benefits of this precise genome editing tool, two aspects need to be considered when interpreting results. First, some genes have different functions during development as compared to the adult animal. For instance, the core clock gene *Bmal1* plays a developmental role that is independent of its function in the TTL in adult mice (Yang et al., 2016). These differences in function cannot be disentangled in the adult animal and might go along with developmental deficits. Second, recombination is a permanent manipulation of the genome that is passed on during mitosis. This includes cells and their progeny that expressed the promoter of the driver line only transiently during development or in specific situations, which needs to be considered during the interpretation of results. In order to investigate the loss of a certain gene in a specific cell population at a certain time period, there are ways to add a temporal component to the Cre-loxP-based conditional knockout. These include drug inducible activation of the Cre driving promoter or viral delivery of components of the Cre-loxP-system by stereotactical injection into target regions (Kim et al., 2018; Landgraf et al., 2016a).

1.2.3. The Circadian System and the Regulation of Mood and Anxiety

Mood disorders such MDD, BD and anxiety disorders are frequently accompanied by circadian disruptions (Difrancesco et al., 2019; Pinho et al., 2016). The most common tool to assess circadian abnormalities in clinical patients is the monitoring of sleep-wake cycles. However, it is important to consider that while being under circadian control, sleep affects mood in manifold ways of which some are independent of the circadian system. Instead, reports of altered skin and body temperature rhythms in depressive patients clearly support a purely circadian disruption in this disorder (Lorenz et al., 2019; van Londen et al., 2001). Further evidence for a circadian component in mood regulation stems from the fact that, healthy individuals show circadian variation in mood and altered rhythms of psychological symptoms like pessimism or motivation to exercise are

associated with a higher risk for psychiatric disorders (Emens et al., 2020; Pilz et al., 2018). On the molecular level, a pioneer study which reconstructed circadian gene expression rhythms in human post-mortem brain samples, reported dampened rhythms of circadian gene expression in mood regulating regions such as the nucleus accumbens (NAc) and the amygdala in MDD patients, indicating a disruption of molecular clocks in this disorder (Li et al., 2013).

The presence of circadian disruption in mood and anxiety disorders poses the question, whether they play a causal role or are a secondary consequence of the underlying disorders. There are several studies linking variants of circadian genes with mood-related disorders, indicating an endogenous circadian predisposition (Hua et al., 2014; Karthikeyan et al., 2014; Kovanen et al., 2013; Kripke et al., 2009). In line with this hypothesis, a late chronotype, a circadian trait that is influenced by genetic variation, has been associated with a higher risk to suffer from depression (Z. Chen et al., 2021; Jones et al., 2019). Further support for a causal role of circadian disruption in mood- and anxiety-related disorders emerges from studies in shift workers. Shift workers are exposed to exogenous disruptions of their endogenous circadian rhythms and suffer more frequently from depressive symptoms and anxiety than individuals working under a regular schedule (Pereira et al., 2021). As a consequence, the emerging field of chronotherapy has developed which aims at reinforcing endogenous rhythms by light therapy and reestablishing sleep-wake, social and eating rhythms in order to improve depressive symptoms (Geoffroy and Palagini, 2021).

Studies in rodents further confirm the ability of circadian disruption to induce altered mood- and anxiety- associated behavior. As in humans, exogenous disruptions of circadian rhythms in rodent shift work or jet lag models induce depression-like behavior (R. Chen et al., 2021; Horsey et al., 2019). In addition, there are several mouse models of clock gene mutations that display altered mood- and anxiety-related behavior. For instance, *Clock-d19* mutant mice show mania-like behavior while *Per1/2*- but also *Cry1/*2-deficient mice behave more anxiously (Hühne et al., 2020; Roybal et al., 2007; Spencer et al., 2013).

While full body clock mutants highlight very strikingly the relevance of the individual clock genes, they are of limited translational value since clinical phenotypes are rather determined by clock gene variants than complete loss of function mutations. Zhang and colleagues tried to overcome this limitation by studying a human *Per3* variant associated with SAD in mice and found a mild depression-like phenotype (Zhang et al., 2016). Another limitation of full body clock mutants is that it is nearly impossible to unravel the contribution of subordinate circadian clocks in distinct neuronal networks, since the master pacemaker, the SCN, is affected. As a consequence, the field

has moved to region specific disruption of clock genes instead. Landgraf et al., demonstrated the significance of the master pacemaker by knocking down *Bmal1* exclusively in the SCN while leaving subordinate clocks in the rest of the body undisturbed (Landgraf et al., 2016a). These mice showed a depression-like phenotype in several behavioral tests. Regarding the role of subordinate circadian clocks in other brain regions, a study demonstrated that knock down of *Clock* in the ventral tegmental area (VTA) induces a state of hyperactivity, reduced anxiety but also increased depression-like behavior (Mukherjee et al., 2010). Furthermore, experiments manipulating the clock in the NAc emphasize that the behavioral phenotype is highly dependent on which clock gene is being manipulated. While simultaneous knockdown of *Per1* and *Per2* in the NAc increased anxiety, down-regulation of *Rev-erbα* in the same brain region led to a reduction in anxiety and increased sociability in female mice, but not in male mice (Spencer et al., 2013; Zhao and Gammie, 2018).

With the establishment of the Cre-loxP-system as a genetic tool, it has become possible to investigate the contribution of circadian clocks in individual cellular populations to behavioral phenotypes. For instance, Bering and colleagues demonstrated that the loss of *Bmal1* in neurons of the cerebral cortex induces depression-like behavior (Bering et al., 2018). In contrast, deletion of *Per2* in glial cells reduces anxiety and despair (Martini et al., 2021). Further, knockout of *Bmal1* only in medium spiny projection neurons of the striatum impacts alcohol consumption in mice, suggesting a link to the reward system (de Zavalia et al., 2021). Considering, that with the advent of single cell sequencing the number of distinct cellular populations in the brain is constantly growing, we are just at the beginning of detangling the role of circadian rhythms in single cellular populations in mood- and anxiety-related behavior.

1.2.4. The Circadian System and Metabolic Regulation

The division into an active and inactive phase is the most prominent feature of the circadian rhythm in vertebrates and manifests in segregated states of opposing metabolic needs. The active phase is characterized by high locomotion and increased energy expenditure, both of which are decreased during the rest phase. Each state is associated with distinct profiles of molecular and cellular signaling whose temporal organization is governed by the circadian clock in order to optimize energy efficiency. Accordingly, many genes involved in metabolic pathways show circadian rhythmicity (Mure et al., 2018; Storch et al., 2002). For instance, insulin sensitivity of the liver displays a circadian rhythm which depends on transcriptional regulation by the CLOCK:BMAL1 heterodimer (Zhou et al., 2014). As a consequence, there is an optimal time window in the circadian

cycle during which nutrition can be most efficiently metabolized. This is most evident in shift workers, whose eating rhythms are disrupted due to the circadian misalignment introduced by their work schedule and who are at higher risk to suffer from metabolic diseases (Antunes et al., 2010). In addition to the long-term consequences of shiftwork, Scheer and colleagues demonstrated the immediate impact of short time circadian disruption. After exposing individuals to only 10 days of artificial circadian misalignment, they observed decreased leptin and increased glucose levels, altered circadian cortisol rhythms and increased mean arterial pressure (Scheer et al., 2009). This is further supported by studies in mice, that show that additional light exposure during the otherwise dark period leads to weight gain and reduced glucose tolerance (Fonken et al., 2010). Even more strikingly, they show that restricting food consumption to the active phase, cannot only ameliorate obesity induced by night light exposure but also high fat diet (HFD) induced weight gain (Arble et al., 2009; Fonken et al., 2010; Hatori et al., 2012). This suggests a high therapeutic potential of chronobiological interventions in metabolic disorders.

In addition to the impact of the circadian system on metabolism, the overall metabolic state of an organism affects the circadian clock. Food acts as a strong *Zeitgeber* in particular for subordinate clocks in peripheral tissue (Damiola et al., 2000). Furthermore, mice show food anticipatory behavior when entrained to a daily feeding schedule (Weaver and Reppert, 1989). This food entrainable oscillator is independent of the SCN although its exact anatomical correlates remain unknown (Pendergast and Yamazaki, 2018; Weaver and Reppert, 1989). On the molecular level, the circadian clock interacts with nutrient/energy status sensors of the cell, such as mammalian/mechanistic target of rapamycin (mTOR), thereby integrating the cellular metabolic state with circadian function (Gopalakrishnan and Kannan, 2021). As a result of this coupling, nutritional composition influences endogenous circadian rhythmicity. For instance, HFD induced obesity in mice is accompanied by dampened expression rhythms of clock genes and CCGs in the liver, kidney, hypothalamus and adipose tissue (Barnea et al., 2009; Hsieh et al., 2010; Kohsaka et al., 2007).

Similar to mood-related disorders, human genetic association studies suggest a genetic circadian predisposition for metabolic diseases. As an example, *BMAL1* haplotypes have been linked to type-2-diabetes and a polymorphism in the *CLOCK* gene was associated with the effect of appetite on waist circumference (Espinosa-Salinas et al., 2020; Woon et al., 2007). Moreover, another study demonstrated a protective effect of a *CLOCK* gene haplotype as it was connected to lower waist and hip circumference as well as decreased body mass index and leptin levels (Scott et al., 2008).

Additional support for a genetic circadian predisposition in metabolic disorders stems from rodent studies of clock genes. In particular *Bmal1*-deficient and *Clock-d19* mutant mice have been extensively studied regarding their metabolic phenotype. While *Bmal1*-deficient mice are characterized by reduced body weight and decreased adipose tissue, *Clock-d19* mutant mice are obese and hyperphagic (Kondratov et al., 2006; Turek et al., 2005). In spite of their opposing weight phenotypes, they share common metabolic pathologies such as the loss of glucose and triglyceride rhythms in the blood , reduced gluconeogenesis and altered insulin signaling (Marcheva et al., 2010; Rudic et al., 2004; Shi et al., 2013; Zhou et al., 2014). In addition to *Bmal1* and *Clock*, there is evidence for a metabolic role of other clock genes: *Per3*- and *Per1/2/3*-deficient mice are more prone to HFD induced obesity and mice lacking *Rev-erbα* lose their feeding rhythm in constant darkness (Dallmann and Weaver, 2010; Sen et al., 2018).

Again, full body clock mutants do not allow conclusions regarding the contribution of subordinate clocks in local tissues to the overall phenotype. Nevertheless, they provide clues on potential candidate regions. In case of metabolic pathologies, they indicate an interplay between subordinate clocks in peripheral tissues and central brain regions. For instance, the metabolic phenotype in *Clock-d19* mutant mice is accompanied by the loss of expression rhythms of genes involved in insulin signaling and glucose sensing in the pancreas but also appetite regulating genes in the hypothalamus (Marcheva et al., 2010; Turek et al., 2005). Accordingly, researchers have been specifically manipulating clock genes in peripheral but also central tissues.

Regarding the role of peripheral subordinate clocks, several tissues have been targeted. These experiments revealed, that the loss of *Bmal1* in the liver is sufficient to induce obesity along with altered glucose metabolism, disrupted rhythms of hepatic insulin sensitivity and hepatotoxicity (Johnson et al., 2014; Lamia et al., 2008; Zhou et al., 2014). Moreover, genetic ablation of *Bmal1* exclusively in the pancreas results in disrupted glucose metabolism and reduced insulin secretion (Marcheva et al., 2010). Similarly, mice with dysfunctional TTL in adipocytes of brown and white adipose tissue suffer from higher body weight, altered food intake rhythms and higher susceptibility to HFD induced obesity (Hasan et al., 2021; Paschos et al., 2012). Highlighting the tight connection between peripheral and central clocks, these mice have additional altered gene expression rhythms in the hypothalamus (Paschos et al., 2012). In contrast to studies indicating a protective role of the circadian clock in metabolic dysfunction, Yu and colleagues demonstrate that loss of circadian rhythmicity can also be beneficial, since *Bmal1*-deletion in the intestine is preventive of HFD induced obesity (Yu et al., 2021).

More recently, studies investigated the contribution of subordinate clocks in the brain to metabolic pathologies. When *Bmal1* is deleted specifically from the central and peripheral nervous system, mice lose their ability to entrain to feeding schedules and knockout of *Rev-erbα* using the same Cre driver disrupts food intake rhythms in constant darkness (Mieda and Sakurai, 2011; Sen et al., 2018). In addition, both studies report lower body weight of their clock mutant mice. However, studies have shown that this can rather be attributed to secondary effects of the used Cre driver line than to the disruption of the circadian clock (Giusti et al., 2014; Sen et al., 2018). Examination of mice with astrocyte-specific *Bmal1* knockout shows altered glucose homeostasis and an initial increase in weight which is followed by a weight reduction due to accelerated aging (Barca-Mayo et al., 2017). Again, not all evidence points towards a protective role of circadian rhythms in metabolic disease, as microglia-specific deletion of *Bmal1* protects mice against HFD induced obesity (Wang et al., 2021).

Several of the described clock mutants report associated circadian abnormalities in the hypothalamus (Barca-Mayo et al., 2017; Paschos et al., 2012; Turek et al., 2005; Wang et al., 2021). Since many major appetite and energy expenditure regulating neuronal populations reside in the hypothalamus, circadian clocks of this brain area are frequently in the focus of interest (Timper and Brüning, 2017). Forebrain specific manipulations of the circadian clock, which include the hypothalamus show an impact on feeding rhythms and glucose metabolism (Cedernaes et al., 2019; Mieda et al., 2017). Emphasizing the impact of the master pacemaker, it has been shown that down-regulation of *Bmal1* only in the SCN increases weight gain in mice (Landgraf et al., 2016a). Likewise, loss of *Bmal1* in neurons of the paraventricular hypothalamus causes weight gain while deletion of *Rev-erbα* in the anterior ventral hypothalamus increases vulnerability to diet induced obesity (Adlanmerini et al., 2021; Kim et al., 2020). Further studies indicate a role of molecular clocks in hypothalamic AgRP neurons in the control of hepatic glucose metabolism and of Sf1 neurons in the regulation of brown adipose tissue dependent thermogenesis (Cedernaes et al., 2019; Orozco-Solis et al., 2016). These studies have already provided valuable insights into the impact of subordinate clocks in the hypothalamus on metabolic regulation. Nevertheless, considering the vast heterogeneity of hypothalamic neuronal populations and the complex neuronal network they form to control metabolic processes, there remain many open questions regarding the interplay between subordinate clocks in distinct neuronal subpopulations of the hypothalamus and their impact on metabolic regulation. For instance, to this date, the role of subordinate clocks in ORX neurons of the LH in metabolic regulation has not been examined.

1.3. The ORX System

The neuropeptides ORX-A and B (also hypocretin-1 and 2) were independently discovered by two research groups towards the end of the last century (de Lecea et al., 1998; Sakurai et al., 1998). While both initial reports included their exceptionally restricted and specific localization in certain areas of the hypothalamus, their name choices focused on different features of the neuropeptides: Due to similarities in amino acid structure to the already known hormone secretin, De Lecea and colleagues termed the newly discovered neuropeptides as a hypothalamic secretin, short hypocretin. Instead, the group around Sakurai observed that rats display increased food consumption following central administration of the neuropeptides, which motivated the name after the Greek word for appetite, orexi. Since then, numerous of studies have described various features of the ORX system regarding their anatomy and functions in various species. In the following, some of the key features of ORX anatomy, signaling and functioning are going to be exposed.

1.3.1. Molecular Components of the ORX System

ORX-A and B originate by proteolytic cleavage from a common precursor peptide, prepro-orexin, which is encoded on the human chromosome 17 and the murine chromosome 11 (Sakurai et al., 1998). The amino acid sequence is highly conserved between humans and mice: While the 33 amino acid long sequence of ORX-A is identical between both species, the 28 amino acid sequence of ORX-B only differs in two amino acids (Sakurai et al., 1998). The neuropeptides bind to two G protein-coupled receptors, ORX-R1 and ORX-R2 (de Lecea et al., 1998; Sakurai et al., 1998). ORX-R1 has a higher affinity for ORX-A while ORX-R2 binds both neuropeptides equally (Sakurai et al., 1998).

1.3.2. Anatomy of the ORX System

Central ORX

To this date, the ORX system is well known for its specific localization in neuronal somas in confined areas of the hypothalamus. This is highly conserved among investigated vertebrate species, although the exact position within the hypothalamus has been shown to differ (Azeez et al., 2021; Cutler et al., 1999; Soya and Sakurai, 2020). In human, rats and mice, *PPOX* expressing neurons are

mainly found in the lateral, dorsal, dorsomedial and perifornical hypothalamus and comprise an overall population of around 50,000 to 70,000 neurons in humans and 3,000 to 4,000 in rodents (Azeez et al., 2021). In birds, they reside additionally in the hypothalamic ventricular zone, which is where they can be found in fish as well, while in amphibians they populate the SCN (Soya and Sakurai, 2020). However, it is important to mention, that *Ppox* expression has also been described in extra-hypothalamic regions of the rodent brain which challenges the idea of the hypothalamus as exclusive central production site (Ciriello et al., 2003; Kim et al., 2015; Saad et al., 2019; Yamamoto et al., 2010). Independent of their source, ORX projections span the entire brain, including the cortex, several hypothalamic regions, the locus coeruleus, the amygdala, the VTA and the spinal cord (Azeez et al., 2021; Cutler et al., 1999; Peyron et al., 1998). Similarly, ORX receptors have been described in the majority of brain structures (Azeez et al., 2021).

Peripheral ORX

ORX is detectable in the plasma and its receptors can be found across a range of peripheral organs (Li et al., 2021; Randeva et al., 2001; Takahashi et al., 2006). However, the sources of peripheral ORX are not completely clear. While it is possible, that central ORX is secreted into the blood stream through which it reaches its peripheral target structures, local ORX production sites have been discussed as well (Heinonen et al., 2008; Kastin and Akerstrom, 1999). In particular following the first years after its discovery, several efforts were taken to investigate the presence of *Ppox* expressing cells in the periphery, as it has been described for other neuropeptides like somatostatin (Lucey, 1986). As a result, *PPOX* expression was detected in the human pancreas, gastrointestinal tract, epididymis, penis, kidney, adrenal gland, pituitary and placenta (Blanco et al., 2003; Ehrström et al., 2005; Karteris et al., 2004; Kirchgessner, 2002; Nakabayashi et al., 2003; Randeva et al., 2001; Takahashi et al., 2006). Similarly, a range of studies have reported several peripheral ORX production sites in the rat (Barreiro et al., 2005; Jöhren et al., 2001; Liguori et al., 2018; Näslund et al., 2002; Patel et al., 2018; Silveyra et al., 2007; Tafuri et al., 2009; Takahashi et al., 2006). In the mouse however, the available data on ORX synthesis in the periphery, is rather incomprehensive. Although its presence in the testis is well established (Joshi and Singh, 2017), there are only few studies reporting expression in the adrenal glands, white adipose tissue, pancreas and the gastrointestinal system (Arafat et al., 2014; de Miguel and Burrell, 2002; Kirchgessner, 2002; Zhang et al., 2010). In addition, many major organs like the kidneys or the heart remain uninvestigated. **Table 1** holds a summary of the available data on peripheral *Ppox* expression and immunohistochemical ORX detection in human, mice and rats. It highlights the gap of knowledge

on peripheral *Ppox* expression in mice as compared to human and rats. This deficit is particularly drastic, since the mouse represents the major clinical research model and many manipulations of the ORX system such as ORX-deficiency or conditional knockouts in *Ppox* expressing cells target the population of ORX cells as a whole. As a consequence, the ignorance regarding the entity of anatomical correlates of the ORX system in the mouse impedes the correct interpretation of preclinical studies.

Table 1 Summary of the literature on Ppox expression and immunohistochemical detection of ORX in peripheral tissues in humans, mice and rats.

Tissue	Human		Mouse		Rat		References
	RNA	Protein	RNA	Protein	RNA	Protein	
Adrenal glands	+ (3)	+ (4) - (3)	+ (1)		- (2)		Arafat et al., 2014 (1) Jöhren et al., 2001 (2) Nakabayashi et al., 2003 (3) Randeva et al., 2001 (4)
Amygdala			+ (6,7,8,9)	+ (6)		+ (5)	Ciriello et al., 2003 (5) Kim et al., 2015 (6) Kim and Han, 2016 (7) Kim et al., 2017 (8) Yamamoto et al., 2010 (9)
Aorta	- (3)	- (3)			- (2)		Jöhren et al., 2001 (2) Nakabayashi et al., 2003 (3)
Bone marrow	- (3)						Nakabayashi et al., 2003 (3)
Breast		- (3)					Nakabayashi et al., 2003 (3)
Bronchus	- (3)	- (3)					Nakabayashi et al., 2003 (3)
Colon	+ (3)	+ (3)					Nakabayashi et al., 2003 (3)
Epididymis	+ (10)				+ (12)	+ (11,12)	Karteris et al., 2004 (10) Liguori et al., 2018 (11) Tafuri et al., 2009 (12)
Esophagus	- (3)	- (3)					Nakabayashi et al., 2003 (3)
Eye		- (3)					Nakabayashi et al., 2003 (3)
Heart	- (3)	- (3)			+ (2,13)	+ (13)	Jöhren et al., 2001 (2) Nakabayashi et al., 2003 (3) Patel et al., 2018 (13)
Kidney	+ (3)	+ (14) - (3)			- (2)	+ (14)	Jöhren et al., 2001 (2) Nakabayashi et al., 2003 (3) Takahashi et al., 2006 (14)
Lacrimal gland						+ (15)	Adeghate and Hameed, 2005 (15)
Liver	- (3)	- (3)			- (2)		Jöhren et al., 2001 (2) Nakabayashi et al., 2003 (3)
Lung	- (3)	- (3)			- (2)		Jöhren et al., 2001 (2) Nakabayashi et al., 2003 (3)
Muscle					- (2)		Jöhren et al., 2001 (2)
Ovaries		- (3)			- (2,16)		Jöhren et al., 2001 (2) Nakabayashi et al., 2003 (3) Silveyra et al., 2007 (16)

Pancreas	+ (3)	+ (3,18)	+ (1)		- (2)	+ (1,17,19)	Adeghate & Hameed, 2011 (17) Arafat et al., 2014 (1) Ehrström et al., 2005 (18) Jöhren et al., 2001 (2) Nakabayashi et al., 2003 (3) Ouedraogo et al., 2003 (19)
Penis	+ (10)						Karteris et al., 2004 (10)
Pituitary Gland		+ (20)			- (2)		Blanco et al., 2003 (20) Jöhren et al., 2001 (2)
Placenta	+ (3)	+ (3)					Nakabayashi et al., 2003 (3)
Prostate		- (3)					Nakabayashi et al., 2003 (3)
Rectum		+ (3) - (21)		- (21)			Baumann et al., 2008 (21) Nakabayashi et al., 2003 (3)
Skin		- (3)					Nakabayashi et al., 2003 (3)
Small Intestine		+ (18)		+ (22)			Baumann et al., 2008 (21) De Miguel & Burrell et al., 2002 (22) Ehrström et al., 2005 (18) Jöhren et al., 2001 (2) Kirchgessner et al., 1999 (23) Nakabayashi et al., 2003 (3) Näslund et al., 2002 (24)
Duodenum	- (3)	+ (3)			- (2)	+ (24)	
Jejunum		+ (3)			- (2)		
Illeum	+ (3)	+ (3,23) - (21)		+ (23) - (21)		+ (23)	
Spleen	- 3	- 3			- (2)		Jöhren et al., 2001 (2) Nakabayashi et al., 2003 (3)
Stomach	+ (3) - (21)	+ (3,18)		- (21) + (22)	- (2)		Baumann et al., 2008 (21) de Miguel & Burrell et al., 2002 (22) Ehrström et al., 2005 (18) Jöhren et al., 2001 (2) Nakabayashi et al., 2003 (3)
Striatum			+ (25,26)				Saad et al., 2019 (25) Saad et al., 2021 (26)
Submandibular gland		- (3)					Nakabayashi et al., 2003 (3)
Testis	- (10)	- (3)	+ (28,29)	+ (28,29)	+ (2,27,30)	+ (27,30)	Barreiro et al., 2005 (27) Jöhren et al., 2011 (2) Joshi & Singh, 2016 (28) Joshi & Singh, 2017 (29) Karteris et al., 2004 (10) Nakabayashi et al., 2003 (3) Tafuri et al., 2010 (30)
Thyroid Gland		- (3)			- (2)		Jöhren et al., 2001 (2) Nakabayashi et al., 2003 (3)
Thymus	- (3)						Nakabayashi et al., 2003 (3)
Tonsil		- (3)					Nakabayashi et al., 2003 (3)
White adipose tissue			+ (1,31)		- (2)		Arafat et et al., 2014; (1) Jöhren et al., 2001 (2) Zhang et al., 2010 (31)

1.3.3. The ORX System and Arousal

The extensive magnitude of ORX projections and receptors within the brain is the anatomical correlate of the manifold physiological and psychological functions that are modulated by the ORX system. Most importantly, it is responsible for the maintenance of wakefulness which manifests in particular in the pathology of narcoleptic patients, who suffer from excessive day time sleepiness due to chronically low ORX levels (Reading, 2019). This correlation between low ORX signaling and narcolepsy-like phenotypes is highly conserved among species including human, mice, dog and fish, which highlights the central role of ORX in promoting wakefulness (Chemelli et al., 1999; Elbaz et al., 2012; Lin et al., 1999). Further, it has been demonstrated, that in addition to ensuring sufficient levels of wakefulness throughout an animal's active phase, ORX also provides arousal on demand as it is upregulated during stressful events which require particular high states of vigilance (James et al., 2017a). In line with their role in wake promotion, ORX neurons were shown to project to many of the major arousal promoting brain regions such as the locus coeruleus, the dorsal raphe nucleus or tuberomammillary nucleus (Peyron et al., 1998). Since states of elevated alertness coincide with higher metabolic needs as well as behavioral changes, it is not surprising that the impact of ORX extends beyond simply increasing wakefulness.

1.3.4. Regulation of the ORX System

The exceptional role of the ORX system as key mediator of wakefulness during the active phase along with guaranteeing arousal on demand requires a fine-tuned regulation that ensures the appropriate levels of ORX at any given time. Similar to glucocorticoids, they need to react to the recurrent changes between day and night as well as unexpected environmental events (Kling and Landgraf, 2021). Hence a model of circadian as well as well as a reactive regulation that is involved in maintaining the ORX homeostasis has been discussed (Azeez et al., 2021). Within this model, the circadian system induces a pattern of high ORX levels in the animal's active phase and low levels during its resting phase. This rhythm can be superimposed by immediate surges of ORX release in situations that require acute alertness. In the subsequent paragraphs, evidence in support of this model is going to be explored.

Reactive Homeostatic Regulation

The ORX system is highly reactive to internal and external factors which ensures its activation in situations that require high levels of arousal. The ability of glucocorticoid receptors to bind to the ORX promoter links it tightly to the stress system (Grafe et al., 2017). As a consequence, ORX is upregulated in response to stressors such as electric foot shock or high arousal awakening during the resting phase (Chen et al., 2014; España et al., 2010). Further, ORX neurons are activated during high locomotor activity, which acts as a positive feedback that reinforces the state of high alertness maintained by the ORX system (Nixon and Smale, 2004). In addition to the response to environmental stimuli, the ORX system also reacts to physiological stressors including sleep deprivation and food restriction (Estabrooke et al., 2001; Fujiki et al., 2001). These examples highlight the homeostatic nature of the ORX system since deprivation induced upregulation is a classical feature of homeostatic regulation. The persistence of sleep deprivation induced upregulation of ORX in SCN lesioned rats emphasizes a partial separation between the circadian and the reactive homeostatic regulation (Deboer et al., 2004; Desarnaud et al., 2004; Yoshida et al., 2001; Zhang et al., 2004). However, it can be speculated that circadian gating also affects the reactive homeostatic regulation of ORX with respect to the magnitude of the evoked response similar as it has been described for glucocorticoids (Helfrich-Förster, 2017; Kling and Landgraf, 2021). The immense reactiveness of the ORX system can hinder the identification of underlying endogenous oscillations. This is illustrated by a study that observed circannual rhythms in human CSF ORX levels with highest levels during summer time (Boddum et al., 2016). Since to this date, there is no known circannual oscillator in humans, seasonal differences in environmental factors such as light and weather conditions, as well as seasonal changes in social patterns and physical activity are discussed as source of these variations.

Circadian Regulation

The circadian regulation of ORX signalling in rodents has been shown to persist throughout all levels from synthesis to its action in target regions. On the transcriptional level, *Ppox* belongs to the group of CCGs as the circadian transcription factor DEC2 binds to the *Ppox* promoter (Hirano et al., 2018). Accordingly, at least nine studies demonstrated rhythmic expression across the circadian cycle in mice (Amador et al., 2016; Hühne et al., 2022; Justinussen et al., 2015; Sen et al., 2018; Stütz et al., 2007; Taheri et al., 2000; Turek et al., 2005; Ventzke et al., 2019; Wang et al., 2017). Despite being unanimous regarding its overall rhythmicity, the exact circadian time point of peak expression varies among publications. This could be due to superimposing influences of the reactive

homeostatic regulation caused by handling of the mice before sacrifice. However, the fact that rhythms are lost in three different full body clock mutants strongly argues for an endogenous circadian regulation of *Ppox* transcription and against an exogenous induction of the observed variations (masking effect) (Amador et al., 2016; Hühne et al., 2022; Sen et al., 2018; Turek et al., 2005).

There are fewer studies investigating the circadian rhythm of ORX peptides in the LH due to several technical issues. For instance, the technique of western blot does not allow a differentiation between released and cellular ORX peptides, and thus does not enable conclusions regarding translational rhythms. Furthermore, the alternative method of immunohistochemistry mainly assesses the number of ORX immunoreactive cells. Evaluation of circadian rhythmicity using this method is based on the assumption, that ORX levels drop below the detection level in individual cells which excludes the identification of more subtle changes. To this date, more advanced staining and imaging techniques that would allow the distinction between cellular and extracellular ORX have not been applied to answer the question of whether the abundancy of ORX protein in ORX neurons of the LH displays circadian rhythmicity. Another issue using immunohistochemistry has been addressed by McGregor and colleagues who have shown that transport of ORX peptide from the soma to the dendrites further diminishes the immunohistochemical signal (McGregor et al., 2017). Nevertheless, the authors found a circadian difference in the number of ORX expressing cells in mice that indicate more ORX producing neurons in the dark phase than in the light phase, which matches the pattern expected in a nocturnal animal (McGregor et al., 2017).

Several studies have demonstrated that cFos, a marker for neuronal activation, displays a circadian rhythm in ORX neurons of the LH suggesting rhythmic activity of this neuronal population (Estabrooke et al., 2001; Marston et al., 2008; Martínez et al., 2002; Nixon and Smale, 2004). In line with the role of ORX in wake promotion during the active phase, cFos in ORX neurons peaks during the night for nocturnal and during the day for diurnal rodents (Martínez et al., 2002; Nixon and Smale, 2004). Further, these rhythms persist in constant conditions, ruling out masking effects caused by external light rhythms (Estabrooke et al., 2001; Marston et al., 2008). In addition, electrophysiological *in vivo* recordings in head-fixed rats confirm that ORX neurons fire most during wake states and least during sleep (Hassani et al., 2009; Lee et al., 2005).

Since activation of ORX neurons leads to the subsequent release of ORX peptides, it is not surprising that ORX levels in the cerebrospinal fluid (CSF) display a circadian rhythm in rats with peak levels towards the end of the night (Deboer et al., 2004; Desarnaud et al., 2004; Fujiki et al., 2001; Yoshida et al., 2001; Zhang et al., 2004). This rhythm is evidently of endogenous origin, as it persists even in

constant conditions and is lost in SCN lesioned rats (Deboer et al., 2004; Zhang et al., 2004). Although this does not necessarily identify the master pacemaker as the source of these rhythms, reports of direct projections from the SCN to ORX neurons in nocturnal and diurnal animals suggest a direct influence of the SCN on ORX signaling (Abrahamson et al., 2001; Schwartz et al., 2011).

Finally, ORX signaling in target regions is gated by the circadian system. For instance, ORX receptors in brain areas such as the cortex and the SCN cycle in a circadian manner (Belle et al., 2014; Ventzke et al., 2019). Even more striking, the olivary pretectal nucleus displays a phase response curve to ORX stimulation and it can be assumed that this is the case for other orexinergically innervated brain regions (Chrobok et al., 2021).

There are only very few studies investigating circadian ORX rhythms in humans. One study compared the amount of ORX immunoreactive cells in the brains of individuals who died during the night with those of individuals who deceased during the day and found a diurnal difference (Lu et al., 2017). This suggests that even in humans, *PPOX* transcription and translation follow a circadian rhythm. Against expectations for a diurnal species, the number of ORX neurons was higher in individuals who passed away during the night. However, this might have been due to the chosen time intervals for night and day which might have not provided the necessary resolution. Regarding studies focusing on ORX release, the majority of them reports no impact of circadian timing (Arihara et al., 2001; Grady et al., 2006; Mäkelä et al., 2018). Several reasons can account for the lack of detectable rhythms in these studies. For instance, some only assessed two different time points, which bears the risk of missing circadian differences if those time points do not match peak and trough (Arihara et al., 2001; Grady et al., 2006). Further, one study measured ORX levels in the plasma and did not find circadian variation (Mäkelä et al., 2018). It is possible that central rhythms do not persist into the periphery, due to the contribution of local peripheral ORX production sites, which might be regulated by the circadian system differently. Another complicating factor is that it is more difficult to control for the homeostatic regulation of ORX signaling in humans, since individuals might vary in nutritional status and wakefulness or might perceive the intervention as stressful, all factors that could evoke acute releases of ORX and obscure underlying circadian rhythms. Despite all the challenges, Salomon et al. continuously measured ORX levels in the lumbar CSF of healthy controls and revealed a circadian rhythm peaking at the beginning of the dark phase (Salomon et al., 2003). Considering the delay between lumbar and central CSF, highest levels probably appear at the end of the light phase in central CSF. This in line with the pattern of ORX rhythms in the CSF of a diurnal primate as well as rodents, where ORX levels peak at the end of the respective active phase (Fujiki et al., 2001; Zeitzer et al., 2003). The peak at the end of the active phase might seem surprising. However, it is important to keep in mind that CSF measurements are

merely a correlate of signaling taking place in the brain. Temporal dynamics might be compromised by the delay between the initial ORX release at the target site and its abundancy in the CSF. Moreover, degradation kinetics of the ORX peptides affect the amount detectable in the CSF. Hence, it is possible, that ORX accumulates in the CSF throughout the active phase.

Interestingly, the relationship between the circadian and the ORX system seems to be bidirectional as the gene encoding for the ORX-R2 has been associated with morningness in humans (Hu et al., 2016). Anatomically, this interaction manifests in ORX projections to the SCN, which expresses ORX-R1 in rats (Belle et al., 2014; Peyron et al., 1998). These orexinergic efferents are capable of inhibiting the SCN without resetting it (Belle et al., 2014; Brown et al., 2008). Since the activity of SCN neurons is highest during the light phase and ORX neuron activity peaks during the active phase, their activity rhythms are antiphasic in nocturnal rodents. Thus, the inhibitory effect of ORX on SCN neurons does not only stabilize this phase relationship , but also allows a downregulation of SCN activity following unexpected arousal promoting events during the resting phase (Belle et al., 2014). It would be of great interest to investigate the interaction between the SCN and ORX neurons in diurnal animals, in which the neuronal activity of these two brain regions is in phase.

In summary, evidence has accumulated over the past 20 years that ORX signaling is subjected to diurnal variations in humans, rodents and primates with peak signaling during the active phase. Moreover, studies under constant conditions, in SCN-lesioned rats and clock mutant mice have demonstrated that these variations depend on the circadian clock. What remains unclear is the question where these rhythms are generated within the hierarchy of the circadian system, meaning whether they are maintained by the SCN or by local subordinate clocks in ORX neurons.

1.3.5. The ORX System and the Regulation of Mood and Anxiety

Several aspects of the ORX system support the idea of ORX dysregulation in mood and anxiety disorders. For instance, ORX neurons of the hypothalamus project to central structures involved in the regulation of mood, anxiety and reward such as the amygdala, the NAc, the VTA and the bed nucleus of the stria terminalis (BNST), which, in turn, express ORX receptors (Peyron et al., 1998; Trivedi et al., 1998). Further, the ORX system is strongly associated with stress and sleep regulation, two major processes involved in mood- and anxiety-related pathology. In the following, evidence regarding the role of ORX in mood and anxiety disorders is going to be discussed.

Low ORX Signaling in Depression and Anxiety

The observation that narcolepsy is frequently associated with a higher risk for depressive comorbidity motivates the concept of pathological downregulation of ORX in depression (Dodel et al., 2007). Although, this could also be due to the burden of living with a chronic disease, the fact that increased reward seeking behavior in addictive patients is associated with high ORX levels argues for an independent impact of the ORX system (James et al., 2017b). Further a study described high ORX levels during laughter and positive emotions in the amygdala of psychologically healthy individuals (Blouin et al., 2013). More direct evidence comes from Brundin et al., who showed that ORX levels in the CSF of MDD patients are reduced following a suicide attempt (Brundin et al., 2007). They also accompanied patients throughout the first year after their suicide attempt and found the reduction of suicidal behavior to be associated with an increase in CSF ORX levels (Brundin et al., 2009).

In rodents, a reduced number of *Ppox* expressing neurons was found in the hypothalamus of genetic and stress induced depression models as well as a model of SAD (Allard et al., 2004; Deats et al., 2014; Ito et al., 2009). Accordingly, rodents with depression-like behavior have lower ORX levels in the hypothalamus along with other brain regions including the amygdala (Hou et al., 2020; Nocjar et al., 2012; Taheri et al., 2001). Furthermore, C57BL/6J mice have lower baseline ORX levels than other mouse strains along with increased depression-like behavior (Feng et al., 2014; Lin et al., 2002). Restoration of a chromosome displacement in this strain rescued not only ORX levels but also some of the behavioral phenotypes (Feng et al., 2014). In support of a causal role of ORX in mood- and anxiety-related disorders, ORX-deficient mice display increased anxiety in several behavioral tests, although studies assessing their depression-like behavior did not detect any differences (Khalil and Fendt, 2017; Lutter et al., 2008; Matsuo et al., 2011). However, OXR-R1-deficient mice show anxiety- as well as depression-like behavior and reduced social interaction, which demonstrates that reduced signaling in this component of the ORX system can induce mood- and anxiety-related phenotypes (Abbas et al., 2015). Even more specifically, Ji et al., showed that the knockdown of ORX receptors exclusively in the ventral pallidum is sufficient to induce depression-like behavior in mice (Ji et al., 2019). In line with these findings, several studies report antidepressant effects of ORX. In healthy animals, intracerebroventricular injection of ORX-A increases neurogenesis in the hippocampus and reduces immobility in the forced swim test (Ito et al., 2008). Similarly, microinjection of ORX into the ventrolateral periaqueductal gray or amygdala reduces anxiety-like behavior (Pan et al., 2020; Pourrahimi et al., 2021). In addition, the antidepressant effect of calorie restriction depends on the reactive upregulation of ORX (Lutter et al., 2008). Since sleep deprivation, a known antidepressant treatment in humans, also increases

ORX levels, it has been hypothesized that the ORX system is mediating this effect although it has not been confirmed yet (Allard et al., 2007).

High ORX Signaling in Depression and Anxiety

In contrast to the multitude of studies supporting the downregulation of the ORX system in disorders with low mood and increased anxiety, there is evidence indicating overactive ORX signaling in these conditions. In particular anxiety seems to be associated with higher ORX levels (Akça et al., 2020; Johnson et al., 2010). Considering that anxiety represents a state of high alertness and stress, this is in line with the role of ORX as promoter of arousal on demand. Further, plasma ORX was positively correlated with depression in anxiety disorder patients and higher ORX levels were reported in BD and MDD patients than in healthy controls (Akça et al., 2020; Li et al., 2021). The notion of high ORX levels as driver of states of low mood and high anxiety is promoted by clinical studies demonstrating the ability of ORX receptor antagonists to improve symptoms of depression and anxiety (Nakamura and Nagamine, 2017; Recourt et al., 2019; Savitz et al., 2021). However, since the amelioration is accompanied by enhanced sleep quality, it is possible that the main impact of ORX receptor antagonists on depression severity is rather indirect via the improvement of sleep quality instead of direct antidepressant actions.

On the rodent side, increased numbers of ORX neurons were reported in Flinders Sensitive Line rats, a genetic model of depression as well a mouse depression model based on corticosterone injections (Jalewa et al., 2014; Mikrouli et al., 2011). In line with this observation, ORX levels and ORX neuron activation are enhanced in several rodent models of depression-like behavior and panic disorder (Feng et al., 2008; Johnson et al., 2010; Nollet et al., 2011; Tenorio-Lopes et al., 2020). Additionally, anxiety-like behavior can be induced by injection of ORX into the amygdala, ventricle or BNST (Avolio et al., 2011; Lungwitz et al., 2012; Suzuki et al., 2005). Last but not least, almorexant, a dual ORX-R antagonist reduces depression-like behavior in mice (Nollet et al., 2012).

Why are Results so Heterogeneous?

It is obvious, that at this stage, there is no clear answer regarding the directionality of ORX dysregulation in mood and anxiety disorders. The heterogeneity among results can be explained by several confounding factors but also the ORX system's unique properties.

One major aspect is the fact that, like other psychiatric disorders, mood and anxiety disorder are inherently heterogeneous and lack biomarker-based classification. As a consequence, it is possible that dysregulation of ORX signaling is only present in a subgroup of patients which so far could not be identified based on current diagnostics. Further, human studies are either based on ORX levels in the CSF or plasma. Since there are additional peripheral ORX production sites, it is possible that plasma ORX is not a correlate of central ORX production and hence might not be comparable to CSF ORX. Another point is that it can be assumed, that there are interindividual differences in ORX baseline levels due to the genetic background as it has been reported for different mouse strains (Lin et al., 2002). These might further obscure results.

Another challenge rises from the extraordinary reactivity of the ORX system to physiological factors such as metabolic state and wakefulness, which can be difficult to correct for in a clinical setting. Although these are more controllable in preclinical animal studies, rodent depression models are frequently stressor based which directly activate the ORX system. Hence, results strongly depend on the nature and duration of the applied stressor as the ORX system has been shown to react differently to acute versus chronic stress (James et al., 2017a).

There is increasing evidence that in contrast to a generally overactive or inhibited ORX system, its individual components might be differentially regulated in anxiety and mood disorders. Multiple studies show that up- or downregulation are region specific and occur within the same animal (Arendt et al., 2013; Feng et al., 2008, 2007). For instance, while injection of ORX into the BNST increased anxiety-like behavior, injections into the medial septum did not have any impact (Lungwitz et al., 2012). Furthermore, ORX-A and ORX-B can be differentially regulated within one brain region and induce contrasting behavior upon injection (Chung et al., 2014; Feng et al., 2007; Hsu and Wang, 2021; Pan et al., 2020). Finally, OXR-R1 and 2 have distinct expression patterns in the brain and their respective knockout mice display opposite mood-related behavior indicating distinct roles for the two receptors (Marcus et al., 2001; Scott et al., 2011). In support of a more differential role of ORX depending on peptide and receptor subtypes, so far only genetic variants of the genes encoding for OXR-R1 or 2 were associated with MDD or treatment outcome but not the *Ppox* gene itself (Cengiz et al., 2019; Firouzabadi et al., 2020; Rainero et al., 2011).

Finally, the ORX system underlies circadian control and hence differences between patients and healthy controls might vary across the 24h cycle. However, most studies assess only one circadian time point. Indeed, Salomon et al., who measured continuously ORX levels in the CSF found a dampened amplitude of ORX rhythmicity in depressed patients along with a trend towards higher mean ORX levels (Salomon et al., 2003). In this study, the comparison of the sinusoidal fits for ORX

in the CSF of depressive and control patients suggests, that in depressive patients ORX levels were relatively higher during one half of the circadian cycle and relatively lower during the other half. This could explain the lack of differences between patients and controls in case samples were taken at various time points throughout the day or the chosen time point missed the maximal differences at peak and trough (Lu et al., 2019; Ozsoy et al., 2017; Schmidt et al., 2011, 2010). In support of the idea that ORX rhythmicity is required for healthy behavior, *Clock-d19* mutant mice display mania-like and less depression-like behavior along with a lack of ORX rhythmicity (Roybal et al., 2007; Turek et al., 2005). Interestingly, while depressive patients had increased mean ORX levels, *Ppox* expression in manic *Clock-d19* mutant mice remained lower than in control mice (Salomon et al., 2003; Turek et al., 2005). This demonstrates that in addition to the lack of rhythmicity, the mean levels of ORX across 24h have an impact on mood. These studies clearly suggest circadian dysregulation of the ORX system in mood disorders. However, they cannot answer the question on whether local subordinate clock in ORX neurons are important to maintain a healthy affective state or whether the loss of ORX rhythmicity is secondary to the disease in depressed patients or to the loss of overall circadian rhythmicity in *Clock-d19* mice.

1.3.6. The ORX System and Metabolic Regulation

The link between the ORX system and metabolic regulation has been evident since its first discovery more than 20 years ago, as ORX central ORX administration increased appetite in rats (Sakurai et al., 1998). Accordingly, narcoleptic patients with ORX-deficiency frequently suffer from comorbid metabolic diseases (Nishino et al., 2000). In the following, the role of ORX in metabolic regulation is going to be explored.

A Protective Role for ORX in Metabolic Regulation

In contrast to what one would expect from the lack of an appetite stimulating neuropeptide, metabolic disruptions in narcoleptic patients include mainly obesity and diabetes, suggesting a protective role of ORX against metabolic syndrome (Kovalská et al., 2016; Nishino et al., 2000). Years of research have investigated the relationship between ORX and metabolic processes and have confirmed its protective impact, which Devanjan Sikder summarized as a “couch potato’s dream” (Cell Press, 2011; Sellayah et al., 2011). In line with the initial reports, ORX indeed directly stimulates appetite and food consumption, however it simultaneously increases the metabolic rate and initiates metabolic processes that lead to an optimal utilization of nutrients instead of

unhealthy fat deposition (Adeghate et al., 2020; Sellayah et al., 2011). Consequently, chronic central administration of ORX increases food intake without affecting body weight (Yamanaka et al., 1999). This serves the key role of ORX in providing arousal on demand which is associated with increased metabolic needs.

A number of rodent studies confirm the protective effect of ORX on metabolic pathologies. Similar to narcoleptic patients, female ORX-deficient mice show higher body weight along with higher fat levels (Fujiki et al., 2006; Ramanathan and Siegel, 2014). Although male ORX knockout mice are of normal weight, animals of both sexes have lower metabolic rates and respiratory quotient as well as higher insulin resistance than control mice (Ramanathan and Siegel, 2014). Vice versa, ORX signaling is decreased in different rodent models of obesity. For instance, HFD induced obesity is accompanied by lower ORX serum levels and number of ORX neurons in the LH along with increased insulin resistance (Moslehi et al., 2021; Nobunaga et al., 2014). Further, two models of genetic obesity show reduced *Ppox* transcription in the LH (Yamamoto et al., 1999).

Mechanisms of Metabolic Regulation by the ORX System

Mechanistically, the ORX system acts as monitor of the overall metabolic state. While HFD dampens the ORX system, fasting enhances ORX signaling in humans and rodents (Almeneessier et al., 2018; Fujiki et al., 2001; Funabashi et al., 2009). Accordingly, signals of satiety such as glucose and leptin inhibit orexin neuron activity, while the appetite stimulating hormone ghrelin stimulates it (Yamanaka et al., 2003). Once activated, the ORX system modulates a variety of metabolic processes to ensure optimal energy expenditure. These include positive effects on lipid profile, insulin sensitivity and brown adipose tissue development and function(Goldstein et al., 2021; Sellayah et al., 2011; Zarifkar et al., 2017).

Sleep represents another possible mechanism via which the ORX system affects metabolism, since sleep disturbances highly associate with metabolic pathologies (St-Onge, 2017). In line with this idea, suvorexant, a dual ORX-R antagonist ameliorates sleep and glucose metabolism not only in a diabetic mouse model with sleep disruption but also in diabetic patients with comorbid insomnia (Toi et al., 2019; Tsuneki et al., 2016; Yoshikawa et al., 2020). However, research in the mouse model demonstrates that not all effects are sleep dependent by using different ORX-R antagonists: while some did not enhance REM sleep efficiency, they all improved glucose intolerance (Kon et al., 2019).

Open Questions Concerning the Role of ORX in Metabolic Regulation

Despite the consensus on the beneficial effects of ORX on metabolism, there still remain many unanswered questions. For instance, a study showed that ORX-R 1 and 2 in serotonergic neurons of the dorsal raphne have opposing effects on insulin sensitivity (Xiao et al., 2021). Further, ORX-R-deficient mice do not have a weight phenotype despite their deficiency in ORX signaling (Kakizaki et al., 2019). In fact, ORX-R1-deficient mice are even more reluctant to diet induced obesity (Kakizaki et al., 2019). This suggests that the strong metabolic phenotype in narcoleptic patients might not be solely mediated by ORX. Indeed, contrary to ORX-deficient mice, narcoleptic patients do not only lack the ORX peptide but the whole population of ORX neurons. Since ORX neurons co-express a range of other neurotransmitters and neuropeptides, these could equally contribute to the observed metabolic pathologies (Mickelsen et al., 2017). This is supported by observations in mice in which ORX neurons were ablated. In contrast to mice lacking the *Ppox* gene, the overweight phenotype of these mice manifests in both sexes (Fujiki et al., 2006; Hara et al., 2005, 2001). In addition, more recent evidence implicates dynorphin, a neuropeptide co-expressed in ORX neurons, in hedonic food intake (Mattar et al., 2020).

Interaction between the Circadian System and the ORX System in Metabolic Regulation

In the murine suvorexant studies, the drug was only given during the inactive phase (Kon et al., 2019; Tsuneki et al., 2016). Strikingly, when ORX-R antagonists were administered during the active phase, the positive effect on glucose metabolism vanished, which indicates a strong circadian component in ORX mediated metabolic regulation (Kon et al., 2019; Tsuneki et al., 2016). The connection to the circadian system was already evident in the early days of ORX research, when it was observed that chronic central ORX administration only increases food consumption during the day but not at night (Yamanaka et al., 1999). Further, despite having normal feeding rhythms, ORX-deficient mice lose the circadian variation of blood glucose (Tsuneki et al., 2015). Moreover, HFD induced obesity as well as obesity in *Clock-d19* mutant mice is accompanied by a loss of *Ppox* expression rhythms in the LH (Kohsaka et al., 2007; Turek et al., 2005). In line with the protective function of ORX against metabolic disease, ORX expression levels remained constantly low throughout the circadian cycle in both models (Kohsaka et al., 2007; Turek et al., 2005). Taken together, it is undebatable that the metabolic regulation by the ORX system underlies circadian gating. Still, whether the observed circadian gating of metabolic regulation by the ORX system is achieved by the master pacemaker or by local subordinate clocks in ORX neurons has not been investigated.

1.4. Summary

The circadian and the ORX system are both involved in the regulation of metabolic processes as well as mood and anxiety-related behavior. The circadian system consists of local subordinate clocks, which are present in nearly all cells of the body and are ruled by the SCN, the master pacemaker. In contrast, anatomical correlates of the ORX system in the mouse are not as well characterized. The major source of central ORX are ORX neurons of the LH which project throughout the entire brain. In humans and rats, ORX production in peripheral organs has been reported, while in the mouse many peripheral organs remain uninvestigated. Further, some studies suggest extra-hypothalamic expression of *Ppox* in the rodent brain, that have not been confirmed. The ignorance of the entity of ORX production sites impedes the interpretation of studies that target the ORX system as a whole, including Cre-loxP-based conditional knockouts using the *Ppox* promoter.

In the brain, a strong link between the circadian and the ORX system has been established. The circadian system induces rhythmicity of ORX signaling on different levels including *Ppox* expression, neuronal firing and ORX release into the CSF. This relationship is bidirectional since the ORX system directly signals to the SCN. Although it is undebated that ORX signaling underlies circadian regulation, it is unclear whether ORX rhythmicity depends on the master pacemaker or local subordinate clocks in ORX neurons. Similarly, although evidence support a contribution of ORX rhythmicity to a healthy metabolic and affective output, the role of subordinate clocks in ORX neurons in metabolic and affective regulation has not been investigated.

Figure 2 depicts the current knowledge on the relationship between the SCN and ORX neuron rhythmicity in affective and metabolic phentoypes in mice. In healthy Wt animals, both the SCN and ORX neurons display circadian rhythms that are synchronized to the external light-dark-cycle. In this scenario, it is not obvious whether ORX neuron rhythmicity depends on the external cues like the light-dark cycle (masking), the SCN or local subordinate clocks. In *Clock-d19* mice, all clocks throughout the entire body including the SCN and subordinate clocks in ORX neurons are disrupted which disables the synchronization of internal processes with the external environment and leads to an obese and manic phenotype. The loss of *Ppox* rhythms in these mice suggests, that ORX neuron rhythmicity is driven by the endogenous circadian clock and not the results of masking by the external light-dark cycle. However, in this model, it is not possible to draw conclusions regarding the contribution of the loss of circadian rhythms in ORX neurons to the observed phenotypes due to the overall disruption of the circadian clock. Further, it cannot be concluded, whether ORX neuron rhythmicity depends on the SCN or on local subordinate clocks. In mice who specifically lack the molecular clock in the master pacemaker, depression-like behavior and increased weight gain

is observed. There is no data on ORX neuron rhythmicity in these mice. However, the molecular clock is still present in ORX neurons of these mice which leads to the assumption, that ORX neuron rhythmicity might still be present but desynchronized with the environment. Finally, a mouse model in which exclusively the clock in ORX neurons is disabled would provide insights on whether ORX neuron rhythmicity depends on local subordinate clocks and whether the loss of this rhythmicity affects metabolic and affective phenotypes independent of the SCN.

A mouse line with in which the molecular clock is specifically lost in ORX neurons can be generated with the help of the Cre-loxP-system. In the classical approach, a *Ppox* Cre-driver line is bred with a line carrying two floxed alleles of *Bmal1*. In the progeny of these mice, the entity of *Ppox* expressing cells will be devoid of *Bmal1* expression throughout their entire development. Since, *Bmal1* has known developmental effects that are independent of its adult function as a clock gene, an additional experimental approach in which *Bmal1* deletion in ORX neurons takes place postnatally would be of great interest.

Figure 2 Current knowledge on the relationship between the SCN and ORX neuron rhythmicity in affective and metabolic phenotypes in mice. Green indicates the presences of molecular clocks, red signals the loss of molecular clocks and orange symbols desynchronized molecular clocks. In the healthy state both, the SCN and ORX neurons display circadian rhythms that are synchronized with the environment. In *Clock-d19* mice, all molecular clocks are dysfunctional including the ones in the SCN and ORX neurons. These mice display a manic and obese phenotype. Mice in which solely the molecular clocks in the SCN are ablated behave more depression-like and gain more weight. There is no data on ORX neuron rhythmicity in these mice. It is hypothesized that while still present, molecular clocks in ORX neurons in these mice are desynchronized with the environment. A mouse model in which the molecular clock is exclusively lost in ORX neurons has not been generated yet. Created with BioRender.com.

2. Hypotheses of this Thesis

The following hypotheses were investigated in this thesis:

(1) There are ORX producing cells outside of the LH in central and peripheral tissues of the mouse.

(2) Rhythmicity of ORX neurons of the LH depends on local subordinate clocks in ORX neurons.

(3) Disruption of local subordinate clocks in ORX neurons affects the mood- and anxiety-related behavior as well as metabolic phenotype in mice.

3. Aims and Objectives

In order to investigate the three working hypothesis of this thesis, the following aims and objectives were formulated:

(1) Characterization of the anatomical correlates of ORX production sites in the mouse.
- Detection and quantification of *Ppox* expression on the RNA level in central and peripheral tissues of the mouse using polymerase chain reaction (PCR) and quantitative polymerase chain reaction (qPCR).
- Visualization of ORX peptide and *Ppox* expressing cells in central and peripheral tissues of the mouse using immunohistochemistry in a lineage tracing experiment based on the Cre-loxP-system.

(2) Abolishment of the circadian clock in ORX neurons of the LH.
- Deletion of *Bmal1* expression specifically in ORX neurons of the LH by generating Orx-Bmal1$^{-/-}$ mice using the Cre-loxP-system.

(3) Examination of the dependence of *Ppox* expression rhythms on subordinate clocks in ORX neurons in the LH.
- Analysis of the expression rhythms of *Ppox* in the LH of Wt, Orx-Bmal1$^{-/-}$ mice and Cry1/2$^{-/-}$ mice using qPCR.

(4) Investigation of the effect of the loss of the circadian clock in ORX neurons on gene expression rhythms in the LH.
- Analysis of gene expression rhythms in the LH of Wt and Orx-Bmal1$^{-/-}$ mice using qPCR.

(5) Analysis of the impact of the loss of the circadian clock in ORX neurons of the LH on circadian, behavioral and metabolic phenotypes in mice.
- Analysis of rhythms of the SCN oscillator using the PER2::LUC system.
- Evaluation of locomotor activity rhythms under normal and constant conditions.
- Testing of Wt and Bmal1$^{-/-}$ mice in several behavioral paradigms for mood and anxiety-related behavior.

- Monitoring of the body weight of Wt and Orx-Bmal1$^{-/-}$ mice throughout their postnatal development.
- Measurement of metabolic activity using the metabolic cage system.

(6) Generation of a model for conditional postnatal loss of the circadian rhythmicity in ORX neurons of the LH in mice.

- Generation of a virus for conditional *Bmal1* knockdown based on the Cre-loxP-system.

4. Methods

4.1. Mouse Lines

4.1.1. Housing

Mice were housed in groups of up to 6 animals and separated according to sex unless stated otherwise. Mice were kept at 12:12 light-dark (LD) conditions. Lights turned on at 7 am (ZT0) and were switched off at 7 pm (ZT12). Water and food were available ad libitum. All experiments were conducted in accordance with the German Animal Protection Law and approved by the Government of Upper Bavaria.

4.1.2. ORX-Bmal1$^{-/-}$ Mice

The abbreviation Orx-Bmal1$^{-/-}$ refers to the genotype of *Orx-Cre* $^{tg/0}$ - *Bmal1*$^{fl/fl}$ – *Per2*^{Luc} $^{tg/tg}$ mice which were the result of breeding *Orx-Cre* mice (Matsuki et al., 2009) with *Per2*^{Luc} (Yoo et al., 2004) and *Bmal1-fl* mice (Storch et al., 2007). *Orx-Cre* mice were kindly provided by Prof. Roland Liblau, Toulouse, France; *Per2*^{Luc} mice were generously gifted by Prof. Michael Hastings, Cambridge, UK and *Bmal1-fl* mice by Prof. Henrik Oster, Lübeck, Germany. The *Orx-Cre* transgene consists of the coding sequence for the Cre recombinase under the control of the human *PPOX* promoter, which represents an area of 3.2 kb upstream of the human *PPOX* gene (Matsuki et al., 2009). In order to reduce possible adverse effects at the insertion site of the transgene, the *Orx-Cre* construct was kept heterozygous. Further, in all breedings the *Orx-Cre* transgene was passed on by the mother to avoid possible germline recombination due to *Ppox* expression in the testis (Joshi and Singh, 2017). In *Bmal1-fl* mice, the endogenous *Bmal1* gene is flanked by the loxP sequence thereby allowing its conditional knockout in *Cre* expressing cells (Storch et al., 2007). In *Per2*^{Luc} mice, the endogenous *Per2* gene is fused to the luciferase coding sequence, which results in the expression of a PER2::LUC fusion protein that enables the monitoring of circadian oscillations *ex vivo* (Yoo et al., 2004). The background of all lines is C57BL/6J mice. Except for the experiments investigating gene expression rhythms, Orx-Cre$^{tg/0}$ - Bmal1$^{fl/fl}$ -*Per2*^{Luc} $^{/tg}$ littermates were used as wildtype (Wt) control. In the assessment of gene expression rhythms, *Per2*^{Luc} mice were used as Wt control. Primers for genotyping are listed in **table 2**.

4.1.3. Cry1/2$^{-/-}$ Mice

Cry1/2$^{-/-}$ mice refer to C57BL/6J mice deficient for both *Cry* genes, *Cry1* and *Cry2* which were kindly provided by by Prof. Michael Hastings, Cambridge, UK (van der Horst et al., 1999). After breeding with *Per2*^{Luc} mice, they additionally carry the *Per2*^{Luc} transgene homozygously. Primers for genotyping are listed in **table 2**.

4.1.4. LSL-Cas9-Egfp Mice

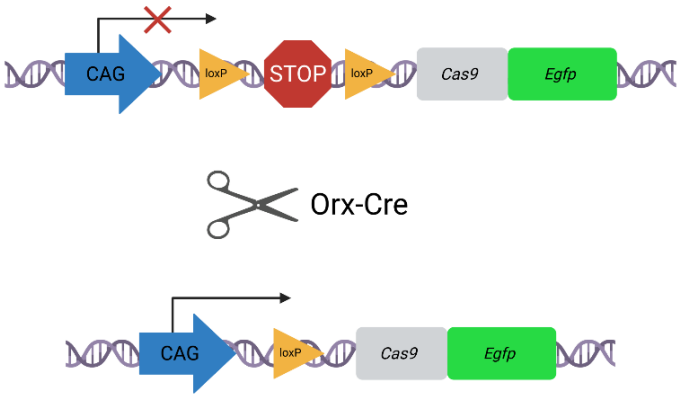

Figure 3 Schematic representation of the *LSL-Cas9-Egfp* transgene. Following Cre induced recombination, the stop sequence is excised and expression of *Cas9-Egfp* initiated. Created with BioRender.com.

LSL-Cas9-Egfp mice carry a transgene consisting of the sequence for 3x FLAG-tagged *Streptococcus pyogenes Cas9* which is linked via a self-cleaving P2A peptide to the enhanced *green fluorescent protein* (*Egfp*) gene (**figure 3**) (Platt et al., 2014). Expression is controlled by the CAG promoter followed by a floxed stop sequence (3x poly-A-signal), which disables expression of the CAS9-EGFP protein in the absence of a Cre recombinase (Platt et al., 2014). When Cre is present, the stop sequence is excised and *Cas9-Egfp* expressed. Hence, the EGFP signal enables the detection of Cre induced recombination which qualifies this line as Cre reporter line that can be used for lineage tracing experiments. Since the CAS9 protein is not able to act without a guide RNA, it does not affect the lineage tracing. The mice have a C57BL/6N genetic background and were kindly provided by Prof. Dr. Moritz Rossner, Munich, Germany. Primers for genotyping are listed in **table 2**.

4.2. Tissue Dissection

After immobilization with isofluorane, animals were sacrificed by cervical dislocation between 10 and 11 am (ZT3 to ZT4), unless stated otherwise. For the characterization of peripheral and central *Ppox* expression, three 21 weeks old male LSL-Cas9-Egfp mice were sacrificed. For the determination of circadian gene expression rhythms in the LH, for each combination of sex and genotype 3 to 8 adult mice (8 to 22 weeks) per time point were sacrificed. For *Per2*^{Luc} and Orx-Bmal1$^{-/-}$ mice, animals of both sexes were used. In case of Cry1/2$^{-/-}$ mice, only female animals were used due to limited availability. Peripheral organs and the cerebellum were snap frozen in liquid nitrogen immediately after sacrifice and stored at – 80 °C until RNA isolation. Fresh brains were cut with a Leica vibratome in 300 µm thin slices, in order to allow a more accurate dissection of relevant brain structures according to the Paxinos and Franklin mouse atlas (cortex: bregma 1.7 mm to -2.7 mm, hippocampus: bregma -1.06 mm to -2.7 mm, amygdala: bregma -0.7 mm to -2.06 mm, SCN: bregma -0.34 mm) (Paxinos and Franklin, 2019). In case of the LH, only the area containing ORX neurons was chosen (bregma -1.2 mm to -1.8 mm, **figure 4**) (Mickelsen et al., 2017). Dissected brain tissue was kept for one night in RNAlater™ (ThermoFisher scientific, Catalog no. AM7024) at 4 °C and was then stored at – 80 °C until further use.

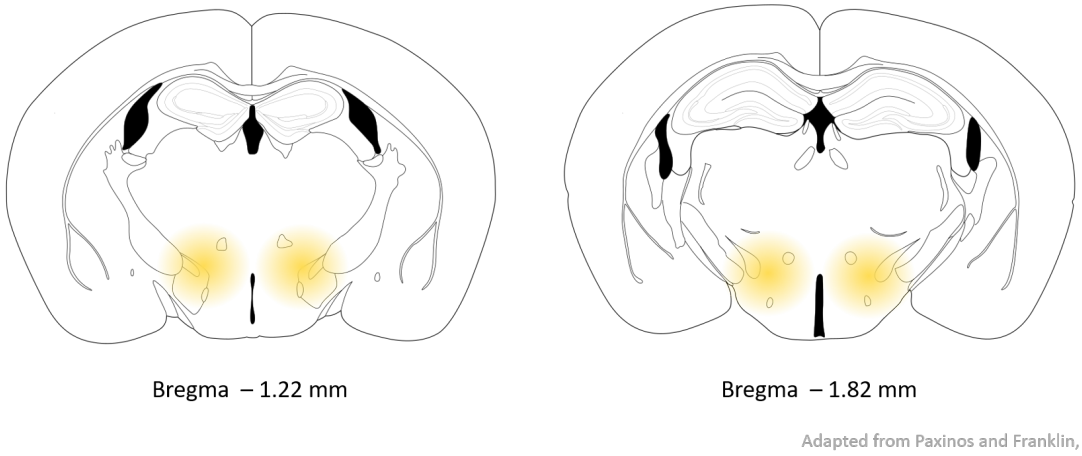

Figure 4 Schematic representation of the bregmata chosen for LH dissection. The yellow circles indicate the dissected area.

4.3. RNA Isolation and cDNA Synthesis

RNA was isolated using QIAzol Lysis Reagent (Qiagen, catalog no. 79306) and the RNeasy Mini Kit (Qiagen, catalog no. GR8RNA) including DNAse treatment (Qiagen, catalog no. 79254). Quality of RNA isolates was confirmed by gel electrophoresis with a 1 % agarose gel. The High-Capacity RNA-to-cDNA™ Kit (TermoFisher Scientific, catalog no. 4368813) was used to synthetize cDNA from 1 µg RNA along with random primers.

4.4. Polymerase Chain Reaction (PCR)

For PCR, the HotStarTaq *Plus* DNA Polymerase (Qiagen, catalog no. 203605) was used along with 1 µl of undiluted cDNA and the PCR primers listed in **table 2**. PCR products were visualized using gel electrophoresis with a 2 % agarose gel.

4.5. Quantitative PCR (qPCR)

For qPCR, cDNA was further diluted 1:20. All qPCR were run with the GoTaq® qPCR kit (Promega, catalog no. A6001) and the primers listed in **table 2**. The threshold for *Ppox* expression was set according to the exponential phase of the amplification curve of LH samples, since this is the major known source of *Ppox* expression. Primer efficiencies were determined with a standard curve using a mixture of all cDNA samples. Fold changes were calculated according to Pfaffl with the testis as reference organ for the assessment of peripheral and extra-hypothalamic *Ppox* expression (Pfaffl, 2001). For the analysis of gene expression rhythms in the LH, the mean expression across all circadian time points in Wt animals was used as reference.

Table 2 Primers used in this thesis. The Oligo ID refers to the documentation system used in this institute and is intended for internal use. The description stock primer refers to the stock of the institute of molecular neurobiology in Munich.

Name	Primer	Sequence	Application	Source	Oligo ID
Orx-Cre	Forward	TCCAATTTACTGACCGTACAC	Genotyping	(Ovchinnikov et al., 2000)	O2604
	Reverse	CATCAGCTACACCAGAGACGG	Genotyping	Inserm	O2605
Per2::Luc	Forward	CTGTGTTTACTGCGAGAGT	Genotyping	(Yoo et al., 2004)	O2064

	Reverse	GGGTCCATGTGATTAGAAAC	Genotyping		O2065
	Reverse	TAAAACCGGGAGGTAGATGAG	Genotyping		O2066
Bmal1-fl	Forward	ACTGGAAGTAACTTTATCAAACTG	Genotyping	Marius Stephan	O3462
	Forward	TTTACTGTGCTGCCTGTAG	Genotyping		O3463
	Reverse	CTGACCAACTTGCTAACAATTA	Genotyping		O3464
Cry1	Forward	CAGGAGGAGAAACTGACGCACT	Genotyping	(Anand et al., 2013)	O2057
	Reverse	GTGTCTGGCTAAATGGTGG	Genotyping		O2059
	Forward	GGGTGGCAAACTTTGAACGAC	Genotyping	Niels Jensen	O2258
	Reverse	GCATCGCCTTCTATCGCCTT	Genotyping	Niels Jensen	O2259
Cry2	Forward	CCAGAGACGGGAAATGTTCTTist	Genotyping	(Anand et al., 2013)	O2062
	Reverse	GAGATCAGCAGCCTCTGTTCC	Genotyping		O2061
	Reverse	GCTTCATCCACATCGGTAACTC	Genotyping		O2063
LSL-Cas9-Egfp	Forward	AAGGGAGCTGCAGTGGAGTA	Genotyping	oIMR9020 The Jackson Laboratory	O1982
	Reverse	CCTTTTGATAAGGCTGCAGAAGGAGC	Genotyping	Niels Jensen	O1991
	Forward	TGATTTGATACCGCGGGCCCTA	Genotyping	Niels Jensen	O2226
	Reverse	CCTTGTAGTCTCCGTCGTGGTCCTTAT	Genotyping	Niels Jensen	O2225
Ppox	Forward	TGTTCCTGCCGTCTCTACGAA	PCR	(Ventzke et al., 2019)	O3080
	Reverse	TGGTTACCGTTGGCCTGAA	PCR		O3081
Actinb	Forward	CCCTGAAGTACCCCATTGAA	PCR / qPCR	Dominic Landgraf	O3064
	Reverse	AGGTGTGGTGCCAGATCTTC	PCR / qPCR		O3065
Ppox	Forward	TTGGACCACTGCACTGAAGA	qPCR	(Kim et al., 2015)	O3583
	Reverse	CCCAGGGAACCTTTGTAGAAG	qPCR		O3584
Bmal1	Forward	CCTAATTCTCAGGGCAGCAGAT	qPCR	Dominic Landgraf	O3066
	Reverse	TCCAGTCTTGGCATCAATGAGT	qPCR		O3067
Pmch	Forward	GTCTGGCTGTAAAACCTTACCTC	qPCR	Nirmal Kannaiyan	O3583
	Reverse	CCTGAGCATGTCAAAATCTCTCC	qPCR		O3584
Per2	Forward	GCCAAGTTTGTGGAGTTCCTG	qPCR	Dominic Landgraf	O3074
	Reverse	CTTGCACCTTGACCAGGTAGG	qPCR		O3075
pSico_mU6	Forward	CGAAGGTACCGATCCGACGCGCCATCTCTAGG	Cloning	Charlotte Kling /Alexander Herholt	O2839
pSico_Xho1_Hpa1	Reverse	CGAAAAGCTTTCGTGAAGCGAGCTTATCGATACCG	Cloning	Charlotte Kling /Alexander Herholt	O2840
cPPT/CTS	Forward	ATTGGGGGGTACAGTGCAGGGG	Sequencing	Stock primer	O2838
WPRE-R	Reverse	CATAGCGTAAAAGGAGCAACA	Sequencing	Stock primer	O1105
EGFP-200bp-dummy_attB1	Forward	GGGGACAAGTTTGTACAAAAAAGCAGGCTATGGTGAGCAAGGGCGAGGAG	Sequencing	Stock primer	O1077
mU6-F	Forward	CAGCACAAAAGGAAACTCACC	Sequencing	Stock primer	O2101
CMVprom_5' rev	Reverse	CCTATTGGCGTTACTATG	Sequencing	Stock primer	O137

4.6. Immunohistochemistry and Imaging

Mice were perfused with 4 % paraformaldehyde (PFA) at 11 am (ZT4) and tissues were dissected. Samples were kept in PFA overnight, followed by a sequence of overnight incubations with phosphate-buffered saline (PBS), 15 % sucrose and 30 % sucrose. Finally, they were embedded in OCT embedding matrix (Roth, catalog. No 6478.1) and transferred to -80 °C. Tissues were cut into 14 µm sections and instantly collected onto object slides, which were stored at -80 °C until staining. In addition to the brain, the following tissues were immunohistochemically stained: adrenal glands, caecum, colon, heart, kidney, liver, muscle, pancreas, spleen, and stomach. Slides were air dried for 40 min and then rinsed with PBS. A permeabilization step with 0.2 % TritonX-100 (Sigma-Aldrich, catalog no. T8787) in PBS was followed by 1 h incubation with blocking solution (5 % bovine serum albumin (Sigma-Aldrich, catalog no. A3059), 0.1 % TritonX-100 in PBS) at room temperature (RT). Primary antibodies were diluted in blocking solution according to **table 3**. Primary antibody solution was applied to the slides and incubated over night at 4 °C. After several washing steps with PBS, secondary antibodies diluted in blocking solution according to **table 3** were applied for 2 h at RT. Following additional washing steps, sections were stained with diamidin-2-phenylindol (DAPI, 1:1000 in PBS and 0.1 % TritonX-100) before being mounted with EverBrite™ (Biotrend, catalog no. 23004). In case of peripheral organs, an additional heat induced antigen retrieval step was performed before blocking, which consisted of an incubation in sodium citrate buffer (10 mM tri-sodium citrate dihydrate, 0.05 % TWEEN®20 (Sigma-Aldrich, catalog no. P1379), ph = 6.0) over night at 60 °C. Stainings were imaged with a 20x objective using a ZEISS Axio Observer Z1 microscope and the ZEISS ZEN blue software. Images were processes with Fiji/ImageJ (Schindelin et al., 2012).

Table 3 Antibodies used in this thesis.

Antigen	Source	Catalog Number	Dilution
ORX-A	Abcam	ab6214	1:1000
ORX-B	Invitrogen	PA5-78389	1:600
GFP	abm	G095	1:500
Alexa 594 anti-rabbit	Dianova	711-585-152	1:500
Alexa 488 anti-goat	Abcam	ab150129	1:500

4.7. Behavioral Tests

A cohort of 26 Orx-Bmal1$^{-/-}$ (15 females and 11 males) and 20 Wt (9 females and 11 males) mice underwent a sequence of behavioral tests when they turned 8 weeks of age (**figure 5**). Open field test (OFT), elevated plus maze (EPM), light dark test (LDT) and tail suspension test (TST) were conducted within the first week of testing on consecutive days. Testing of the prepulse inhibition of the startle reflex (PPI) took place in the second week of testing, followed by one week without any tests. In the following week, the learned helplessness paradigm (LHP) was started which took a total of two weeks until all animals were tested. For all experiments, animals were left to habituate for 10 min in the experimental room before starting the test and the apparatus was thoroughly cleaned with 5 % sodium dodecyl sulfate in water, water and ethanol between mice. The mice were left to recover for 16 weeks until the sucrose preference test (SPT) was performed, followed by the assessment of locomotor activity rhythms in the IntelliCage system.

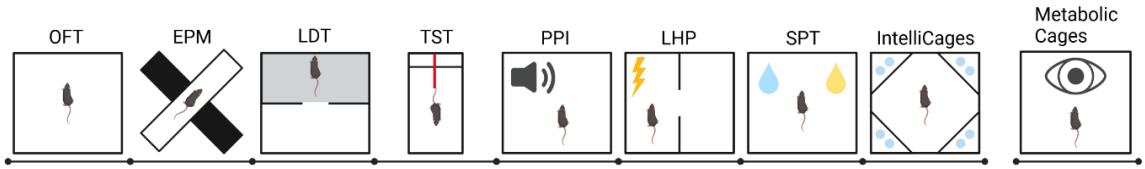

Figure 5 Sequence of behavioral tests and metabolic assessment. One cohort of Orx-Bmal1$^{-/-}$ and Wt mice of both sexes was subjected to a series of behavioral tests. A separate cohort was investigated using the metabolic cage system. OFT = Open field test; EPM = elevated plus maze; LDT = light dark test; TST = tail suspension test; PPI = prepulse inhibition; LHP = learned helplessness paradigm; SPT = sucrose preference test. Created with BioRender.com.

4.7.1. Open Field Test (OFT)

The OFT was used to assess anxiety-related behavior. Mice were left to freely explore an open field surrounded by high walls. In this test, time spent in the proximity of the corners or the walls (periphery) represents more anxious behavior, while entering the unprotected center is interpreted as less anxious behavior (Prut and Belzung, 2003). At the start of the experiment, mice were placed into the open field box facing the wall and video recorded for 10 min. Time spent in the periphery, center and corner was analyzed automatically with the ANY-maze tracking software (Stoelting). All animals were tested between ZT2 and ZT7 of the same day with a light intensity between 1500 and 1700 lux.

4.7.2. Elevated Plus Maze (EPM)

Animals were tested for anxiety in the EPM. In this test, animals are positioned onto an elevated platform in the shape of a plus. Two arms of the plus are closed and two arms are open. At the start of the experiment, mice are placed into the center of the maze facing the open arm and video recorded for 10 min. Tendency to spend time the closed arm correlates with more anxious behavior, while time spent in the open arm is associated with less anxiety (Walf and Frye, 2007). Time spent in the open and closed arm as well as the center was measured automatically using the ANY-maze tracking software (Stoelting). All animals were tested on consecutive days between ZT2 and ZT7 with a light intensity between 10 and 30 lux.

4.7.3. Light Dark Test (LDT)

The LDT was used to examine anxiety-related behavior. In the LDT, mice are exposed to a test arena with a closed dark compartment and an open light compartment. Tendency of the mice to spend more time in the light compartment reflects lower anxiety while preference of the dark compartment is associated with more anxiety (Bourin and Hascoët, 2003). Animals were placed in the dark compartment facing the wall away from the light compartment at the start of the experiment. Movement between the two compartments was recorded for 10 min and videos were manually analyzed regarding time spent in each compartment and latency to first enter the light compartment. All animals were tested between ZT1 and ZT8 of the same day with a light intensity between 800 and 900 lux.

4.7.4. Tail Suspension Test (TST)

The TST was used to test for depression-like behavior. Mice were suspended approximately 30 cm above an even surface by attaching adhesive tape to their tails. Plastic caps were placed around the tail to prevent the mice from climbing up during the experiment. Time immobile and mobile was measured for 6 min via video recording and assessed using the ANY-maze tracking software (Stoelting). In this test, time spent immobile in response to this unescapable stressful situation correlates with a lower motivation to escape, hence more depression-like behavior (Cryan et al., 2005). In contrast longer times of mobility reflect high motivation to escape and less depression-

like behavior (Cryan et al., 2005). All animals were tested between ZT2 and ZT6 of the same day with a light intensity between 1500 and 1700 lux.

4.7.5. Prepulse Inhibition (PPI)

The term PPI describes the inhibition of the startle reflex in response to a stimulus (pulse), when this main pulse has been preceded by a prepulse (Geyer et al., 2002). Since PPI is impaired in patients with schizophrenia, the test is used to assess a schizophrenia-like phenotype in mice (Geyer et al., 2002; Sato, 2020). The PPI of the startle response was investigated by measuring the amplitude of movement-induced vibration of the base plate in startle-response-enclosures using the SR-Lab system and software (San Diego Instruments). Mice were habituated to the apparatus during two consecutive days for 10 min each at 65 dB of the background noise present during the testing. On the test day, the paradigm started with a short time habituation of 10 times 40 ms of the 115 dB main pulse. This was followed by 10 trials of PPI for each prepulse level (70, 75, 80 or 85 dB). One trial consisted of 20 ms prepulse, 100 ms inter pulse interval and 40 ms main pulse. The PPI trials were randomly mixed with 10 trials each of 40 ms main pulse only and 20 ms of the 85 dB prepulse. The relative startle response of each animal at each dB level was calculated using the formula below, in which the baseline equals the mean baseline startle response during the main pulse only trials.

$$\text{Relative startle response}_{\text{x dB}} = \frac{mean(Amplitude\ x\ dB)}{Baseline}$$

$$\text{PPI}_{\text{x dB}} = 1 - \text{Relative startle response}_{\text{x dB}}$$

4.7.6. Learned Helplessness Paradigm (LHP)

The LHP was performed as described before in order to test for helpless behavior in response to an uncontrollable stress, which reflects depression-like behavior (Landgraf et al., 2015). The paradigm consists of two consecutive days of training and one final day of testing. Training was performed between ZT5 and ZT9 while testing was carried out between ZT3 and ZT7. Training times were kept constant for each animal, while testing time differed in order to avoid temporal association. Due to the large sample size, animals were trained and tested during two consecutive weeks. During training, mice were placed in restraining tubes and exposed to an unavoidable series of electric

shocks. Within 60 min, 120 electrical shocks that were gradually increased every 15 shocks (0.25 to 0.6 mA) and lasted 5 s each, were applied with random intertrial interval length (20-30 s). On the testing day, mice were put into shuttle boxes (Panlab Harvard Apparatus) with two chambers separated by an automatic sliding gate. 30 electrical shocks of 0.1 mA were applied for 30 s through a metallic grid on the floor. The mice could terminate the shocks prematurely by moving through the gate into the adjacent chamber. The testing consisted of two phases, fixed ratio (FR) 1 and 2. During FR1 animals had to cross the gate once to end the shock, while during FR2 they had to cross twice. 5 trials of FR1 were followed by 25 trials of FR2. The gate remained closed between trials. A trial was considered as failed, when the mouse did not end the shock within the 30 s. Latency to escape the shock as well as failures during FR2 were recorded automatically by the ShutAvoid software (Panlab Harvard Apparatus). On a separate day, the individual pain threshold of each animal was determined by applying increasingly higher electric shocks until the animal jumped.

4.7.7. The IntelliCage System

The IntelliCage system and software (TSE-Systems GmbH) were used for the assessment of locomotor activity rhythms and the SPT. These cages consist of four corners equipped with two drinking bottles each, which are place behind a gate. Mice can access the fluid by poking the gate with their nose. Animals are implanted with a subcutaneous RFID transponder which is recognized in the corner and enables the tracking of corner visits, nose pokes and licks for each individual mouse. For this surgery, mice were anesthetized using isofluorane. Eyes were protected from drying out by application of Dexpanthenol ointment. Hair was removed from the dorsocervical area and skin was sterilized with 70 % ethanol before opening of the skin and implantation of the RFID transponder. The opening was stitched up and the mice were given several days to recover before entering the IntelliCages. Surgery was performed by Jessica Bly. One cage holds space for up to 16 mice allowing the measurement of behavior in their familiar social group. The measurement was preceded by a habituation time of 2 days allowing the mice to get used to their new environment.

4.7.7.1. SPT

For the SPT, one of the two bottles in each corner was filled with 1 % sucrose solution in water. In this experiment, gates were kept open and mice were able to freely chose between the sucrose

solution and autoclaved tap water for 24 h. A preference score was calculated for each animal based on the number of licks on the respective bottle according to this formula:

$(Licks_{Sucrose} - Licks_{Water}) / (Licks_{Sucrose} + Licks_{Water})$

Preference for sugar over water is interpreted as increased hedonistic behavior. In the graphs depicting the 24 h consumption of sucrose and water, licks were summarized across 30 minutes.

4.7.7.2. Activity Measurements

Corner visits of each mouse across the circadian cycle were used as a correlate of locomotor activity in order to investigate circadian rhythms of rest-wake behavior. Mice were first recorded for 7 days in 12:12 LD conditions followed by 14 days in constant darkness. Since mice tend to stay for longer period in the corners, only the start of the corner visit was documented as one event.

4.8. Vaginal Smears

Mice were restrained and the opening of the vaginal canal was gently flushed with PBS. The liquid was collected onto object slides and left to dry. Smears were stained for 30 s with Wright-Giemsa stain (Sigma-Aldrich, catalog no. WG32-1L) and then washed for 3 min in deionized water followed by a brief rinse with deionized water. The smears were then left to dry before investigation under the microscope.

4.9. Body Weight Measurement

The cohort of Wt and Orx-Bmal1$^{-/-}$ mice that underwent behavioral testing was weighed once a week from the moment they were weaned (3 weeks of age). The weighing was performed every week on the same day of the week and at the same time (ZT7 to ZT8) until the mice reached 22 weeks of age.

4.10. Luciferase Assays in Organotypic SCN Slices

The cohort of Wt and Orx-Bmal1$^{-/-}$ mice that underwent behavioral testing and was monitored for their body weight, was sacrificed at 32 to 34 weeks of age and processed for bioluminescence recording of the Per2^{Luc} transgene in organotypic SCN slices. They were immobilized with isoflurane and subsequently sacrificed by cervical dislocation. Brains were immediately dissected and transferred to a half-frozen PBS solution. A Leica vibratome was used to cut the brain into 300 µm thin organotypic slices. The brains were kept in ice cold PBS throughout the whole procedure. The SCN was dissected using a pair of extra thin scissors and transferred to tissue culture inserts (Millicell Cell Culture Inserts, 30 mm, Millipore, catalog no. PICMORG50) in 35 mm petri dishes containing explant media [DMEM (Corning®, catalog no. 90-013-PB), 4 mM sodium bicarbonate (Sigma-Aldrich, catalog no. S8761), 10 mM HEPES (PAN-Biotech, catalog no. P05-01100), 52 U/ml penicillin, 52 µg/ml streptomycin, 4 mM L-glutamine, 2 % B-27™ Supplement (50x, Gibco™, catalog no. 17504044), 1 mM luciferin (PJK GmbH, catalog no. 102111)]. The dishes were covered with glass cover slips and sealed with silicon grease before entering a LumiCycle™ luminometer (Actimetrics) in which luciferase activity was measured every 10 min at 37 °C and in unmodified room air. Luciferase signaling was measured for seven days.

4.11. Metabolic Cages

A separate cohort of 8 Orx-Bmal1$^{-/-}$ (4 females and 4 males) and 8 Wt (4 females and 4 males) mice between the age of 8 to 12 weeks was analyzed using the metabolic cage system. The PhenoMaster system and software (TSE-Systems GmbH) was used to continuously monitor locomotor activity, food and water consumption as well as the respiratory exchange rate (RER, $\frac{\mathrm{VCO2\ [ml/h/kg]}}{\mathrm{VO2[ml/h/kg]}}$). Activity, food and water consumption were summed up across 15 min while the RER was determined once every 15 min. Mice were single housed at a 12:12 LD cycle during the experiment and given 3 days to habituate to the new environment. For analysis, only the 4th day was considered.

4.12. Cloning

4.12.1. Cloning of pSico into Adeno-Associated Virus Backbone

Cre dependent knockdown of *Bmal1* was based on the commercially available plasmid pSico (Addgene, catalog no. 11578) (Ventura et al., 2004). In this construct, the sequence of the murine U6 promoter is interrupted by the floxed coding sequence for *Egfp* driven by the CMV promoter. Upon recombination, the sequence of the U6 promoter is unified and initiates the expression of subsequent short hairpin RNAs (shRNA) targeting *Bmal1* (**figure 6**). In order to clone the U6 construct into a backbone for adeno-associated viruses (AAV), it was isolated using the primers O2839 and O2840 along with adding Kpn1 and Hind3 restriction sites. PCR was performed using 400 nM of each primer, 1 ng pSico and the PWO polymerase (Roche, catalog no. 3789403001). The PCR product was purified by gel electrophoresis and subsequent clean up with the NucleoSpin Gel and PCR Clean-up kit (Machery-Nagel, catalog no. 740.609.50). The PCR product and the vector V824 containing the AAV backbone were digested with the restriction enzymes Kpn1-HF (New England BioLabs, catalog no. R3142L) and Hind3-HF (New England BioLabs, catalog no. R3104L) for 12 h at 37 °C. After digestion, the fragments of V824 were separated by gel electrophoresis with a 1 % agarose gel and the largest fragment of 4389 bp was isolated and purified using the NucleoSpin Gel and PCR Clean-up kit (Machery-Nagel, catalog no. 740.609.50). The U6 construct and the V824 AAV backbone were ligated using the T4 DNA ligase (NewEngland BioLabs, catalog no. M0202L) and vector-insert-ratio of 1:3 for 1 h at RT followed by 4 °C overnight. The pSico-AAV plasmid was amplified by heat shock transformation (42 s at 42 °C and 2 min on ice) into self-made Mach1 bacterial cells. Single clones were grown in liquid lysogeny broth (LB) medium cultures and 200

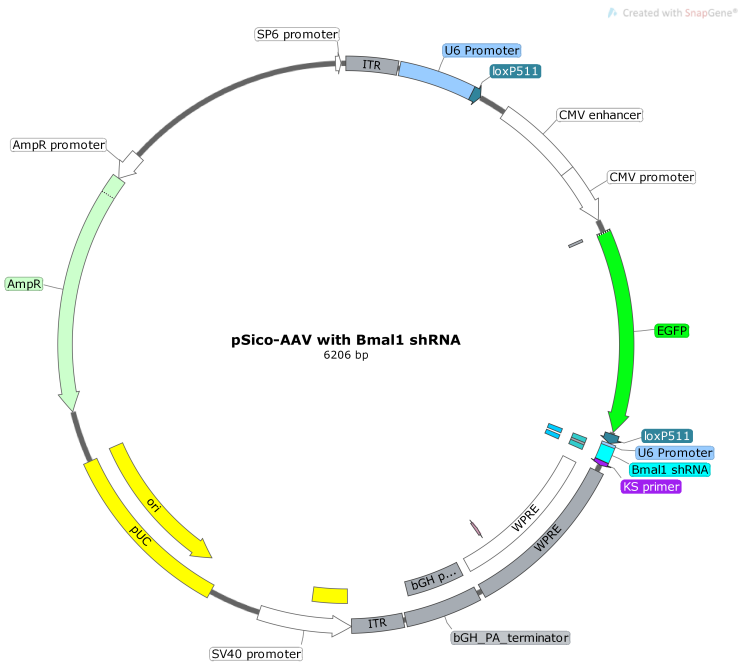

Figure 6 Vector map of the pSICO-AAV with inserted shRNA targeting *Bmal1*. Blue shows the two separated parts of the U6 promoter. In between, there is the coding sequence for *Egfp* in green under the control of the CMV promoter (white). The two loxP sites (loxP511) are marked in dark turquoise, while the inserted shRNA is pictured in cyan. All other elements are either required for the bacterial amplification or virus production.

μg/ml ampicillin (Sigma-Aldrich, catalog no. A9518-5G). Plasmid DNA was isolated using the NucleoSpin Plasmid kit (Machery-Nagel, catalog no. 740588.250). Sequence identity was confirmed after each step by sequencing with the primers O2838, O1105, O1077, O2101, O137 listed in **table 2** (Eurofins Genomics).

4.12.2. Insertion of shRNA into pSico-AAV

Short RNAs (shRNAs) for the RNA interference mediated knockdown of gene expression were purchased form Eurofins Genomics (**table 4**). Ligation was performed with the T4 Ligase (New England BioLabs, catalog no. M0202L) for 3 min at 90°C followed by 2 h at room temperature. The pSico-AAV plasmid was opened for shRNA insertion by digestion with the restriction enzymes Hpa1 (New England BioLabs, catalog no. R0105S) and Xho1 (New England, BioLabs, catalog no. R0146S) for 12 h at 37 °C, followed by gel electrophoresis and gel clean up (NucleoSpin Gel and PCR Clean-up kit (Machery-Nagel, catalog no. 740.609.50)). Ligation of the different shRNAs with the pSico-AAV plasmid was achieved using the T4 ligase (New England BioLabs, catalog no. M0202L) for 1 h at RT followed by 4 °C overnight and a vector- insert-ratio of 1:10. In total, four plasmids with different shRNAs were generated, of which two target *Bmal1* and two have no known murine targets and served as controls (scrambled shRNAs) (Landgraf et al., 2016a). The final plasmids of pSico-AAV with the different shRNAs were amplified by heat shock transformation (42 s at 42 °C and 2 min on ice) into self-made Mach1 bacterial cells. Single clones were grown in liquid LB medium cultures and 200 μg/ml ampicillin (Sigma-Aldrich, catalog no. A9518-5G). Plasmid DNA was isolated using the (Machery-Nagel, catalog no. 740588.250). Sequence identity of the shRNAs was confirmed by sequencing using the primer O1105 (Eurofins Genomics) (**table 2**).

Table 4 ShRNA used in this thesis.

Name	Target	Strand	Sequence	Oligo ID	Virus ID
Bmal1 shRNA 1	*Bmal1*	Sense	TGTCGATGGTTCAGTTTCATTTCAAGAGAATGAAACTGAACCATCGACTTTTTTC	O2920	A384
		Antisense	TCGAGAAAAAAGTCGATGGTTCAGTTTCATTCTCTTGAAATGAAACTGAACCATCGACA	O2921	
Bmal1 shRNA 2	*Bmal1*	Sense	TGCATCGATATGATAGATAATTCAAGAGATTATCTATCATATCGATGCTTTTTTC	O2922	A385
		Antisense	TCGAGAAAAAAGCATCGATATGATAGATAATCTCTTGAATTATCTATCATATCGATGCA	O2923	
SCR shRNA 1	None	Sense	TGCAACAAGATGAAGAGCACTTCAAGAGAGTGCTCTTCATCTTGTTGCTTTTTTC	O2924	A386
		Antisense	TCGAGAAAAAAGCAACAAGATGAAGAGCACTCTCTTGAAGTGCTCTTCATCTTGTTGCA	O2925	
SCR shRNA 2	None	Sense	TGCGCTTAGCTGTAGGATTCTTCAAGAGAGAATCCTACAGCTAAGCGCTTTTTTC	O2926	A383
		Antisense	TCGAGAAAAAAGCGCTTAGCTGTAGGATTCTCTCTTGAAGAATCCTACAGCTAAGCGCA	O2927	

4.13. Virus Generation

Virus generation was performed in 293FT cells (Invitrogen, catalog no. R70007) in HEK culture medium [DMEM (4.5 g/l Glucose), 10 % FBS, 1% Glutamax (Gibco, catalog no. 35050-038)] on poly-L-lysine coated dishes. The plasmids of pSico-AAV with the different shRNA were transfected along with the AAV packaging plasmids pFΔ6, pRV1, pH21 using OptiMEM (LifeTech, catalog no. 504730) and polyethylenimine (Polysciences, catalog no. 23966-2). Cells were incubated with the plasmid mixture for 3 days at 37°C and then harvested using lysis buffer. The lysate was 3 times frozen for 20 min at -80 °C and thawed in a 37°C water bath. After 30 min of benzonase (Sigma-Aldrich, catalog no. E1015-5KU) treatment at 37 °C in a water bath, the suspension was centrifuged for 10 min at 3,000 rpm and the supernatant collected and filtered using 0.45 µm filter units (Millipore, catalog no. SLHA033SS). The virus was further enriched by centrifugation at 3,000 rpm using ultra-15 centrifugal filter units (100kDa, Amicon, catalog no. UFC910024). The AAV IDs referring to the corresponding shRNAs are listed in **table 4**. Virus generation was carried out by Beate Kauschat.

4.14. Luciferase Assays in Primary Neurons

AAVs A383 to A386 were tested in primary neurons of mice carrying the *Per2*^{Luc} reporter construct. On day *in vitro* (DIV) 0, cells were dissected from the cortex of E15.5 embryonic pups. Cells were singularized using papain treatment (Cell Systems, catalog no. LS003126) and trituration by pipetting. Cells were suspended in plating medium [Neurobasal medium (Gibco™, catalog no. 12348017), 2% B-27™ Supplement (50x, Gibco™, catalog no. 17504044), 1% Glutamax (Gibco™ catalog no. 35050-038)] and seeded on poly-d-lysine coated dishes. On DIV 1, plating medium was replaced by culture medium [Neurobasal medium, 2% B-27™ Supplement (50x, Gibco™, catalog no. 17504044), 1% Glutamax (Gibco™, catalog no. 35050-038)]. In all experiments, lentiviral infection of L31-2 was done along with the media change at DIV 1 and AAV infection was combined with feeding the cells at DIV 5. The condition "*Bmal1* shRNA" refers to an equimolar mixture of A384 and A385 and "scrambled shRNA" to an equimolar mixture of A383 and A386. On DIV 8, cells were pulsed with 10 µM forskolin (Tocris Bioscience, catalog no. 1099) for 2 h. Since primary neurons are highly dependent on cellular factors secreted into the media, only half of the media was replaced by forskolin containing fresh media. The removed media was mixed with fresh phenol red free culture media with 0.1 mM luciferin (PJK GmbH, catalog no. 102111) and was reapplied after the pulse. Plastic lids were replaced by thin glass lids that were attached with parafilm.

Luciferase signaling was measured in 10 min intervals using a LumiCycle™ luminometer (Actimetrics) in an incubator with 5 % CO_2 at 37 °C.

4.15. Statistical Analysis

Statistical analysis was done in R. Outlier detection was done using the Grubbs' test and a maximum of one outlier per genotype independent of sex was identified for each investigated parameter. In experimental set ups, were the circadian phase or circadian time points were taken into account, a maximum of one outlier per genotype per phase or time point were determined independent of sex. Outliers were excluded from further analysis. The impact of genotype, sex, ZT, circadian phase and their interactions on any given variable were investigated using analysis of variance (ANOVA). Since ANOVA is considered robust towards violations of normality, only the normality of the residuals of the linear model was inspected using quantile-quantile plots. All investigated variables showed normal distribution of the residuals in the linear model and allowed the application of ANOVA. Further significance was assessed using post-hoc pairwise t-test. Within one analysis, bonferroni correction was used to correct for multiple testing. Data was visualized using the R package ggplot2.

4.16. Rhythmicity Analysis

4.16.1. Gene Expression Data

Rhythmicity across the circadian cycle was determined using cosinor analysis with a period of 24 h using the *cosinor.lm* function from the R package *cosinor*. The function *cosinor.detect* from the R package cosinor2 was used to test for rhythmicity based on the zero-amplitude test. In this test, the null hypothesis is the absence of a rhythm and the alternative hypothesis the presence of a rhythm (Cornelissen, 2014). Expression data and the respective cosinor fit were plotted together using *ggplot.cosinor.lm* (cosinor package). ZT1 is plotted twice (ZT25) but the cosinor fit was only performed for ZT1, ZT7, ZT13 and ZT19.

4.16.2. IntelliCage and Metabolic Cage Data

Activity, drinking, feeding and calorimetry data from the metabolic cages and the IntelliCages were analyzed using the R package rethomics (Geissmann et al., 2019). The group averages across the 24 h circadian cycle were done using the function *ggetho* and *stat_pop_etho* with summary_time_window=mins(30) and default settings. For the metabolic cages, this results in the mean of two measurement intervals of 15 min each. In case of the IntelliCages the recording of visits is not based on a regular sampling interval but on single events at second resolution. Since the package requires a continuous time scale in seconds, the start of each visit was matched to a time line of the experiment in seconds as an event of 1. All time points at which no visit took place, were documented as an event of 0. Due to the second time scale, there were relatively more seconds when there was no visit happening, which lead to very small means across 30 min for the IntelliCages. Therefore, visits were multiplied with 1800 in order to plot the total visits in 30 minutes. Lomb-Scargle periodograms were calculated using the function *periodogram* with resample_rate = 1 (IntelliCage) and 1/mins(15) (Metabolic Cages). The period with the highest power was extracted for each animal. Visualization of periodograms was done using the function *ggperio*.

4.16.3. LumiCycler Data

PER2::LUC measurements of organotypic slices and primary neurons were obtained in the LumiCycle™ luminometer (Actimetrics) and analyzed using the corresponding LumiCycle™ software (Actimetrics). For all recordings, the first 24 h of recording were dismissed. In case of the SCN organotypic slices, 5 days were analyzed while for the primary neuron experiments 4 days were analyzed. The analyzed time window was kept identical between samples of one experiment day. On each experiment day, the start of analysis was the first real trough after the discarded first 24 h. The amplitude was determined using the LM Fit (Sin) setting. Since the amplitude is influenced by the amount of cells in the dish or organotypic slices, the amplitude was normalized to the number of cells, by dividing the amplitude by the average bioluminescence of each dish across the analyzed time frame (Welsh and Noguchi, 2012). The period was determined using the Sin Fit (Damped) setting.

5. Results

5.1. *Orx-Cre* Construct Validation

In this thesis, the abolishment of *Bmal1* expression in ORX neurons of the LH depends on the cell-specific expression of the *Orx-Cre* transgene in *Ppox* expressing cells. In order to ensure the cell-specificity for all following experiments, the expression pattern of the *Orx-Cre* transgene was validated in the founder animals of the *Orx-Cre* line in our laboratory. Therefore, *Orx-Cre* mice were bred with LSL-Cas9-Egfp mice, which serve as a Cre reporter line in order to perform a lineage tracing experiment. In Cre reporter lines, Cre induced recombination leads to the expression of a reporter gene such as *Egfp* (**figure 3**). As a consequence, all cells that have expressed the *Orx-Cre* transgene at any given time point of their development, are labelled with EGFP. Since this also includes cells, that originate from cells expressing the *Ppox* promoter, this kind of experiment is called lineage tracing.

There was extensive ectopic *Orx-Cre* expression in the progeny of one homozygous *Orx-Cre* mouse. In addition to the LH, EGFP was found throughout the hypothalamus, including the entire SCN (**figure 7**). Further EGFP positive cells were present in the hippocampus, cortex and cerebellum (**figure 8**). While EGFP positive cells in the LH additionally stained for ORX, none of the *Egfp* expressing cells in any of the other brain regions co-labelled for ORX (**figure 8**). The ectopic expression was strongly reduced in offspring from heterozygous *Orx-Cre* founder animals that had been further bred with $Per2^{Luc}$ mice during the generation of Orx-Bmal1$^{-/-}$ mice (data not shown). Animals of the final Orx-Bmal1$^{-/-}$ line were checked again for cell-specific *Orx-Cre* expression by

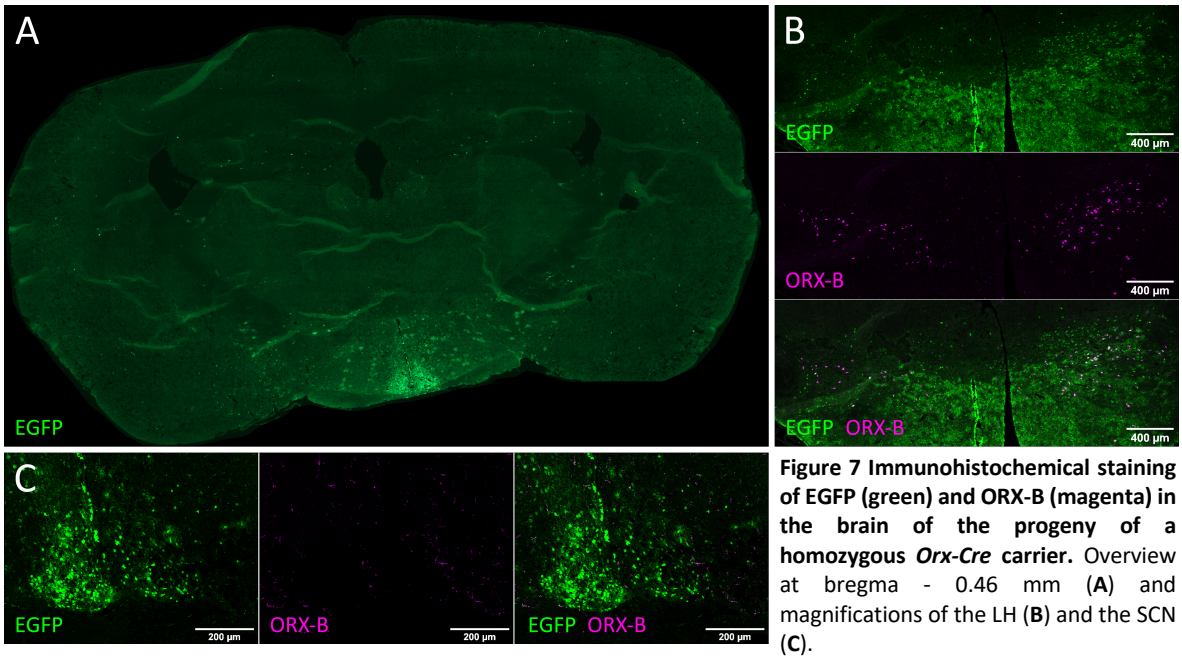

Figure 7 Immunohistochemical staining of EGFP (green) and ORX-B (magenta) in the brain of the progeny of a homozygous *Orx-Cre* carrier. Overview at bregma - 0.46 mm (**A**) and magnifications of the LH (**B**) and the SCN (**C**).

breeding with LSL-Cas9-EGFP mice. In these animals, there were only very sparse EGFP labelled cells in the hippocampus, cortex and cerebellum while the SCN was devoid of any *Egfp* expression (**figure 9**). In the LH, *Orx-Cre* expression was restricted to ORX neurons although the overlap was not complete, leaving cells exclusively stained for ORX-A but not EGFP. Further, while EGFP was restricted to the soma of cells, ORX-A additionally labelled projections of ORX neurons (**figure 10**).Projections can be visually distinguished from somas, since they do not have a nucleus but localize in between nuclei. Although the staining for ORX-A revealed projections throughout the entire brain, somas were exclusively found in the LH.

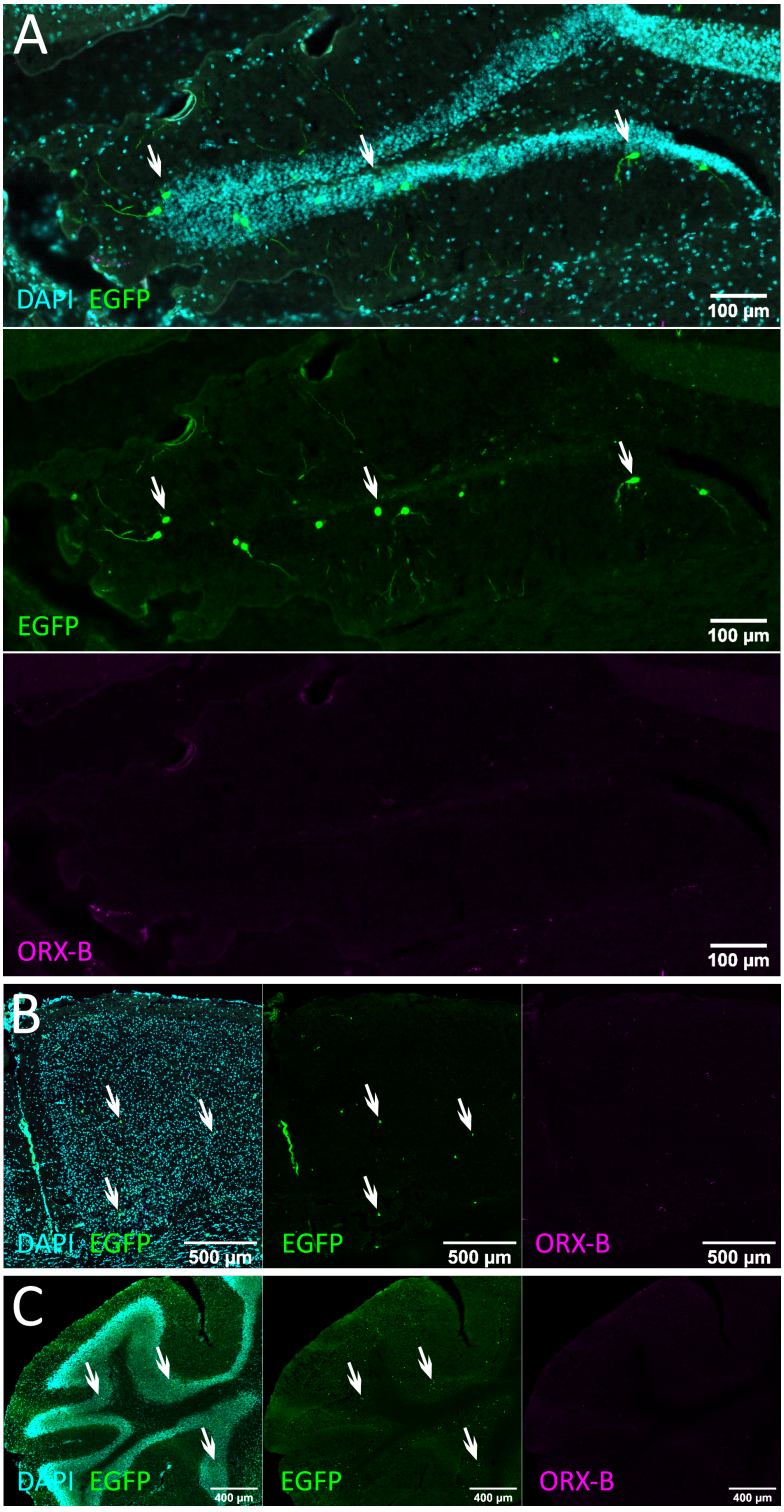

Figure 8 Immunohistochemical staining of EGFP (green) and ORX-B (magenta) in the brain of the progeny of a homozygous Orx-Cre *carrier*. Magnifications of the hippocampus (**A**), cortex (**B**) and the cerebellum (**C**). The white arrows indicate exemplary somas stained with EGFP. Nuclei were visualized by staining with DAPI (cyan).

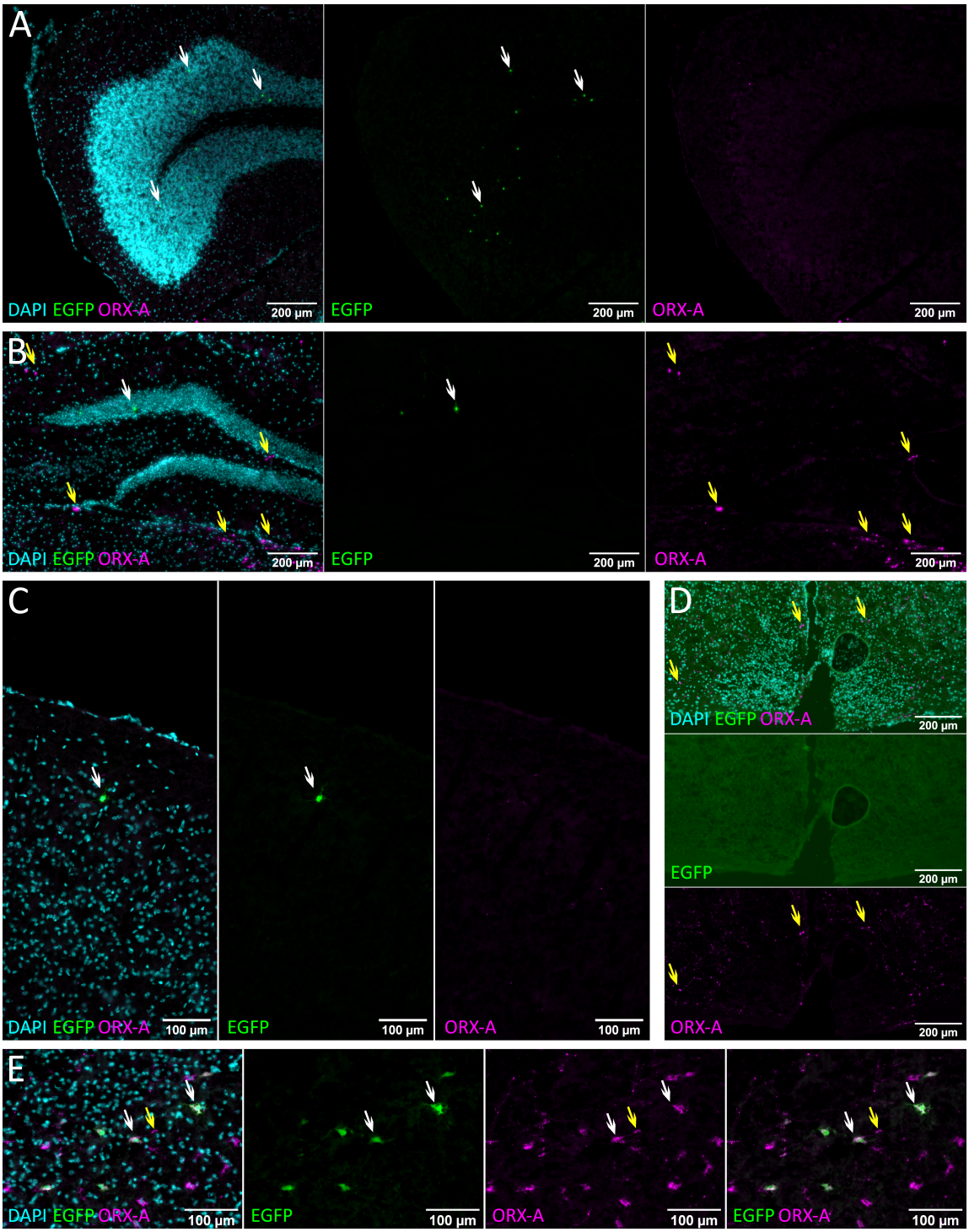

Figure 9 Immunohistochemical staining of EGFP (green) and ORX-A (magenta) in the brain of progeny of a heterozygous *Orx-Cre* carrier of the final Orx-Bmal1$^{-/-}$ line. Magnifications of the cerebellum (**A**), hippocampus (**B**), cortex (**C**), SCN (**D**) and LH (**E**). Arrows indicate examples of stained somas (white) and projections (yellow). Nuclei were visualized by staining with DAPI (cyan).

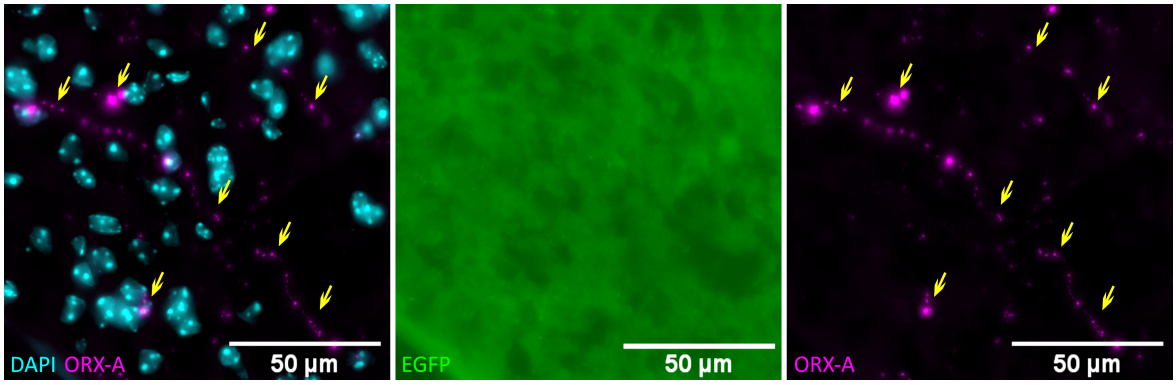

Figure 10 Projections of ORX neurons in the brain of progeny of a heterozygous *Orx-Cre* carrier of the final Orx-Bmal1$^{-/-}$ line. Immunohistochemical staining of ORX-A (magenta) and EGFP (green). Nuclei were visualized by staining with DAPI (cyan). Yellow arrows indicate examples of stained projections.

5.2. Characterization of Central and Peripheral *Ppox* Expression

Several studies report *Ppox* expression in peripheral organs in humans and rats (**table 1**). In contrast, knowledge on peripheral *Ppox* expression in the mouse is rather incomplete. Further, there are a few studies describing *Ppox* expression in extra-hypothalamic regions in the rodent brain such as the striatum or the amygdala (Kim et al., 2015; Saad et al., 2019). Since manipulations using the *Orx-Cre* transgene target all *Ppox* expressing cells, it is important to identify the entire population of *Ppox* expressing cells in the mouse. In order to achieve this, RNA was isolated from 21 central and peripheral tissues of LSL-Cas9-Egfp mice without Cre recombinase, which represent the wildtype state. Standard PCR was used for a first screen of *Ppox* expressing tissues. In addition, differences in expression among tissues were relatively quantified using qPCR. Two different sets of primers were used in order to increase reproducibility. Finally, in a lineage tracing experiment, *Orx-Cre* mice were crossed with LSL-Cas9-Egfp mice with the aim of visualizing cells expressing the *Orx-Cre* transgene and/or the endogenous *Ppox* in peripheral tissues by immunohistochemistry.

5.2.1. Quality Assessment of RNA Isolates from Different Tissues

Quality of the isolated RNA was judged based on gel electrophoresis, in which the presence of the 18s and 28s rRNA bands (1.9 and 4.7 kb, respectively) indicated successful RNA isolation. Except for pancreatic RNA, all tissues showed well-defined bands at the expected positions (**figure 11**). The smear observed in the low base range of the pancreatic RNA suggests degradation of the 18s and 28s rRNA and thus most likely other RNA species. The rather small brain regions of the LH, the SCN

and the amygdala were not included in the RNA gel, since due to their small size, comparatively low amounts of RNA were isolated and were saved for PCR analysis. However, since these three regions were dissected at the same time and based on the same protocol as the remaining 3 brain tissues, hippocampus, cortex and cerebellum, the same level of quality can be expected.

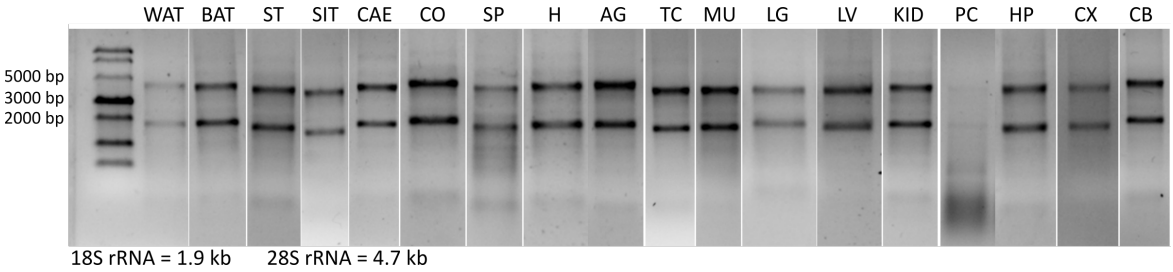

Figure 11 Quality assessment of RNA isolates. Quality was assessed by visualization of the 18S and 28S rRNA. White adipose tissue (WAT), brown adipose tissue (BAT), stomach (ST), small intestine (SIT), caecum (CAE), colon (CO), spleen (SP), heart (H), adrenal glands (AG), testicle (TC), muscle (MU), lung (LG), liver (LV), kidney (KID), pancreas (PC), hippocampus (HP), cortex (CX), cerebellum (CB).

5.2.2. Screening for *Ppox* Expression in Different Tissues

Following cDNA synthesis, PCR was performed as a first screening of *Ppox* expression (**figure 12**). All tissues showed clear bands for the housekeeping gene, confirming successful mRNA isolation and accurate cDNA synthesis. Regarding the presence of *Ppox* cDNA, only testis, kidney and LH showed strong bands at the expected size (131 – 137 bp, depending on splice variants). In addition weak bands could be observed in samples of the hippocampus, cortex, amygdala, SCN and cerebellum. All remaining 13 tissues showed no indication of *Ppox* expression in the PCR screen.

5.2.3. Relative Quantification of *Ppox* Expression in Different Tissues

In order to quantify the difference between *Ppox* expression in the individual tissues, qPCR analysis was performed on the same samples and the expression fold change was calculated relative to *Ppox* expression in the testis (**figure 12**, **table 5**). Highest expression was observed in the LH, whose *Ppox* levels were up to 3,000x higher than in the testis. Second highest expression was detected in the SCN and amygdala followed by the testis. All other brain regions and the kidney displayed stable *Ppox* expression across all 3 biological replicates but at a very low level. In contrast, there was no *Ppox* expression in most of the remaining peripheral tissues, except for the muscle, liver, stomach,

small intestine and adrenal gland of which some but not all of the 3 of the biological replicates displayed low level *Ppox* expression.

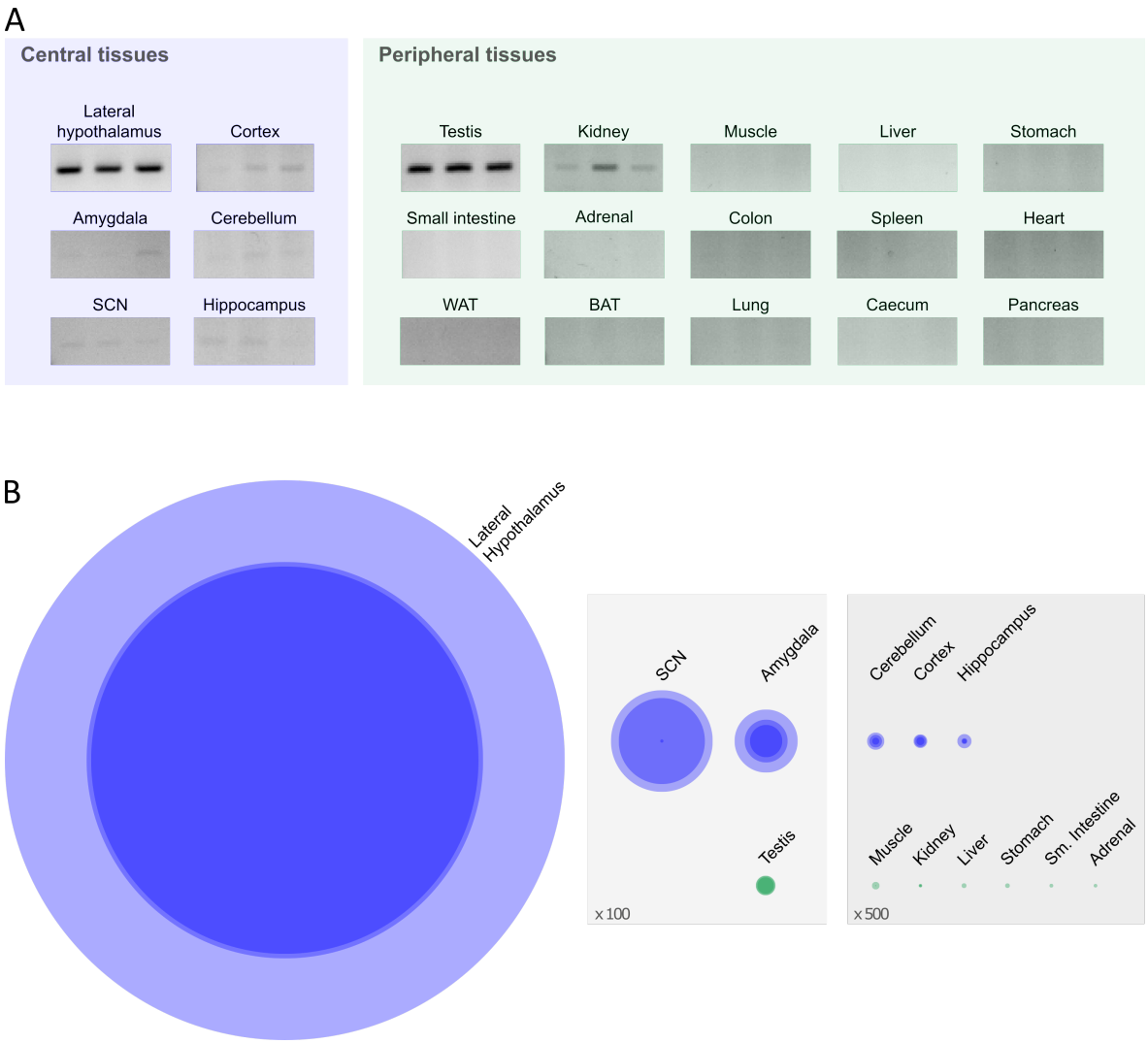

Figure 12 Analysis of *Ppox* expression in different central (blue) and peripheral (green) tissues. (**A**) Gel electrophoresis of a PCR targeting *Ppox* cDNA in 3 biological replicates per tissue. (**B**) Fold change of *Ppox* relative to *Ppox* expression in the testis as determined by qPCR. Each circle represents a biological replicate and the diameter equals the relative fold change compared to average *Ppox* expression in the testis. Due to the superimposition of the biological replicates of one tissue (n=3), the color intensity represents the abundancy across the 3 replicates, with darker shades indicating presence in more biological replicates. Except for the LH, the circle size was magnified either 100x or 500x to increase visibility.

Table 5 Analysis of *Ppox* expression in different central (blue) and peripheral (green) tissues. For each of the biological replicates of one tissue (n=3), the relative fold change compared to average *Ppox* expression in the testis was calculated. BAT = brown adipose tissue; WAT = white adipose tissue.

Organ	Replicate	Fold Change
Amygdala	1	2.34
Amygdala	2	1.76
Amygdala	3	3.44
Cerebellum	1	0.08
Cerebellum	2	0.14
Cerebellum	3	0.19
Cortex	1	0.15
Cortex	2	0.13
Cortex	3	0.09
Hippocampus	1	0.05
Hippocampus	2	0.06
Hippocampus	3	0.15
LH	1	2160.11
LH	2	2110.54
LH	3	3050.22
SCN	1	4.69
SCN	2	5.54
SCN	3	0.17
Adrenal Glands	1	0.00
Adrenal Glands	2	0.04
Adrenal Glands	3	0.00
BAT	1	0.00
BAT	2	0.00
BAT	3	0.00
Caecum	1	0.00
Caecum	2	0.00
Caecum	3	0.00
Colon	1	0.00
Colon	2	0.00
Colon	3	0.00
Heart	1	0.00
Heart	2	0.00
Heart	3	0.00
Kidney	1	0.01
Kidney	2	0.04
Kidney	3	0.04
Liver	1	0.00
Liver	2	0.05
Liver	3	0.00
Lung	1	0.00
Lung	2	0.00
Lung	3	0.00
Muscle	1	0.00
Muscle	2	0.01
Muscle	3	0.08
Pancreas	1	0.00
Pancreas	2	0.00
Pancreas	3	0.00
Small Intestine	1	0.00
Small Intestine	2	0.04
Small Intestine	3	0.00
Spleen	1	0.00
Spleen	2	0.00
Spleen	3	0.00
Stomach	1	0.00
Stomach	2	0.05
Stomach	3	0.00
Testis	1	0.89
Testis	2	1.07
Testis	3	1.03
WAT	1	0.00
WAT	2	0.00
WAT	3	0.00

5.2.4. Visualization of *Ppox* Expressing Cells in Peripheral Tissues

The results of the PCR and qPCR represent a snap shot of *Ppox* expression at a certain time of day and developmental stage. They do not provide information on whether the gene has been expressed at a different developmental or circadian time point. In contrast, in *Orx-Cre* mice crossed with the Cre reporter line LSL-Cas9-Egfp (Orx-Cre-LSL-Cas9-Egfp) the recombination takes place on the genomic level and cells continue the expression of *Egfp* even in the absence of Cre. As a result, all cells that have activated the *Ppox* promoter at any given time or that originate from cells that have previously expressed *Ppox,* will be labeled with EGFP. Since the central *Egfp* expression in these mice was already described in the section concerning the *Orx-Cre* construct validation (5.1.), the following focuses on peripheral organs.

Due to technical limitations, not all organs included in qPCR analysis could be analyzed immunohistochemically. The investigated organs include adrenal glands, caecum, colon, heart, kidney, liver, muscle, pancreas, spleen, and stomach. Most investigated organs were devoid of EGFP labelled cells, except pancreas, stomach and spleen (**figure 13**). While in the spleen only very few single cells were labelled, multiple cells in the stomach and entire islets of Langerhans were stained in the pancreas (indicated by the arrow in **figure 13 A**).

The *Orx-Cre* transgene is based on the human *Ppox* promoter and it cannot be assured, that the transgene mimics exactly the endogenous murine *Ppox* expression. In order to compare the EGFP labelled cells in the periphery with the acute presence of endogenous ORX, immunohistochemical staining of ORX in peripheral tissues was pursued. However, despite several attempts of assay optimization including different antigen retrieval methods, neither ORX-A nor ORX-B could be visualized in any of the peripheral organs, including the testis which according to qPCR analysis yields the highest levels of peripheral *Ppox* expression.

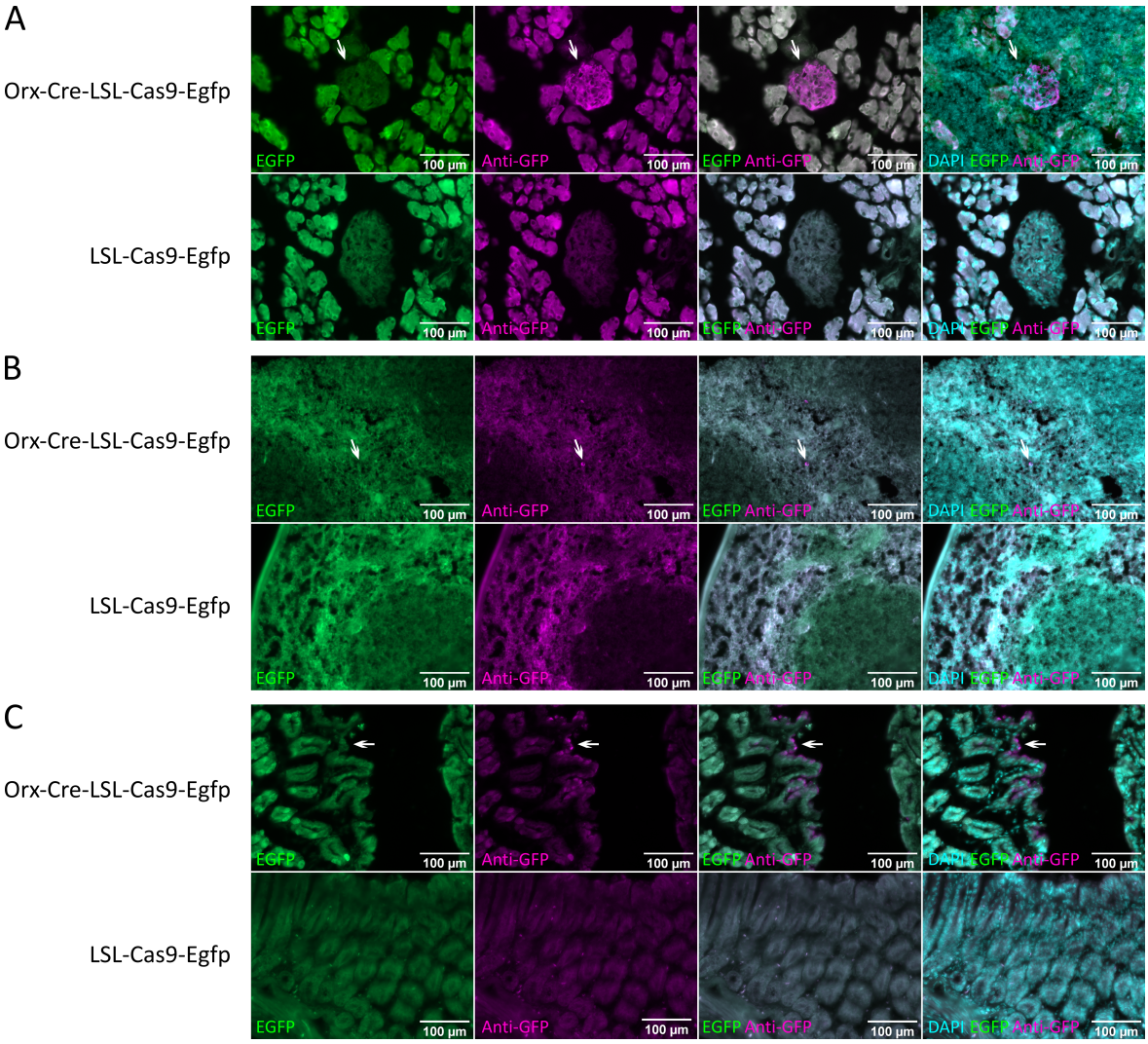

Figure 13 Recombination induced expression of *Egfp* in peripheral organs of Orx-Cre-LSL-Cas9-Egfp mice and LSL-Cas9-EGFP. EGFP was imaged (green) and further visualized by immunohistochemical staining (magenta). Magnifications of the pancreas (**A**), spleen (**B**), and stomach (**C**).White arrows indicate immunohistochemically stained somas. In this experiment, LSL-Cas9-EGFP mice serve as a negative control for the absence of Cre.

5.3. Circadian Rhythms of Gene Expression in the LH

ORX neurons of the LH represent a highly circadian cell population, since ORX release in the CSF, ORX neuron activity and *Ppox* expression display diurnal rhythms. While studies in full body clock mutant mice show that the rhythm of *Ppox* expression depends on the circadian system, the role of local subordinate clocks in ORX neurons in the generation of these rhythms has not been examined. This is why the expression of *Ppox* across the circadian cycle was investigated in the LH of Orx-Bmal1$^{-/-}$ mice which specifically lack *Bmal1* and hence a functional clock in ORX neurons of the LH. Further, the expression in the LH of Wt and full body clock mutant Cry1/2$^{-/-}$ mice was analyzed was a control for the presence and absence of *Ppox* rhythms, respectively. In all genotypes, at least one clock gene was analyzed to investigate the overall output of the circadian clock in these regions in each genotype. Furthermore, in Orx-Bmal1$^{-/-}$ and Wt mice, the circadian expression of *Pro-melanin-concentrating hormone (Pmch)* was studied. The expression of *Pmch* is the hallmark of a second cell type residing in the LH, the MCH-neurons, which is distinct from ORX-neurons and displays an anti-phasic activity pattern (Hassani et al., 2009; Mickelsen et al., 2017; Ono and Yamanaka, 2017). It is of great interest to understand how the loss of the molecular clock in one neuronal population affects the rhythmicity of neighboring cells in the same area.

5.3.1. Cry1/2$^{-/-}$ Mice

Due to limited availability, only female Cry1/2$^{-/-}$ and Wt mice were sacrificed at four time points across the circadian cycle in a random order. Their LH was dissected for RNA isolation and subsequent analysis of gene expression. The impact of genotype and ZT was assessed using two-way ANOVA and circadian rhythmicity was determined by cosinor analysis and the zero-amplitude test.

Ppox

There was a significant impact of ZT and the interaction genotype x ZT on *Ppox* expression (**figure 14**, **supplementary table S1**). Post-hoc testing determined, that in Cry1/2$^{-/-}$ mice, *Ppox* expression was higher than in Wt mice at ZT13 and 19 and lower at ZT7 (**supplementary table S2**). Further, cosinor analysis and the zero-amplitude test revealed that *Ppox* expression was significantly rhythmic in Wt animals but arrhythmic in Cry1/2$^{-/-}$ mice (**supplementary table S3**).

Per2

Two-way ANOVA showed no impact of ZT or the interaction genotype x ZT but only genotype on *Per2* expression with higher mean *Per2* expression levels in Cry1/2$^{-/-}$ mice independent of circadian time point (**figure 14**, **supplementary table S1**). Accordingly, *Per2* expression did not cycle in either genotype according to cosinor analysis and zero-amplitude test (**supplementary table S3**).

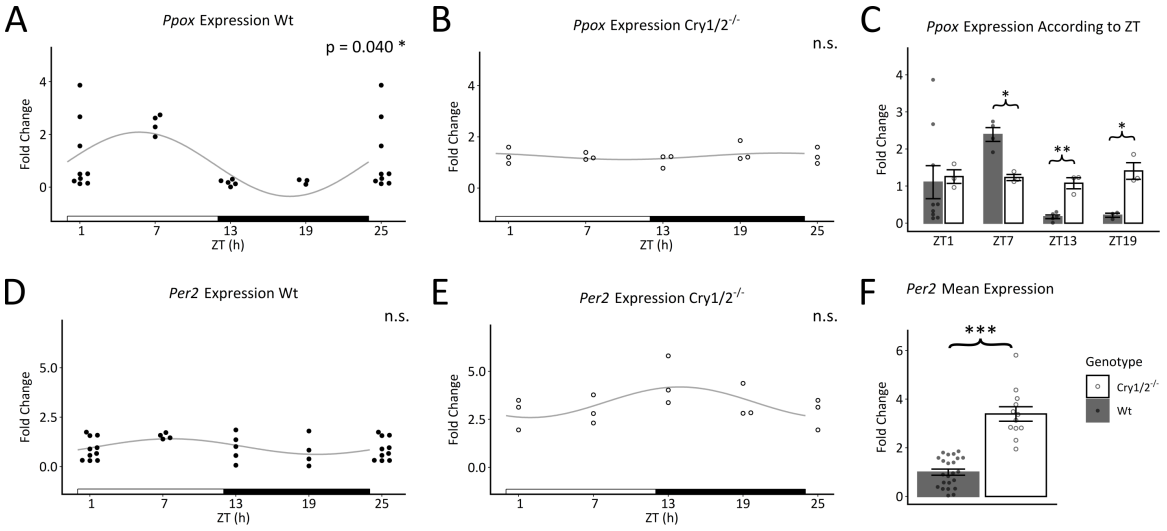

Figure 14 Investigation of circadian gene expression rhythms of *Ppox* and *Per2* in Wt and Cry1/2$^{-/-}$ mice. Gene expression of each gene was analyzed relative to the mean expression across time points in Wt mice. **A**,**B**,**D** and **E** show cosinor fits of the gene expression at different time points with a period of 24 h. ZT1 is plotted twice (ZT25) but ZT25 was not included in the cosinor analysis. In these graphs, p-values and asterisk refer to rhythmicity testing based on the zero-amplitude test with bonferroni correction *(Cornelissen, 2014)*. The white and black bars along the x-axis represent light and dark phases. **C** visualizes the mean *Ppox* expression of each genotype at the different time points and **F** the mean *Per2* expression in each genotype independent of circadian time point. In these graphs, error bars represent the standard error of the mean (SEM) and asterisk indicates a significant effect according to either two-way ANOVA or post-hoc testing with bonferroni correction. For all graphs: group sizes (n) per time point Wt/ Cry1/2$^{-/-}$ were ZT1 = 9-10/3, ZT7 = 4/3, ZT13 = 5/3, ZT19 =3-4/3; *p < 0.05, **p < 0.01, ***p < 0.001;

5.3.2. Orx-Bmal1$^{-/-}$ Mice

RNA was isolated from the LH of Wt and Orx-Bmal1$^{-/-}$ mice of both sexes that were sacrificed at four different time points across the circadian cycle in a random order. The expression of *Ppox, Bmal1* and *Pmch* was investigated using qPCR. The impact of sex, genotype and ZT was analyzed by three-way ANOVA and circadian rhythmicity was determined by cosinor analysis and the zero-amplitude test.

Ppox

Three-way ANOVA revealed a significant impact of genotype, ZT, sex and the interaction genotype x ZT on *Ppox* expression (**figure 15**, **supplementary tables S4** and **S5**). Since there was no interaction between sex and genotype, cosinor analysis was performed independent of sex. In Wt mice, *Ppox* expression peaked at ZT7 and remained low throughout the rest of the cycle. Post-hoc comparison of mean *Ppox* expression levels at the different circadian time points showed that *Ppox* expression was significantly lower in Orx-Bmal1$^{-/-}$ mice than in Wt mice at ZT7 and higher at ZT13 and ZT19 although the effect on ZT19 was not robust towards correction for multiple testing (**supplementary table S6**). Further, female mice of both genotypes had higher mean *Ppox* expression levels than their male littermates independent of circadian time point. Assessment of rhythmicity of *Ppox* expression using cosinor analysis and the zero-amplitude test confirmed a loss of circadian rhythmicity in Orx-Bmal1$^{-/-}$ mice as compared to Wt mice (**supplementary table S7**).

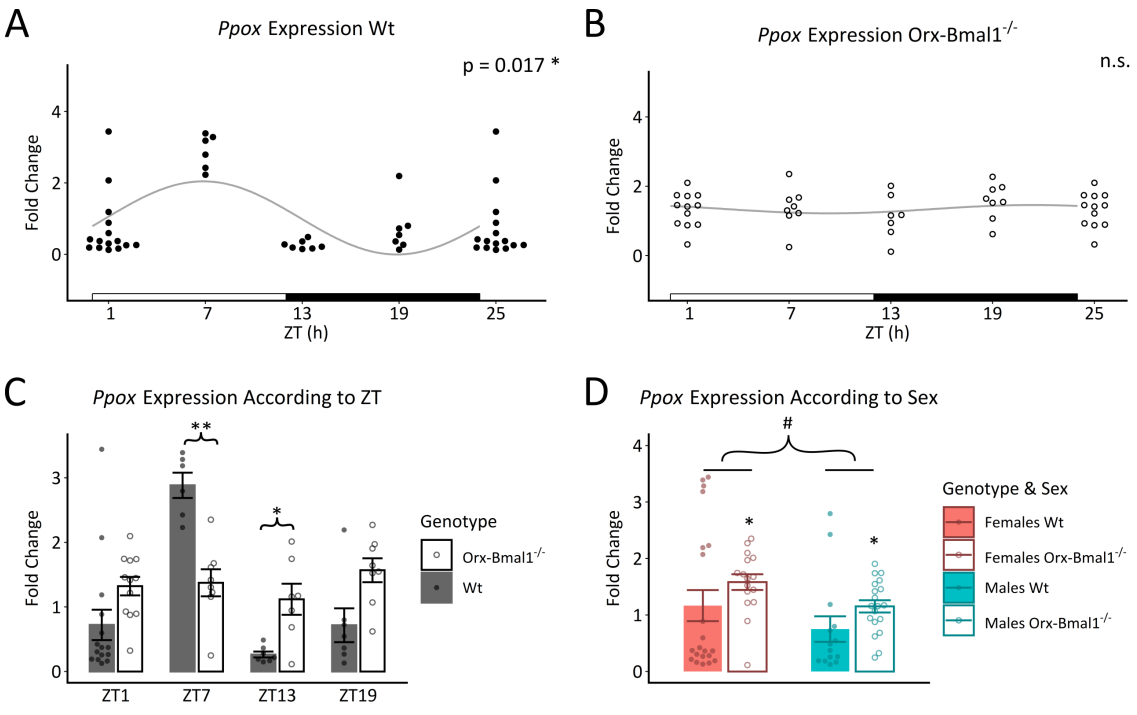

Figure 15 Investigation of circadian *Ppox* expression rhythms in Wt and in Orx-Bmal1$^{-/-}$ mice. Gene expression was analyzed relative to the mean expression across time points in Wt mice. **A** and **B** show cosinor fits of the gene expression at different time points with a period of 24 h. ZT1 is plotted twice (ZT25) but ZT25 was not included in the cosinor analysis. In these graphs, p-values and asterisk refer to rhythmicity testing based on the zero-amplitude test with bonferroni correction *(Cornelissen, 2014)*. The white and black bars along the x-axis represent light and dark phases. **C** visualizes the mean *Ppox* expression of each genotype at the different time points and **D** the mean *Ppox* expression in each genotype and sex independent of circadian time point. In these graphs, error bars represent the SEM and asterisk indicates a significant genotype effect and # a significant sex effect according to either three-way ANOVA or post-hoc testing with bonferroni correction. For all graphs: group sizes (n) per time point Wt/ Orx-Bmal1$^{-/-}$ were ZT1 = 15/12, ZT7 = 6/8, ZT13 = 7/7, ZT19 =7/8; *p or # p < 0.05, **p < 0.01.

Bmal1

Three-way ANOVA detected a significant impact of genotype and the interaction ZT x sex on *Bmal1* expression (**figure 16**, **supplementary tables S4** and **S5**). There was no interaction effect between sex and genotype which is why both sexes were analyzed together. The genotype effect manifested in elevated mean expression levels of *Bmal1* Orx-Bmal1$^{-/-}$ mice as compared to Wt mice, independent of circadian time point. *Bmal1* expression in the LH of Wt animals was not significantly rhythmic according to cosinor analysis and the zero-amplitude test, but gained rhythmicity in Orx-Bmal1$^{-/-}$ animals with highest expression at ZT1 and lowest between ZT7 and 13 (**supplementary figure S7**).

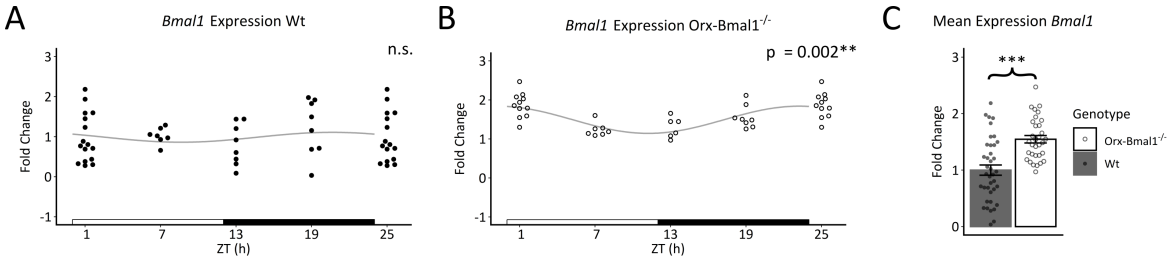

Figure 16 Investigation of circadian *Bmal1* expression rhythms in Wt and in Orx-Bmal1$^{-/-}$ mice. Gene expression was analyzed relative to the mean expression across time points in Wt mice. **A** and **B** show cosinor fits of the gene expression at different time points with a period of 24 h. ZT1 is plotted twice (ZT25) but ZT25 was not included in the cosinor analysis. In these graphs, p-values and asterisk refer to rhythmicity testing based on the zero-amplitude test with bonferroni correction (Cornelissen, 2014). The white and black bars along the x-axis represent light and dark phases. **C** visualizes the mean *Bmal1* expression in each genotype independent of circadian time point. In these graphs, error bars represent the SEM and asterisk indicates a significant effect according to either three-way ANOVA or post-hoc testing with bonferroni correction. For all graphs: group sizes (n) per time point Wt/ Orx-Bmal1$^{-/-}$ were ZT1 = 16/11, ZT7 = 7/7, ZT13 = 8/6, ZT19 =8/8; **p < 0.01, ***p < 0.001;

Pmch

Three-way ANOVA of *Pmch* expression exposed a significant impact of genotype, ZT and the interactions genotype x ZT as well as genotype x ZT X sex (**figure 17**, **supplementary tables S4** and **S5**). Post-hoc testing revealed no significant difference between female Wt and Orx-Bmal1$^{-/-}$ mice at ZT1, 7 and 19 (**supplementary table S6**). At ZT13 the sample number in Orx-Bmal1$^{-/-}$ was too small for statistical testing. Similarly, ZT1, 13 and 19 were not different between male Wt and Orx-Bmal1$^{-/-}$ mice. Although mean *Pmch* levels were higher in male Wt mice at ZT7, statistical analysis could not be performed due to the low sample number in Wt mice at this time point. Due to the interaction genotype x ZT x sex, rhythm detection was performed for each sex separately

(**supplementary figure S7**). Male Wt mice displayed a rhythm of *Pmch* expression according to cosinor analysis and the zero-amplitude test, however it was not significant after correction for multiple testing. The cosinor model for female Wt mice followed the same shape but did not reach statistical significance. Similarly, neither female nor male Orx-Bmal1$^{-/-}$ mice displayed rhythmic *Pmch* expression.

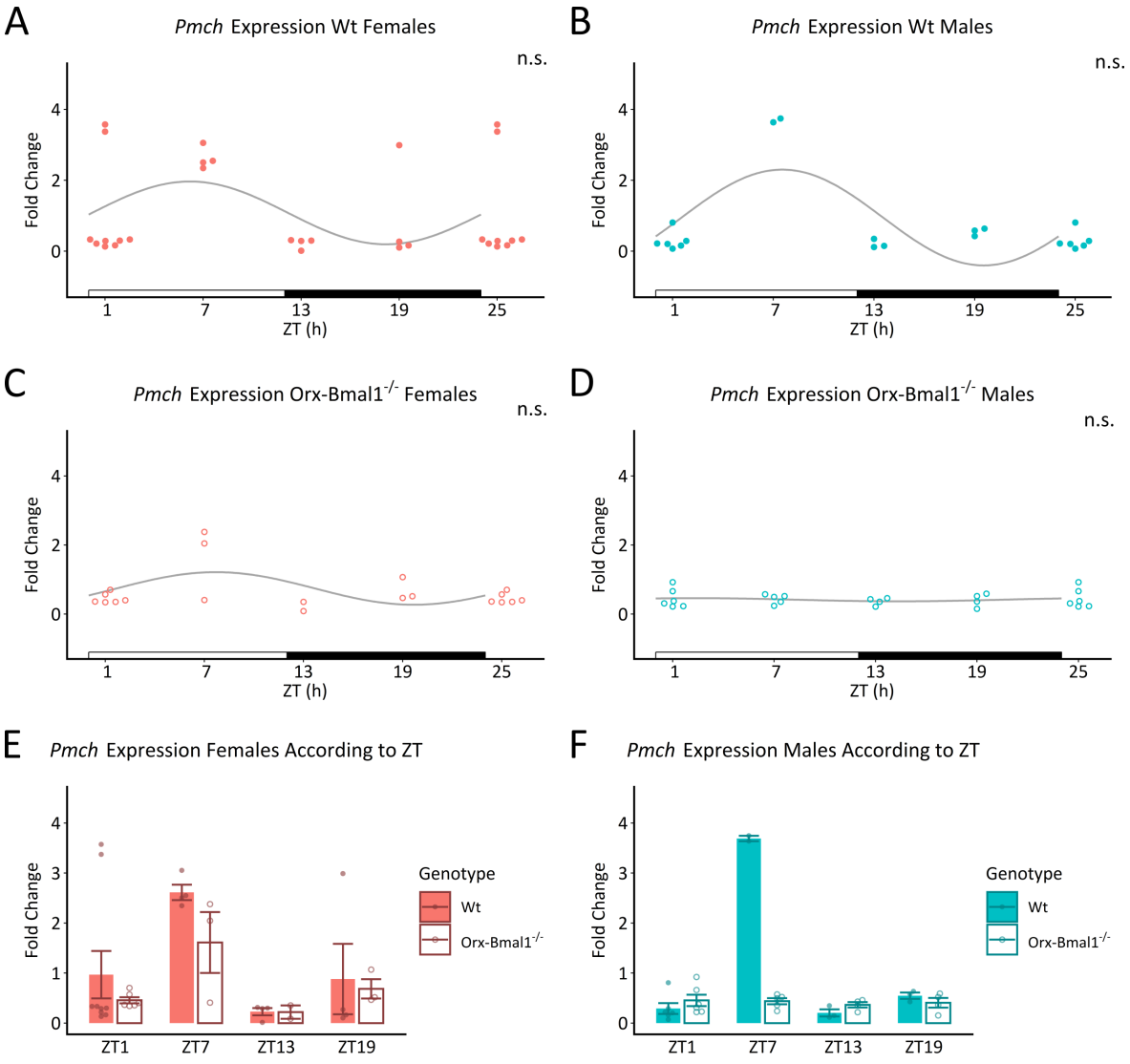

Figure 17 Investigation of circadian gene expression rhythms of *Pmch* in Wt and in Orx-Bmal1$^{-/-}$ mice. Gene expression was analyzed relative to the mean expression across time points in Wt mice. **A** - **D** show cosinor analysis of the gene expression at different time points with a period of 24 h. ZT1 is plotted twice (ZT25) but ZT25 was not included in the cosinor fit. In these graphs, p-values and asterisk refer to rhythmicity testing based on the zero-amplitude test with bonferroni correction *(Cornelissen, 2014)*. The white and black bars along the x-axis represent light and dark phases. **E** and **F** visualize the mean Ppox expression of each genotype at different time points for each sex. In these graphs, error bars represent the SEM. For all graphs: group sizes (n) per time point Wt/ Orx-Bmal1$^{-/-}$ were for females: ZT1 = 9/6, ZT7 = 4/3, ZT13 = 4/2, ZT19 =4/3 and for males: ZT1 = 6/6, ZT7 = 2/5, ZT13 = 3/4, ZT19 =3/4;

5.4. Metabolic, Behavioral and Circadian Phenotyping of Orx-Bmal1$^{-/-}$ mice

The ORX and the circadian system are tightly linked and are both involved in the regulation of mood- and anxiety-related behavior as well as metabolic processes. In order to investigate the role of subordinate clocks in ORX neurons of the LH in mood- and anxiety-related behavior as well as metabolic regulation, a cohort of male and female Orx-Bmal1$^{-/-}$ and Wt mice underwent a series of tests to determine their circadian, behavioral and metabolic phenotype. Since the relationship between the ORX and the circadian system is bidirectional (Belle et al., 2014; Brown et al., 2008), rhythmicity of locomotor activity and PER2::LUC oscillations in the SCN were investigated to gain insights on the overall rhythmicity of the circadian system in these animals. The series of behavioral tests included several tests for anxiety- and depression-like behavior. Further, due to recent reports of ORX dysregulation in schizophrenic patients, measurement of the PPI of the startle reflex was included, since disrupted PPI is a common feature displayed in schizophrenic patients (Lu et al., 2021; Sato, 2020). For assessment of the metabolic phenotype, the mice were weighed weekly from the moment they were weaned as a correlate of their overall metabolic state. In addition, circadian variations of food and water consumption as well as the RER were assessed in a separate cohort of Orx-Bmal1$^{-/-}$ and Wt mice of both sexes using the metabolic cage system.

5.4.1. Circadian Phenotyping of Orx-Bmal1$^{-/-}$ Mice

5.4.1.1. Circadian Rhythms of Locomotor Activity

Locomotor activity of Orx-Bmal1$^{-/-}$ and Wt mice was monitored for 1 week in a 12:12 LD cycle and for 2 weeks in constant darkness (DD) using the IntelliCage system (**figure 18**). Under LD conditions, both genotypes and sexes displayed strong locomotor rhythms with maximum activity in the dark phase and approximately 24 h periodicity according to the lomb-scargle periodogram. This was confirmed by three-way ANOVA investigating the impact of genotype, sex and phase on activity, which revealed a significant effect of circadian phase (**supplementary table S8** and **S9**). The significant interactions between genotype and sex as well as genotype, sex and phase were further explored with post-hoc tests, showing that female Wt mice, compared to female Orx-Bmal1$^{-/-}$ mice were more active during the night but not during the day (**supplementary table S10**). This effect was not present in male mice. Two-way ANOVA was used to analyze differences in the period of locomotor activity according to genotype and sex (**supplementary table S11**). It did not expose any significant differences in the period of activity rhythms between any of the groups. Animals were

transferred into DD in order to assess endogenous rhythms of locomotor activity in the absence of the *Zeitgeber* light (**supplementary table S8**). Data was analyzed according to the ZT and circadian phases of the previous LD cycle. Locomotor activity rhythms persisted in, which manifested in a significant impact of phase and a period of approximately 24 h. There was a significant effect of genotype, the interaction genotype and sex, as well as the interaction genotype, sex and phase in the three-way ANOVA (**supplementary table S9**). Post-hoc testing revealed that this was due to higher activity in female Wt mice as compared to female Orx-Bmal1$^{-/-}$ mice during both, day and night, of the previous light-dark cycle (**supplementary table S10**). In contrast, no significant differences between the activity of male Wt and Orx-Bmal1$^{-/-}$ mice were detected in either phase. Analysis of the period of locomotor activity in DD exposed, that female mice of both genotypes had slightly longer periods than male mice. Still, periods of all groups were approximately 24 h (**supplementary table S11**).

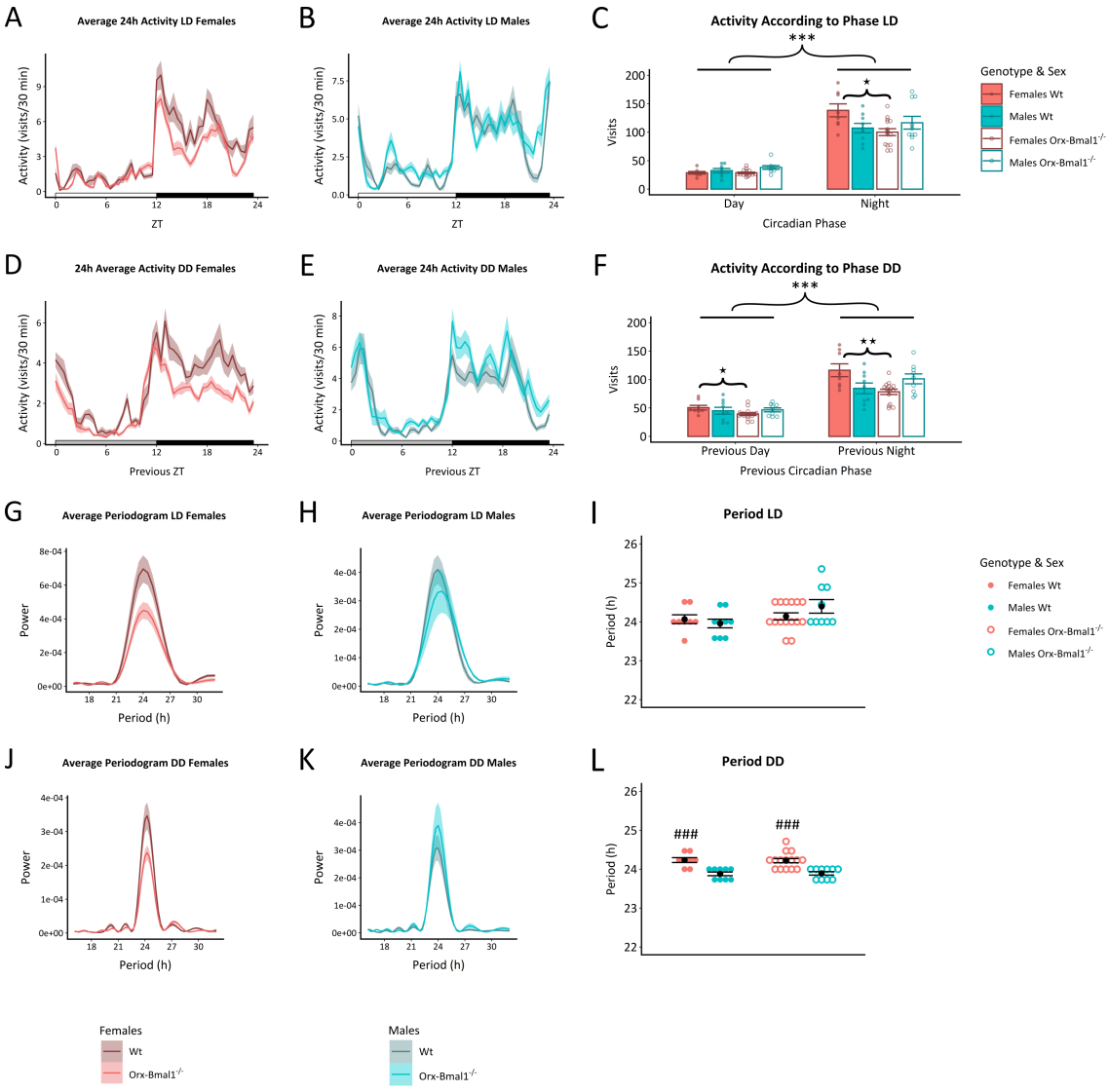

Figure 18 Analysis of locomotor activity rhythms in Wt and Orx-Bmal1$^{-/-}$ mice. Average 24 h locomotor activity of male and female mice of both genotypes under 12:12 LD (**A,B**) and DD conditions (**D,E**). Activity was measured as corner visits in the IntelliCage system. The white and black bars along the x-axis indicate light and dark phases. Gray represents the previous light phase during DD. Data from DD was analyzed according to the ZT and circadian phases of the previous LD cycle. The shaded area and the error bars represents the SEM. **C** and **F** show the mean visits ± SEM of each group according to circadian phase. Rhythmicity of locomotor activity in LD and DD was assessed using the lomb-scargle periodogram (**G,H,J,K**). **I** and **L** show the mean period of locomotor activity ± SEM of each group in LD and DD. Asterisk indicates significant phase effect and hashtag indicates significant sex effect determined by three- or one-way ANOVA. Star indicates significant differences between female Wt and female Orx-Bmal1$^{-/-}$ mice determined by post-hoc testing with bonferroni correction. ***p < 0.001, ###p < 0.001, p * < 0.05 p ** < 0.01; Group sizes of Wt/Orx-Bmal1$^{-/-}$ mice: females n = 8/15 and males n = 8-9/9-10.

5.4.1.2. PER2::LUC Rhythms in the SCN

Endogenous rhythmicity of the animals was further examined based on organotypic slices of the master pacemaker, the SCN. Parameters of SCN rhythmicity were assessed *ex vivo* using the PER2::LUC reporter system (**figure 19**, **supplementary table S12**). Two-way ANOVA revealed no significant differences in the amplitude, period or dampening of rhythms between the two genotypes as well as sexes.

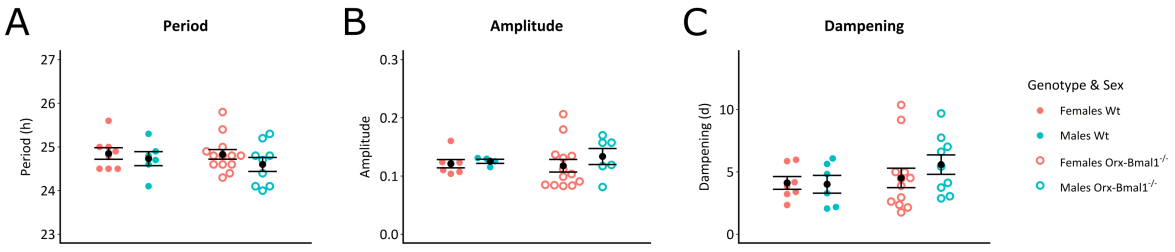

Figure 19 Analysis of PER2::LUC rhythms in the SCN of female and male Wt and Orx-Bmal1$^{-/-}$ mice. A Mean period ± SEM with group sizes Wt/ Orx-Bmal1$^{-/-}$ mice: females n = 8/13 and males n = 6/9. **B** Mean amplitude ± SEM with group sizes Wt/ Orx-Bma1l$^{-/-}$ mice: females n = 7/13 and males n = 4/6. **C** Mean dampening ± SEM with group sizes Wt/ Orx-Bmal1$^{-/-}$ mice: females n = 7/12 and males n = 6/9. Two-way ANOVA did not reveal any significant effects.

5.4.2. Behavioral Phenotyping of Orx-Bmal1$^{-/-}$ Mice

Orx-Bmal1$^{-/-}$ and Wt mice of both sexes were subjected to a behavioral test battery in order to assess the impact of loss of ORX neuron rhythmicity on anxiety related and depression-like behavior, as well as one schizophrenia-associated phenotype. The impact of genotype and sex on the behavioral tests was analyzed using two-way ANOVA and are summarized **supplementary tables S13** to **S20**.

5.4.2.1. Anxiety-Related Behavior

Anxiety-related behavior was measured in the OFT, EPM and LDT. In the OFT, no significant impact of genotype on any of the measured parameters was found (**figure 20**, **supplementary table S13**). There were no striking differences between male and female mice expect that male mice spent significantly more time in the corners as determined by a significant impact of sex on corner time. Genotype did not affect the behavior in the EPM although Orx-Bmal1$^{-/-}$ mice tended to spend more time in the open arm but without reaching significance (**figure 21**, **supplementary table S14**). In both genotypes, male mice entered less often the open arms and spent less time in the open arms than female mice as shown by a significant sex effect on the parameters. Neither sex nor genotype had an effect on the total distance travelled or mean speed during the EPM or OFT. In the LDT, Orx-Bmal1$^{-/-}$ spent significantly more time in the light compartment than Wt mice along with similar total amounts of light entries and latency until first light entry (**figure 22**, **supplementary table S15**). Sex did not affect the behavior in the LDT.

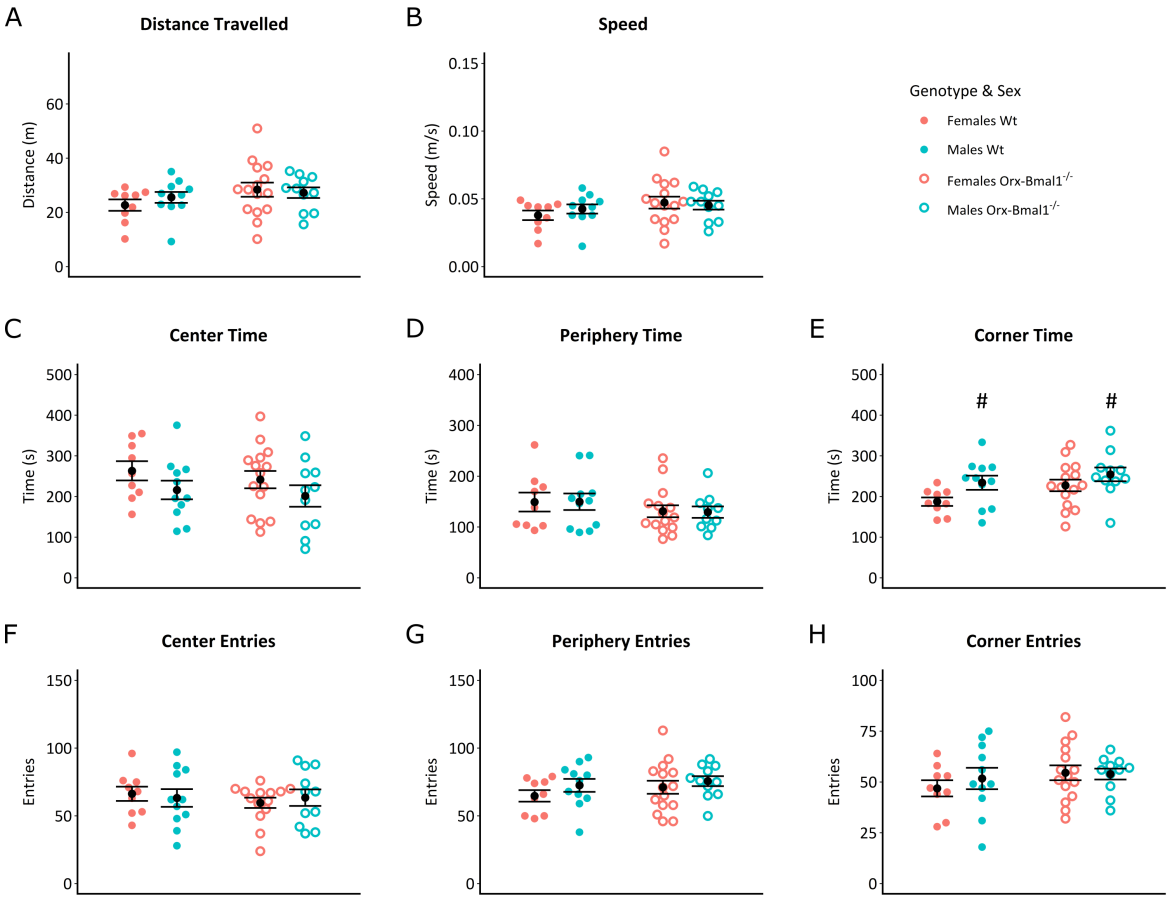

Figure 20 OFT of female and male Wt and Orx-Bmal1$^{-/-}$ mice. Graphs show the mean ± SEM of the distance travelled (**A**), speed (**B**), center time (**C**), periphery time (**D**), corner time (**E**), center entries (**F**), periphery entries (**G**) and corner entries (**H**) in each group. Hashtag indicates significant sex effect determined by two-way ANOVA. #p < 0.05; Group sizes Wt/Orx-Bmal1$^{-/-}$ mice: females n = 9/14-15 and males n = 11/10-11.

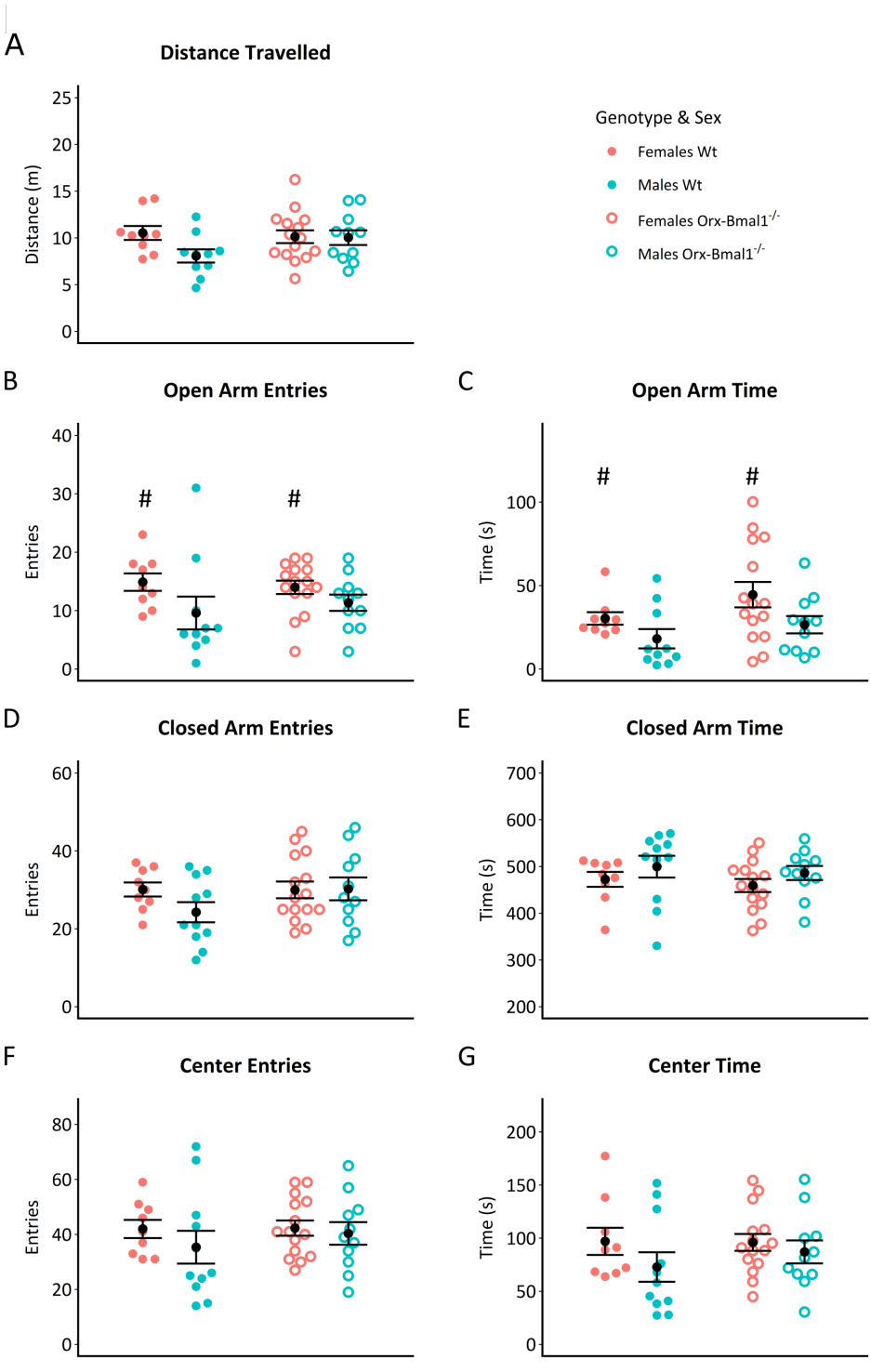

Figure 21 EPM of female and male Wt and Orx-Bmal1$^{-/-}$ mice. Data plotted as mean ± SEM of the distance travelled (**A**), open arm entries (**B**), open arm time (**C**), closed arm entries (**D**), closed arm time (**E**), center entries (**F**) and center time (**G**) in each group. Hashtag indicates significant sex effect determined by two-way ANOVA. #$p < 0.05$; Group sizes Wt/Orx-Bmal1$^{-/-}$ mice: females n = 9/15 and males n = 10-11/11.

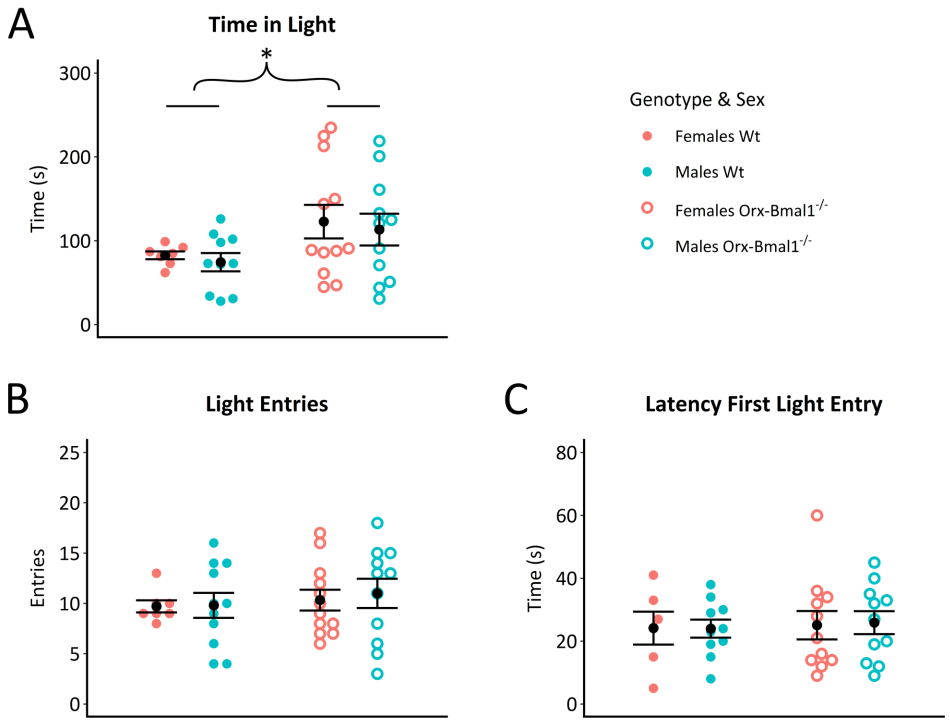

Figure 22 LDT of female and male Wt and Orx-Bmal1$^{-/-}$ mice. Graphs show the mean ± SEM of the time spent in light (**A**), light entries (**B**) and latency until the first light entry (**C**) in each group. Asterisk indicates significant genotype effect determined by two-way ANOVA. *p < 0.05; Group sizes Wt/Orx-Bmal1$^{-/-}$ mice: females n = 6-7/11-12 and males n = 10-11/11.

5.4.2.2. Depression-Like Behavior

Depression-like behavior was investigated based on the TST, LHP and SPT. Time immobile, the number of immobile episodes and the latency until the first immobile episode in the TST were not affected by genotype or sex (**figure 23**, **supplementary table S16**).

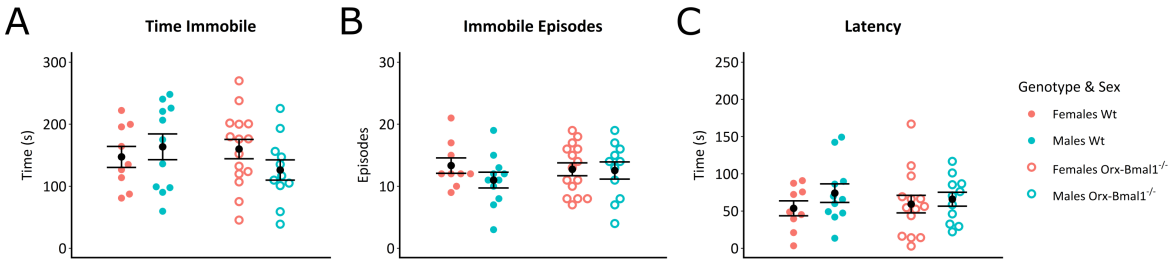

Figure 23 TST of female and male Wt and Orx-Bmal1$^{-/-}$ mice. Graphs show the mean ± SEM of the time immobile (**A**), immobile episodes (**B**) and latency until first immobile episode (**C**) in each group. Two-way ANOVA did not reveal any significant effects. Group sizes Wt/Orx-Bmal1$^{-/-}$ mice: females n = 9/14-15 and males n = 11/11.

In the LHP, Orx-Bmal1$^{-/-}$ mice displayed a significantly reduced latency to escape the electrical shocks along with a reduction in complete failures to avoid the shocks as compared to Wt mice (**figure 24, supplementary table S17**). As the reaction to electrical shocks depends on the perception of pain in the animals, pain sensitivity was measured which revealed a significant interaction between sex and genotype. Post-hoc testing exposed, that this was due to lower pain sensitivity in female Orx-Bmal1$^{-/-}$ mice. However, this difference was not robust against p-value correction for multiple testing (**supplementary table S18**).

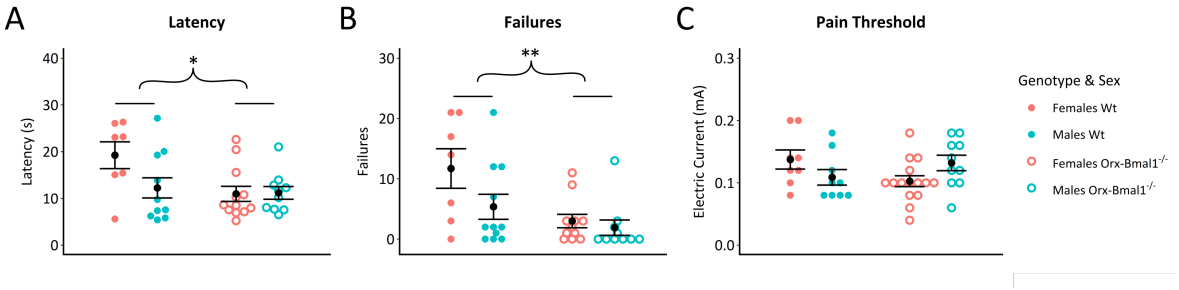

Figure 24 LHP of female and male Wt and Orx-Bmal1$^{-/-}$ mice. Graphs show the mean ± SEM of the latency to escape shock (**A**), failures to escape shock (**B**) and pain threshold (**C**) in each group. Asterisk indicates significant genotype effect determined by two-way ANOVA. *p < 0.05, p** < 0.01; Group sizes Wt/Orx-Bmal1$^{-/-}$ mice: females n = 7-8/11-15 and males n = 9-11/10.

During the SPT, in both genotypes liquid consumption varied diurnally with higher consumption during the dark phase (**figure 25**). In Wt mice of both sexes, mice consumed similar amounts of water and sucrose independent of circadian phase. In female Orx-Bmal1$^{-/-}$ mice, the mean sucrose consumption was above the mean water consumption. Similarly, male Orx-Bmal1$^{-/-}$ mice chose sucrose over water and nearly completely abolished water consumption. These observations were quantified by calculation of the sucrose preference score (**supplementary table S19**). Two-way ANOVA confirmed that independent of sex, Orx-Bmal1$^{-/-}$ mice preferred sucrose above water while Wt mice consumed equal amounts of both liquids. This effect was more pronounced in male than in female mice, as indicated by a significant interaction between genotype and sex.

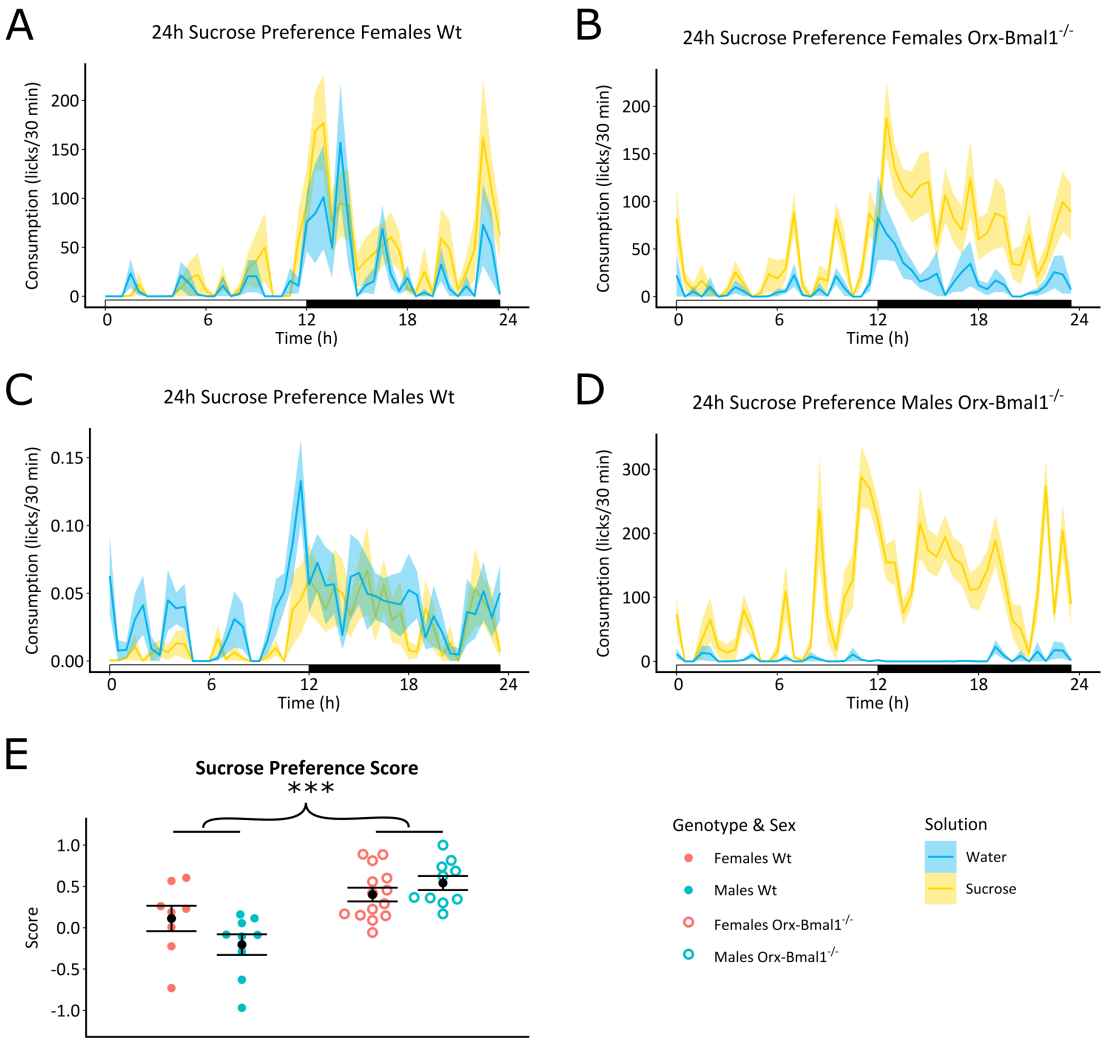

Figure 25 SPT of female and male Wt and Orx-Bmal1$^{-/-}$ mice. Graphs **A**-**D** show the average 24 h consumption of sucrose (yellow) and water (blue) measured as licks in the IntelliCage system. The white and black bars along the x-axis represent light and dark phases. The shaded area represents the SEM. **E** shows the mean preference score ± SEM in each group. Asterisk indicates significant genotype effect determined by two-way ANOVA. ***p < 0.001; Group sizes Wt/Orx-Bmal1$^{-/-}$ mice: females n = 8/14 and males n = 9/10.

5.4.2.3. Schizophrenia-Associated Phenotype

PPI of the startle response was measured for four different dB levels of prepulses as schizophrenia-associated phenotype (**figure 26**, **supplementary table S20**). In all groups, PPI increased along with the decibel level of the prepulse. PPI was neither influenced by genotype nor sex at any of the tested prepulse levels.

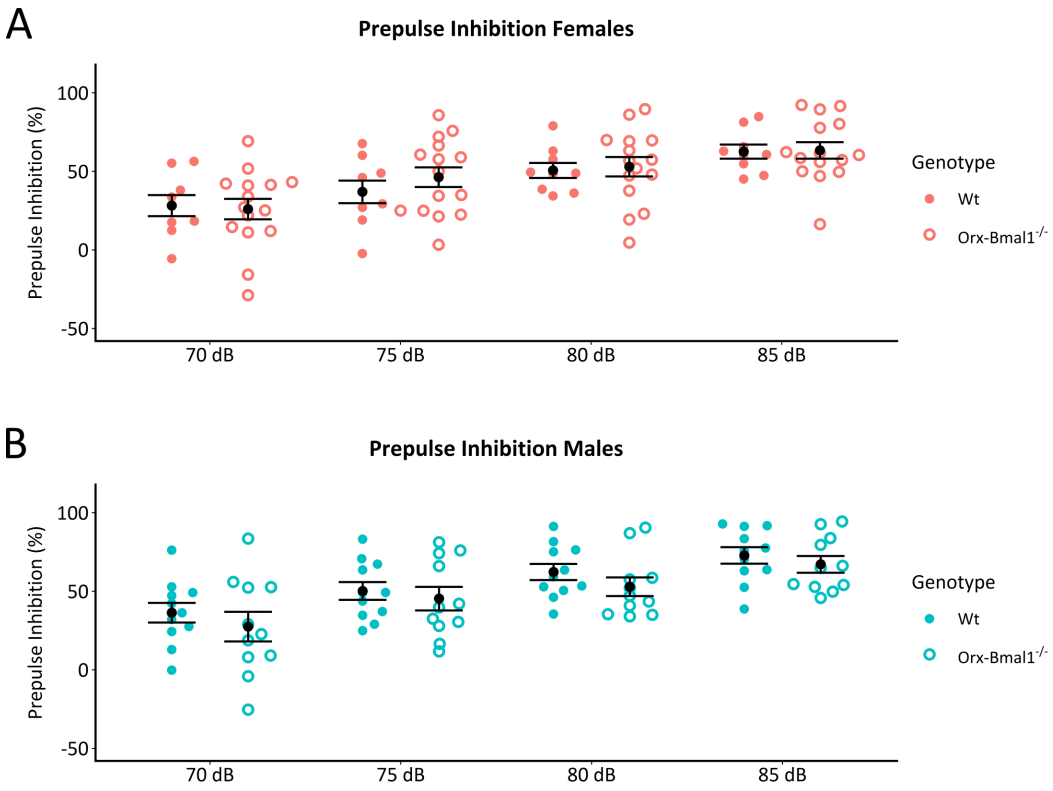

Figure 26 PPI of female and male Wt and Orx-Bmal1$^{-/-}$ mice. Graphs **A** and **B** show the mean PPI ± SEM at different decibel levels in each group. Two-way ANOVA did not reveal any significant effects. Group sizes Wt/Orx-Bmal1$^{-/-}$ mice: females n = 9/115 and males n = 11/11.

5.4.2.4. Impact of Estrus Cycle in Female Mice

Vaginal smears were taken after the testing of female mice in the OFT, EPM, LDT, TST, LHP and PPI. They were grouped according to high and low estrus phases. A two-way ANOVA revealed neither an impact of estrus cycle phase on its own, nor in interaction with the genotype for any of the behavioral tests (data not shown).

5.4.3. Metabolic Phenotyping of Orx-Bmal1$^{-/-}$ mice

5.4.3.1 Body Weight

The same cohort of Orx-Bmal1$^{-/-}$ and Wt mice that underwent behavioral testing was weighed weekly from the moment they were weaned (3 weeks) until the age of 22 weeks (**figure 27**, **supplementary table S21** and **S22**). The monitoring of the weight was measured as a correlate of the impact of loss of ORX neuron rhythmicity on the overall metabolic state of the animals. Since it is well established, that male and female mice differ strongly in weight, the two sexes were analyzed separately. A two-way repeated measure ANOVA showed a strong impact of age on the weight of both sexes (**supplementary table S23**). In case of male mice, a significant impact of the interaction genotype and age was identified. Post-hoc testing revealed that this effect was not due to differences between the two genotypes at any age (**supplementary table S24**). Instead, the effect is probably caused by the relatively steeper increase in weight in Orx-Bmal1$^{-/-}$ males from the age of 5 to 6 weeks (indicated by the arrow in **figure 27**).

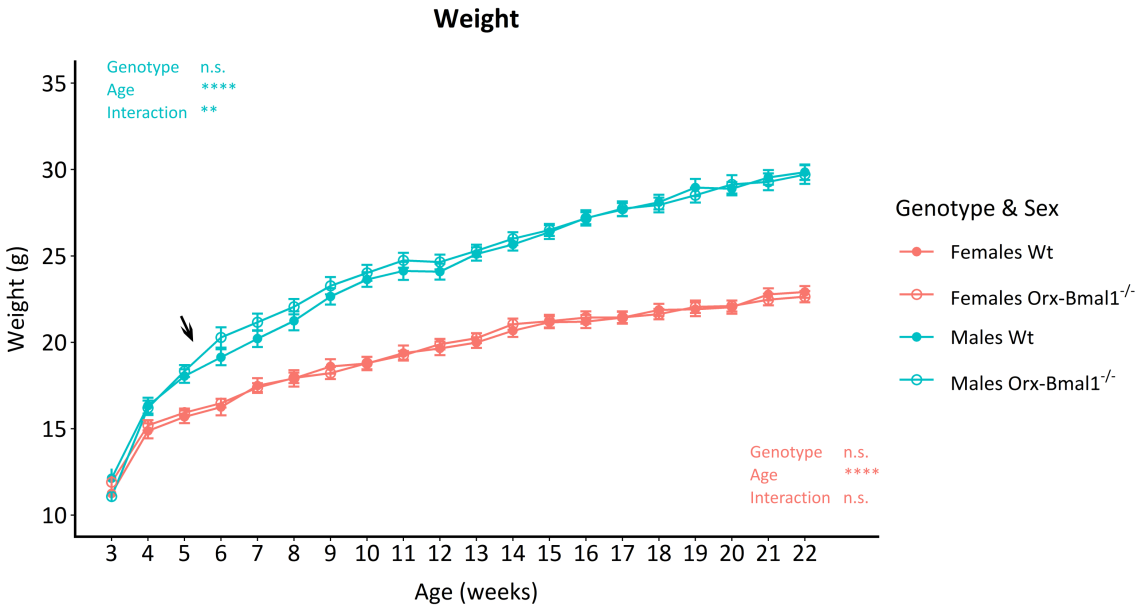

Figure 27 Weight of Wt and Orx-Bmal1$^{-/-}$ mice of both sexes from the age of 3 weeks to the age of 22 weeks. Graph shows the mean weight ± SEM in each group. The arrow highlights a steeper increase in weight in male Orx-Bmal1$^{-/-}$ mice than male Wt mice from the age of 5 to 6 weeks. Asterisk indicates significant effects determined by two-way repeated measure ANOVA. p** < 0.01, ***p < 0.001, n.s. = not significant; Group sizes Wt/Orx-Bmal1$^{-/-}$ mice: females n = 8/15 and males n = 9/11.

5.4.3.2 Metabolic Cages

In order to gain more insights on the role of ORX neuron rhythmicity in metabolic regulation, a separate cohort of Orx-Bmal1$^{-/-}$ and Wt mice was placed in metabolic cages to measure their RER, food and water consumption as well as activity over 24 h (**figure 28**, **supplementary table S25**). Three-way ANOVA revealed a significant impact of phase on all measured parameters indicating circadian rhythmicity for all genotypes and sexes (**figure 28, supplementary table S26**). Moreover, the shape of the observed rhythms was similar across groups with peak activity, RER as well as food and water consumption during the dark phase. In both sexes, the peak of food consumption in the middle of the dark phase was more pronounced in Orx-Bmal1$^{-/-}$ than in Wt mice as indicated by the arrow. Further, there was a significant effect of sex on food and water consumption, as well as activity, since female mice of both genotypes were more active and had higher food and water intake. Due to the significant interaction between phase and sex in food consumption and activity, post-hoc testing was performed to determine phase specific sex differences (**supplementary table S27**). Post-hoc testing revealed, that the higher activity and food consumption in female mice was restricted to the night. However, there was no effect of genotype on RER, food and water consumption or locomotor activity.

5.5. Virus Mediated Knockdown of *Bmal1* in ORX Neurons of the LH

Circadian arrhythmicity in ORX neurons of the LH as modeled in Orx-Bmal1$^{-/-}$ mice suffers from two limitations. First, as demonstrated in the previous sections, *Ppox* is not exclusively expressed in the LH but also in other brain regions and peripheral tissues. Although the lineage tracing experiment revealed that *Orx-Cre* expression in the brain is mainly restricted to the LH, we found some EGFP labeled cells in the pancreas, stomach, spleen and cerebellum. Consequently, *Bmal1* is lost in these cells which might contribute to the observed phenotype. Second, *Bmal1* is known for interacting with a pleiotropy of proteins throughout development of which not all are associated with circadian function. This is most evident in *Bmal1*$^{-/-}$ mice which have a reduced life span along with other severe pathologies (Kondratov et al., 2006). Strikingly, when *Bmal1* expression is abolished after the mice have reached adulthood, many of these pathologies do not develop and the mice show a normal life span (Yang et al., 2016). These findings strongly underline a developmental role for *Bmal1* independent of the generation of molecular oscillations.

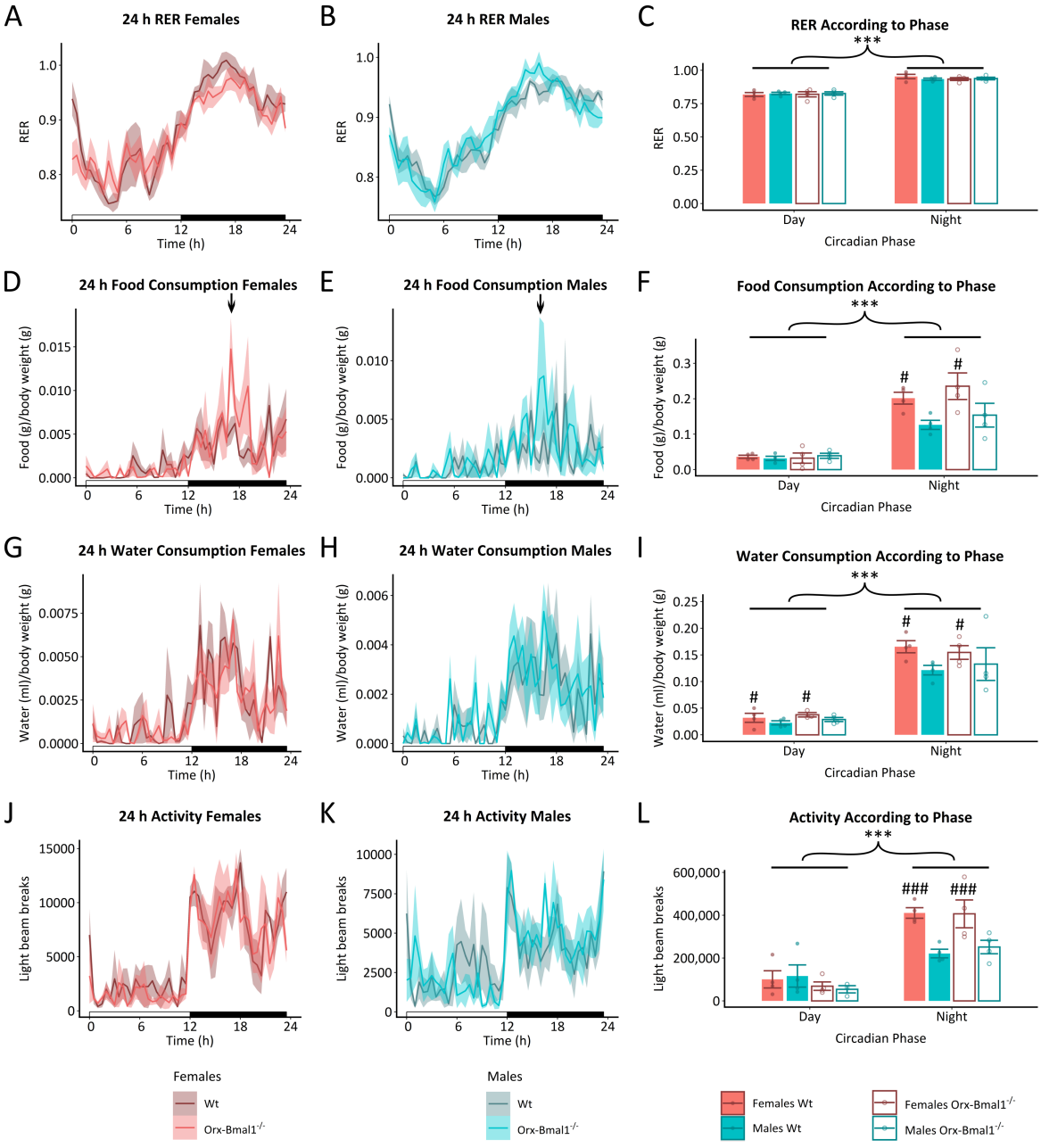

Figure 28 Metabolic cage measurements of female and male Wt and Orx-Bmal1$^{-/-}$ mice. Graphs **A**, **B, D, E, G, H, J,** and **K** show the average 24 h RER, food and water consumption as well as activity determined by light beam breaks. The white and black bars along the x-axis indicate light and dark phases. The shaded area represents the SEM. **C,F, I** and **L** show the mean ± SEM of the RER, food and water consumption, and activity according to circadian phase in each group. Asterisk indicates significant phase effect and hashtag indicates significant sex effect determined by three-way ANOVA. ***p < 0.001, #p < 0.05, ###p < 0.001; Group sizes Wt/Orx-Bmal1$^{-/-}$ mice: females n = 4/3-4 and males n = 4/3-4.

To circumvent these limitations, a virus was generated that enables the Cre mediated knockdown of *Bmal1*. When stereotactically injected into the LH of adult Orx-Cre mice, it allows a region and cell-specific post-developmental *Bmal1* knockdown. This approach combines the spatial restriction of the manipulation of the molecular clock to ORX neurons of the LH with a temporal restriction given by the time point of injection. The virus is based on a vector designed by Ventura and colleagues that initiates the expression of shRNAs for RNA interference based knockdown of a given gene, only after Cre mediated recombination (Ventura et al., 2004). It was cloned into an AAV backbone before adding shRNAs targeting *Bmal1* as described in material and methods (**figure 6**). AAV was chosen as a vector, since the stable integration into the genome as achieved by lentiviruses bears the risk of genetic alterations at the integration site and undesired site effects *in vivo*.

In vitro virus testing for proof of concept was carried out in primary neurons carrying the *Per2*^{Luc} reporter transgene in order to investigate the effect of the viral constructs on molecular oscillations. In these experiments, Cre was provided by the lentivirus L31-2 carrying the coding sequence for the Cre recombinase under the control of the *Synapsin* promoter, which specifically expresses in cells of neuronal fate. L31-2 was already readily available and the integrating nature of the lentivirus was irrelevant in the *in vitro* proof of concept experiments. In a pre-experiment, the optimal multiplicity of infection (MOI) for lentiviral and AAV infection was determined. In all experiments, circadian rhythms in primary neurons were synchronized by a forskolin pulse before recording luciferase activity.

5.5.1. MOI Test

5.5.1.1 Lentivirus L31-2

Different MOIs of L31-2 were tested in primary neurons of *Per2*^{Luc}*-Bmal1-fl* mice. In this experiment, *Bmal1* is excised in neurons infected with the lentivirus due to Cre induced recombination. PER2::LUC rhythms were dampened across all different MOI conditions as compared to untreated control neurons (**figure 29**). One-way ANOVA testing revealed a significant impact of the MOI on the amplitude of PER2::LUC oscillations (**supplementary table 28**). In post-hoc testing, all MOIs were significantly different from the control, although this effect was not robust towards p-value correction (**supplementary table S29**). There were no difference among the amplitudes of neurons treated with the different MOIs.

5.5.1.2 AAV

Primary neurons of *Per2*^{Luc} mice were infected with different MOIs of the AAV mixture containing *Bmal1* shRNA. Due to the absence of Cre in this experiment, the expression of the *Bmal1* shRNA should not be initiated. This experiment served as a control for the sole impact of AAV infection, independent of the molecular manipulation of the clock, on PER2::LUC rhythmicity. Although PER2::LUC rhythms were visually dampened in AAV infected neurons as compared to untreated control cells, this effect did not reach statistical significance according to one-way ANOVA (**figure 29**, **supplementary table S28**). EGFP encoded on the AAV construct was used to determine infection efficiency. Counting of *Egfp* expressing cells showed, that independent of MOI, a maximum of ~ 60 % of the neurons was infected (**figure 29**, **supplementary table S28**).

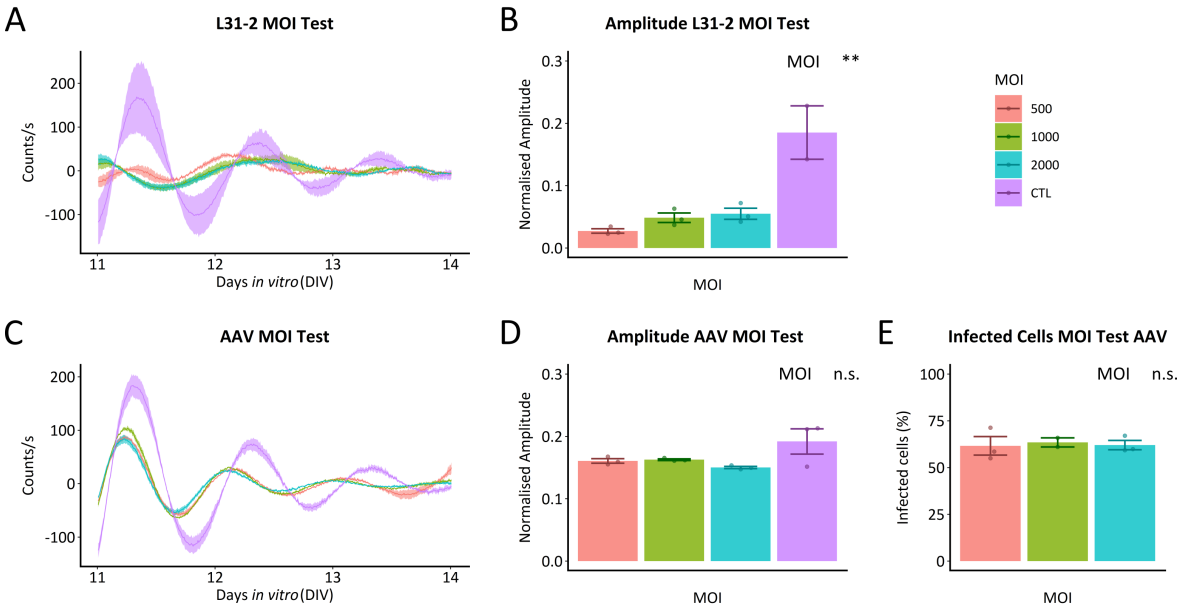

Figure 29 Testing the impact of different MOIs of the lentivirus L31-2 and AAV on PER2::LUC oscillations in primary neurons. The lentivirus L31-2 was tested in *Per2*^{Luc}*-Bmal1-fl* primary neurons and the AAV mixture in *Per2*^{Luc}primary neurons. Graphs in **A** and **C** show the average PER2::LUC signal per group across the investigated time frame. The shaded area represents the SEM. **B** and **D** show the mean amplitude of PER2::LUC oscillations ± SEM of each condition. **E** depicts the percentage of AAV infected cells determined by counting *Egfp* expressing cells. Asterisk indicates significant MOI effect determined by one-way ANOVA. **p < 0.01, n.s. = not significant; Group sizes per MOI n = 2-3.

5.5.2. Cre Dependent Knockdown of *Bmal1*

The proof of concept of the Cre induced shRNA mediated *Bmal1* knockdown was tested in *Per2*^{Luc} primary neurons (**figure 30**). In this experiment, only when the Cre recombinase (delivered by L31-2) and the AAV with the *Bmal1* shRNA are present within the same cell, the knockdown of *Bmal1* can occur. In 5.5.1.1., the amplitude was reduced in neurons treated with any MOI of L31-2 as compared to untreated control neurons although this effect was not robust towards p-value correction. Since there were no differences among the MOIs, the lowest MOI was chosen to continue in order to reduce undesirable effects due to lentiviral integration. In case of the AAV, higher MOIs did not increase the percentage of infected cells and the amplitude was not significantly affected by any MOI. Therefore, a MOI of 500 was chosen for the following experiment. AAVs with scrambled shRNAs without any known murine targets served as a control for ectopic shRNA expression. Furthermore, in order to control for the effects of viral infection on cellular circadian rhythms, additional conditions infected with either only AAVs or lentivirus or no virus at all, were included. Neurons were synchronized twice, once at DIV 8 and once at DIV 13. PER2::LUC oscillations displayed higher amplitude rhythms after the pulse at DIV 13 than after synchronization at DIV 8. From DIV 9 to 13, there was no significant effect of treatment on the amplitude of PER2::LUC rhythms as determined by one-way ANOVA (**supplementary table S30**). This changed after the second synchronization pulse at DIV 13, when treatment significantly impacted the amplitude of PER2::LUC oscillations. Post-hoc testing revealed that the conditions “Bmal1 shRNA + Cre*”, “Bmal1* shRNA” and “Scrambled shRNA + Cre” had lower amplitudes than the untreated control. Further, the amplitude of cells treated with “*Bmal1* shRNA + Cre” was also lower than the amplitude in neurons only treated with Cre. However, none of these effects were robust against correction for multiple testing (**supplementary table S31**).

In the AAVs, the EGFP coding sequence between the two loxP sites is excised after Cre induced recombination (**figure 6**). As a consequence, *Egfp* expression can provide a visual impression on whether recombination took place. By visual inspection, there were more *Egfp* expressing cells in dishes only infected with the *Bmal1* shRNA expressing AAV as compared to cells that were additionally infected with the Cre lentivirus (**figure 31**).

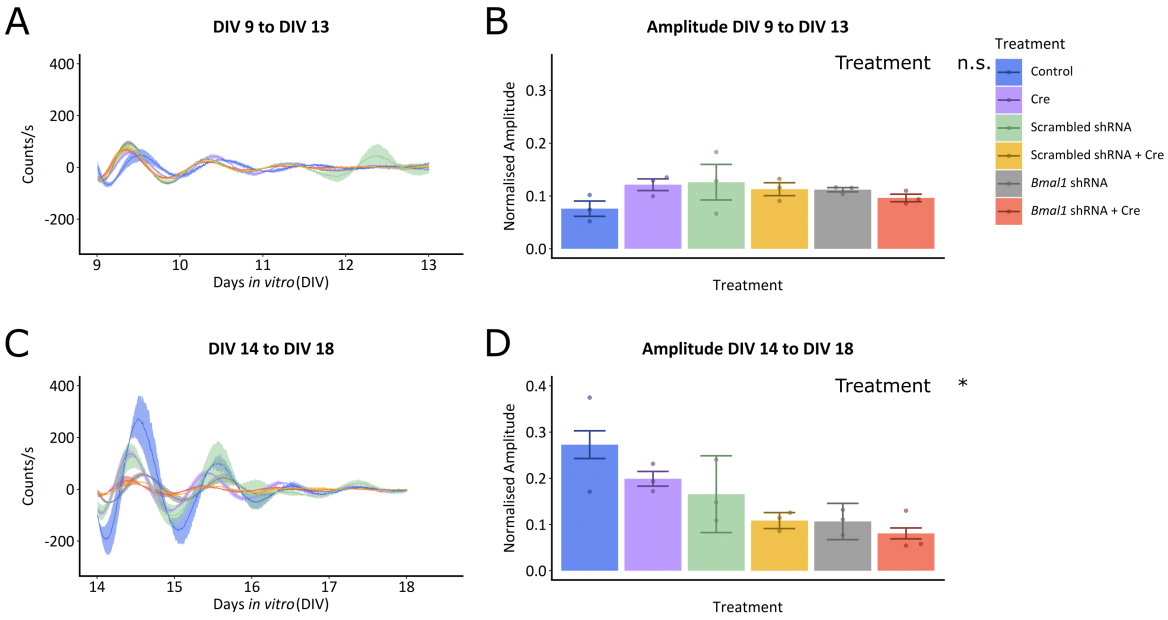

Figure 30 Virus mediated and Cre dependent knockdown of *Bmal1* in *Per2*^{Luc} primary neurons. Two time frames, DIV 9 to DIV 13 and DIV 14 to DIV 18 were analyzed. Graphs in **A** and **C** show the average PER2::LUC signal in each group across the investigated time frames. The shaded area represents the SEM. **B** and **D** show the mean amplitude of PER2::LUC oscillations ± SEM in each group. Asterisk indicates significant MOI effect determined by one-way ANOVA. *p < 0.05, n.s. = not significant; Group sizes per treatment n = 2-3.

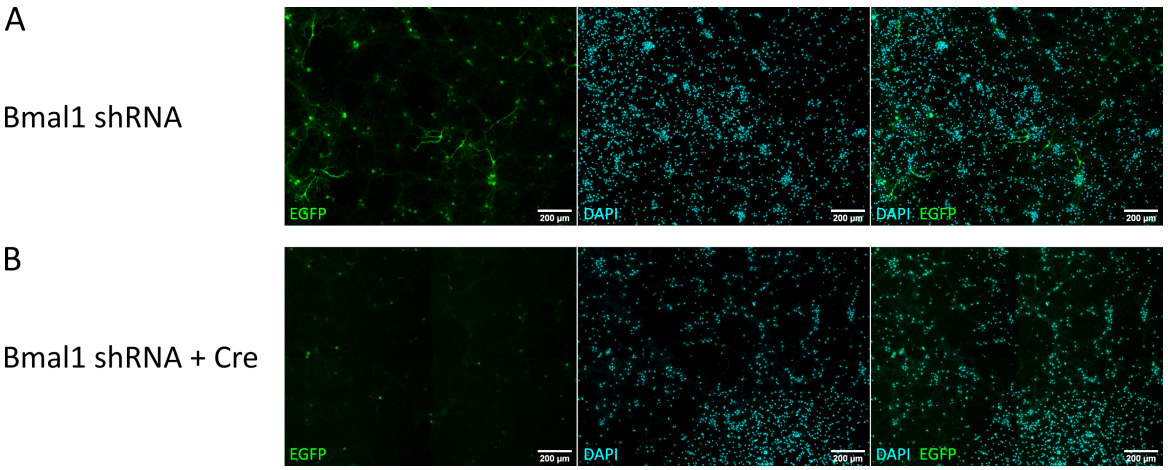

Figure 31 Visual inspection of Cre dependent recombination. EGFP (green) and DAPI (cyan) in primary neurons infected with *Bmal1* shRNA (**A**) or *Bmal1* shRNA + Cre (**B**).

6. Discussion

6.1. *Orx-Cre* Construct Validation

In this thesis, the role of subordinate clocks of ORX neurons of the LH in the regulation of mood- and anxiety-related behavior as well as metabolic processes was investigated. For this purpose, *Bmal1* expression was abolished specifically in this neuronal population This approach was based on the cell-specific expression of the *Orx-Cre* transgene in ORX neurons of the LH. Therefore, as a first step in the generation of Orx-Bmal1$^{-/-}$ mice, the cell-specific expression of the *Orx-Cre* transgene was validated by breeding *Orx-Cre* mice with a Cre reporter mouse line (LSL-Cas9-Egfp mice) in a lineage tracing experiment. In the progeny of these mice, Cre induced recombination leads to the expression of *Egfp*. As a consequence, all cells that have expressed *Orx-Cre* at any given time point of their development or that originate from *Ppox* expressing cells, are labelled by EGFP.

During the validation of *Orx-Cre* transgene specificity in the brain, extensive ectopic recombination appeared in several brain regions, including the SCN, in the progeny of one homozygous *Orx-Cre* mouse. This effect was strongly reduced in the offspring of heterozygous animals and in the final Orx-Bmal1$^{-/-}$ line. In these mice, recombination was mainly restricted to the LH with only very sparse EGFP labeled cells in other brain regions while the SCN was completely devoid of *Egfp* expression.

The discovery of unspecific *Orx-Cre* expression contrasts with the original publication of this transgenic mouse line, where a similar reporter assay for Cre induced recombination was performed (Matsuki et al., 2009). In this study, the authors did not find any ectopic recombination in the brain. However, there are some methodological differences between the assay used in the study of Matsuki and colleagues and the one used in this thesis. In the Cre reporter line used for this thesis, Cre induced *Egfp* expression is driven by the CAG promoter, while Matsuki and colleagues used the promoter of the phosphoglycerate kinase (PGK) (Matsuki et al., 2009). The PGK promoter has been shown to drive comparatively low expression levels that depend strongly on the investigated tissue (Cheng et al., 1993; Qin et al., 2010). In contrast, the CAG promoter is known for its high expression levels (Qin et al., 2010). As a consequence, it is possible that the assay used in this thesis was more sensitive to reveal Cre induced recombination that could not be captured by the previous approach.

Even though it is methodologically possible that the results of this thesis differ from the initial publication of the *Orx-Cre* line, it is still difficult to explain the presence of the strong ectopic recombination in the progeny of the homozygous *Orx-Cre* carrier versus the rather restricted expression of the construct in the heterozygous carrier. However, a previous publication describes

a similar scenario, in which lineage tracing experiments of two groups using one particular Cre driver line led to different results (Gil-Sanz et al., 2015). The authors show that homozygous inbreeding of Cre transgenes can compromise the cell-specific expression of the construct. They attribute the effect to epigenetic changes. Further they demonstrate, that by outbreeding the unspecific expressing Cre line with mice of a different genetic background, construct specificity can be restored. Interestingly, an unpublished study recently identified that the human *PPOX* promoter, which is the promoter driving *Cre* expression in the *Orx-Cre* transgene, is sensitive to methylation and hence susceptible to epigenetic modulation (Seifinejad et al., 2021). Although it is difficult to prove, I assume that this happened in the *Orx-Cre* mice, since the massive ectopic expression was only present in the progeny of the homozygous *Orx-Cre* carrier and was strongly reduced after further breeding heterozygous carriers with other mouse lines to obtain triple transgenic Orx-Cre$^{tg/0}$-Bmal1$^{fl/fl}$-Per2Luc$^{tg/tg}$ mice. Since sparse ectopic recombination is present in most *Cre* transgenes, and the few observed cells in the cortex, hippocampus and cerebellum were neglectable as compared to the whole cellular population of these brain regions, the final Orx-Bmal1$^{-/-}$ line was continued for further analysis. To ensure sustained construct specificity, the *Orx-Cre* construct was kept heterozygous.

6.2. Characterization of Central and Peripheral *Ppox* Expression

In addition to ORX neurons of the LH, *Ppox* expression has been reported in several peripheral tissues in humans and rats and even in some extra-hypothalamic regions of the rodent brain (**table 1**). In contrast, *Ppox* expression in peripheral and extra-hypothalamic central tissues has never been systematically screened in mice. Similarly, the expression of the *Orx-Cre* transgene has mainly been investigated within the brain. Since the Cre induced deletion of *Bmal1* is targeting all *Ppox* expressing cells, 15 peripheral tissues along with 6 brain regions were analyzed for *Ppox* expression, in order to identify the entity of *Ppox* expressing cells in the mouse. Moreover, the expression of the *Orx-Cre* construct in peripheral tissues was investigated by breeding *Orx-Cre* mice with LSL-Cas9-Egfp mice, in which Cre induced recombination is reported by the expression of *Egfp*. Importantly, *Ppox* expression in the hypothalamus has been shown to display a circadian rhythm (Hühne et al., 2022). It is possible that extra-hypothalamic central and peripheral *Ppox* expression sites also underlie circadian control. Since all animals were sacrificed between ZT3 and ZT4, the data presented here is only representative for this particular circadian time frame. In the following, central and peripheral extra-hypothalamic *Ppox* expression is discussed separately.

6.2.1. Peripheral *Ppox* Expression

Peripheral *Ppox* expression was found to be a lot less abundant than expected from previous reports in humans and rats. In a first PCR based screen of cDNA from different peripheral tissues, only testis and kidney showed clear bands of the *Ppox* product. Subsequent qPCR analysis revealed, that *Ppox* expression in the LH, as most known central ORX source, is nearly 3,000 times higher than in the testis, the highest peripheral ORX production site. In comparison, expression in the kidney was 0.03 times lower than in the testis and other peripheral organs failed to display stable expression across all biological replicates. This is in line with Jöhren et al., who reported that *Ppox* expression levels in the rat testis were dramatically decreased as compared to the entire hypothalamus and could only be detected with qPCR but not with the less sensitive method of in-situ-hybridization (Jöhren et al., 2001). In the present work, the difference between LH and testis is even more drastic, since RNA was specifically isolated from the LH of two consecutive 300 µm thin sections, in which most of *Ppox* expressing neurons reside as opposed to the whole hypothalamus.

Still, the results of this work are in contrast to the broad range of human and rat tissues that have been identified as *Ppox* expressing in previous studies as well as the few reports of murine *Ppox* expression in the adrenal glands, pancreas, small intestine, stomach and white adipose tissue. However, this is not the first report of difficulties in reproducing these findings. Baumann et al., reported that they failed to visualize ORX-A or ORX-B in the human and murine rectum, ileum and stomach, despite testing several methods (Baumann et al., 2008). This is in line with attempts of staining for ORX-A or ORX-B in peripheral tissues during the work of this thesis, as it was not possible to visualize the supposedly higher ORX levels in the testis despite several methodological optimization strategies. However, taking into account how low *Ppox* expression is in the periphery, it could also be that the affinity and sensitivity of the antibody used in this thesis was not high enough to detect it.

Another explanation could be differences in *Ppox* baseline expression among different mouse strains. Lin et al., demonstrated that whole brain ORX peptide levels differ significantly among different mouse strains (Lin et al., 2002). In particular, C57BL/6J mice used in this thesis and Baumann's study have comparatively little central amounts of ORX peptide, suggesting that peripheral ORX levels might be even lower (Lin et al., 2002). In line with this hypothesis, the majority of studies on peripheral *Ppox* expression in mice was not done in C57BL/6J but Swiss mice bred, Parks P strain and BALB/c mice (Arafat et al., 2014; de Miguel and Burrell, 2002; Joshi and Singh, 2017).

Despite the fact that it was not possible to directly visualize ORX in any peripheral organ, *Ppox* promoter activity could be investigated with a reporter-based lineage tracing approach, in which all cells that activated their *Ppox* promoter throughout any time point of their development were labeled with EGFP. EGFP could not be detected directly but was visualized by immunohistochemical staining in the pancreas, spleen and stomach. It is important to keep in mind, that *ORX-Cre* is a transgene and is based on the human *PPOX* promoter. This affects the findings on two levels. First, transgenes are subjected to unspecific expression and position effects at their integration site in the genome. Second, it cannot be assured that the human promoter reproduces the murine *Ppox* expression pattern. Due to the lack of success in the present work to visualize ORX in any peripheral organ, it was not possible to confirm the acute presence of ORX in peripheral *Egfp* expressing cells. Therefore, all interpretations regarding developmental activation of *Ppox* remain speculative. While in the spleen, there are only very few single EGFP positive cells, which could represent random unspecific activation of the *ORX-Cre* construct, in the pancreas it is striking how entire pancreatic islets are labelled with EGFP. This matches the cellular location of ORX described in rat pancreatic islets (Adeghate and Hameed, 2011).

The identification of peripheral sources of ORX is linked to the question whether these comparatively low expression sites are of functional relevance. As mentioned, ORX-R have been detected in various peripheral tissues and the peripheral actions of ORX are generally undebated (Skrzypski et al., 2018). However, these do not necessarily require local production sites since central ORX could easily reach its peripheral targets via the bloodstream (Kastin and Akerstrom, 1999). Regarding the testis, a role for ORX in the regulation of testicular development as well as steroidogenesis, spermatogenesis, oxidative stress management and glucose homeostasis in the adult mouse testis was described (Joshi et al., 2018; Joshi and Singh, 2018, 2016). In case of the pancreas, several studies have demonstrated, that ORX is released from rat pancreatic islets and that this is modulated by glucagon and glucose concentrations (Adeghate and Hameed, 2011; Arafat et al., 2014; Ouedraogo et al., 2003). Furthermore, pancreatic *Ppox* expression seems to be sensitive to the overall metabolic state, since it is altered in obesity and diabetes (Adeghate and Hameed, 2011; Arafat et al., 2014). Although I could not demonstrate *Ppox* expression in the mouse pancreas, the results of the PCR screen and qPCR are questionable since the RNA gel indicated a strong degree of RNA degradation in this particular tissue.

6.2.2. Central *Ppox* expression

As expected, *Ppox* expression was highest in the LH. Immunohistochemical staining confirmed the presence of ORX-A positive somas in this area and in the lineage tracing experiment, the majority of these cells also stained for EGFP. The few cells that were only labelled for ORX-A but not EGFP are in line with studies reporting a 50 – 80 % penetrance and 98 % specificity of the human *PPOX* promoter in the mouse hypothalamus (Mickelsen et al., 2017; Moriguchi et al., 2002). Surprisingly, *Ppox* mRNA was detected in extra-hypothalamic brain regions like the cortex, hippocampus, amygdala and cerebellum. The expression levels were substantially decreased as compared to the LH, although expression in the SCN and amygdala was even greater than in the testis. *Ppox* expression in extra-hypothalamic brain regions appeared stably across three biological replicates and in two assays using different primer pairs, which is why the possibility of a methodological artefact can be excluded.

Indeed, although the predominant opinion in the field states the LH as exclusive *Ppox* expression site in the brain, this is not the first report of possible ORX production in other brain regions. Three groups independently described *Ppox* expression in the rodent amygdala and one further observed its expression in the murine striatum (Ciriello et al., 2003; Kim et al., 2017, 2015; Kim and Han, 2016; Saad et al., 2021, 2019; Yamamoto et al., 2010). In line with the observations made in this thesis, when compared to hypothalamic expression, *Ppox* in the striatum was considerably lower (Saad et al., 2019). In case of the amygdala, the authors even observed ORX positive somas (Ciriello et al., 2003; Kim et al., 2015). In contrast, the ORX antibody used in this thesis did not visualize any somas outside the LH. However, this could again be due to insufficient sensitivity of the antibody used in this study. This issue should be circumvented in the lineage tracing experiment, since the CAG promoter driving *Egfp* expression promoter should amplify even low-level endogenous activation of the *Ppox* promoter. Still, only very sparse EGFP labeled cells were observed in the hippocampus, cortex and the cerebellum but not in any other brain region.

As discussed in 6.1., the few *Egfp* expressing cells in the hippocampus, cortex and cerebellum could be the result of unspecific random activation of the *Orx-Cre* transgene. Nevertheless, they could also reflect an earlier transient activation of *Ppox* during development in these cells or in their precursor cells. In the mouse brain, *Ppox* mRNA is first detected at E18 but protein can already be observed at E13/E14 (Ogawa et al., 2017). The same study showed, that the human *PPOX* promoter is able to drive *Egfp* expression in cells within the zone of the developing hypothalamus from E12 onwards. Since there was no further characterization of these cells, no statement on their future

fate can be made. However, since EGFP labelled cells in extra-hypothalamic brain regions were so rare, it is very unlikely that they represent a specific developmental subpopulation.

Saad et al., discuss the possibility of local translation of *Ppox* mRNA in projections of hypothalamic ORX neurons in their target regions (Saad et al., 2019). This could explain the lack of extra-hypothalamic somas stained for ORX in the majority of immunohistochemical assays. Still, *Ppox* mRNA was also detected in the cerebellum, which was nearly devoid of ORX projections in the present and previous studies (Peyron et al., 1998).

Again, these findings of low extra-hypothalamic *Ppox* expression in the brain pose the question of functional relevance. In case of the amygdala, increased *Ppox* expression is associated with depression-like behavior in mice (Kim et al., 2017, 2015; Kim and Han, 2016; Yamamoto et al., 2010). Further it was shown that amygdaloid ORX counteracts the ameliorative impact of exercise on stress induced depression-like behavior and that this effect depends on local *Ppox* expression in this area (Kim et al., 2015). Interestingly, narcoleptic patients, whose ORX levels are chronically decreased, frequently suffer from a symptom called cataplexy, which has been associated with the amygdala (Schiappa et al., 2018). Cataplexy involves the sudden loss of muscle tonus and is frequently triggered by strong emotions. In ORX knockout mice, lesions of the amygdala as well as gene-transfer of the *Ppox* gene to this brain area can reduce cataplectic episodes (Burgess et al., 2013; Liu et al., 2016). One can only speculate that this might be associated with local *Ppox* expression in this region. With respect to *Ppox* expression in the striatum, it was found to be altered following the consumption of sucrose and cocaine, indicating a role in reward and addiction related behavior (Saad et al., 2021, 2019). To my knowledge, there is no data available on *Ppox* expression in any of the other extra-hypothalamic brain regions that were investigated in this thesis. Further studies are required to determine whether the local *Ppox* expression sites in these brain areas are of biological significance and whether they stem from neurons situated in these regions or are the product of local translation in projections of hypothalamic neurons as proposed by Saad and colleagues.

6.3. Circadian Rhythms of Gene Expression in the LH

Signaling of ORX neurons of the LH underlies strong circadian rhythmicity, including rhythmic *Ppox* expression. However, the role of subordinate clocks in ORX neurons in the maintenance of this rhythm has not been investigated. In order to investigate the contribution of subordinate clocks in ORX neurons of the LH to gene expression rhythms in this area, the LH of Orx-Bmal1$^{-/-}$ and Cry1/2$^{-/-}$ mice was isolated at four different time points of the circadian cycle and processed for qPCR analysis.

6.3.1. *Ppox*

Independent of sex, Wt animals displayed significant *Ppox* expression rhythms in the LH. Expression was highest at ZT7 and remained low throughout the rest of the circadian cycle. This is in line with previous publications of *Ppox* expression rhythms in the hypothalamus of nocturnal rodents (Amador et al., 2016; Kohsaka et al., 2007; Taheri et al., 2000; Turek et al., 2005). A range of studies has investigated the rhythmicity of ORX signaling on different levels in nocturnal rodents (**figure 32**). They have unanimously demonstrated that ORX neuron activity is mainly restricted to the active phase (Estabrooke et al., 2001; Hassani et al., 2009; Lee et al., 2005; Marston et al., 2008; Martínez et al., 2002; Nixon and Smale, 2004). Accordingly, the amount of ORX peptide released in the CSF is high during the active phase and low during the rest phase (Deboer et al., 2004; Desarnaud et al., 2004; Fujiki et al., 2001; Yoshida et al., 2001; Zhang et al., 2004). Similarly, more ORX neurons can be immunohistochemically detected during the dark phase indicating increased storage of ORX peptide in the cell during this time (McGregor et al., 2017). Since there is a temporal delay between gene expression and protein availability, the transcriptional peak during the inactive phase provides sufficient time for neuropeptide synthesis and storage, therefore ORX can fulfill its task as the promoter of wakefulness during the active phase.

The fact that the *Ppox* rhythms are lost in Cry1/2$^{-/-}$ mice, which globally lack the molecular oscillator, shows that they are truly generated by the endogenous circadian clock and are not a result of masking by the light-dark cycle. This is in agreement with observations in *Clock-d19* mutant and *Rev-erbα*-deficient mice, which also fail to display *Ppox* expression rhythms in the hypothalamus (Sen et al., 2018; Turek et al., 2005). The lack of the molecular oscillator in Cry1/2$^{-/-}$ results in lower *Ppox* levels when Wt mice reach their peak expression and relatively higher levels throughout the rest of the circadian cycle. In Wt mice, it is probably the peak that is important in order to provide

sufficient levels of arousal throughout the active phase. Interestingly, Cry1/2$^{-/-}$ mice display a hyperactive phenotype which could be indicative of ADHD-like behavior, a disorder that has been associated with hypoarousal and low ORX signaling (Baykal et al., 2019; Strauß et al., 2018). Supporting the idea of an ADHD-like state in Cry1/2$^{-/-}$ mice, *CRY1* variants are linked to ADHD in humans (Onat et al., 2020). However, whether the lack of the *Ppox* expression peak is accompanied by lower ORX peptide levels and hypoarousal in the active phase in Cry1/2$^{-/-}$ mice remains speculative. Another feature of this mouse line is their reduced addictive behavior (Hühne et al., 2022). The increased *Per2* expression supports the negative impact of CRY proteins on addictive behavior: Elevated *Per2* levels are the result of the disabled inhibition of the PER/CRY dimer on their own transcription and as a consequence, Cry1/2$^{-/-}$ mice are not only a model of *Cry* deficiency but also *Per* overexpression. Conversely, studies in mice with decreased *Per* signaling, such as dysfunctional *Per* variants display higher addictive behavior (Gamsby et al., 2013; Spanagel et al., 2005). Similar to the CRY proteins, ORX is negatively correlated to addiction (James et al., 2017a). Hence, the loss of *Ppox* rhythms and particularly the peak expression at ZT7 could be a mechanism on how *Cry* deficiency leads to reduced alcohol consumption in mice (Hühne et al., 2022).

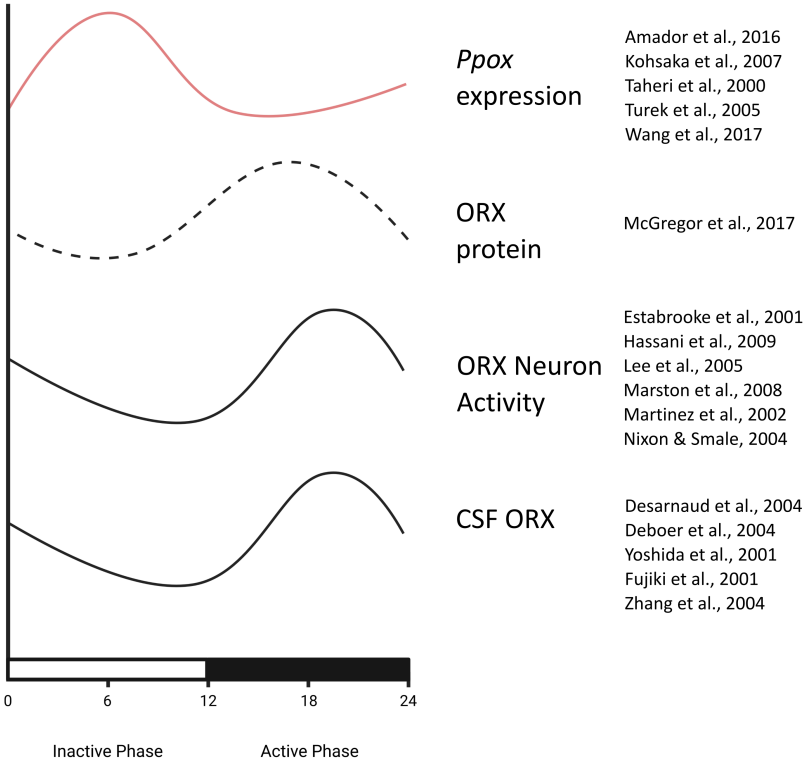

Figure 32 Circadian rhythms of ORX signaling in nocturnal rodents according to results of this thesis (red) and published data (black). *Ppox* expression levels peak during the inactive phase, while ORX neuron activity and CSF levels of ORX peptide are highest during the active phase. The circadian rhythm of ORX protein abundancy is hypothesized based on the ability to detect ORX neurons by immunohistochemical staining at two different time points (the light versus during the dark phase) (dashed line). Created with BioRender.com.

Since Cry1/2$^{-/-}$ mice globally lack the molecular oscillator, they cannot reveal the contribution of local circadian clocks in ORX neurons to *Ppox* rhythms. In contrast, the loss of *Ppox* rhythms in Orx-Bmal1$^{-/-}$ mice, which lack the essential clock gene *Bmal1* specifically in ORX neurons, demonstrates that local subordinate circadian clocks in ORX neurons of the LH are sufficient to generate *Ppox* expression rhythms. In Orx-Bmal1$^{-/-}$ mice, *Ppox* is expressed relatively low at the Wt peak at ZT7 and relatively high during the dark phase. The fact that *Ppox* expression remains at a constant intermediate level throughout the circadian cycle argues against negative effects of *Bmal1* deficiency on ORX neuron development. However, it is not clear how the lack of transcriptional rhythms in ORX neurons affects the circadian fluctuation of ORX peptides and ORX neuron activity. ORX rhythms in the CSF can be abolished by SCN lesion and the SCN has been shown to directly project to ORX neurons (Abrahamson et al., 2001; Deboer et al., 2004; Zhang et al., 2004). This suggests that rhythmic ORX release is under the influence of the master pacemaker whose oscillator is still intact in Orx-Bmal1$^{-/-}$ mice. Further, ORX neurons interact with many other neuronal populations, that could superimpose rhythmic activity of ORX neurons externally. Nevertheless, it can be assumed that the lack of transcriptional rhythms in ORX neurons severely alters the temporal synchronization between transcription, translation, activation, and release. ORX neurons undergo circadian synaptic remodeling, a concept referred to as “chronoconnectivity” (Azeez et al., 2018). This process impacts the circadian responsiveness of the neurons to external stimuli and is most likely impaired in Orx-Bmal1$^{-/-}$ mice. Further, even if ORX release rhythms persist, their amplitude might be dampened due to altered synthesis rhythms, which affect the amount of peptide available to be released. It would be of great interest to further investigate ORX neuron reactivity, synaptic remodeling, and ORX release into the CSF in Orx-Bmal1$^{-/-}$ mice in order to untangle the contribution of local clocks in ORX neurons to different aspects of circadian rhythms of ORX signaling.

6.3.2. *Bmal1*

Due to the specific expression in ORX neurons, *Ppox* rhythms of the LH reflect the rhythms of this neuronal population. In contrast, *Bmal1* is presumably expressed in other cellular populations in this brain region. As a consequence, *Bmal1* expression can be only interpreted as the overall circadian output of the dissected area. In Wt mice, *Bmal1* expression in the LH is not significantly rhythmic. This observation is in line with other studies that do not observe *Bmal1* rhythmicity in the LH of rodents and primates (Mure et al., 2018; Wang et al., 2017). In contrast, *Bmal1* gained rhythmicity in the LH of Orx-Bmal1$^{-/-}$ mice. This observation led to the assumption that the arrhythmicity observed in the LH of Wt mice, might be the result of the interference of two neuronal

populations with antiphasic rhythms (**figure 33**). In this scenario, the antiphasic peaks and troughs of the two neuronal populations cancel each other out and result in an overall arrhythmic output of the circadian oscillator. In support of this hypothesis, *Bmal1* expression levels of biological replicates in Wt mice showed a higher variance than in Orx-Bmal1$^{-/-}$ mice which could indicate the presence of different cellular subpopulations.

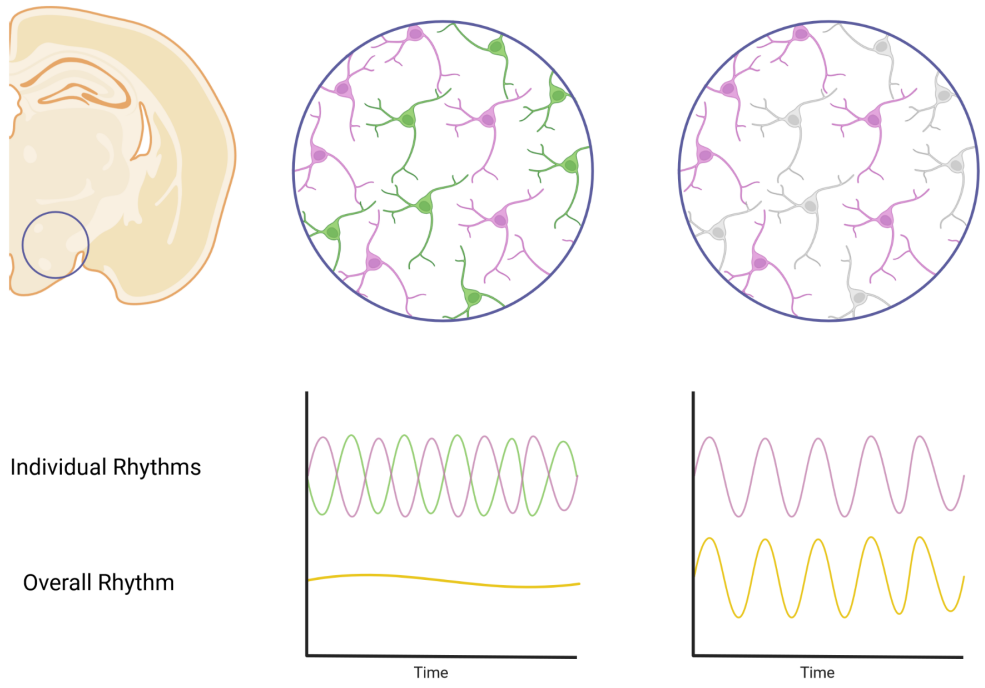

Figure 33 Hypothetical impact of the presence of two anti-phasic rhythmic neuronal populations and the loss of rhythms in one population on the overall rhythmicity of the LH. The molecular oscillators of the green and purple neurons are running in anti-phase. As a consequence, the overall rhythms of the LH (yellow) appears arrhythmic. If the molecular oscillator in the green population is disabled (gray neurons), the rhythm of the purple population dominates and the overall circadian output of the LH becomes rhythmic. Created with BioRender.com.

To further investigate this assumption, the circadian expression of *Pmch* as candidate marker for an antiphasic neuronal population in the LH was analyzed. MCH neurons are often described as the antagonistic players of ORX neurons, due to their prominent role in sleep regulation (Hassani et al., 2009; Ono and Yamanaka, 2017). Due to the interaction effect between genotype, ZT and sex, female and male mice were analyzed separately. For male Wt mice the zero-amplitude test detected a rhythm, however it was not robust towards correction for multiple testing. Male Wt mice showed highest *Pmch* expression at ZT7. Similarly, female Wt mice showed highest expression at ZT7, but no rhythm was detected by the zero-amplitude test. In conclusion, although the impact of ZT in the ANOVA and the detection of a rhythm in male Wt mice before correction for multiple testing suggest rhythmic *Pmch* expression in Wt mice, the evidence is not very strong. Looking into the literature, there is only limited data on *Pmch* expression rhythms and these yield mixed results:

While one study found peak *Pmch* expression at the beginning of the dark phase in rats, no significant rhythms have been reported in other rodent studies (Bluet-Pajot et al., 1995; Stütz et al., 2007; Wang et al., 2017). Similarly, regarding the number of MCH neurons which reflect the amount of immunohistochemically detectable neuropeptide, both the presence and absence of circadian variation has been reported (Gerics et al., 2017; McGregor et al., 2017). With respect to MCH levels in the CSF, studies in rats failing to report circadian differences are contrasted by a report of peak levels during the dark but also a study showing peak levels during the light phase (Dias Abdo Agamme et al., 2015; Noble et al., 2018; Pelluru et al., 2013). Along with methodological differences, the great heterogeneity among results might emerge from rodent sleep structure. Rodents display a polyphasic sleep pattern, meaning that they display several smaller sleep bouts instead of one long consolidated sleep phase (Hiyoshi et al., 2014; Toth and Bhargava, 2013). Although they still mainly sleep during their inactive phase, sleeping bouts can also be observed during their active phase (Hiyoshi et al., 2014). Accordingly, MCH neuron firing has mainly been associated with sleep independent of circadian phase but no overall circadian rhythm of MCH neuron activation has been shown yet (Hassani et al., 2009). As a consequence, MCH signaling might not show such a clear restriction to the inactive phase. Regarding the hypothesis of antiphasic molecular oscillators in ORX and MCH neurons, no clear answer can be given at this stage. In case the observed pattern in *Pmch* expression is the result of a circadian rhythm, it would be in phase with *Ppox* expression. This does not necessarily argue against the presence of antiphasic TTLs in ORX and MCH neurons, since the rhythms could be generated by opposing arms of the TTL. Nevertheless, the presence of *Pmch* expression rhythms needs to be first confirmed, before this hypothesis can be further explored.

ORX and MCH neurons are known to interact (Apergis-Schoute et al., 2015). Therefore, it is possible, that alterations in ORX neuron rhythmicity affect MCH signaling, which is why the expression of *Pmch* in Orx-Bmal1$^{-/-}$ mice was investigated. The zero-amplitude test did not detect *Pmch* rhythms in Orx-Bmal1$^{-/-}$ mice of either sex. Since the existence of *Pmch* expression rhythms in Wt mice is still unclear, no conclusion can be drawn from the lack of it in Orx-Bmal1$^{-/-}$ mice. Further, post-hoc testing did not reveal any significant differences between Wt and Orx-Bmal1$^{-/-}$ mice of each sex despite the significant interaction between ZT and genotype. As a consequence, despite known interactions between ORX and MCH neurons, the current study does not indicate an impact of the loss of circadian rhythmicity in ORX neurons on MCH neurons (Apergis-Schoute et al., 2015).

6.4. Characterization of Orx-Bmal1$^{-/-}$ Mice

6.4.1. Characterization of the Circadian Phenotype

Analysis of locomotor activity rhythms in Orx-Bmal1$^{-/-}$ mice revealed strong circadian rhythmicity of locomotor activity in LD and DD. Analysis of the period revealed no significant differences between genotypes in either condition. In addition, period, amplitude, and dampening of SCN oscillations were not affected by the loss of *Bmal1* in ORX neurons despite known interactions between the two brain areas (Belle et al., 2014; Brown et al., 2008). Regarding the overall locomotor activity, female Orx-Bmal1$^{-/-}$ mice were less active than their Wt counterparts in both LD and DD. However, this is probably due to the different housing numbers in the IntelliCage system (8 Wt vs. 15 Orx-Bmal1$^{-/-}$ mice). In the IntelliCage system, locomotor activity is measured on the basis of corner visits of each individual mouse. The probability of entering a corner is much higher when there is less animals in the cage. This issue is further aggravated by the tendency of mice to fall asleep in the corners. Accordingly, female Wt and Orx-Bmal1$^{-/-}$ mice had similar activity levels in the metabolic cages where animals are single housed and activity is measured by beam breaks. Furthermore, speed and distance travelled were not altered in any of the behavioral tests. In summary, the loss of *Bmal1* rhythms in ORX neurons of the LH did neither affect overall locomotor activity levels nor the rhythmicity of locomotor activity or the SCN.

6.4.2. Characterization of the Behavioral and Metabolic Phenotype

Orx-Bmal1$^{-/-}$ mice underwent a series of behavioral tests in order to evaluate their mood- and anxiety-related phenotype. These tests revealed that Orx-Bmal1$^{-/-}$ behave less anxious in the LDT, are more robust towards stress-induced depression-like behavior in the LHP and more hedonistic in the SPT, which concludes in an overall more resilient phenotype.

As discussed above, it is difficult to draw conclusions about how the altered *Ppox* expression rhythms affect ORX levels in the brain. Behavioral experiments were conducted in the morning, when ORX levels are low in CSF of Wt mice. Hence, the relatively reduced *Ppox* expression in Orx-Bmal1$^{-/-}$ mice at the time of the *Ppox* peak in Wt mice is probably not relevant at this time point. Instead, effects can rather be attributed to the increased mean *Ppox* expression, which is particularly prominent during the active phase in Orx-Bmal1$^{-/-}$ mice, when *Ppox* expression is low in Wt mice. The increased *Ppox* expression during the active phase could be accompanied by increased synthesis and storage of ORX peptide. As a consequence, the stress associated with the

behavioral tests might induce a higher stress-induced ORX release in Orx-Bmal1$^{-/-}$ than in Wt mice. However, further experiments investigating the relationship between the stress response and the ORX system in Orx-Bmal1$^{-/-}$ mice at different circadian time points are required to answer this question.

As mentioned before, both high and low ORX levels have been associated with increased anxiety in rodents (Johnson et al., 2010; Khalil and Fendt, 2017). In support of reduced anxiety-like behavior as a consequence of increased mean *Ppox* expression in Orx-Bmal1$^{-/-}$ mice, ORX-deficient as well as ORX-R1-deficient mice display increased anxiety-like behavior arguing for a negative correlation between ORX signaling and anxiety (Abbas et al., 2015; Khalil and Fendt, 2017). Further, rodent experiments supporting a positive correlation are frequently based on findings of increased anxiety after ORX administration (Avolio et al., 2011; Lungwitz et al., 2012; Suzuki et al., 2005). These exogenously induced states of high ORX might differ from underlying baseline differences as present in Orx-Bmal1$^{-/-}$ and ORX-deficient mice. For instance, the increase in *Ppox* expression in Orx-Bmal1$^{-/-}$ is comparatively smaller and probably in a more physiological range then the injected dose of ORX in other mouse models. Moreover, the effect of exogenously administered ORX on anxiety depends on the investigated brain region, while in mice with baseline differences in ORX signaling all ORX projections sites are affected simultaneously (Lungwitz et al., 2012). Another aspect might be that in experiments in which anxiety-like behavior is induced by exogenous administration of ORX, activation of ORX neurons or in which anxiety is reduced by the inhibition of ORX neurons, the manipulation is transient in otherwise healthy animals. In contrast, ORX-deficient and Orx-Bmal1$^{-/-}$ suffer from chronically altered ORX levels throughout their entire development. As a consequence, the heterogeneous results obtained in different models could reflect different roles for ORX in acute states of anxiety while animal models with underlying genetic manipulations that alter ORX signaling permanently could give more insights on the role of ORX in the development of anxiety-disorders. Nevertheless, at this stage it is still unclear whether the increased mean *Ppox* expression is associated with higher ORX release in Orx-Bmal1$^{-/-}$ mice. Future studies are required to answer this question and enable a full interpretation of the role of ORX signaling in anxiety-related behavior.

In humans, the loss of circadian ORX rhythms in the CSF along with elevated mean ORX levels has been shown to be associated with depression (Salomon et al., 2003). In contrast, loss of *Ppox* rhythms and increased mean expression led to higher resilience to stress-induced depression and increased hedonistic behavior in Orx-Bmal1$^{-/-}$ mice in the present work. Although these results are conflicting, there is one major aspect to be considered when comparing these two studies: In Orx-Bmal1$^{-/-}$ there is only a disruption of the molecular oscillator in ORX neurons and we are

investigating the consequence of the loss of rhythmicity in this particular neuronal population. In the human study however, depressive patients were only assessed for ORX rhythmicity, which does not exclude any other underlying circadian abnormalities such as altered sleep-wake cycles, which might have secondary effects on the rhythmicity of the ORX system. Hence, the dampened circadian ORX rhythms in depressive patients could also be the consequence of an overall dampened rhythmicity whose effects go beyond the loss of ORX rhythms. In line with this assumption, loss of *Ppox* rhythmicity in overall arrhythmic *Clock-d19* mutant mice is associated with decreased mean *Ppox* levels and mania-like behavior, despite other studies indicating a link between lower ORX levels and depression (Brundin et al., 2007; Feng et al., 2014; Hou et al., 2020; Nocjar et al., 2012; Roybal et al., 2007; Turek et al., 2005). In case of Orx-Bmal1$^{-/-}$ mice, it has been demonstrated that C57BL/6J mice, which have reduced ORX levels as compared to other mouse strains, show higher depression-like behavior at baseline (Feng et al., 2014; Lin et al., 2002). It is possible, that the increased mean *Ppox* expression in Orx-Bmal1$^{-/-}$ restored ORX signaling to the physiological range of other mouse strains along with reducing the depression-like behavior. In compliance with this hypothesis, in contrast to Orx-Bmal1$^{-/-}$, Wt mice did not prefer sucrose over water in the SPT indicating anhedonic behavior. Accordingly, lower ORX levels have been associated with reduced addictive behavior (James et al., 2017b).

Another point to be considered is the interaction between the ORX and the stress system which could be an explanation why depression-like behavior in Orx-Bmal1$^{-/-}$ was not detected in the TST but in the LHP. Not only is the LHP associated with higher exposure to acute stress, but also the paradigm represents a complex interaction between learning processes and the stress system in the face of uncontrollable stress. Although it did not reach statistical significance, the effect was slightly more pronounced in female mice, which displayed higher mean *Ppox* expression levels independent of genotype. This is supported by a study that demonstrated that ORX mediates sex differences in response to repeated stress (Grafe et al., 2017). They also reported higher ORX levels in female mice, which were associated with reduced habituation to repeated stress. Another reason for the more pronounced effect in females, could be a reduced pain sensitivity in female Orx-Bmal1$^{-/-}$ mice, although this effect was not robust against correction for multiple testing. As ORX is known to be involved in pain modulation, the generally higher *Ppox* expression in female mice combined with increased *Ppox* expression in Orx-Bmal1$^{-/-}$ could contribute to this phenotype (Razavi and Hosseinzadeh, 2017). Since stress induced reactions depend highly on the nature and duration of the applied stressor it is difficult to compare results from different stress paradigms. Still, a more recent study shed more light on the complex impact of the LHP on the ORX system: Hsu and Wang showed that the LHP affects ORX abundancy in the brain not only in a region specific manner but

also depending on whether ORX-A or ORX-B is investigated (Hsu and Wang, 2021). This implies that the question of whether ORX signaling is up or down regulated in depression strongly depends on the studied brain area and neuropeptide.

The impact of stress needs to be considered as well when interpreting the results of the SPT, since it was conducted after the LHP. Orx-Bmal1$^{-/-}$ mice chose sucrose over water, indicating more hedonistic behavior than Wt mice, who drunk equal amounts of both solutions. Landgraf et al., showed that sucrose preference does not correlate with helplessness in mice (Landgraf et al., 2015). Furthermore, LHP is not considered a trauma-like experience, since it is not capable of inducing persistent behavioral changes in rodents (Schöner et al., 2017). Hence, the 16 weeks between the LHP and SPT in the present study should allow sufficient time for the mice to recover.

The assessment of the metabolic phenotype did not reveal any alterations in Orx-Bmal1$^{-/-}$ mice. Apart from a steeper increase in weight between the age of 5 to 6 weeks in male Orx-Bmal1$^{-/-}$, there were no significant differences to the weight of Wt mice at any age in either sex. Further, within the same sex, animals of both genotypes consumed similar amounts of food and water. Regarding circadian rhythmicity, animals of both genotypes and sexes displayed strong circadian rhythms of the RER along with drinking and feeding behavior. In female and male Orx-Bmal1$^{-/-}$ mice the mean food consumption around ZT17 lay above the mean food consumption in Wt mice. This roughly coincides with the peak of ORX levels in the CSF and could be indicative of altered ORX signaling at this time point. However, since at this stage there is no information on how the loss of *Ppox* expression rhythms affects the signaling of ORX neurons and the release of ORX into the CSF, no further conclusions can be drawn.

The normal weight in Orx-Bmal1$^{-/-}$, whose mean *Ppox* expression levels are higher than in Wt mice, is in line with the protective role of ORX in metabolic dysregulation (Adeghate et al., 2020). Accordingly, *Clock-d19* mutant mice, whose *Ppox* expression remains constantly low, show an obese and hyperphagic phenotype (Turek et al., 2005). It would be interesting to investigate the coping of Orx-Bmal1$^{-/-}$ mice with a metabolic challenge such as HFD. Due to their higher mean *Ppox* expression, they would be expected to be less prone to diet induced obesity. Although a preliminary experiment with HFD was performed which did not find differences to Wt mice (data not shown), this experiment might be inconclusive, since the animals in this experiment varied strongly in age and housing conditions, all factors that are known to influence body weight in mice (Pasquarelli et al., 2017). Further, it would be an option to test different kinds of metabolically challenging diets including high sugar diet.

Kohsaka and colleagues demonstrated that *Ppox* expression rhythms in the LH are lost in mice under HFD (Kohsaka et al., 2007). In their study *Ppox* expression remained at an intermediate level and was even higher than in Wt mice throughout one half of the circadian cycle (Kohsaka et al., 2007). At the moment, it is unclear whether this loss of rhythmicity in Wt mice under HFD represents a pathological consequence of obesity or a protective compensatory mechanism. Investigating the impact of HFD in Orx-Bmal1$^{-/-}$ mice could shed further light on the role of circadian rhythms of ORX signaling in metabolic dysregulation.

Other interesting metabolic aspects that could be examined in Orx-Bmal1$^{-/-}$ mice include food anticipatory behavior and diurnal variations of blood glucose, both of which are lost in animals with deficient ORX signaling (Akiyama et al., 2004; Tsuneki et al., 2015). In summary, although so far there is no evidence for metabolic dysregulation in Orx-Bmal1$^{-/-}$ mice, they still offer the possibility to further explore the role of ORX rhythmicity in the circadian regulation of metabolic processes.

There are some factors limiting the interpretation of the behavioral and metabolic assessment of Orx-Bmal1$^{-/-}$ mice. For instance, to provide a full picture of the effects caused by the loss of *Ppox* rhythmicity, it would be necessary to include *Orx-Cre*$^{tg/0}$*-Per2*$^{Luc\ tg/tg}$ mice as a control, since some transgenic Cre lines display altered behavior independent of recombination (Giusti et al., 2014). Still, it can be assumed that by keeping the mice heterozygous for the transgene, as done in this study, this impact is reduced.

Another point to keep in mind is that although ORX is the dominant marker that defines the population of ORX neurons, it is not the only neuropeptide and neurotransmitter these neurons express. A recent study has provided the full transcriptomic profile of ORX neurons and suggests further subpopulations that might have distinct roles (Mickelsen et al., 2017). At the moment, it is unclear how the loss of *Bmal1* in ORX neurons affects co-expressed genes and how these might contribute to the observed phenotypes. As an example, dynorphin, which is co-expressed in ORX neurons has been associated with reward and stress related behavior (Muschamp et al., 2014; Nocjar et al., 2012). Modern technologies such as single-cell sequencing combined with a circadian experimental design could delineate the full consequences of the loss of *Bmal1* on the circadian expression profile of ORX neurons in the LH.

Finally, there is the issue that *Bmal1*, which has known ubiquitous functions independent of the circadian clock, is missing throughout the entire development of Orx-Bmal1$^{-/-}$ mice. Although the increased mean *Ppox* expression levels argue for a healthy state of ORX neurons, it cannot be known for sure. To overcome this limitation, there are two options. One would be the implementation of an inducible *Orx-Cre* transgene, which can be selectively activated during adulthood. The other

option is based on virus mediated knockdown of *Bmal1* by stereotactic injection into the LH of adult mice. First steps towards this approach have been taken as such a virus has been generated within the work of this thesis.

6.5. Virus Mediated Knockdown of *Bmal1* in ORX Neurons of the LH

In Orx-Bmal1$^{-/-}$ mice *Bmal1* expression is abolished in all *Ppox* expressing cells throughout their entire development. As a consequence, *Bmal1* expression is not exclusively disrupted in the population of ORX neurons of the LH but also other *Ppox* expressing cell populations. Further, due to the strong developmental role of *Bmal1*, loss of *Bmal1* might have additional effects in ORX neurons independent of the disruption of molecular oscillations. In order to circumvent these limitations, a virus was generated that allows the post-developmental knockdown of *Bmal1* in *Ppox* expressing neurons of the LH by Cre induced RNA interference.

Functionality of the virus was tested in primary neurons of *Pe2r*^{Luc} mice that were co-infected with a Cre recombinase. Circadian rhythms were synchronized twice, once at DIV 8 and once at DIV 13. The amplitude of PER2::LUC rhythms was larger after the second synchronization pulse than after the first. This effect is probably due to the increased maturation of primary neurons at DIV 13 as compared to DIV 8. Primary neurons undergo a series of developmental changes after the seeding at DIV 0. This maturation process is associated with the increased formation of intercellular contacts and synapses (Baj et al., 2014; Herholt, 2017). Since cellular coupling is an important feature of circadian synchronization, this could explain the stronger rhythms at DIV 13 (Pilorz et al., 2020). Hence, in future experiments it would be best to determine the earliest time point between DIV 9 and DIV 13 for a strong synchronization and only synchronize once. Both, the handling for the synchronization as well as the environment of the luminometer pose unnecessary stress to the neurons and should be kept as minimal as possible.

None of the treatments had an impact on PER2::LUC rhythms in the time window after the first synchronization pulse at DIV 8. However, treatment did have a significant effect on the amplitude after the second synchronization although none of the differences between any of the groups reached significance after correction for multiple testing in the post-hoc test. In addition, visual inspection of infected primary neurons indicated, that Cre recombination took place since the EGFP signal appeared weaker in primary neurons infected with "*Bmal1* shRNA + Cre" than only with "*Bmal1* shRNA".

When comparing the mean amplitudes of the different conditions, it is obvious, that all viruses-treated conditions have lower mean amplitudes than the untreated control, indicating that viral infection itself affects circadian rhythmicity. In favor of this hypothesis, lowest mean amplitudes are observed in the conditions "*Bmal1* shRNA + Cre" and "Scrambled shRNA + Cre". Since the scrambled shRNA should not interfere with molecular oscillations, the low amplitudes in these two conditions point rather towards a cumulative effect of viral infection on circadian rhythms as these are the only two conditions that were infected with both AAVs and lentivirus. In order to control for this, the conditions "*Bmal1* shRNA" and "Scrambled shRNA" could be co-infected with a dummy lentivirus, which expresses GFP under the control of the *Synapsin* promoter. Further, the AAVs generated by Landgraf et al., that constitutively express the same shRNAs used in this thesis, could be included to assess the efficiency of the conditional knockdown (Landgraf et al., 2016b).

Another aspect that could be optimized is the infection MOI. Although the effect did not reach significance after correction for multiple testing, a MOI of 500 was enough to dampen rhythms in *Per2*^{Luc}*-Bmal1-fl* primary neurons by L31-2 infection. In contrast, the AAVs did not infect more than 60 % of the cells at an MOI of 2000. Consequently, it is possible that not enough neurons were infected to affect the overall luciferase readout of the dish. Nevertheless, it can be expected that increasing the viral load could also increase the negative effects of viral infections on circadian rhythmicity in general.

Primary neurons are highly sensitive and delicate in handling. Since circadian rhythms are strongly coupled to the overall wellbeing and metabolic state of a cell, it is possible that primary neurons are too sensitive as a test system. Another possibility would be to move to organotypic SCN slices from mice ubiquitously expressing the Cre recombinase along with the *Per2*^{Luc} construct. Not only are circadian rhythms in organotypic SCN slices extremely robust but moreover, lentiviral infection could be circumvented.

In summary, at this stage, it is not evident whether the generated virus can achieve the conditional Cre mediated *Bmal1* knockdown it was designed for. However, this might simply be due to the insufficient test system. This question could be finally answered by implementing the optimizations of the test assay as discussed above.

7. Conclusions

This thesis aimed at characterizing the anatomy of ORX production sites and exploring the role of local subordinate clocks in ORX neurons of the LH in the generation of the circadian rhythms in this brain area and their impact on circadian, mood and metabolic phenotypes in mice.

Hypothesis 1:

There are ORX producing cells outside of the LH in central and peripheral tissues of the mouse.

Regarding the characterization of peripheral ORX production sites in the mouse, there were much fewer than expected based on previous reports in humans and rats. Only the testis and the kidney displayed stable *Ppox* expression across 3 biological replicates in 2 independent assays. ORX protein could not be visualized in any of the peripheral tissues, probably due to the low amounts of available peptide, as *Ppox* expression in the testis, which is known for high peripheral *Ppox* expression, was up to 3,000x lower than in the LH. These extremely low levels might be associated with the mouse strain chosen in this thesis, as C57BL/6J mice are known to have comparatively low ORX levels even in the LH. Moreover, all other investigated brain regions showed low but stable *Ppox* expression across the 3 biological replicates in both assays. This challenges the view of the LH as exclusive central ORX production site. No somas could be identified in any brain regions but the LH based on immunohistochemical stainings. As a consequence, the question whether the *Ppox* mRNA in other brain regions indicates the presence of previously unidentified ORX synthetizing neurons or is the product of local translation in ORX projections originating in the LH as well as the functional relevance of this findings remains to be clarified.

Hypothesis 2:

Rhythmicity of ORX neurons of the LH depends on local subordinate clocks in ORX neurons.

Bmal1 expression was successfully abolished in ORX neurons of the LH which lead to the loss of *Ppox* expression rhythms in this area. This is the first evidence showing that *Ppox* expression rhythms in the LH directly depend on the local circadian clock in ORX neurons. In Orx-Bmal1$^{-/-}$ mice, *Ppox* expression was relatively increased at least one circadian time point and relatively decreased during the Wt peak at ZT7. Overall, mean *Ppox* expression across the circadian cycle was increased.

It will be the task of future studies, to resolve how the loss of *Ppox* rhythmicity in the LH affects the circadian rhythms of ORX neuron activity and ORX release into the CSF as well as other target sites.

Interestingly, loss of *Bmal1* in ORX neurons led to a gain of *Bmal1* rhythmicity in the LH. This could be indicative of the presence of two distinct neuronal populations in the LH of Wt animals with antiphasic circadian rhythms which cancel each other out and whose rhythms only become visible once one of the populations loses its rhythm. To further investigate this hypothesis, circadian rhythms of *Pmch* expression in the LH were analyzed as a promising candidate marker for the second antiphasic neuronal population. However, *Pmch* rhythmicity was questionable and peak levels were in phase with peak *Ppox* levels. Although this does not exclude that the TTL in MCH neurons is antiphasic to the TTL in ORX neurons, it also does not support this idea.

Hypothesis 3:

Disruption of local subordinate clocks in ORX neurons affects the mood- and anxiety related behavior, as well as metabolic phenotypes in mice.

Orx-Bmal1$^{-/-}$ mice were extensively characterized regarding their circadian, mood- and anxiety-related as well as metabolic phenotype. They showed normal circadian rhythms of locomotor activity which coincided with functional molecular rhythms in the SCN.

In the behavioral test battery, Orx-Bmal1$^{-/-}$ mice were less anxious in the LDT, more resilient to stress induced depression in the LHP and more hedonic in the SPT. This indicates that the loss of circadian rhythms in ORX neurons has protective effects against depression- and anxiety-like behavior in mice. One mechanism, on how the loss of circadian rhythmicity in ORX neurons positively affects depression- and anxiety-like behavior is the mean increase of *Ppox* expression throughout the circadian cycle, which might rescue the lower baseline ORX levels in C57BL/6J mice. However, it is not clear, how the increase in *Ppox* expression and the loss of the molecular clock in ORX neurons affects rhythms of ORX neuron firing and ORX peptide release. Studies have shown that the effect of ORX on mood- and anxiety-related behavior depends strongly on the investigated target site, which adds a spatial component. In order to fully understand how the loss of rhythmic *Ppox* expression contributes to the observed mood- and anxiety-related phenotypes, it would be necessary to examine its impact on the rhythmicity of ORX neuron firing and ORX peptide release in the CSF and at ORX projection sites in order to provide a full picture of the temporal and spatial dynamics of ORX signaling.

Regarding the metabolic characterization, no differences regarding body weight, diurnal food and water consumption, as well as circadian rhythms of drinking, feeding and RER were detected. As a result, the loss of *Ppox* expression rhythms in the LH and the associated increased mean *Ppox* expression does not seem to cause any obvious metabolic dysregulation. This is in line with the protective role of ORX against metabolic disease. Furthermore, the increase in *Ppox* expression in Orx-Bmal1$^{-/-}$ mice seems to be within a physiological range, compared to the appetite stimulating injections of ORX into the mouse brain, since no increase in food consumption was observed in the present study. Nevertheless, Orx-Bmal1$^{-/-}$ mice might represent an exciting model to study the relevance of ORX rhythms in the circadian regulation of metabolic processes including blood glucose levels and food anticipatory behavior.

Summary

In summary, this thesis has provided important insights into the anatomy of the ORX system and the role of circadian rhythms in ORX neurons in the mouse. It shows that *Ppox* expression in the mouse is not restricted to the LH, although expression levels in other tissues are considerably lower. Moreover, the results show that the *Ppox* expression rhythm directly depends on the local TTL in ORX neurons and that the loss of this rhythm, which results in elevated mean *Ppox* expression, is accompanied by alterations in mood- and anxiety-related behavior pointing towards higher resilience against anxiety- and depression-like behavior.

8. References

Abbas, M.G., Shoji, H., Soya, S., Hondo, M., Miyakawa, T., Sakurai, T., 2015. Comprehensive Behavioral Analysis of Male Ox1r (-/-) Mice Showed Implication of Orexin Receptor-1 in Mood, Anxiety, and Social Behavior. Front Behav Neurosci 9, 324. https://doi.org/10.3389/fnbeh.2015.00324

Abrahamson, E.E., R. K. Leak, Moore, R.Y., 2001. The suprachiasmatic nucleus projects to posterior hypothalamic arousal systems. Neuroreport 12, 435–440.

Adeghate, E., Hameed, R., 2011. Mechanism of orexin B-stimulated insulin and glucagon release from the pancreas of normal and diabetic rats. Pancreas 40, 131–136. https://doi.org/10.1097/MPA.0b013e3181f74b4b

Adeghate, E., Lotfy, M., D'Souza, C., Alseiari, S.M., Alsaadi, A.A., Qahtan, S.A., 2020. Hypocretin/orexin modulates body weight and the metabolism of glucose and insulin. Diabetes Metab Res Rev 36, e3229. https://doi.org/10.1002/dmrr.3229

Adlanmerini, M., Krusen, B.M., Nguyen, H.C.B., Teng, C.W., Woodie, L.N., Tackenberg, M.C., Geisler, C.E., Gaisinsky, J., Peed, L.C., Carpenter, B.J., Hayes, M.R., Lazar, M.A., 2021. REV-ERB nuclear receptors in the suprachiasmatic nucleus control circadian period and restrict diet-induced obesity. Sci. Adv. 7, eabh2007. https://doi.org/10.1126/sciadv.abh2007

Akça, Ö.F., Uzun, N., Kılınç, İ., 2020. Orexin A in adolescents with anxiety disorders. Int J Psychiatry Clin Pract 24, 127–134. https://doi.org/10.1080/13651501.2019.1711425

Akiyama, M., Yuasa, T., Hayasaka, N., Horikawa, K., Sakurai, T., Shibata, S., 2004. Reduced food anticipatory activity in genetically orexin (hypocretin) neuron-ablated mice. Eur J Neurosci 20, 3054–3062. https://doi.org/10.1111/j.1460-9568.2004.03749.x

Allard, J.S., Tizabi, Y., Shaffery, J.P., Manaye, K., 2007. Effects of rapid eye movement sleep deprivation on hypocretin neurons in the hypothalamus of a rat model of depression. Neuropeptides 41, 329–337. https://doi.org/10.1016/j.npep.2007.04.006

Allard, J.S., Tizabi, Y., Shaffery, J.P., Trouth, C.O., Manaye, K., 2004. Stereological analysis of the hypothalamic hypocretin/orexin neurons in an animal model of depression. Neuropeptides 38, 311–315. https://doi.org/10.1016/j.npep.2004.06.004

Almeneessier, A.S., Alzoghaibi, M., BaHammam, A.A., Ibrahim, M.G., Olaish, A.H., Nashwan, S.Z., BaHammam, A.S., 2018. The effects of diurnal intermittent fasting on the wake-promoting neurotransmitter orexin-A. Ann Thorac Med 13, 48–54. https://doi.org/10.4103/atm.ATM_181_17

Amador, A., Wang, Y., Banerjee, S., Kameneka, T.M., Solt, L.A., Burris, T.P., 2016. Pharmacological and Genetic Modulation of REV-ERB Activity and Expression Affects Orexigenic Gene Expression. PLoS One 11, e0151014. https://doi.org/10.1371/journal.pone.0151014

American Psychiatric Association (Ed.), 2013. Diagnostic and statistical manual of mental disorders: DSM-5, 5th ed. ed. American Psychiatric Association, Washington, D.C.

Anand, S.N., Maywood, E.S., Chesham, J.E., Joynson, G., Banks, G.T., Hastings, M.H., Nolan, P.M., 2013. Distinct and separable roles for endogenous CRY1 and CRY2 within the circadian molecular clockwork of the suprachiasmatic nucleus, as revealed by the Fbxl3(Afh) mutation. J Neurosci 33, 7145–7153. https://doi.org/10.1523/JNEUROSCI.4950-12.2013

Antunes, L.C., Levandovski, R., Dantas, G., Caumo, W., Hidalgo, M.P., 2010. Obesity and shift work: chronobiological aspects. Nutr Res Rev 23, 155–168. https://doi.org/10.1017/S0954422410000016

Apergis-Schoute, J., Iordanidou, P., Faure, C., Jego, S., Schöne, C., Aitta-Aho, T., Adamantidis, A., Burdakov, D., 2015. Optogenetic evidence for inhibitory signaling from orexin to MCH neurons via local microcircuits. J Neurosci 35, 5435–5441. https://doi.org/10.1523/JNEUROSCI.5269-14.2015

Arafat, A.M., Kaczmarek, P., Skrzypski, M., Pruszyńska-Oszmałek, E., Kołodziejski, P., Adamidou, A., Ruhla, S., Szczepankiewicz, D., Sassek, M., Billert, M., Wiedenmann, B., Pfeiffer, A.F.H., Nowak, K.W., Strowski, M.Z., 2014. Glucagon regulates orexin A secretion in humans and rodents. Diabetologia 57, 2108–2116. https://doi.org/10.1007/s00125-014-3335-4

Arble, D.M., Bass, J., Laposky, A.D., Vitaterna, M.H., Turek, F.W., 2009. Circadian timing of food intake contributes to weight gain. Obesity (Silver Spring) 17, 2100–2102. https://doi.org/10.1038/oby.2009.264

Arendt, D.H., Ronan, P.J., Oliver, K.D., Callahan, L.B., Summers, T.R., Summers, C.H., 2013. Depressive behavior and activation of the orexin/hypocretin system. Behav. Neurosci. 127, 86–94. https://doi.org/10.1037/a0031442

Arihara, Z., Takahashi, K., Murakami, O., Totsune, K., Sone, M., Satoh, F., Ito, S., Mouri, T., 2001. Immunoreactive orexin-A in human plasma. Peptides 22, 139–142. https://doi.org/10.1016/s0196-9781(00)00369-7

Avolio, E., Alò, R., Carelli, A., Canonaco, M., 2011. Amygdalar orexinergic-GABAergic interactions regulate anxiety behaviors of the Syrian golden hamster. Behav Brain Res 218, 288–295. https://doi.org/10.1016/j.bbr.2010.11.014

Azeez, I.A., Del Gallo, F., Cristino, L., Bentivoglio, M., 2018. Daily Fluctuation of Orexin Neuron Activity and Wiring: The Challenge of "Chronoconnectivity." Front Pharmacol 9, 1061. https://doi.org/10.3389/fphar.2018.01061

Azeez, I.A., Igado, O.O., Olopade, J.O., 2021. An overview of the orexinergic system in different animal species. Metab Brain Dis 36, 1419–1444. https://doi.org/10.1007/s11011-021-00761-0

Baj, G., Patrizio, A., Montalbano, A., Sciancalepore, M., Tongiorgi, E., 2014. Developmental and maintenance defects in Rett syndrome neurons identified by a new mouse staging system in vitro. Front Cell Neurosci 8, 18. https://doi.org/10.3389/fncel.2014.00018

Barca-Mayo, O., Pons-Espinal, M., Follert, P., Armirotti, A., Berdondini, L., De Pietri Tonelli, D., 2017. Astrocyte deletion of Bmal1 alters daily locomotor activity and cognitive functions via GABA signalling. Nat Commun 8, 14336. https://doi.org/10.1038/ncomms14336

Barnea, M., Madar, Z., Froy, O., 2009. High-fat diet delays and fasting advances the circadian expression of adiponectin signaling components in mouse liver. Endocrinology 150, 161–168. https://doi.org/10.1210/en.2008-0944

Barreiro, M.L., Pineda, R., Gaytan, F., Archanco, M., Burrell, M.A., Castellano, J.M., Hakovirta, H., Nurmio, M., Pinilla, L., Aguilar, E., Toppari, J., Dieguez, C., Tena-Sempere, M., 2005. Pattern of orexin expression and direct biological actions of orexin-a in rat testis. Endocrinology 146, 5164–5175. https://doi.org/10.1210/en.2005-0455

Baumann, C.R., Clark, E.L., Pedersen, N.P., Hecht, J.L., Scammell, T.E., 2008. Do enteric neurons make hypocretin? Regul Pept 147, 1–3. https://doi.org/10.1016/j.regpep.2007.11.006

Baykal, S., Albayrak, Y., Durankuş, F., Güzel, S., Abbak, Ö., Potas, N., Beyazyüz, M., Karabekiroğlu, K., Donma, M.M., 2019. Decreased serum orexin A levels in drug-naive children with attention deficit and hyperactivity disorder. Neurol Sci 40, 593–602. https://doi.org/10.1007/s10072-018-3692-8

Belle, M.D.C., Hughes, A.T.L., Bechtold, D.A., Cunningham, P., Pierucci, M., Burdakov, D., Piggins, H.D., 2014. Acute suppressive and long-term phase modulation actions of orexin on the mammalian circadian clock. J Neurosci 34, 3607–3621. https://doi.org/10.1523/JNEUROSCI.3388-13.2014

Bering, T., Carstensen, M.B., Wörtwein, G., Weikop, P., Rath, M.F., 2018. The Circadian Oscillator of the Cerebral Cortex: Molecular, Biochemical and Behavioral Effects of Deleting the Arntl Clock Gene in Cortical Neurons. Cereb Cortex 28, 644–657. https://doi.org/10.1093/cercor/bhw406

Blanco, M., Gallego, R., García-Caballero, T., Diéguez, C., Beiras, A., 2003. Cellular localization of orexins in human anterior pituitary. Histochem Cell Biol 120, 259–264. https://doi.org/10.1007/s00418-003-0562-z

Blouin, A.M., Fried, I., Wilson, C.L., Staba, R.J., Behnke, E.J., Lam, H.A., Maidment, N.T., Karlsson, K.Æ., Lapierre, J.L., Siegel, J.M., 2013. Human hypocretin and melanin-concentrating hormone levels are linked to emotion and social interaction. Nat Commun 4, 1547. https://doi.org/10.1038/ncomms2461

Bluet-Pajot, M.T., Presse, F., Voko, Z., Hoeger, C., Mounier, F., Epelbaum, J., Nahon, J.L., 1995. Neuropeptide-E-I antagonizes the action of melanin-concentrating hormone on stress-induced release of adrenocorticotropin in the rat. J Neuroendocrinol 7, 297–303. https://doi.org/10.1111/j.1365-2826.1995.tb00761.x

Boddum, K., Hansen, M.H., Jennum, P.J., Kornum, B.R., 2016. Cerebrospinal Fluid Hypocretin-1 (Orexin-A) Level Fluctuates with Season and Correlates with Day Length. PLoS ONE 11, e0151288. https://doi.org/10.1371/journal.pone.0151288

Bourin, M., Hascoët, M., 2003. The mouse light/dark box test. Eur J Pharmacol 463, 55–65. https://doi.org/10.1016/s0014-2999(03)01274-3

Brown, T.M., Coogan, A.N., Cutler, D.J., Hughes, A.T., Piggins, H.D., 2008. Electrophysiological actions of orexins on rat suprachiasmatic neurons in vitro. Neurosci Lett 448, 273–278. https://doi.org/10.1016/j.neulet.2008.10.058

Brundin, L., Björkqvist, M., Petersén, A., Träskman-Bendz, L., 2007. Reduced orexin levels in the cerebrospinal fluid of suicidal patients with major depressive disorder. Eur Neuropsychopharmacol 17, 573–579. https://doi.org/10.1016/j.euroneuro.2007.01.005

Brundin, L., Björkqvist, M., Träskman-Bendz, L., Petersén, A., 2009. Increased orexin levels in the cerebrospinal fluid the first year after a suicide attempt. J Affect Disord 113, 179–182. https://doi.org/10.1016/j.jad.2008.04.011

Burgess, C.R., Oishi, Y., Mochizuki, T., Peever, J.H., Scammell, T.E., 2013. Amygdala lesions reduce cataplexy in orexin knock-out mice. J Neurosci 33, 9734–9742. https://doi.org/10.1523/JNEUROSCI.5632-12.2013

Carroll, D., Phillips, A.C., Thomas, G.N., Gale, C.R., Deary, I., Batty, G.D., 2009. Generalized anxiety disorder is associated with metabolic syndrome in the Vietnam experience study. Biol Psychiatry 66, 91–93. https://doi.org/10.1016/j.biopsych.2009.02.020

Cedernaes, J., Huang, W., Ramsey, K.M., Waldeck, N., Cheng, L., Marcheva, B., Omura, C., Kobayashi, Y., Peek, C.B., Levine, D.C., Dhir, R., Awatramani, R., Bradfield, C.A., Wang, X.A., Takahashi, J.S., Mokadem, M., Ahima, R.S., Bass, J., 2019. Transcriptional Basis for Rhythmic Control of Hunger and Metabolism within the AgRP Neuron. Cell Metab. 29, 1078-1091.e5. https://doi.org/10.1016/j.cmet.2019.01.023

Cell Press, 2011. Why narcoleptics get fat. ScienceDaily. URL www.sciencedaily.com/releases/2011/10/111004123558.htm (accessed 3.3.22).

Cengiz, M., Karaj, V., Kocabasoğlu, N., Gozubatik-Celik, G., Dirican, A., Bayoglu, B., 2019. Orexin/hypocretin receptor, Orx1, gene variants are associated with major depressive disorder. Int J Psychiatry Clin Pract 23, 114–121. https://doi.org/10.1080/13651501.2018.1551549

Chemelli, R.M., Willie, J.T., Sinton, C.M., Elmquist, J.K., Scammell, T., Lee, C., Richardson, J.A., Williams, S.C., Xiong, Y., Kisanuki, Y., Fitch, T.E., Nakazato, M., Hammer, R.E., Saper, C.B., Yanagisawa, M., 1999. Narcolepsy in orexin knockout mice: molecular genetics of sleep regulation. Cell 98, 437–451.

Chen, R., Weitzner, A.S., McKennon, L.A., Fonken, L.K., 2021. Chronic circadian phase advance in male mice induces depressive-like responses and suppresses neuroimmune activation. Brain Behav Immun Health 17, 100337. https://doi.org/10.1016/j.bbih.2021.100337

Chen, X., Wang, H., Lin, Z., Li, S., Li, Y., Bergen, H.T., Vrontakis, M.E., Kirouac, G.J., 2014. Orexins (hypocretins) contribute to fear and avoidance in rats exposed to a single episode of footshocks. Brain Struct Funct 219, 2103–2118. https://doi.org/10.1007/s00429-013-0626-3

Chen, Z., Zhao, S., Tian, S., Yan, R., Wang, H., Wang, X., Zhu, R., Xia, Y., Yao, Z., Lu, Q., 2021. Diurnal Mood Variation Symptoms in Major Depressive Disorder Associated with Evening

Chronotype: Evidence from a Neuroimaging Study. J Affect Disord S0165-0327(21)01155–1. https://doi.org/10.1016/j.jad.2021.10.087

Cheng, L., Ziegelhoffer, P.R., Yang, N.S., 1993. In vivo promoter activity and transgene expression in mammalian somatic tissues evaluated by using particle bombardment. Proc. Natl. Acad. Sci. U.S.A. 90, 4455–4459. https://doi.org/10.1073/pnas.90.10.4455

Chrobok, L., Alwani, A., Pradel, K., Daniela Klich, J., Henryk Lewandowski, M., 2021. Orexin A excites the rat olivary pretectal nucleus via OX2 receptor in a daily manner. Brain Res 147603. https://doi.org/10.1016/j.brainres.2021.147603

Chung, H.-S., Kim, J.-G., Kim, J.-W., Kim, H.-W., Yoon, B.-J., 2014. Orexin administration to mice that underwent chronic stress produces bimodal effects on emotion-related behaviors. Regul. Pept. 194–195, 16–22. https://doi.org/10.1016/j.regpep.2014.11.003

Ciriello, J., Rosas-Arellano, M.P., Solano-Flores, L.P., de Oliveira, C.V.R., 2003. Identification of neurons containing orexin-B (hypocretin-2) immunoreactivity in limbic structures. Brain Res 967, 123–131. https://doi.org/10.1016/s0006-8993(02)04233-6

Cornelissen, G., 2014. Cosinor-based rhythmometry. Theor Biol Med Model 11, 16. https://doi.org/10.1186/1742-4682-11-16

Cryan, J.F., Mombereau, C., Vassout, A., 2005. The tail suspension test as a model for assessing antidepressant activity: review of pharmacological and genetic studies in mice. Neurosci Biobehav Rev 29, 571–625. https://doi.org/10.1016/j.neubiorev.2005.03.009

Cutler, D.J., Morris, R., Sheridhar, V., Wattam, T.A.K., Holmes, S., Patel, S., Arch, J.R.S., Wilson, S., Buckingham, R.E., Evans, M.L., Leslie, R.A., Williams, G., 1999. Differential distribution of orexin-A and orexin-B immunoreactivity in the rat brain and spinal cord☆. Peptides 20, 1455–1470. https://doi.org/10.1016/S0196-9781(99)00157-6

Dallmann, R., Weaver, D.R., 2010. Altered body mass regulation in male mPeriod mutant mice on high-fat diet. Chronobiol Int 27, 1317–1328. https://doi.org/10.3109/07420528.2010.489166

Damiola, F., Le Minh, N., Preitner, N., Kornmann, B., Fleury-Olela, F., Schibler, U., 2000. Restricted feeding uncouples circadian oscillators in peripheral tissues from the central pacemaker in the suprachiasmatic nucleus. Genes Dev 14, 2950–2961. https://doi.org/10.1101/gad.183500

de Lecea, L., Kilduff, T.S., Peyron, C., Gao, X., Foye, P.E., Danielson, P.E., Fukuhara, C., Battenberg, E.L., Gautvik, V.T., Bartlett, F.S., Frankel, W.N., van den Pol, A.N., Bloom, F.E., Gautvik, K.M., Sutcliffe, J.G., 1998. The hypocretins: hypothalamus-specific peptides with neuroexcitatory activity. Proc. Natl. Acad. Sci. U.S.A. 95, 322–327.

de Miguel, M.J.S., Burrell, M.A., 2002. Immunocytochemical detection of orexin A in endocrine cells of the developing mouse gut. J. Histochem. Cytochem. 50, 63–69. https://doi.org/10.1177/002215540205000107

de Zavalia, N., Schoettner, K., Goldsmith, J.A., Solis, P., Ferraro, S., Parent, G., Amir, S., 2021. Bmal1 in the striatum influences alcohol intake in a sexually dimorphic manner. Commun Biol 4, 1227. https://doi.org/10.1038/s42003-021-02715-9

Deats, S.P., Adidharma, W., Lonstein, J.S., Yan, L., 2014. Attenuated orexinergic signaling underlies depression-like responses induced by daytime light deficiency. Neuroscience 272, 252–260. https://doi.org/10.1016/j.neuroscience.2014.04.069

Deboer, T., Overeem, S., Visser, N. a. H., Duindam, H., Frölich, M., Lammers, G.J., Meijer, J.H., 2004. Convergence of circadian and sleep regulatory mechanisms on hypocretin-1. Neuroscience 129, 727–732. https://doi.org/10.1016/j.neuroscience.2004.07.049

Desarnaud, F., Murillo-Rodriguez, E., Lin, L., Xu, M., Gerashchenko, D., Shiromani, S.N., Nishino, S., Mignot, E., Shiromani, P.J., 2004. The diurnal rhythm of hypocretin in young and old F344 rats. Sleep 27, 851–856. https://doi.org/10.1093/sleep/27.5.851

Dias Abdo Agamme, A.L., Aguilar Calegare, B.F., Fernandes, L., Costa, A., Lagos, P., Torterolo, P., D'Almeida, V., 2015. MCH levels in the CSF, brain preproMCH and MCHR1 gene expression

during paradoxical sleep deprivation, sleep rebound and chronic sleep restriction. Peptides 74, 9–15. https://doi.org/10.1016/j.peptides.2015.10.001

Difrancesco, S., Lamers, F., Riese, H., Merikangas, K.R., Beekman, A.T.F., van Hemert, A.M., Schoevers, R.A., Penninx, B.W.J.H., 2019. Sleep, circadian rhythm, and physical activity patterns in depressive and anxiety disorders: A 2-week ambulatory assessment study. Depress Anxiety 36, 975–986. https://doi.org/10.1002/da.22949

Dodel, R., Peter, H., Spottke, A., Noelker, C., Althaus, A., Siebert, U., Walbert, T., Kesper, K., Becker, H.F., Mayer, G., 2007. Health-related quality of life in patients with narcolepsy. Sleep Med 8, 733–741. https://doi.org/10.1016/j.sleep.2006.10.010

Ehrström, M., Gustafsson, T., Finn, A., Kirchgessner, A., Grybäck, P., Jacobsson, H., Hellström, P.M., Näslund, E., 2005. Inhibitory effect of exogenous orexin a on gastric emptying, plasma leptin, and the distribution of orexin and orexin receptors in the gut and pancreas in man. J. Clin. Endocrinol. Metab. 90, 2370–2377. https://doi.org/10.1210/jc.2004-1408

Elbaz, I., Yelin-Bekerman, L., Nicenboim, J., Vatine, G., Appelbaum, L., 2012. Genetic ablation of hypocretin neurons alters behavioral state transitions in zebrafish. J Neurosci 32, 12961–12972. https://doi.org/10.1523/JNEUROSCI.1284-12.2012

Emens, J.S., Berman, A.M., Thosar, S.S., Butler, M.P., Roberts, S.A., Clemons, N.A., Herzig, M.X., McHill, A.W., Morimoto, M., Bowles, N.P., Shea, S.A., 2020. Circadian rhythm in negative affect: Implications for mood disorders. Psychiatry Res 293, 113337. https://doi.org/10.1016/j.psychres.2020.113337

España, R.A., Oleson, E.B., Locke, J.L., Brookshire, B.R., Roberts, D.C.S., Jones, S.R., 2010. The hypocretin-orexin system regulates cocaine self-administration via actions on the mesolimbic dopamine system. Eur. J. Neurosci. 31, 336–348. https://doi.org/10.1111/j.1460-9568.2009.07065.x

Espinosa-Salinas, I., San-Cristobal, R., Colmenarejo, G., Loria-Kohen, V., Molina, S., Reglero, G., Ramirez de Molina, A., Martinez, J.A., 2020. Polymorphic Appetite Effects on Waist Circumference Depend on rs3749474 CLOCK Gene Variant. Nutrients 12, E1846. https://doi.org/10.3390/nu12061846

Estabrooke, I.V., McCarthy, M.T., Ko, E., Chou, T.C., Chemelli, R.M., Yanagisawa, M., Saper, C.B., Scammell, T.E., 2001. Fos expression in orexin neurons varies with behavioral state. J. Neurosci. 21, 1656–1662.

Feng, P., Hu, Y., Vurbic, D., Akladious, A., Strohl, K.P., 2014. Chromosome 1 replacement increases brain orexins and antidepressive measures without increasing locomotor activity. J Psychiatr Res 59, 140–147. https://doi.org/10.1016/j.jpsychires.2014.08.008

Feng, P., Vurbic, D., Wu, Z., Hu, Y., Strohl, K.P., 2008. Changes in brain orexin levels in a rat model of depression induced by neonatal administration of clomipramine. J. Psychopharmacol. (Oxford) 22, 784–791. https://doi.org/10.1177/0269881106082899

Feng, P., Vurbic, D., Wu, Z., Strohl, K.P., 2007. Brain orexins and wake regulation in rats exposed to maternal deprivation. Brain Res 1154, 163–172. https://doi.org/10.1016/j.brainres.2007.03.077

Firouzabadi, N., Navabzadeh, N., Moghimi-Sarani, E., Haghnegahdar, M., 2020. Orexin/Hypocretin Type 2 Receptor (HCRTR2) Gene as a Candidate Gene in Sertraline-Associated Insomnia in Depressed Patients. Neuropsychiatr Dis Treat 16, 1121–1128. https://doi.org/10.2147/NDT.S250141

Fonken, L.K., Workman, J.L., Walton, J.C., Weil, Z.M., Morris, J.S., Haim, A., Nelson, R.J., 2010. Light at night increases body mass by shifting the time of food intake. Proc Natl Acad Sci U S A 107, 18664–18669. https://doi.org/10.1073/pnas.1008734107

Fujiki, N., Yoshida, Y., Ripley, B., Honda, K., Mignot, E., Nishino, S., 2001. Changes in CSF hypocretin-1 (orexin A) levels in rats across 24 hours and in response to food deprivation. Neuroreport 12, 993–997. https://doi.org/10.1097/00001756-200104170-00026

Fujiki, N., Yoshida, Y., Zhang, S., Sakurai, T., Yanagisawa, M., Nishino, S., 2006. Sex difference in body weight gain and leptin signaling in hypocretin/orexin deficient mouse models. Peptides 27, 2326–2331. https://doi.org/10.1016/j.peptides.2006.03.011

Funabashi, T., Hagiwara, H., Mogi, K., Mitsushima, D., Shinohara, K., Kimura, F., 2009. Sex differences in the responses of orexin neurons in the lateral hypothalamic area and feeding behavior to fasting. Neurosci Lett 463, 31–34. https://doi.org/10.1016/j.neulet.2009.07.035

Gamsby, J.J., Templeton, E.L., Bonvini, L.A., Wang, W., Loros, J.J., Dunlap, J.C., Green, A.I., Gulick, D., 2013. The circadian Per1 and Per2 genes influence alcohol intake, reinforcement, and blood alcohol levels. Behav Brain Res 249, 15–21. https://doi.org/10.1016/j.bbr.2013.04.016

Geissmann, Q., Garcia Rodriguez, L., Beckwith, E.J., Gilestro, G.F., 2019. Rethomics: An R framework to analyse high-throughput behavioural data. PLoS ONE 14, e0209331. https://doi.org/10.1371/journal.pone.0209331

Geoffroy, P.A., Palagini, L., 2021. Biological rhythms and chronotherapeutics in depression. Prog Neuropsychopharmacol Biol Psychiatry 106, 110158. https://doi.org/10.1016/j.pnpbp.2020.110158

Gerics, B., Szalay, F., Sótonyi, P., Jancsik, V., 2017. Diurnal variation of the melanin-concentrating hormone level in the hypothalamus. Acta Biol Hung 68, 14–21. https://doi.org/10.1556/018.68.2017.1.2

Geyer, M.A., McIlwain, K.L., Paylor, R., 2002. Mouse genetic models for prepulse inhibition: an early review. Mol Psychiatry 7, 1039–1053. https://doi.org/10.1038/sj.mp.4001159

Gil-Sanz, C., Espinosa, A., Fregoso, S.P., Bluske, K.K., Cunningham, C.L., Martinez-Garay, I., Zeng, H., Franco, S.J., Müller, U., 2015. Lineage Tracing Using Cux2-Cre and Cux2-CreERT2 Mice. Neuron 86, 1091–1099. https://doi.org/10.1016/j.neuron.2015.04.019

Giusti, S.A., Vercelli, C.A., Vogl, A.M., Kolarz, A.W., Pino, N.S., Deussing, J.M., Refojo, D., 2014. Behavioral phenotyping of Nestin-Cre mice: implications for genetic mouse models of psychiatric disorders. J Psychiatr Res 55, 87–95. https://doi.org/10.1016/j.jpsychires.2014.04.002

Goldstein, N., Tsuneki, H., Bhandarkar, N., Aimaretti, E., Haim, Y., Kon, K., Sato, K., Wada, T., Liberty, I.F., Kirshtein, B., Dukhno, O., Maixner, N., Gepner, Y., Sasaoka, T., Rudich, A., 2021. Human adipose tissue is a putative direct target of daytime orexin with favorable metabolic effects: A cross-sectional study. Obesity (Silver Spring) 29, 1857–1867. https://doi.org/10.1002/oby.23262

Gopalakrishnan, S., Kannan, N.N., 2021. Only time will tell: the interplay between circadian clock and metabolism. Chronobiol Int 38, 149–167. https://doi.org/10.1080/07420528.2020.1842436

Grady, S.P., Nishino, S., Czeisler, C.A., Hepner, D., Scammell, T.E., 2006. Diurnal variation in CSF orexin-A in healthy male subjects. Sleep 29, 295–297. https://doi.org/10.1093/sleep/29.3.295

Grafe, L.A., Cornfeld, A., Luz, S., Valentino, R., Bhatnagar, S., 2017. Orexins Mediate Sex Differences in the Stress Response and in Cognitive Flexibility. Biol Psychiatry 81, 683–692. https://doi.org/10.1016/j.biopsych.2016.10.013

Guha, P., Bhowmick, K., Mazumder, P., Ghosal, M., Chakraborty, I., Burman, P., 2014. Assessment of insulin resistance and metabolic syndrome in drug naive patients of bipolar disorder. Indian J Clin Biochem 29, 51–56. https://doi.org/10.1007/s12291-012-0292-x

Hara, J., Beuckmann, C.T., Nambu, T., Willie, J.T., Chemelli, R.M., Sinton, C.M., Sugiyama, F., Yagami, K., Goto, K., Yanagisawa, M., Sakurai, T., 2001. Genetic ablation of orexin neurons in mice results in narcolepsy, hypophagia, and obesity. Neuron 30, 345–354.

Hara, J., Yanagisawa, M., Sakurai, T., 2005. Difference in obesity phenotype between orexin-knockout mice and orexin neuron-deficient mice with same genetic background and

environmental conditions. Neurosci Lett 380, 239–242. https://doi.org/10.1016/j.neulet.2005.01.046

Hasan, N., Nagata, N., Morishige, J.-I., Islam, M.T., Jing, Z., Harada, K.-I., Mieda, M., Ono, M., Fujiwara, H., Daikoku, T., Fujiwara, T., Maida, Y., Ota, T., Shimba, S., Kaneko, S., Fujimura, A., Ando, H., 2021. Brown adipocyte-specific knockout of Bmal1 causes mild but significant thermogenesis impairment in mice. Mol Metab 101202. https://doi.org/10.1016/j.molmet.2021.101202

Hassani, O.K., Lee, M.G., Jones, B.E., 2009. Melanin-concentrating hormone neurons discharge in a reciprocal manner to orexin neurons across the sleep-wake cycle. Proc Natl Acad Sci U S A 106, 2418–2422. https://doi.org/10.1073/pnas.0811400106

Hatori, M., Vollmers, C., Zarrinpar, A., DiTacchio, L., Bushong, E.A., Gill, S., Leblanc, M., Chaix, A., Joens, M., Fitzpatrick, J.A.J., Ellisman, M.H., Panda, S., 2012. Time-restricted feeding without reducing caloric intake prevents metabolic diseases in mice fed a high-fat diet. Cell Metab 15, 848–860. https://doi.org/10.1016/j.cmet.2012.04.019

Heinonen, M.V., Purhonen, A.K., Mäkelä, K.A., Herzig, K.H., 2008. Functions of orexins in peripheral tissues. Acta Physiol (Oxf) 192, 471–485. https://doi.org/10.1111/j.1748-1716.2008.01836.x

Helfrich-Förster, C., 2017. Interactions between psychosocial stress and the circadian endogenous clock: Psychosocial stress and the endogenous clock. PsyCh Journal 6, 277–289. https://doi.org/10.1002/pchj.202

Herholt, A., 2017. Development of a multiplexed RNAi-coupled sensor assay to study neuronal function on the large-scale. Georg-August-University Göttingen. https://doi.org/10.53846/goediss-6199

Hirano, A., Hsu, P.-K., Zhang, L., Xing, L., McMahon, T., Yamazaki, M., Ptáček, L.J., Fu, Y.-H., 2018. DEC2 modulates orexin expression and regulates sleep. Proc Natl Acad Sci U S A 115, 3434–3439. https://doi.org/10.1073/pnas.1801693115

Hiyoshi, H., Terao, A., Okamatsu-Ogura, Y., Kimura, K., 2014. Characteristics of sleep and wakefulness in wild-derived inbred mice. Exp Anim 63, 205–213. https://doi.org/10.1538/expanim.63.205

Horsey, E.A., Maletta, T., Turner, H., Cole, C., Lehmann, H., Fournier, N.M., 2019. Chronic Jet Lag Simulation Decreases Hippocampal Neurogenesis and Enhances Depressive Behaviors and Cognitive Deficits in Adult Male Rats. Front Behav Neurosci 13, 272. https://doi.org/10.3389/fnbeh.2019.00272

Hou, Y., Liu, Y., Liu, C., Yan, Z., Ma, Q., Chen, Jianbei, Zhang, M., Yan, Q., Li, X., Chen, Jiaxu, 2020. Xiaoyaosan regulates depression-related behaviors with physical symptoms by modulating Orexin A/OxR1 in the hypothalamus. Anat Rec (Hoboken) 303, 2144–2153. https://doi.org/10.1002/ar.24386

Hsieh, M.-C., Yang, S.-C., Tseng, H.-L., Hwang, L.-L., Chen, C.-T., Shieh, K.-R., 2010. Abnormal expressions of circadian-clock and circadian clock-controlled genes in the livers and kidneys of long-term, high-fat-diet-treated mice. Int J Obes (Lond) 34, 227–239. https://doi.org/10.1038/ijo.2009.228

Hsu, C.-W., Wang, S., 2021. Changes in the Orexin System in Rats Exhibiting Learned Helplessness Behaviors. Brain Sci 11, 1634. https://doi.org/10.3390/brainsci11121634

Hu, Y., Shmygelska, A., Tran, D., Eriksson, N., Tung, J.Y., Hinds, D.A., 2016. GWAS of 89,283 individuals identifies genetic variants associated with self-reporting of being a morning person. Nat Commun 7, 10448. https://doi.org/10.1038/ncomms10448

Hua, P., Liu, W., Chen, D., Zhao, Y., Chen, L., Zhang, N., Wang, C., Guo, S., Wang, L., Xiao, H., Kuo, S.-H., 2014. Cry1 and Tef gene polymorphisms are associated with major depressive disorder in the Chinese population. J Affect Disord 157, 100–103. https://doi.org/10.1016/j.jad.2013.11.019

Hühne, A., Echtler, L., Kling, C., Stephan, M., Schmidt, M.V., Rossner, M.J., Landgraf, D., 2022. Circadian gene × environment perturbations influence alcohol drinking in Cryptochrome-deficient mice. Addict Biol 27, e13105. https://doi.org/10.1111/adb.13105

Hühne, A., Volkmann, P., Stephan, M., Rossner, M., Landgraf, D., 2020. An in-depth neurobehavioral characterization shows anxiety-like traits, impaired habituation behavior, and restlessness in male Cryptochrome-deficient mice. Genes Brain Behav 19, e12661. https://doi.org/10.1111/gbb.12661

Hühne, A., Welsh, D.K., Landgraf, D., 2018. Prospects for circadian treatment of mood disorders. Ann. Med. 50, 637–654. https://doi.org/10.1080/07853890.2018.1530449

Ito, N., Yabe, T., Gamo, Y., Nagai, T., Oikawa, T., Yamada, H., Hanawa, T., 2008. I.c.v. administration of orexin-A induces an antidepressive-like effect through hippocampal cell proliferation. Neuroscience 157, 720–732. https://doi.org/10.1016/j.neuroscience.2008.09.042

Ito, N., Yabe, T., Nagai, T., Oikawa, T., Yamada, H., Hanawa, T., 2009. A possible mechanism underlying an antidepressive-like effect of Kososan, a Kampo medicine, via the hypothalamic orexinergic system in the stress-induced depression-like model mice. Biol Pharm Bull 32, 1716–1722. https://doi.org/10.1248/bpb.32.1716

Jalewa, J., Wong-Lin, K., McGinnity, T.M., Prasad, G., Hölscher, C., 2014. Increased number of orexin/hypocretin neurons with high and prolonged external stress-induced depression. Behav. Brain Res. 272, 196–204. https://doi.org/10.1016/j.bbr.2014.05.030

James, M.H., Campbell, E.J., Dayas, C.V., 2017a. Role of the Orexin/Hypocretin System in Stress-Related Psychiatric Disorders. Curr Top Behav Neurosci 33, 197–219. https://doi.org/10.1007/7854_2016_56

James, M.H., Mahler, S.V., Moorman, D.E., Aston-Jones, G., 2017b. A Decade of Orexin/Hypocretin and Addiction: Where Are We Now? Curr Top Behav Neurosci 33, 247–281. https://doi.org/10.1007/7854_2016_57

Ji, M.-J., Zhang, X.-Y., Chen, Z., Wang, J.-J., Zhu, J.-N., 2019. Orexin prevents depressive-like behavior by promoting stress resilience. Mol Psychiatry 24, 282–293. https://doi.org/10.1038/s41380-018-0127-0

Johnson, B.P., Walisser, J.A., Liu, Y., Shen, A.L., McDearmon, E.L., Moran, S.M., McIntosh, B.E., Vollrath, A.L., Schook, A.C., Takahashi, J.S., Bradfield, C.A., 2014. Hepatocyte circadian clock controls acetaminophen bioactivation through NADPH-cytochrome P450 oxidoreductase. Proc. Natl. Acad. Sci. U.S.A. 111, 18757–18762. https://doi.org/10.1073/pnas.1421708111

Johnson, P.L., Truitt, W., Fitz, S.D., Minick, P.E., Dietrich, A., Sanghani, S., Träskman-Bendz, L., Goddard, A.W., Brundin, L., Shekhar, A., 2010. A key role for orexin in panic anxiety. Nat Med 16, 111–115. https://doi.org/10.1038/nm.2075

Jöhren, O., Neidert, S.J., Kummer, M., Dendorfer, A., Dominiak, P., 2001. Prepro-orexin and orexin receptor mRNAs are differentially expressed in peripheral tissues of male and female rats. Endocrinology 142, 3324–3331. https://doi.org/10.1210/endo.142.8.8299

Jones, S.E., Lane, J.M., Wood, A.R., van Hees, V.T., Tyrrell, J., Beaumont, R.N., Jeffries, A.R., Dashti, H.S., Hillsdon, M., Ruth, K.S., Tuke, M.A., Yaghootkar, H., Sharp, S.A., Jie, Y., Thompson, W.D., Harrison, J.W., Dawes, A., Byrne, E.M., Tiemeier, H., Allebrandt, K.V., Bowden, J., Ray, D.W., Freathy, R.M., Murray, A., Mazzotti, D.R., Gehrman, P.R., Lawlor, D.A., Frayling, T.M., Rutter, M.K., Hinds, D.A., Saxena, R., Weedon, M.N., 2019. Genome-wide association analyses of chronotype in 697,828 individuals provides insights into circadian rhythms. Nat Commun 10, 343. https://doi.org/10.1038/s41467-018-08259-7

Joshi, D., Sarkar, D., Singh, S.K., 2018. The hypothalamic neuropeptide orexin A- a possible regulator in glucose homeostasis and germ cell kinetics in adult mice testes. Biochimie 152, 94–109. https://doi.org/10.1016/j.biochi.2018.06.021

Joshi, D., Singh, S.K., 2018. The neuropeptide orexin A - search for its possible role in regulation of steroidogenesis in adult mice testes. Andrology 6, 465–477. https://doi.org/10.1111/andr.12475

Joshi, D., Singh, S.K., 2017. Localization and expression of Orexin A and its receptor in mouse testis during different stages of postnatal development. Gen Comp Endocrinol 241, 50–56. https://doi.org/10.1016/j.ygcen.2016.05.006

Joshi, D., Singh, S.K., 2016. Localization, expression and role of Orexin A and its receptor in testes of neonatal mice. Gen Comp Endocrinol 239, 62–70. https://doi.org/10.1016/j.ygcen.2015.11.005

Justinussen, J.L., Holm, A., Kornum, B.R., 2015. An optimized method for measuring hypocretin-1 peptide in the mouse brain reveals differential circadian regulation of hypocretin-1 levels rostral and caudal to the hypothalamus. Neuroscience 310, 354–361. https://doi.org/10.1016/j.neuroscience.2015.09.050

Kakizaki, M., Tsuneoka, Y., Takase, K., Kim, S.J., Choi, J., Ikkyu, A., Abe, M., Sakimura, K., Yanagisawa, M., Funato, H., 2019. Differential Roles of Each Orexin Receptor Signaling in Obesity. iScience 20, 1–13. https://doi.org/10.1016/j.isci.2019.09.003

Karing, C., 2021. Prevalence and predictors of anxiety, depression and stress among university students during the period of the first lockdown in Germany. J Affect Disord Rep 5, 100174. https://doi.org/10.1016/j.jadr.2021.100174

Karteris, E., Chen, J., Randeva, H.S., 2004. Expression of human prepro-orexin and signaling characteristics of orexin receptors in the male reproductive system. J. Clin. Endocrinol. Metab. 89, 1957–1962. https://doi.org/10.1210/jc.2003-031778

Karthikeyan, R., Marimuthu, G., Ramasubramanian, C., Arunachal, G., BaHammam, A.S., Spence, D.W., Cardinali, D.P., Brown, G.M., Pandi-Perumal, S.R., 2014. Association of Per3 length polymorphism with bipolar I disorder and schizophrenia. Neuropsychiatr Dis Treat 10, 2325–2330. https://doi.org/10.2147/NDT.S73765

Kastin, A.J., Akerstrom, V., 1999. Orexin A but not orexin B rapidly enters brain from blood by simple diffusion. J Pharmacol Exp Ther 289, 219–223.

Khalil, R., Fendt, M., 2017. Increased anxiety but normal fear and safety learning in orexin-deficient mice. Behav Brain Res 320, 210–218. https://doi.org/10.1016/j.bbr.2016.12.007

Kim, E.R., Xu, Yuanzhong, Cassidy, R.M., Lu, Y., Yang, Y., Tian, J., Li, D.-P., Van Drunen, R., Ribas-Latre, A., Cai, Z.-L., Xue, M., Arenkiel, B.R., Eckel-Mahan, K., Xu, Yong, Tong, Q., 2020. Paraventricular hypothalamus mediates diurnal rhythm of metabolism. Nat Commun 11, 3794. https://doi.org/10.1038/s41467-020-17578-7

Kim, H., Kim, M., Im, S.-K., Fang, S., 2018. Mouse Cre-LoxP system: general principles to determine tissue-specific roles of target genes. Lab Anim Res 34, 147–159. https://doi.org/10.5625/lar.2018.34.4.147

Kim, T.-K., Han, P.-L., 2016. Functional Connectivity of Basolateral Amygdala Neurons Carrying Orexin Receptors and Melanin-concentrating Hormone Receptors in Regulating Sociability and Mood-related Behaviors. Exp Neurobiol 25, 307–317. https://doi.org/10.5607/en.2016.25.6.307

Kim, T.-K., Kim, J.-E., Choi, J., Park, J.-Y., Lee, J.-E., Lee, E.-H., Lee, Y., Kim, B.Y., Oh, Y.J., Han, P.-L., 2017. Local Interleukin-18 System in the Basolateral Amygdala Regulates Susceptibility to Chronic Stress. Mol Neurobiol 54, 5347–5358. https://doi.org/10.1007/s12035-016-0052-7

Kim, T.-K., Kim, J.-E., Park, J.-Y., Lee, J.-E., Choi, J., Kim, H., Lee, E.-H., Kim, S.-W., Lee, J.-K., Kang, H.-S., Han, P.-L., 2015. Antidepressant effects of exercise are produced via suppression of hypocretin/orexin and melanin-concentrating hormone in the basolateral amygdala. Neurobiol. Dis. 79, 59–69. https://doi.org/10.1016/j.nbd.2015.04.004

Kirchgessner, A.L., 2002. Orexins in the brain-gut axis. Endocr. Rev. 23, 1–15. https://doi.org/10.1210/edrv.23.1.0454

Kling, C., Landgraf, D., 2021. Circadian Clocks, Stress, and Psychiatric Disorders, in: Stress: Genetics, Epigenetics and Genomics. Elsevier, pp. 95–108. https://doi.org/10.1016/B978-0-12-813156-5.00008-X

Kohsaka, A., Laposky, A.D., Ramsey, K.M., Estrada, C., Joshu, C., Kobayashi, Y., Turek, F.W., Bass, J., 2007. High-fat diet disrupts behavioral and molecular circadian rhythms in mice. Cell Metab 6, 414–421. https://doi.org/10.1016/j.cmet.2007.09.006

Kon, K., Tsuneki, H., Ito, H., Takemura, Y., Sato, K., Yamazaki, M., Ishii, Y., Sasahara, M., Rudich, A., Maeda, T., Wada, T., Sasaoka, T., 2019. Chronotherapeutic effect of orexin antagonists on glucose metabolism in diabetic mice. J Endocrinol JOE-18-0708.R3. https://doi.org/10.1530/JOE-18-0708

Kondratov, R.V., Kondratova, A.A., Gorbacheva, V.Y., Vykhovanets, O.V., Antoch, M.P., 2006. Early aging and age-related pathologies in mice deficient in BMAL1, the core componentof the circadian clock. Genes Dev. 20, 1868–1873. https://doi.org/10.1101/gad.1432206

Kovalská, P., Kemlink, D., Nevšímalová, S., Maurovich Horvat, E., Jarolímová, E., Topinková, E., Šonka, K., 2016. Narcolepsy with cataplexy in patients aged over 60 years: a case-control study. Sleep Medicine 26, 79–84. https://doi.org/10.1016/j.sleep.2016.05.011

Kovanen, L., Kaunisto, M., Donner, K., Saarikoski, S.T., Partonen, T., 2013. CRY2 genetic variants associate with dysthymia. PLoS ONE 8, e71450. https://doi.org/10.1371/journal.pone.0071450

Kripke, D.F., Nievergelt, C.M., Joo, E., Shekhtman, T., Kelsoe, J.R., 2009. Circadian polymorphisms associated with affective disorders. J Circadian Rhythms 7, 2. https://doi.org/10.1186/1740-3391-7-2

Lamia, K.A., Storch, K.-F., Weitz, C.J., 2008. Physiological significance of a peripheral tissue circadian clock. Proc Natl Acad Sci U S A 105, 15172–15177. https://doi.org/10.1073/pnas.0806717105

Landgraf, D., Long, J., Der-Avakian, A., Streets, M., Welsh, D.K., 2015. Dissociation of Learned Helplessness and Fear Conditioning in Mice: A Mouse Model of Depression. PLoS ONE 10, e0125892. https://doi.org/10.1371/journal.pone.0125892

Landgraf, D., Long, J.E., Proulx, C.D., Barandas, R., Malinow, R., Welsh, D.K., 2016a. Genetic Disruption of Circadian Rhythms in the Suprachiasmatic Nucleus Causes Helplessness, Behavioral Despair, and Anxiety-like Behavior in Mice. Biol. Psychiatry 80, 827–835. https://doi.org/10.1016/j.biopsych.2016.03.1050

Landgraf, D., Long, J.E., Welsh, D.K., 2016b. Depression-like behaviour in mice is associated with disrupted circadian rhythms in nucleus accumbens and periaqueductal grey. Eur. J. Neurosci. 43, 1309–1320. https://doi.org/10.1111/ejn.13085

Lee, M.G., Hassani, O.K., Jones, B.E., 2005. Discharge of identified orexin/hypocretin neurons across the sleep-waking cycle. J Neurosci 25, 6716–6720. https://doi.org/10.1523/JNEUROSCI.1887-05.2005

Li, H., Lu, J., Li, S., Huang, B., Shi, G., Mou, T., Xu, Y., 2021. Increased Hypocretin (Orexin) Plasma Level in Depression, Bipolar Disorder Patients. Front Psychiatry 12, 676336. https://doi.org/10.3389/fpsyt.2021.676336

Li, J.Z., Bunney, B.G., Meng, F., Hagenauer, M.H., Walsh, D.M., Vawter, M.P., Evans, S.J., Choudary, P.V., Cartagena, P., Barchas, J.D., Schatzberg, A.F., Jones, E.G., Myers, R.M., Watson, S.J., Akil, H., Bunney, W.E., 2013. Circadian patterns of gene expression in the human brain and disruption in major depressive disorder. Proc. Natl. Acad. Sci. U.S.A. 110, 9950–9955. https://doi.org/10.1073/pnas.1305814110

Li, M.-D., Li, C.-M., Wang, Z., 2012. The role of circadian clocks in metabolic disease. Yale J Biol Med 85, 387–401.

Liguori, G., Tafuri, S., Miyoshi, C., Yanagisawa, M., Squillacioti, C., De Pasquale, V., Mirabella, N., Vittoria, A., Costagliola, A., 2018. Localization of orexin B and orexin-2 receptor in the rat epididymis. Acta Histochem. 120, 292–297. https://doi.org/10.1016/j.acthis.2018.02.011

Lin, L., Faraco, J., Li, R., Kadotani, H., Rogers, W., Lin, X., Qiu, X., de Jong, P.J., Nishino, S., Mignot, E., 1999. The sleep disorder canine narcolepsy is caused by a mutation in the hypocretin (orexin) receptor 2 gene. Cell 98, 365–376.

Lin, L., Wisor, J., Shiba, T., Taheri, S., Yanai, K., Wurts, S., Lin, X., Vitaterna, M., Takahashi, J., Lovenberg, T.W., Koehl, M., Uhl, G., Nishino, S., Mignot, E., 2002. Measurement of hypocretin/orexin content in the mouse brain using an enzyme immunoassay: the effect of circadian time, age and genetic background. Peptides 23, 2203–2211. https://doi.org/10.1016/s0196-9781(02)00251-6

Liu, M., Blanco-Centurion, C., Konadhode, R.R., Luan, L., Shiromani, P.J., 2016. Orexin gene transfer into the amygdala suppresses both spontaneous and emotion-induced cataplexy in orexin-knockout mice. Eur J Neurosci 43, 681–688. https://doi.org/10.1111/ejn.13158

Lorenz, N., Spada, J., Sander, C., Riedel-Heller, S.G., Hegerl, U., 2019. Circadian skin temperature rhythms, circadian activity rhythms and sleep in individuals with self-reported depressive symptoms. J Psychiatr Res 117, 38–44. https://doi.org/10.1016/j.jpsychires.2019.06.022

Lu, J., Huang, M.-L., Li, J.-H., Jin, K.-Y., Li, H.-M., Mou, T.-T., Fronczek, R., Duan, J.-F., Xu, W.-J., Swaab, D., Bao, A.-M., 2021. Changes of Hypocretin (Orexin) System in Schizophrenia: From Plasma to Brain. Schizophrenia Bulletin 47, 1310–1319. https://doi.org/10.1093/schbul/sbab042

Lu, J., Li, S., Li, H., Mou, T., Zhou, L., Huang, B., Huang, M., Xu, Y., 2019. Changes In Plasma NPY, IL-1β And Hypocretin In People Who Died By Suicide. Neuropsychiatr Dis Treat 15, 2893–2900. https://doi.org/10.2147/NDT.S219962

Lucey, M.R., 1986. Endogenous somatostatin and the gut. Gut 27, 457–467. https://doi.org/10.1136/gut.27.4.457

Lungwitz, E.A., Molosh, A., Johnson, P.L., Harvey, B.P., Dirks, R.C., Dietrich, A., Minick, P., Shekhar, A., Truitt, W.A., 2012. Orexin-A induces anxiety-like behavior through interactions with glutamatergic receptors in the bed nucleus of the stria terminalis of rats. Physiol Behav 107, 726–732. https://doi.org/10.1016/j.physbeh.2012.05.019

Lutter, M., Krishnan, V., Russo, S.J., Jung, S., McClung, C.A., Nestler, E.J., 2008. Orexin signaling mediates the antidepressant-like effect of calorie restriction. J. Neurosci. 28, 3071–3075. https://doi.org/10.1523/JNEUROSCI.5584-07.2008

Mäkelä, K.A., Karhu, T., Jurado Acosta, A., Vakkuri, O., Leppäluoto, J., Herzig, K.-H., 2018. Plasma Orexin-A Levels Do Not Undergo Circadian Rhythm in Young Healthy Male Subjects. Front Endocrinol (Lausanne) 9, 710. https://doi.org/10.3389/fendo.2018.00710

Mansur, R.B., Brietzke, E., McIntyre, R.S., 2015. Is there a “metabolic-mood syndrome”? A review of the relationship between obesity and mood disorders. Neurosci Biobehav Rev 52, 89–104. https://doi.org/10.1016/j.neubiorev.2014.12.017

Marcheva, B., Ramsey, K.M., Buhr, E.D., Kobayashi, Y., Su, H., Ko, C.H., Ivanova, G., Omura, C., Mo, S., Vitaterna, M.H., Lopez, J.P., Philipson, L.H., Bradfield, C.A., Crosby, S.D., JeBailey, L., Wang, X., Takahashi, J.S., Bass, J., 2010. Disruption of the clock components CLOCK and BMAL1 leads to hypoinsulinaemia and diabetes. Nature 466, 627–631. https://doi.org/10.1038/nature09253

Marcus, J.N., Aschkenasi, C.J., Lee, C.E., Chemelli, R.M., Saper, C.B., Yanagisawa, M., Elmquist, J.K., 2001. Differential expression of orexin receptors 1 and 2 in the rat brain. J Comp Neurol 435, 6–25. https://doi.org/10.1002/cne.1190

Marston, O.J., Williams, R.H., Canal, M.M., Samuels, R.E., Upton, N., Piggins, H.D., 2008. Circadian and dark-pulse activation of orexin/hypocretin neurons. Molecular Brain 1, 19. https://doi.org/10.1186/1756-6606-1-19

Martínez, G.S., Smale, L., Nunez, A.A., 2002. Diurnal and nocturnal rodents show rhythms in orexinergic neurons. Brain Res. 955, 1–7.

Martini, T., Ripperger, J.A., Stalin, J., Kores, A., Stumpe, M., Albrecht, U., 2021. Deletion of the clock gene Period2 (Per2) in glial cells alters mood-related behavior in mice. Sci Rep 11, 12242. https://doi.org/10.1038/s41598-021-91770-7

Matsuki, T., Nomiyama, M., Takahira, H., Hirashima, N., Kunita, S., Takahashi, S., Yagami, K., Kilduff, T.S., Bettler, B., Yanagisawa, M., Sakurai, T., 2009. Selective loss of GABA(B) receptors in orexin-producing neurons results in disrupted sleep/wakefulness architecture. Proc. Natl. Acad. Sci. U.S.A. 106, 4459–4464. https://doi.org/10.1073/pnas.0811126106

Matsuo, E., Mochizuki, A., Nakayama, K., Nakamura, S., Yamamoto, T., Shioda, S., Sakurai, T., Yanagisawa, M., Shiuchi, T., Minokoshi, Y., Inoue, T., 2011. Decreased intake of sucrose solutions in orexin knockout mice. J Mol Neurosci 43, 217–224. https://doi.org/10.1007/s12031-010-9475-1

Mattar, P., Uribe-Cerda, S., Pezoa, C., Guarnieri, T., Kotz, C.M., Teske, J.A., Morselli, E., Perez-Leighton, C., 2020. Brain site-specific regulation of hedonic intake by orexin and DYN peptides: role of the PVN and obesity. Nutr Neurosci 1–10. https://doi.org/10.1080/1028415X.2020.1840049

McGregor, R., Shan, L., Wu, M.-F., Siegel, J.M., 2017. Diurnal fluctuation in the number of hypocretin/orexin and histamine producing: Implication for understanding and treating neuronal loss. PLoS ONE 12, e0178573. https://doi.org/10.1371/journal.pone.0178573

Meinke, G., Bohm, A., Hauber, J., Pisabarro, M.T., Buchholz, F., 2016. Cre Recombinase and Other Tyrosine Recombinases. Chem. Rev. https://doi.org/10.1021/acs.chemrev.6b00077

Mickelsen, L.E., Kolling, F.W., Chimileski, B.R., Fujita, A., Norris, C., Chen, K., Nelson, C.E., Jackson, A.C., 2017. Neurochemical Heterogeneity Among Lateral Hypothalamic Hypocretin/Orexin and Melanin-Concentrating Hormone Neurons Identified Through Single-Cell Gene Expression Analysis. eNeuro 4. https://doi.org/10.1523/ENEURO.0013-17.2017

Mieda, M., Hasegawa, E., Kessaris, N., Sakurai, T., 2017. Fine-Tuning Circadian Rhythms: The Importance of Bmal1 Expression in the Ventral Forebrain. Front Neurosci 11, 55. https://doi.org/10.3389/fnins.2017.00055

Mieda, M., Sakurai, T., 2011. Bmal1 in the nervous system is essential for normal adaptation of circadian locomotor activity and food intake to periodic feeding. J. Neurosci. 31, 15391–15396. https://doi.org/10.1523/JNEUROSCI.2801-11.2011

Mikrouli, E., Wörtwein, G., Soylu, R., Mathé, A.A., Petersén, Å., 2011. Increased numbers of orexin/hypocretin neurons in a genetic rat depression model. Neuropeptides 45, 401–406. https://doi.org/10.1016/j.npep.2011.07.010

Milaneschi, Y., Simmons, W.K., van Rossum, E.F.C., Penninx, B.W., 2019. Depression and obesity: evidence of shared biological mechanisms. Mol Psychiatry 24, 18–33. https://doi.org/10.1038/s41380-018-0017-5

Moreira, F.P., Jansen, K., Cardoso, T. de A., Mondin, T.C., Magalhães, P.V. da S., Kapczinski, F., Souza, L.D. de M., da Silva, R.A., Oses, J.P., Wiener, C.D., 2017. Metabolic syndrome in subjects with bipolar disorder and major depressive disorder in a current depressive episode: Population-based study: Metabolic syndrome in current depressive episode. J Psychiatr Res 92, 119–123. https://doi.org/10.1016/j.jpsychires.2017.03.025

Moriguchi, T., Sakurai, T., Takahashi, S., Goto, K., Yamamoto, M., 2002. The human prepro-orexin gene regulatory region that activates gene expression in the lateral region and represses it in the medial regions of the hypothalamus. J. Biol. Chem. 277, 16985–16992. https://doi.org/10.1074/jbc.M107962200

Moslehi, E., Minasian, V., Sadeghi, H., 2021. Subcutaneous Adipose Tissue Browning, Serum Orexin-A, and Insulin Resistance Following Aerobic Exercise in High-Fat Diet Obesity Male Wistar Rats. Int J Prev Med 12, 132. https://doi.org/10.4103/ijpvm.IJPVM_110_19

Mukherjee, S., Coque, L., Cao, J.-L., Kumar, J., Chakravarty, S., Asaithamby, A., Graham, A., Gordon, E., Enwright, J.F., DiLeone, R.J., Birnbaum, S.G., Cooper, D.C., McClung, C.A., 2010. Knockdown of Clock in the ventral tegmental area through RNA interference results in a mixed state of mania and depression-like behavior. Biol. Psychiatry 68, 503–511. https://doi.org/10.1016/j.biopsych.2010.04.031

Mure, L.S., Le, H.D., Benegiamo, G., Chang, M.W., Rios, L., Jillani, N., Ngotho, M., Kariuki, T., Dkhissi-Benyahya, O., Cooper, H.M., Panda, S., 2018. Diurnal transcriptome atlas of a primate across major neural and peripheral tissues. Science 359, eaao0318. https://doi.org/10.1126/science.aao0318

Muschamp, J.W., Hollander, J.A., Thompson, J.L., Voren, G., Hassinger, L.C., Onvani, S., Kamenecka, T.M., Borgland, S.L., Kenny, P.J., Carlezon, W.A., 2014. Hypocretin (orexin) facilitates reward

by attenuating the antireward effects of its cotransmitter dynorphin in ventral tegmental area. Proc Natl Acad Sci U S A 111, E1648-1655. https://doi.org/10.1073/pnas.1315542111

Nakabayashi, M., Suzuki, T., Takahashi, K., Totsune, K., Muramatsu, Y., Kaneko, C., Date, F., Takeyama, J., Darnel, A.D., Moriya, T., Sasano, H., 2003. Orexin-A expression in human peripheral tissues. Mol. Cell. Endocrinol. 205, 43–50.

Nakamura, M., Nagamine, T., 2017. Neuroendocrine, Autonomic, and Metabolic Responses to an Orexin Antagonist, Suvorexant, in Psychiatric Patients with Insomnia. Innov Clin Neurosci 14, 30–37.

Näslund, E., Ehrström, M., Ma, J., Hellström, P.M., Kirchgessner, A.L., 2002. Localization and effects of orexin on fasting motility in the rat duodenum. Am. J. Physiol. Gastrointest. Liver Physiol. 282, G470-479. https://doi.org/10.1152/ajpgi.00219.2001

Nishino, S., Ripley, B., Overeem, S., Lammers, G.J., Mignot, E., 2000. Hypocretin (orexin) deficiency in human narcolepsy. Lancet 355, 39–40. https://doi.org/10.1016/S0140-6736(99)05582-8

Nixon, J.P., Smale, L., 2004. Individual differences in wheel-running rhythms are related to temporal and spatial patterns of activation of orexin A and B cells in a diurnal rodent (Arvicanthis niloticus). Neuroscience 127, 25–34. https://doi.org/10.1016/j.neuroscience.2004.04.052

Noble, E.E., Hahn, J.D., Konanur, V.R., Hsu, T.M., Page, S.J., Cortella, A.M., Liu, C.M., Song, M.Y., Suarez, A.N., Szujewski, C.C., Rider, D., Clarke, J.E., Darvas, M., Appleyard, S.M., Kanoski, S.E., 2018. Control of Feeding Behavior by Cerebral Ventricular Volume Transmission of Melanin-Concentrating Hormone. Cell Metab 28, 55-68.e7. https://doi.org/10.1016/j.cmet.2018.05.001

Nobunaga, M., Obukuro, K., Kurauchi, Y., Hisatsune, A., Seki, T., Tsutsui, M., Katsuki, H., 2014. High fat diet induces specific pathological changes in hypothalamic orexin neurons in mice. Neurochem Int 78, 61–66. https://doi.org/10.1016/j.neuint.2014.09.002

Nocjar, C., Zhang, J., Feng, P., Panksepp, J., 2012. The social defeat animal model of depression shows diminished levels of orexin in mesocortical regions of the dopamine system, and of dynorphin and orexin in the hypothalamus. Neuroscience 218, 138–153. https://doi.org/10.1016/j.neuroscience.2012.05.033

Nollet, M., Gaillard, P., Minier, F., Tanti, A., Belzung, C., Leman, S., 2011. Activation of orexin neurons in dorsomedial/perifornical hypothalamus and antidepressant reversal in a rodent model of depression. Neuropharmacology 61, 336–346. https://doi.org/10.1016/j.neuropharm.2011.04.022

Nollet, M., Gaillard, P., Tanti, A., Girault, V., Belzung, C., Leman, S., 2012. Neurogenesis-independent antidepressant-like effects on behavior and stress axis response of a dual orexin receptor antagonist in a rodent model of depression. Neuropsychopharmacology 37, 2210–2221. https://doi.org/10.1038/npp.2012.70

Ogawa, Y., Kanda, T., Vogt, K., Yanagisawa, M., 2017. Anatomical and electrophysiological development of the hypothalamic orexin neurons from embryos to neonates. J. Comp. Neurol. 525, 3809–3820. https://doi.org/10.1002/cne.24261

Onat, O.E., Kars, M.E., Gül, Ş., Bilguvar, K., Wu, Y., Özhan, A., Aydın, C., Başak, A.N., Trusso, M.A., Goracci, A., Fallerini, C., Renieri, A., Casanova, J.-L., Itan, Y., Atbaşoğlu, C.E., Saka, M.C., Kavaklı, İ.H., Özçelik, T., 2020. Human CRY1 variants associate with attention deficit/hyperactivity disorder. J Clin Invest 130, 3885–3900. https://doi.org/10.1172/JCI135500

Ono, D., Yamanaka, A., 2017. Hypothalamic regulation of the sleep/wake cycle. Neuroscience Research 118, 74–81. https://doi.org/10.1016/j.neures.2017.03.013

Orozco-Solis, R., Aguilar-Arnal, L., Murakami, M., Peruquetti, R., Ramadori, G., Coppari, R., Sassone-Corsi, P., 2016. The Circadian Clock in the Ventromedial Hypothalamus Controls Cyclic Energy Expenditure. Cell Metab. 23, 467–478. https://doi.org/10.1016/j.cmet.2016.02.003

Ouedraogo, R., Näslund, E., Kirchgessner, A.L., 2003. Glucose regulates the release of orexin-a from the endocrine pancreas. Diabetes 52, 111–117.

Ovchinnikov, D.A., Deng, J.M., Ogunrinu, G., Behringer, R.R., 2000. Col2a1-directed expression of Cre recombinase in differentiating chondrocytes in transgenic mice. Genesis 26, 145–146.

Ozsoy, S., Olguner Eker, O., Abdulrezzak, U., Esel, E., 2017. Relationship between orexin A and childhood maltreatment in female patients with depression and anxiety. Soc Neurosci 12, 330–336. https://doi.org/10.1080/17470919.2016.1169216

Pan, Y.-P., Liu, C., Liu, M.-F., Wang, Y., Bian, K., Xue, Y., Chen, L., 2020. Involvement of orexin-A in the regulation of neuronal activity and emotional behaviors in central amygdala in rats. Neuropeptides 80, 102019. https://doi.org/10.1016/j.npep.2020.102019

Partch, C.L., Green, C.B., Takahashi, J.S., 2014. Molecular architecture of the mammalian circadian clock. Trends Cell Biol 24, 90–99. https://doi.org/10.1016/j.tcb.2013.07.002

Paschos, G.K., Ibrahim, S., Song, W.-L., Kunieda, T., Grant, G., Reyes, T.M., Bradfield, C.A., Vaughan, C.H., Eiden, M., Masoodi, M., Griffin, J.L., Wang, F., Lawson, J.A., Fitzgerald, G.A., 2012. Obesity in mice with adipocyte-specific deletion of clock component Arntl. Nat. Med. 18, 1768–1777. https://doi.org/10.1038/nm.2979

Pasquarelli, N., Voehringer, P., Henke, J., Ferger, B., 2017. Effect of a change in housing conditions on body weight, behavior and brain neurotransmitters in male C57BL/6J mice. Behav Brain Res 333, 35–42. https://doi.org/10.1016/j.bbr.2017.06.018

Patel, V.H., Karteris, E., Chen, J., Kyrou, I., Mattu, H.S., Dimitriadis, G.K., Rodrigo, G., Antoniades, C., Antonopoulos, A., Tan, B.K., Hillhouse, E.W., Ng, A., Randeva, H.S., 2018. Functional cardiac orexin receptors: role of orexin-B/orexin 2 receptor in myocardial protection. Clin Sci (Lond) 132, 2547–2564. https://doi.org/10.1042/CS20180150

Paxinos, G., Franklin, K.B.J., 2019. Paxinos and Franklin's The mouse brain in stereotaxic coordinates, Fifth edition. ed. Elsevier, Academic Press, London San Diego Cambridge; MA Kidlington, Oxford.

Pelluru, D., Konadhode, R., Shiromani, P.J., 2013. MCH Neurons Are the Primary Sleep-Promoting Group. Sleep 36, 1779–1781. https://doi.org/10.5665/sleep.3196

Pendergast, J.S., Yamazaki, S., 2018. The Mysterious Food-Entrainable Oscillator: Insights from Mutant and Engineered Mouse Models. J Biol Rhythms 33, 458–474. https://doi.org/10.1177/0748730418789043

Pereira, H., Fehér, G., Tibold, A., Monteiro, S., Costa, V., Esgalhado, G., 2021. The Impact of Shift Work on Occupational Health Indicators among Professionally Active Adults: A Comparative Study. Int J Environ Res Public Health 18, 11290. https://doi.org/10.3390/ijerph182111290

Peyron, C., Tighe, D.K., van den Pol, A.N., de Lecea, L., Heller, H.C., Sutcliffe, J.G., Kilduff, T.S., 1998. Neurons containing hypocretin (orexin) project to multiple neuronal systems. J. Neurosci. 18, 9996–10015.

Pfaffl, M.W., 2001. A new mathematical model for relative quantification in real-time RT-PCR. Nucleic Acids Res 29, e45. https://doi.org/10.1093/nar/29.9.e45

Pilorz, V., Astiz, M., Heinen, K.O., Rawashdeh, O., Oster, H., 2020. The Concept of Coupling in the Mammalian Circadian Clock Network. J Mol Biol 432, 3618–3638. https://doi.org/10.1016/j.jmb.2019.12.037

Pilz, L.K., Carissimi, A., Oliveira, M.A.B., Francisco, A.P., Fabris, R.C., Medeiros, M.S., Scop, M., Frey, B.N., Adan, A., Hidalgo, M.P., 2018. Rhythmicity of Mood Symptoms in Individuals at Risk for Psychiatric Disorders. Sci Rep 8, 11402. https://doi.org/10.1038/s41598-018-29348-z

Pinho, M., Sehmbi, M., Cudney, L.E., Kauer-Sant'anna, M., Magalhães, P.V., Reinares, M., Bonnín, C.M., Sassi, R.B., Kapczinski, F., Colom, F., Vieta, E., Frey, B.N., Rosa, A.R., 2016. The association between biological rhythms, depression, and functioning in bipolar disorder: a large multi-center study. Acta Psychiatr Scand 133, 102–108. https://doi.org/10.1111/acps.12442

Platt, R.J., Chen, S., Zhou, Y., Yim, M.J., Swiech, L., Kempton, H.R., Dahlman, J.E., Parnas, O., Eisenhaure, T.M., Jovanovic, M., Graham, D.B., Jhunjhunwala, S., Heidenreich, M., Xavier, R.J., Langer, R., Anderson, D.G., Hacohen, N., Regev, A., Feng, G., Sharp, P.A., Zhang, F.,

2014. CRISPR-Cas9 knockin mice for genome editing and cancer modeling. Cell 159, 440–455. https://doi.org/10.1016/j.cell.2014.09.014

Pourrahimi, A.M., Abbasnejad, M., Raoof, M., Esmaeili-Mahani, S., Kooshki, R., 2021. The involvement of orexin 1 and cannabinoid 1 receptors within the ventrolateral periaqueductal gray matter in the modulation of migraine-induced anxiety and social behavior deficits of rats. Peptides 146, 170651. https://doi.org/10.1016/j.peptides.2021.170651

Prut, L., Belzung, C., 2003. The open field as a paradigm to measure the effects of drugs on anxiety-like behaviors: a review. Eur J Pharmacol 463, 3–33. https://doi.org/10.1016/s0014-2999(03)01272-x

Qin, J.Y., Zhang, L., Clift, K.L., Hulur, I., Xiang, A.P., Ren, B.-Z., Lahn, B.T., 2010. Systematic comparison of constitutive promoters and the doxycycline-inducible promoter. PLoS ONE 5, e10611. https://doi.org/10.1371/journal.pone.0010611

Rainero, I., Ostacoli, L., Rubino, E., Gallone, S., Picci, L.R., Fenoglio, P., Negro, E., Rosso, C., De Martino, P., De Marchi, M., Furlan, P.M., Pinessi, L., 2011. Association between major mood disorders and the hypocretin receptor 1 gene. J Affect Disord 130, 487–491. https://doi.org/10.1016/j.jad.2010.10.033

Ramanathan, L., Siegel, J.M., 2014. Gender differences between hypocretin/orexin knockout and wild type mice: age, body weight, body composition, metabolic markers, leptin and insulin resistance. J. Neurochem. 131, 615–624. https://doi.org/10.1111/jnc.12840

Randeva, H.S., Karteris, E., Grammatopoulos, D., Hillhouse, E.W., 2001. Expression of orexin-A and functional orexin type 2 receptors in the human adult adrenals: implications for adrenal function and energy homeostasis. J. Clin. Endocrinol. Metab. 86, 4808–4813. https://doi.org/10.1210/jcem.86.10.7921

Razavi, B.M., Hosseinzadeh, H., 2017. A review of the role of orexin system in pain modulation. Biomed Pharmacother 90, 187–193. https://doi.org/10.1016/j.biopha.2017.03.053

Reading, P.J., 2019. Update on narcolepsy. J. Neurol. https://doi.org/10.1007/s00415-019-09310-3

Recourt, K., de Boer, P., Zuiker, R., Luthringer, R., Kent, J., van der Ark, P., Van Hove, I., van Gerven, J., Jacobs, G., van Nueten, L., Drevets, W., 2019. The selective orexin-2 antagonist seltorexant (JNJ-42847922/MIN-202) shows antidepressant and sleep-promoting effects in patients with major depressive disorder. Transl Psychiatry 9, 216. https://doi.org/10.1038/s41398-019-0553-z

RKI, 2017. Depressive Symptomatik bei Erwachsenen in Deutschland. https://doi.org/10.17886/RKI-GBE-2017-058

Robert Koch-Institut, 2019. Depressive Symptomatik im europäischen Vergleich – Ergebnisse des European Health Interview Survey (EHIS) 2. https://doi.org/10.25646/6221

Roybal, K., Theobold, D., Graham, A., DiNieri, J.A., Russo, S.J., Krishnan, V., Chakravarty, S., Peevey, J., Oehrlein, N., Birnbaum, S., Vitaterna, M.H., Orsulak, P., Takahashi, J.S., Nestler, E.J., Carlezon, W.A., McClung, C.A., 2007. Mania-like behavior induced by disruption of CLOCK. Proc Natl Acad Sci U S A 104, 6406–6411. https://doi.org/10.1073/pnas.0609625104

Rudic, R.D., McNamara, P., Curtis, A.-M., Boston, R.C., Panda, S., Hogenesch, J.B., Fitzgerald, G.A., 2004. BMAL1 and CLOCK, two essential components of the circadian clock, are involved in glucose homeostasis. PLoS Biol 2, e377. https://doi.org/10.1371/journal.pbio.0020377

Saad, L., Kalsbeek, A., Zwiller, J., Anglard, P., 2021. Rhythmic Regulation of DNA Methylation Factors and Core-Clock Genes in Brain Structures Activated by Cocaine or Sucrose: Potential Role of Chromatin Remodeling. Genes (Basel) 12, 1195. https://doi.org/10.3390/genes12081195

Saad, L., Sartori, M., Pol Bodetto, S., Romieu, P., Kalsbeek, A., Zwiller, J., Anglard, P., 2019. Regulation of Brain DNA Methylation Factors and of the Orexinergic System by Cocaine and Food Self-Administration. Mol Neurobiol 56, 5315–5331. https://doi.org/10.1007/s12035-018-1453-6

Saarni, S.I., Suvisaari, J., Sintonen, H., Pirkola, S., Koskinen, S., Aromaa, A., Lönnqvist, J., 2007. Impact of psychiatric disorders on health-related quality of life: general population survey. Br J Psychiatry 190, 326–332. https://doi.org/10.1192/bjp.bp.106.025106

Sakurai, T., Amemiya, A., Ishii, M., Matsuzaki, I., Chemelli, R.M., Tanaka, H., Williams, S.C., Richardson, J.A., Kozlowski, G.P., Wilson, S., Arch, J.R., Buckingham, R.E., Haynes, A.C., Carr, S.A., Annan, R.S., McNulty, D.E., Liu, W.S., Terrett, J.A., Elshourbagy, N.A., Bergsma, D.J., Yanagisawa, M., 1998. Orexins and orexin receptors: a family of hypothalamic neuropeptides and G protein-coupled receptors that regulate feeding behavior. Cell 92, 573–585.

Salomon, R.M., Ripley, B., Kennedy, J.S., Johnson, B., Schmidt, D., Zeitzer, J.M., Nishino, S., Mignot, E., 2003. Diurnal variation of cerebrospinal fluid hypocretin-1 (Orexin-A) levels in control and depressed subjects. Biol. Psychiatry 54, 96–104.

Sato, K., 2020. Why is prepulse inhibition disrupted in schizophrenia? Med Hypotheses 143, 109901. https://doi.org/10.1016/j.mehy.2020.109901

Savitz, A., Wajs, E., Zhang, Y., Xu, H., Etropolski, M., Thase, M.E., Drevets, W., 2021. Efficacy and safety of seltorexant as adjunctive therapy in major depressive disorder: A phase 2b, randomized, placebo-controlled, adaptive dose-finding study. Int J Neuropsychopharmacol pyab050. https://doi.org/10.1093/ijnp/pyab050

Scheer, F.A.J.L., Hilton, M.F., Mantzoros, C.S., Shea, S.A., 2009. Adverse metabolic and cardiovascular consequences of circadian misalignment. Proc Natl Acad Sci U S A 106, 4453–4458. https://doi.org/10.1073/pnas.0808180106

Schiappa, C., Scarpelli, S., D'Atri, A., Gorgoni, M., De Gennaro, L., 2018. Narcolepsy and emotional experience: a review of the literature. Behav Brain Funct 14, 19. https://doi.org/10.1186/s12993-018-0151-x

Schindelin, J., Arganda-Carreras, I., Frise, E., Kaynig, V., Longair, M., Pietzsch, T., Preibisch, S., Rueden, C., Saalfeld, S., Schmid, B., Tinevez, J.-Y., White, D.J., Hartenstein, V., Eliceiri, K., Tomancak, P., Cardona, A., 2012. Fiji: an open-source platform for biological-image analysis. Nat Methods 9, 676–682. https://doi.org/10.1038/nmeth.2019

Schmidt, F.M., Arendt, E., Steinmetzer, A., Bruegel, M., Kratzsch, J., Strauss, M., Baum, P., Hegerl, U., Schönknecht, P., 2011. CSF-hypocretin-1 levels in patients with major depressive disorder compared to healthy controls. Psychiatry Res 190, 240–243. https://doi.org/10.1016/j.psychres.2011.06.004

Schmidt, F.M., Brügel, M., Kratzsch, J., Strauss, M., Sander, C., Baum, P., Thiery, J., Hegerl, U., Schönknecht, P., 2010. Cerebrospinal fluid hypocretin-1 (orexin A) levels in mania compared to unipolar depression and healthy controls. Neurosci. Lett. 483, 20–22. https://doi.org/10.1016/j.neulet.2010.07.038

Schöner, J., Heinz, A., Endres, M., Gertz, K., Kronenberg, G., 2017. Post-traumatic stress disorder and beyond: an overview of rodent stress models. J Cell Mol Med 21, 2248–2256. https://doi.org/10.1111/jcmm.13161

Schwartz, M.D., Urbanski, H.F., Nunez, A.A., Smale, L., 2011. Projections of the suprachiasmatic nucleus and ventral subparaventricular zone in the Nile grass rat (Arvicanthis niloticus). Brain Res. 1367, 146–161. https://doi.org/10.1016/j.brainres.2010.10.058

Scott, E.M., Carter, A.M., Grant, P.J., 2008. Association between polymorphisms in the Clock gene, obesity and the metabolic syndrome in man. Int J Obes (Lond) 32, 658–662. https://doi.org/10.1038/sj.ijo.0803778

Scott, M.M., Marcus, J.N., Pettersen, A., Birnbaum, S.G., Mochizuki, T., Scammell, T.E., Nestler, E.J., Elmquist, J.K., Lutter, M., 2011. Hcrtr1 and 2 signaling differentially regulates depression-like behaviors. Behav. Brain Res. 222, 289–294. https://doi.org/10.1016/j.bbr.2011.02.044

Seifinejad, A., Neiteler, A., Li, S., Pfister, C., Fronczek, R., Shan, L., Garrett-Sinha, L.A., Frieser, D., Honda, M., Arribat, Y., Grepper, D., Amati, F., Picot, M., Iseli, C., Chartrel, N., Lammers, G.J., Liblau, R., Vassalli, A., Tafti, M., 2021. Narcolepsy with cataplexy is caused by epigenetic

silencing of hypocretin neurons (preprint). Neuroscience. https://doi.org/10.1101/2021.09.21.461046

Sellayah, D., Bharaj, P., Sikder, D., 2011. Orexin is required for brown adipose tissue development, differentiation, and function. Cell Metab. 14, 478–490. https://doi.org/10.1016/j.cmet.2011.08.010

Semenkovich, K., Brown, M.E., Svrakic, D.M., Lustman, P.J., 2015. Depression in type 2 diabetes mellitus: prevalence, impact, and treatment. Drugs 75, 577–587. https://doi.org/10.1007/s40265-015-0347-4

Sen, S., Dumont, S., Sage-Ciocca, D., Reibel, S., de Goede, P., Kalsbeek, A., Challet, E., 2018. Expression of the clock gene Rev-erbα in the brain controls the circadian organisation of food intake and locomotor activity, but not daily variations of energy metabolism. J Neuroendocrinol 30. https://doi.org/10.1111/jne.12557

Shi, S., Ansari, T.S., McGuinness, O.P., Wasserman, D.H., Johnson, C.H., 2013. Circadian disruption leads to insulin resistance and obesity. Curr Biol 23, 372–381. https://doi.org/10.1016/j.cub.2013.01.048

Silarova, B., Giltay, E.J., Van Reedt Dortland, A., Van Rossum, E.F.C., Hoencamp, E., Penninx, B.W.J.H., Spijker, A.T., 2015. Metabolic syndrome in patients with bipolar disorder: comparison with major depressive disorder and non-psychiatric controls. J Psychosom Res 78, 391–398. https://doi.org/10.1016/j.jpsychores.2015.02.010

Silveyra, P., Lux-Lantos, V., Libertun, C., 2007. Both orexin receptors are expressed in rat ovaries and fluctuate with the estrous cycle: effects of orexin receptor antagonists on gonadotropins and ovulation. Am J Physiol Endocrinol Metab 293, E977-985. https://doi.org/10.1152/ajpendo.00179.2007

Sinha, A., Shariq, A., Said, K., Sharma, A., Jeffrey Newport, D., Salloum, I.M., 2018. Medical Comorbidities in Bipolar Disorder. Curr Psychiatry Rep 20, 36. https://doi.org/10.1007/s11920-018-0897-8

Skrzypski, M., Billert, M., Nowak, K.W., Strowski, M.Z., 2018. The role of orexin in controlling the activity of the adipo-pancreatic axis. J. Endocrinol. 238, R95–R108. https://doi.org/10.1530/JOE-18-0122

Soya, S., Sakurai, T., 2020. Evolution of Orexin Neuropeptide System: Structure and Function. Front Neurosci 14, 691. https://doi.org/10.3389/fnins.2020.00691

Spanagel, R., Pendyala, G., Abarca, C., Zghoul, T., Sanchis-Segura, C., Magnone, M.C., Lascorz, J., Depner, M., Holzberg, D., Soyka, M., Schreiber, S., Matsuda, F., Lathrop, M., Schumann, G., Albrecht, U., 2005. The clock gene Per2 influences the glutamatergic system and modulates alcohol consumption. Nat. Med. 11, 35–42. https://doi.org/10.1038/nm1163

Spencer, S., Falcon, E., Kumar, J., Krishnan, V., Mukherjee, S., Birnbaum, S.G., McClung, C.A., 2013. Circadian genes Period 1 and Period 2 in the nucleus accumbens regulate anxiety-related behavior. Eur. J. Neurosci. 37, 242–250. https://doi.org/10.1111/ejn.12010

Steffen, A., Thom, J., Jacobi, F., Holstiege, J., Bätzing, J., 2020. Trends in prevalence of depression in Germany between 2009 and 2017 based on nationwide ambulatory claims data. Journal of Affective Disorders 271, 239–247. https://doi.org/10.1016/j.jad.2020.03.082

St-Onge, M.-P., 2017. Sleep-obesity relation: underlying mechanisms and consequences for treatment. Obes Rev 18 Suppl 1, 34–39. https://doi.org/10.1111/obr.12499

Storch, K.-F., Lipan, O., Leykin, I., Viswanathan, N., Davis, F.C., Wong, W.H., Weitz, C.J., 2002. Extensive and divergent circadian gene expression in liver and heart. Nature 417, 78–83. https://doi.org/10.1038/nature744

Storch, K.-F., Paz, C., Signorovitch, J., Raviola, E., Pawlyk, B., Li, T., Weitz, C.J., 2007. Intrinsic circadian clock of the mammalian retina: importance for retinal processing of visual information. Cell 130, 730–741. https://doi.org/10.1016/j.cell.2007.06.045

Strauß, M., Ulke, C., Paucke, M., Huang, J., Mauche, N., Sander, C., Stark, T., Hegerl, U., 2018. Brain arousal regulation in adults with attention-deficit/hyperactivity disorder (ADHD). Psychiatry Res 261, 102–108. https://doi.org/10.1016/j.psychres.2017.12.043

Stütz, A.M., Staszkiewicz, J., Ptitsyn, A., Argyropoulos, G., 2007. Circadian expression of genes regulating food intake. Obesity (Silver Spring) 15, 607–615. https://doi.org/10.1038/oby.2007.564

Sullivan, P.F., Neale, M.C., Kendler, K.S., 2000. Genetic epidemiology of major depression: review and meta-analysis. Am J Psychiatry 157, 1552–1562. https://doi.org/10.1176/appi.ajp.157.10.1552

Suzuki, M., Beuckmann, C.T., Shikata, K., Ogura, H., Sawai, T., 2005. Orexin-A (hypocretin-1) is possibly involved in generation of anxiety-like behavior. Brain Res 1044, 116–121. https://doi.org/10.1016/j.brainres.2005.03.002

Tafuri, S., Pavone, L.M., Lo Muto, R., Basile, M., Langella, E., Fiorillo, E., Avallone, L., Staiano, N., Vittoria, A., 2009. Expression of orexin A and its receptor 1 in the rat epididymis. Regul. Pept. 155, 1–5. https://doi.org/10.1016/j.regpep.2009.03.010

Taheri, S., Gardiner, J., Hafizi, S., Murphy, K., Dakin, C., Seal, L., Small, C., Ghatei, M., Bloom, S., 2001. Orexin A immunoreactivity and preproorexin mRNA in the brain of Zucker and WKY rats. Neuroreport 12, 459–464. https://doi.org/10.1097/00001756-200103050-00008

Taheri, S., Sunter, D., Dakin, C., Moyes, S., Seal, L., Gardiner, J., Rossi, M., Ghatei, M., Bloom, S., 2000. Diurnal variation in orexin A immunoreactivity and prepro-orexin mRNA in the rat central nervous system. Neurosci. Lett. 279, 109–112.

Takahashi, K., Arihara, Z., Suzuki, T., Sone, M., Kikuchi, K., Sasano, H., Murakami, O., Totsune, K., 2006. Expression of orexin-A and orexin receptors in the kidney and the presence of orexin-A-like immunoreactivity in human urine. Peptides 27, 871–877. https://doi.org/10.1016/j.peptides.2005.08.008

Tenorio-Lopes, L., Fournier, S., Henry, M.S., Bretzner, F., Kinkead, R., 2020. Disruption of estradiol regulation of orexin neurons: a novel mechanism in excessive ventilatory response to CO2 inhalation in a female rat model of panic disorder. Transl Psychiatry 10, 394. https://doi.org/10.1038/s41398-020-01076-x

Timper, K., Brüning, J.C., 2017. Hypothalamic circuits regulating appetite and energy homeostasis: pathways to obesity. Dis Model Mech 10, 679–689. https://doi.org/10.1242/dmm.026609

Toi, N., Inaba, M., Kurajoh, M., Morioka, T., Hayashi, N., Hirota, T., Miyaoka, D., Emoto, M., Yamada, S., 2019. Improvement of glycemic control by treatment for insomnia with suvorexant in type 2 diabetes mellitus. Journal of Clinical & Translational Endocrinology 15, 37–44. https://doi.org/10.1016/j.jcte.2018.12.006

Toth, L.A., Bhargava, P., 2013. Animal models of sleep disorders. Comp Med 63, 91–104.

Trivedi, P., Yu, H., MacNeil, D.J., Van der Ploeg, L.H., Guan, X.M., 1998. Distribution of orexin receptor mRNA in the rat brain. FEBS Lett 438, 71–75. https://doi.org/10.1016/s0014-5793(98)01266-6

Tsuneki, H., Kon, K., Ito, H., Yamazaki, M., Takahara, S., Toyooka, N., Ishii, Y., Sasahara, M., Wada, T., Yanagisawa, M., Sakurai, T., Sasaoka, T., 2016. Timed Inhibition of Orexin System by Suvorexant Improved Sleep and Glucose Metabolism in Type 2 Diabetic db/db Mice. Endocrinology 157, 4146–4157. https://doi.org/10.1210/en.2016-1404

Tsuneki, H., Tokai, E., Nakamura, Y., Takahashi, K., Fujita, M., Asaoka, T., Kon, K., Anzawa, Y., Wada, T., Takasaki, I., Kimura, K., Inoue, H., Yanagisawa, M., Sakurai, T., Sasaoka, T., 2015. Hypothalamic orexin prevents hepatic insulin resistance via daily bidirectional regulation of autonomic nervous system in mice. Diabetes 64, 459–470. https://doi.org/10.2337/db14-0695

Turek, F.W., Joshu, C., Kohsaka, A., Lin, E., Ivanova, G., McDearmon, E., Laposky, A., Losee-Olson, S., Easton, A., Jensen, D.R., Eckel, R.H., Takahashi, J.S., Bass, J., 2005. Obesity and metabolic syndrome in circadian Clock mutant mice. Science 308, 1043–1045. https://doi.org/10.1126/science.1108750

van der Horst, G.T., Muijtjens, M., Kobayashi, K., Takano, R., Kanno, S., Takao, M., de Wit, J., Verkerk, A., Eker, A.P., van Leenen, D., Buijs, R., Bootsma, D., Hoeijmakers, J.H., Yasui, A., 1999.

Mammalian Cry1 and Cry2 are essential for maintenance of circadian rhythms. Nature 398, 627–630. https://doi.org/10.1038/19323

van Londen, L., Goekoop, J.G., Kerkhof, G.A., Zwinderman, K.H., Wiegant, V.M., De Wied, D., 2001. Weak 24-h periodicity of body temperature and increased plasma vasopressin in melancholic depression. Eur Neuropsychopharmacol 11, 7–14. https://doi.org/10.1016/s0924-977x(00)00124-3

van Reedt Dortland, A.K.B., Giltay, E.J., van Veen, T., Zitman, F.G., Penninx, B.W.J.H., 2010. Metabolic syndrome abnormalities are associated with severity of anxiety and depression and with tricyclic antidepressant use. Acta Psychiatr Scand 122, 30–39. https://doi.org/10.1111/j.1600-0447.2010.01565.x

Vancampfort, D., Stubbs, B., Mitchell, A.J., De Hert, M., Wampers, M., Ward, P.B., Rosenbaum, S., Correll, C.U., 2015. Risk of metabolic syndrome and its components in people with schizophrenia and related psychotic disorders, bipolar disorder and major depressive disorder: a systematic review and meta-analysis. World Psychiatry 14, 339–347. https://doi.org/10.1002/wps.20252

Ventura, A., Meissner, A., Dillon, C.P., McManus, M., Sharp, P.A., Van Parijs, L., Jaenisch, R., Jacks, T., 2004. Cre-lox-regulated conditional RNA interference from transgenes. Proc. Natl. Acad. Sci. U.S.A. 101, 10380–10385. https://doi.org/10.1073/pnas.0403954101

Ventzke, K., Oster, H., Jöhren, O., 2019. Diurnal Regulation of the Orexin/Hypocretin System in Mice. Neuroscience 421, 59–68. https://doi.org/10.1016/j.neuroscience.2019.10.002

Vogelzangs, N., Beekman, A.T.F., Boelhouwer, I.G., Bandinelli, S., Milaneschi, Y., Ferrucci, L., Penninx, B.W.J.H., 2011. Metabolic depression: a chronic depressive subtype? Findings from the InCHIANTI study of older persons. J Clin Psychiatry 72, 598–604. https://doi.org/10.4088/JCP.10m06559

Walf, A.A., Frye, C.A., 2007. The use of the elevated plus maze as an assay of anxiety-related behavior in rodents. Nat Protoc 2, 322–328. https://doi.org/10.1038/nprot.2007.44

Wang, D., Opperhuizen, A.-L., Reznick, J., Turner, N., Su, Y., Cooney, G.J., Kalsbeek, A., 2017. Effects of feeding time on daily rhythms of neuropeptide and clock gene expression in the rat hypothalamus. Brain Res 1671, 93–101. https://doi.org/10.1016/j.brainres.2017.07.006

Wang, X.-L., Kooijman, S., Gao, Y., Tzeplaeff, L., Cosquer, B., Milanova, I., Wolff, S.E.C., Korpel, N., Champy, M.-F., Petit-Demoulière, B., Goncalves Da Cruz, I., Sorg-Guss, T., Rensen, P.C.N., Cassel, J.-C., Kalsbeek, A., Boutillier, A.-L., Yi, C.-X., 2021. Microglia-specific knock-down of Bmal1 improves memory and protects mice from high fat diet-induced obesity. Mol Psychiatry 26, 6336–6349. https://doi.org/10.1038/s41380-021-01169-z

Weaver, D.R., Reppert, S.M., 1989. Periodic feeding of SCN-lesioned pregnant rats entrains the fetal biological clock. Brain Res Dev Brain Res 46, 291–296. https://doi.org/10.1016/0165-3806(89)90292-7

Welsh, D.K., Noguchi, T., 2012. Cellular bioluminescence imaging. Cold Spring Harb Protoc 2012, pdb.top070607. https://doi.org/10.1101/pdb.top070607

Woon, P.Y., Kaisaki, P.J., Bragança, J., Bihoreau, M.-T., Levy, J.C., Farrall, M., Gauguier, D., 2007. Aryl hydrocarbon receptor nuclear translocator-like (BMAL1) is associated with susceptibility to hypertension and type 2 diabetes. Proc Natl Acad Sci U S A 104, 14412–14417. https://doi.org/10.1073/pnas.0703247104

World Health Organization, 2017. Depression and other common mental disorders: global health estimates., No. WHO/MSD/MER/2017.2. ed. World Health Organization.

Xiao, X., Yeghiazaryan, G., Hess, S., Klemm, P., Sieben, A., Kleinridders, A., Morgan, D.A., Wunderlich, F.T., Rahmouni, K., Kong, D., Scammell, T.E., Lowell, B.B., Kloppenburg, P., Brüning, J.C., Hausen, A.C., 2021. Orexin receptors 1 and 2 in serotonergic neurons differentially regulate peripheral glucose metabolism in obesity. Nat Commun 12, 5249. https://doi.org/10.1038/s41467-021-25380-2

Yamamoto, Y., Tanahashi, T., Katsuura, S., Kurokawa, K., Nishida, K., Kuwano, Y., Kawai, T., Teshima-Kondo, S., Chikahisa, S., Tsuruo, Y., Sei, H., Rokutan, K., 2010. Interleukin-18 deficiency

reduces neuropeptide gene expressions in the mouse amygdala related with behavioral change. J. Neuroimmunol. 229, 129–139. https://doi.org/10.1016/j.jneuroim.2010.07.024

Yamamoto, Y., Ueta, Y., Date, Y., Nakazato, M., Hara, Y., Serino, R., Nomura, M., Shibuya, I., Matsukura, S., Yamashita, H., 1999. Down regulation of the prepro-orexin gene expression in genetically obese mice. Brain Res Mol Brain Res 65, 14–22. https://doi.org/10.1016/s0169-328x(98)00320-9

Yamanaka, A., Beuckmann, C.T., Willie, J.T., Hara, J., Tsujino, N., Mieda, M., Tominaga, M., Yagami, K. ichi, Sugiyama, F., Goto, K., Yanagisawa, M., Sakurai, T., 2003. Hypothalamic orexin neurons regulate arousal according to energy balance in mice. Neuron 38, 701–713. https://doi.org/10.1016/s0896-6273(03)00331-3

Yamanaka, A., Sakurai, T., Katsumoto, T., Yanagisawa, M., Goto, K., 1999. Chronic intracerebroventricular administration of orexin-A to rats increases food intake in daytime, but has no effect on body weight. Brain Res 849, 248–252. https://doi.org/10.1016/s0006-8993(99)01905-8

Yang, G., Chen, L., Grant, G.R., Paschos, G., Song, W.-L., Musiek, E.S., Lee, V., McLoughlin, S.C., Grosser, T., Cotsarelis, G., FitzGerald, G.A., 2016. Timing of expression of the core clock gene Bmal1 influences its effects on aging and survival. Sci Transl Med 8, 324ra16. https://doi.org/10.1126/scitranslmed.aad3305

Yoo, S.-H., Yamazaki, S., Lowrey, P.L., Shimomura, K., Ko, C.H., Buhr, E.D., Siepka, S.M., Hong, H.-K., Oh, W.J., Yoo, O.J., Menaker, M., Takahashi, J.S., 2004. PERIOD2::LUCIFERASE real-time reporting of circadian dynamics reveals persistent circadian oscillations in mouse peripheral tissues. Proc Natl Acad Sci U S A 101, 5339–5346. https://doi.org/10.1073/pnas.0308709101

Yoshida, Y., Fujiki, N., Nakajima, T., Ripley, B., Matsumura, H., Yoneda, H., Mignot, E., Nishino, S., 2001. Fluctuation of extracellular hypocretin-1 (orexin A) levels in the rat in relation to the light-dark cycle and sleep-wake activities. Eur J Neurosci 14, 1075–1081. https://doi.org/10.1046/j.0953-816x.2001.01725.x

Yoshikawa, F., Shigiyama, F., Ando, Y., Miyagi, M., Uchino, H., Hirose, T., Kumashiro, N., 2020. Chronotherapeutic efficacy of suvorexant on sleep quality and metabolic parameters in patients with type 2 diabetes and insomnia. Diabetes Res Clin Pract 169, 108412. https://doi.org/10.1016/j.diabres.2020.108412

Yu, F., Wang, Z., Zhang, T., Chen, X., Xu, H., Wang, F., Guo, L., Chen, M., Liu, K., Wu, B., 2021. Deficiency of intestinal Bmal1 prevents obesity induced by high-fat feeding. Nat Commun 12, 5323. https://doi.org/10.1038/s41467-021-25674-5

Zarifkar, M., Noshad, S., Shahriari, M., Afarideh, M., Khajeh, E., Karimi, Z., Ghajar, A., Esteghamati, A., 2017. Inverse Association of Peripheral Orexin-A with Insulin Resistance in Type 2 Diabetes Mellitus: A Randomized Clinical Trial. Rev Diabet Stud 14, 301–310. https://doi.org/10.1900/RDS.2017.14.301

Zeitzer, J.M., Buckmaster, C.L., Parker, K.J., Hauck, C.M., Lyons, D.M., Mignot, E., 2003. Circadian and homeostatic regulation of hypocretin in a primate model: implications for the consolidation of wakefulness. J. Neurosci. 23, 3555–3560.

Zhang, L., Hirano, A., Hsu, P.-K., Jones, C.R., Sakai, N., Okuro, M., McMahon, T., Yamazaki, M., Xu, Y., Saigoh, N., Saigoh, K., Lin, S.-T., Kaasik, K., Nishino, S., Ptáček, L.J., Fu, Y.-H., 2016. A PERIOD3 variant causes a circadian phenotype and is associated with a seasonal mood trait. Proc. Natl. Acad. Sci. U.S.A. 113, E1536-1544. https://doi.org/10.1073/pnas.1600039113

Zhang, S., Zeitzer, J.M., Yoshida, Y., Wisor, J.P., Nishino, S., Edgar, D.M., Mignot, E., 2004. Lesions of the suprachiasmatic nucleus eliminate the daily rhythm of hypocretin-1 release. Sleep 27, 619–627.

Zhang, Z., Li, Q., Liu, F., Sun, Y., Zhang, J., 2010. Prevention of diet-induced obesity by safflower oil: insights at the levels of PPARalpha, orexin, and ghrelin gene expression of adipocytes in mice. Acta Biochim. Biophys. Sin. (Shanghai) 42, 202–208. https://doi.org/10.1093/abbs/gmq010

Zhao, C., Gammie, S.C., 2018. The circadian gene Nr1d1 in the mouse nucleus accumbens modulates sociability and anxiety-related behavior. Eur J Neurosci. https://doi.org/10.1111/ejn.14207

Zhou, B., Zhang, Y., Zhang, F., Xia, Y., Liu, J., Huang, R., Wang, Yuangao, Hu, Y., Wu, J., Dai, C., Wang, H., Tu, Y., Peng, X., Wang, Yiqian, Zhai, Q., 2014. CLOCK/BMAL1 regulates circadian change of mouse hepatic insulin sensitivity by SIRT1. Hepatology 59, 2196–2206. https://doi.org/10.1002/hep.26992

9. Supplement

Supplementary table S1 Gene expression in the LH of Cry1/2 $^{-/-}$ mice. Group sizes, mean and standard deviation (SD) of *Ppox* and *Per2* expression in the LH of Wt and Cry1/2$^{-/-}$ mice at different ZT and two-way ANOVA investigating the impact of genotype and ZT on *Ppox* and *Per2* expression. DF = degrees of freedom; n.s. = not significant; *p < 0.05, ***p < 0.001.

Gene	Parameter	Wt				Cry1/2 $^{-/-}$						Source of variation		
		ZT1	ZT7	ZT13	ZT19	ZT1	ZT7	ZT13	ZT19			Genotype	ZT	Genotype x ZT
Ppox	Fold Change (mean ± SD)	1.10 ± 1.33	2.39 ± 0.37	0.17 ± 0.11	0.21 ± 0.09	1.26 ± 0.32	1.23 ± 0.14	1.08 ± 0.26	1.41 ± 0.39	Two-way ANOVA	DF	1	3	3
											F-value	0.7485	4.1701	3.0089
											p-value	0.39517	0.01591	0.04912
	n	9	4	5	3	3	3	3	3		Summary	n.s.	*	*
Per2	Fold Change (mean ± SD)	0.89 ± 0.56	1.54 ± 0.14	0.97 ± 0.69	0.76 ± 0.77	2.86 ± 0.81	2.96 ± 0.75	4.40 ± 1.26	3.35 ± 0.89		DF	1	3	3
											F-value	81.8685	1.2372	2.6758
											p-value	1.16e-09	0.31556	0.06717
	n	10	4	5	4	3	3	3	3		Summary	***	n.s.	n.s.

Supplementary table S2 Gene expression in the LH of Cry1/2 $^{-/-}$ mice. Post-hoc pairwise t-test with bonferroni correction of *Ppox* expression in Wt and Cry1/2$^{-/-}$ mice at different ZT. n.s. = not significant; *p < 0.05, **p < 0.01.

Gene	**ZT**	**Wt vs. Cry1/2 $^{-/-}$**		
		p -value	**Corrected p-value**	**Summary**
Ppox	**ZT1**	**0.854**	**1**	**n.s.**
	ZT7	**0.00403**	**0.01612**	*****
	ZT13	**0.000411**	**0.001644**	******
	ZT19	**0.0067**	**0.0268**	*****

Supplementary table S3 Gene expression in the LH of Cry1/2 $^{-/-}$ mice. Zero-amplitude test for rhythmicity with bonferroni correction in the expression of *Ppox* and *Per2* in Wt and Cry1/2$^{-/-}$ mice. n.s. = not significant; *p < 0.05.

Gene	Genotype	Zero-amplitude test for rhythmicity		
		p -value	Corrected p-value	Summary
Ppox	Wt	0.01005237	0.04020948	*
	Cry1/2 $^{-/-}$	0.5870723	1	n.s.
Per2	Wt	0.1818508	0.7274032	n.s.
	Cry1/2 $^{-/-}$	0.1699096	0.6796384	n.s.

Supplementary table S4 Gene expression in the LH of Orx-Bmal1$^{-/-}$ mice. Group sizes, mean expression and standard deviation (SD) of *Ppox*, *Bmal1* and *Pmch* in the LH of Wt and Orx-Bmal1$^{-/-}$ at ZT1, ZT7, ZT13 and ZT19.

Gene	Parameter		Wt				Orx-Bmal1$^{-/-}$			
			ZT1	ZT7	ZT13	ZT19	ZT1	ZT7	ZT13	ZT19
Ppox	Fold Change (mean ± SD)		0.72 ± 0.91	2.88 ± 0.48	0.26 ± 0.12	0.72 ± 0.69	1.32 ± 0.50	1.37 ± 0.59	1.12 ± 0.64	1.57 ± 0.52
	n		15	6	7	7	12	8	7	8
Bmal1	Fold Change (mean ± SD)		0.97 ± 0.62	1.02 ± 0.20	0.81 ± 0.52	1.23 ± 0.70	1.87 ± 0.32	1.24 ± 0.17	1.29 ± 0.26	1.56 ± 0.29
	n		16	7	8	8	11	7	6	8
Pmch	f	Fold Change (mean ± SD)	0.97 ± 1.42	2.61 ± 0.31	0.23 ± 0.14	0.88 ± 1.41	0.46 ± 0.15	1.61 ± 1.06	0.22 ± 0.19	0.68 ± 0.34
		n	9	4	4	4	6	3	2	3
	m	Fold Change (mean ± SD)	0.29 ± 0.26	3.69 ± 0.08	0.20 ± 0.12	0.55 ± 0.11	0.45 ± 0.28	0.44 ± 0.14	0.37 ± 0.11	0.41 ± 0.19
		n	6	2	3	3	6	5	4	4

Supplementary table S5 Gene expression in the LH of Orx-Bmal1$^{-/-}$ mice. Three-way ANOVA investigating the impact of genotype and ZT on *Ppox*, *Bmal1* and *Pmch* expression in the LH of Wt and Orx-Bmal1$^{-/-}$. DF = degrees of freedom; n.s. = not significant; *p < 0.05, **p < 0.01, ***p < 0.001.

Gene	Three-way ANOVA	Source of Variation						
		Genotype	ZT	Sex	Genotype x ZT	Genotype x Sex	ZT x Sex	Genotype x ZT x Sex
Ppox	DF	1	3	1	3	1	3	3
	F-value	5.5716	11.0832	5.4460	9.4607	0.1402	0.2313	0.3349
	p-value	0.02190	8.927e-06	0.02337	4.017e-05	0.70956	0.87420	0.80015
	Summary	*	***	*	***	n.s.	n.s.	n.s.
Bmal1	DF	1	3	1	3	1	3	3
	F-value	28.4470	2.7240	0.4678	2.4338	0.3528	3.7163	1.9179
	p-value	1.866e-06	0.05294	0.49687	0.07459	0.55495	0.01662	0.13737
	Summary	***	n.s.	n.s.	n.s.	n.s.	*	n.s.
Pmch	DF	1	3	1	3	1	3	3
	F-value	7.9251	13.3520	2.0561	6.2111	0.1122	0.2503	3.0947
	p-value	0.006870	1.4e-06	0.157588	0.001095	0.738992	0.860736	0.034749
	Summary	**	***	n.s.	**	n.s.	n.s.	*

Supplementary table S6 Gene expression in the LH of Orx-Bmal1$^{-/-}$ mice. Post-hoc pairwise t-test with bonferroni correction of *Ppox* and *Pmch* expression in Wt and Orx-Bmal1$^{-/-}$ mice at different ZT. n.a. = not available; n.s. = not significant; *p < 0.05, **p < 0.01.

Gene	ZT		Post-hoc pairwise t-test with bonferroni correction Wt vs. Orx-Bmal1$^{-/-}$		
			p -value	Corrected p-value	Summary
Ppox	ZT1		0.0515	0.206	n.s.
	ZT7		0.000261	0.001044	**
	ZT13		0.0044	0.0176	*
	ZT19		0.018	0.072	n.s.
Pmch	ZT1	f	0.402	1	n.s.
		m	0.326	1	n.s.
	ZT7	f	0.123	0.738	n.s.
		m	n.a.	n.a.	n.a.
	ZT13	f	n.a.	n.a.	n.a.
		m	0.125	0.75	n.s.
	ZT19	f	0.826	1	n.s.
		m	0.315	1	n.s.

Supplementary table S7 Gene expression in the LH of Orx-Bmal1$^{-/-}$ mice. Zero-amplitude test for rhythmicity with bonferroni correction of the expression of *Ppox*, *Bmal1* and *Pmch* in Wt and Orx-Bmal1$^{-/-}$. n.s. = not significant; *p < 0.05, **p < 0.01.

Gene	Genotype		Zero-amplitude test for rhythmicity		
			p -value	Corrected p-value	Summary
Ppox	Wt		0.002087737	0.016701896	*
	Orx-Bmal1$^{-/-}$		0.6834333	1	n.s.
Bmal1	Wt		0.6898291	1	n.s.
	Orx-Bmal1$^{-/-}$		0.00019022	0.00152176	**
Pmch	Wt	f	0.1624085	1	n.s.
		m	0.03644907	0.29159256	n.s.
	Orx-Bmal1$^{-/-}$	f	0.2428334	1	n.s.
		m	0.7743529	1	n.s.

Supplementary table S8 Locomotor activity in the IntelliCages. Group sizes, mean and standard deviation (SD) of activity measured in the IntelliCage system of Wt and Orx-Bmal1$^{-/-}$ mice of both sexes during LD and DD. Data form DD was analyzed according to the circadian phases of the previous LD cycle.

Activity	Day / Previous Day						Night / Previous Night					
	Wt			Orx-Bmal1$^{-/-}$			Wt			Orx-Bmal1$^{-/-}$		
	All	Females	Males	All	Females	Males	All	Females	Males	All	Females	Males
LD (visits) (mean ± SD)	30.7 ± 8.8	28.8 ± 6.4	32.5 ± 10.9	32.2 ± 8.6	28.6 ± 5.5	38.1 ± 9.7	122.0 ± 31.8	138.5 ± 32.1	107.4 ± 24.7	106.8 ± 29.3	100.2 ± 23.3	116.8 ± 35.5
n	16	8	8	24	15	9	17	8	9	25	15	10
DD (visits) (mean ± SD)	47.7 ± 15.2	50.6 ± 11.5	45.2 ± 18.1	42.1 ± 10.3	39.3 ± 9.4	46.7 ± 10.5	99.6 ± 33.4	116.4 ± 31.9	84.6 ± 28.2	87 ± 23.8	78.4 ± 18.1	101.3 ± 26.1
n	17	8	9	24	15	9	17	8	9	24	15	9

Supplementary table S9 Locomotor activity in the IntelliCages. Three-way ANOVA investigating the impact of genotype, sex and circadian phase on activity measured in the IntelliCage system of Wt and Orx-Bmal1$^{-/-}$ mice of both sexes during LD and DD. n.s. = not significant; *p < 0.05, **p< 0.01, ***p < 0.001.

Activity	Three-way ANOVA	Source of Variation						
		Genotype	Sex	Phase	Genotype x Sex	Genotype x Phase	Sex x Phase	Genotype x Sex x Phase
LD	d.f.	1	1	1	1	1	1	1
	F-value	2.0192	0.1479	300.6581	8.0227	3.7912	1.1811	4.6841
	p-value	0.159525	0.701626	< 2.2e-16	0.005948	0.055319	0.280652	0.033670
	Summary	n.s.	n.s.	***	**	n.s.	n.s.	*
DD	d.f.	1	1	1	1	1	1	1
	F-value	14.0044	0.0212	118.5243	14.0292	0.6586	0.0774	5.3545
	p-value	0.0490498	0.8847384	< 2.2e-16	0.0003538	0.4196554	0.7815865	0.0234481
	Summary	*	n.s.	***	***	n.s.	n.s.	*

Supplementary table S10 Locomotor activity in the IntelliCages. Post-hoc pairwise t-test with bonferroni correction comparing activity measured in the IntelliCages during LD and DD conditions between Wt and Orx-Bmal1$^{-/-}$ of the same sex. n.s. = not significant; *p < 0.05, **p< 0.01.

Activity	Phase		Post-hoc pairwise t-test with bonferroni correction Wt vs. Orx-Bmal1$^{-/-}$		
			p –value	Corrected p-value	Summary
LD	f	Day	0.934	1	n.s.
		Night	0.00345	0.0138	*
	m	Day	0.279	1	n.s.
		Night	0.518	1	n.s.
DD	f	Day	0.0184	0.0736	*
		Night	0.00141	0.00564	**
	m	Day	0.823	1	n.s.
		Night	0.21	0.84	n.s.

Supplementary table S11 Locomotor activity in the IntelliCages. Two-way ANOVA assessing the impact of genotype and sex on the period of locomotor activity measured in the IntelliCages during LD and DD conditions in Wt and Orx-Bmal1$^{-/-}$ mice of both sexes. n.s. = not significant; ***p < 0.001.

Period	Wt			Orx-Bmal1$^{-/-}$					Source of Variance		
	All	Females	Males	All	Females	Males			Genotype	Sex	Genotype x Sex
LD (mean ± SD)	24.01 ± 0.32	24.07 ± 0.32	23.96 ± 0.33	24.24 ± 0.43	24.14 ± 0.35	24.59 ± 0.79	Two-way ANOVA	d.f.	1	1	1
								F-value	3.8038	0.6548	2.1697
								p-value	0.05874	0.42358	0.14921
n	17	8	9	24	15	10		Summary	n.s.	n.s.	n.s.
DD (mean ± SD)	24.05 ± 0.24	24.23 ± 0.18	23.88 ± 0.14	24.09 ± 0.24	24.22 ± 0.21	23.89 ± 0.14		d.f.	1	1	1
								F-value	0.0016	38.0249	0.0594
								p-value	0.9682	3.366e-07	0.8088
n	17	8	9	25	15	10		Summary	n.s.	***	n.s.

Supplementary table S12 PER2::LUC oscillations in the SCN. Group sizes, mean and standard deviation (SD) of amplitude, period and dampening of PER2::LUC oscillations in the SCN of Wt and Orx-Bmal1$^{-/-}$ mice of both sexes and two-way ANOVA investigating the impact of genotype and sex on these parameters. DF = degrees of freedom; n.s. = not significant.

Parameter	Wt			Orx-Bmal1$^{-/-}$					Source of variation		
	All	Females	Males	All	Females	Males			Genotype	Sex	Genotype x Sex
Amplitude (mean ± SD)	0.12 ± 0.02	0.12 ± 0.02	0.13 ± 0.01	0.12 ± 0.04	0.12 ± 0.04	0.13 ± 0.03	Two-way ANOVA	DF	1	1	1
								F-value	0.0018	0.8488	0.2182
								p-value	0.9662	0.3654	0.6443
n	11	7	4	19	13	6		Summary	n.s.	n.s.	n.s.
Period (h) (mean ± SD)	24.8 ± 0.37	24.85 ± 0.37	24.73 ± 0.39	24.74 ± 0.44	24.83 ± 0.40	24.60 ± 0.48		DF	1	1	1
								F-value	0.2243	1.7547	0.1573
								p-value	0.6390	0.1947	0.6943
n	14	8	6	22	13	9		Summary	n.s.	n.s.	n.s.
Dampening (d) (mean ± SD)	4.07 ± 1.48	4.12 ± 1.36	4.01 ± 1.75	4.98 ± 2.55	4.52 ± 2.71	5.59 ± 2.34		DF	1	1	1
								F-value	1.3783	0.6345	0.5452
								p-value	0.2496	0.4320	0.4660
n	13	7	6	21	12	9		Summary	n.s.	n.s.	n.s.

Supplementary table S13 OFT. Group sizes, mean and standard deviation (SD) of distance travelled, mean speed, center time, center entries, periphery time, periphery entries, corner time, corner entries in the OFT of Wt and Orx-Bmal1$^{-/-}$ mice of both sexes and two-way ANOVA investigating the impact of genotype and sex on these parameters. DF = degrees of freedom; n.s. = not significant; *p < 0.05.

Parameter	Wt			Orx-Bmal1$^{-/-}$					Source of variation		
	All	Females	Males	All	Females	Males			Genotype	Sex	Genotype x Sex
Distance travelled (m) (mean ± SD)	24.28 ± 6.50	22.71 ± 6.29	25.56 ± 6.68	27.93 ± 8.67	28.40 ± 10.17	27.29 ± 6.50	Two-way ANOVA	DF	1	1	1
								F-value	2.4796	0.0695	0.6948
								p-value	0.1228	0.7933	0.4093
n	20	9	11	26	15	11		Summary	n.s.	n.s.	n.s.
Mean Speed (m/s) (mean ± SD)	0.04 ± 0.01	0.04 ± 0.01	0.04 ± 0.01	0.05 ± 0.01	0.05 ± 0.02	0.05 ± 0.01		DF	1	1	1
								F-value	2.3844	0.0607	0.6814
								p-value	0.1301	0.8066	0.4138
n	20	9	11	26	15	11		Summary	n.s.	n.s.	n.s.
Center time (s) (mean ± SD)	237.35 ± 76.02	263.31 ± 71.34	216.10 ± 76.20	224.58 ± 85.72	241.61 ± 82.90	201.36 ± 87.88		DF	1	1	1
								F-value	0.5721	3.2678	0.0208
								p-value	0.45365	0.07782	0.88603
n	20	9	11	26	15	11		Summary	n.s.	n.s.	n.s.
Center entries (mean ± SD)	64.65 ± 18.87	66.33 ± 15.86	63.27 ± 21.69	61.32 ± 16.89	59.64 ± 14.25	63.45 ± 20.29		DF	1	1	1
								F-value	0.3523	0.0190	0.3944
								p-value	0.3944	0.8910	0.5335
n	20	9	11	25	14	11		Summary	n.s.	n.s.	n.s.
Periphery time (s) (mean ± SD)	149.59 ± 53.33	149.26 ± 55.90	149.86 ± 53.88	130.36 ± 40.89	131.05 ± 45.44	129.34 ± 35.29		DF	1	1	1
								F-value	1.7668	0.0021	0.0063
								p-value	0.1911	0.9639	0.9370
n	20	9	11	25	15	10		Summary	n.s.	n.s.	n.s.
Periphery entries (mean ± SD)	69.05 ± 14.71	64.78 ± 12.70	72.55 ± 15.89	73.04 ± 16.18	71.13 ± 18.77	75.64 ± 12.19		DF	1	1	1
								F-value	1.0266	1.6324	0.1217
								p-value	0.3168	0.2084	0.7290
n	20	9	11	26	15	11		Summary	n.s.	n.s.	n.s.
Corner time (s) (mean ± SD)	213.07 ± 52.26	187.44 ± 31.20	234.04 ± 57.75	238.83 ± 56.44	227.32 ± 55.59	254.54 ± 56.27		DF	1	1	1
								F-value	3.6952	5.2118	0.3778
								p-value	0.06137	0.02756	0.54211
n	20	9	11	26	15	11		Summary	n.s.	*	n.s.
Corner entries	49.55	46.89	51.73	54.27	54.53	53.91		DF	1	1	1

(mean ± SD)	± 15.05	± 11.96	± 17.44	± 11.99	± 14.14	± 8.89		F-value	1.4687	0.1910	0.4482
								p-value	0.2323	0.6643	0.5068
n	20	9	11	26	15	11		Summary	n.s.	n.s.	n.s.

Supplementary table S14 EPM. Group sizes, mean and standard deviation (SD) of open arm entries, open arm time, closed arm entries, closed arm time, center entries, center time and distance travelled in the EPM of Wt and Bmal1$^{-/-}$ mice of both sexes and two-way ANOVA investigating the impact of genotype and sex on these parameters. DF = degrees of freedom; n.s. = not significant; *p < 0.05.

Parameter	Wt			Orx-Bmal1$^{-/-}$					Source of variation		
	All	Females	Males	All	Females	Males			Genotype	Sex	Genotype x Sex
Open arm entries (mean ± SD)	12.11 ± 7.48	14.89 ± 4.48	9.6 ± 8.90	12.88 ± 4.62	14 ± 4.42	11.36 ± 4.63	Two-way ANOVA	DF	1	1	1
								F-value	0.0498	4.7425	0.5745
								p-value	0.82456	0.0352	0.45280
n	19	9	10	26	15	11		Summary	n.s.	*	n.s.
Open arm time (s) (mean ± SD)	23.96 ± 16.26	30.36 ± 11.33	18.2 ± 18.35	36.98 ± 26.20	44.57 ± 29.46	26.62 ± 17.22		DF	1	1	1
								F-value	3.0297	5.6757	0.1951
								p-value	0.08925	0.02192	0.66106
n	19	9	10	26	15	11		Summary	n.s.	*	n.s.
Closed arm entries (mean ± SD)	26.9 ± 7.71	30.11 ± 5.40	24.27 ± 8.53	30.12 ± 8.77	30 ± 8.36	30.27 ± 9.72		DF	1	1	1
								F-value	1.3724	0.9519	1.5128
								p-value	0.2480	0.3348	0.2256
n	20	9	11	26	15	11		Summary	n.s.	n.s.	n.s.
Closed arm time (s) (mean ± SD)	487.58 ± 65.67	472.62 ± 47.89	499.82 ± 77.41	470.79 ± 53.17	459.44 ± 54.11	486.26 ± 50.12		DF	1	1	1
								F-value	0.5782	2.3933	0.0001
								p-value	0.4513	0.1294	0.9916
n	20	9	11	26	15	11		Summary	n.s.	n.s.	n.s.
Center entries (mean ± SD)	38.35 ± 16.13	42 ± 9.90	35.36 ± 19.85	41.5 ± 11.82	42.33 ± 10.73	40.36 ± 13.63		DF	1	1	1
								F-value	0.3976	0.9334	0.3105
								p-value	0.5317	0.3395	0.5803
n	20	9	11	26	15	11		Summary	n.s.	n.s.	n.s.
Center time (s) (mean ± SD)	83.78 ± 43.43	97.04 ± 38.34	72.93 ± 46.05	92.26 ± 32.58	96.02 ± 30.76	87.13 ± 35.76		DF	1	1	1
								F-value	0.3349	1.9482	0.4589
								p-value	0.5659	0.1701	0.5019
n	20	9	11	26	15	11		Summary	n.s.	n.s.	n.s.
Distance travelled (m) (mean ± SD)	9.24 ± 2.52	10.53 ± 2.25	8.07 ± 2.24	10.09 ± 2.58	10.14 ± 2.66	10.03 ± 2.59		DF	1	1	1
								F-value	0.9660	2.2300	2.4621
								p-value	0.3314	0.1430	0.1243
n	19	9	10	26	15	11		Summary	n.s.	n.s.	n.s.

Supplementary table S15 LDT. Group sizes, mean and standard deviation (SD) of time spent in light, light entries and latency until the first light entry in the LDT of Wt and Orx-Bmal1$^{-/-}$ mice of both sexes and two-way ANOVA investigating the impact of genotype and sex on these parameters. DF = degrees of freedom; n.s. = not significant. *p < 0.05.

Parameter	Wt			Orx-Bmal1$^{-/-}$					Source of variation		
	All	Females	Males	All	Females	Males			Genotype	Sex	Genotype x Sex
Time in light (s) (mean ± SD)	77.88 ± 27.35	82.71 ± 12.26	74.5 ± 34.62	118.35 ± 64.90	122.83 ± 69.21	113.45 ± 62.82	Two-way ANOVA	DF	1	1	1
								F-value	5.2209	0.2702	0.0011
								p-value	0.02831	0.60639	0.97340
n	17	7	10	23	12	11		Summary	*	n.s.	n.s.
Light entries (mean ± SD)	9.78 ± 3.30	9.71 ± 1.60	9.82 ± 4.12	10.65 ± 4.13	10.33 ± 3.58	11 ± 4.82		DF	1	1	1
								F-value	0.5705	0.1208	0.0515
								p-value	0.4548	0.7302	0.8217
n	18	7	11	23	12	11		Summary	n.s.	n.s.	n.s.
Latency first light entry (s) (mean ± SD)	24.06 ± 10.19	24.17 ± 12.81	24 ± 9.04	25.5 ± 13.30	25.09 ± 15	25.91 ± 12.10		DF	1	1	1
								F-value	0.1306	0.0105	0.0140
								p-value	0.7200	0.9191	0.9067
n	16	6	10	22	11	11		Summary	n.s.	n.s.	n.s.

Supplementary table S16 TST. Group sizes, mean and standard deviation (SD) of time immobile, immobile episodes and immobility latency in the TST of Wt and Orx-Bmal1$^{-/-}$ mice of both sexes and two-way ANOVA investigating the impact of genotype and sex on these parameters. DF = degrees of freedom; n.s. = not significant

Parameter	Wt			Orx-Bmal1$^{-/-}$					Source of variation		
	All	Females	Males	All	Females	Males			Genotype	Sex	Genotype x Sex
Time immobile (s) (mean ± SD)	156.28 ± 60.51	147.32 ± 50.86	163.6 ± 68.96	144.31 ± 60.39	159.96 ± 60.29	126.23 ± 54.13	Two-way ANOVA	DF	1	1	1
								F-value	0.4994	0.3531	1.8338
								p-value	0.4839	0.5557	0.1833
n	20	9	11	24	15	11		Summary	n.s.	n.s.	n.s.
Immobile episodes (mean ± SD)	12.05 ± 4.07	13.33 ± 3.74	11 ± 4.2	12.63 ± 4.11	12.73 ± 4.03	12.55 ± 4.59		DF	1	1	1
								F-value	0.1419	0.8381	0.7654
								p-value	0.7084	0.3654	0.3869
n	20	9	11	24	15	11		Summary	n.s.	n.s.	n.s.
Immobility latency (s) (mean ± SD)	64.98 ± 37.24	53.79 ± 30.11	74.13 ± 41.28	66.99 ± 36.17	59.45 ± 44.07	65.98 ± 30.96		DF	1	1	1
								F-value	0.0534	0.5522	0.9683
								p-value	0.8184	0.4619	0.3312
n	20	9	11	23	14	11		Summary	n.s.	n.s.	n.s.

Supplementary table S17 LHP. Group sizes, mean and standard deviation (SD) of the latency to escape, failures to escape and the pain threshold in the LHP of Wt and Orx-Bmal1$^{-/-}$ mice of both sexes and two-way ANOVA investigating the impact of genotype and sex on these parameters. DF = degrees of freedom; n.s. = not significant; *p < 0.05, **p < 0.01.

Parameter	Wt			Orx-Bmal1$^{-/-}$					Source of variation		
	All	Females	Males	All	Females	Males			Genotype	Sex	Genotype x Sex
Latency (s) (mean ± SD)	14.97 ± 7.92	19.25 ± 7.59	12.25 ± 7.15	11.07 ± 4.93	10.98 ± 5.59	11.19 ± 4.31	Two-way ANOVA	DF	1	1	1
								F-value	4.8449	2.2406	3.2792
								p-value	0.03423	0.14314	0.07851
n	18	7	11	22	12	10		Summary	*	n.s.	n.s.
Failures (mean ± SD)	7.83 ± 8.04	11.71 ± 8.67	5.36 ± 6.89	2.48 ± 3.80	3 ± 3.69	1.9 ± 4.04		DF	1	1	1
								F-value	9.3450	3.2990	1.8796
								p-value	0.004264	0.077895	0.179112
n	18	7	11	21	11	10		Summary	**	n.s.	n.s.
Pain threshold (mA) (mean ± SD)	0.122 ± 0.042	0.138 ± 0.043	0.109 ± 0.038	0.114 ± 0.038	0.103 ± 0.034	0.132 ± 0.039		DF	1	1	1
								F-value	0.3686	0.2063	5.8561
								p-value	0.54740	0.65227	0.02041
n	17	8	9	25	15	10		Summary	n.s.	n.s.	*

Supplementary table S18 LHP. Post-hoc pairwise t-test with bonferroni correction of the pain threshold in Wt and Orx-Bmal1$^{-/-}$ mice of both sexes. n.s. = not significant.

Parameter	Comparison			p -value	Corrected p-value	Summary
Pain threshold	f	Wt	Orx-Bmal1$^{-/-}$	0.0443	0.1772	n.s.
	m	Wt	Orx-Bmal1$^{-/-}$	0.207	0.828	n.s.
	Wt	f	m	0.165	0.66	n.s.
	Orx-Bmal1$^{-/-}$	f	m	0.0573	0.2292	n.s.

Supplementary table S19 SPT. Group sizes, mean and standard deviation (SD) of the preference score in the SPT of Wt and Orx-Bmal1$^{-/-}$ mice of both sexes and two-way ANOVA investigating the impact of genotype and sex on this parameter. DF = degrees of freedom; n.s. = not significant. *p < 0.05, ***p < 0.001.

Parameter	Wt			Orx-Bmal1$^{-/-}$					Source of variation		
	All	Females	Males	All	Females	Males			Genotype	Sex	Genotype x Sex
Preference score (mean ± SD)	-0.05 ± 0.42	0.11 ± 0.43	-0.20 ± 0.37	0.46 ± 0.30	0.40 ± 0.31	0.54 ± 0.27	Two-way ANOVA	DF	1	1	1
								F-value	21.7543	0.2364	4.3550
								p-value	3.961e-05	0.62969	0.04385
n	17	8	9	24	14	10		Summary	***	n.s.	*

Supplementary table S20 PPI. Group sizes, mean and standard deviation (SD) of the PPI at different dB levels in Wt and Orx-Bmal1$^{-/-}$ mice of both sexes and two-way ANOVA investigating the impact of genotype and sex on these parameters. DF = degrees of freedom; n.s. = not significant.

PPI (%) by Prepulse dB	Wt			Orx-Bmal1$^{-/-}$					Source of Variance		
	All	Females	Males	All	Females	Males			Genotype	Sex	Genotype x Sex
70 dB (mean ± SD)	32.75 ± 20.36	28.26 ± 20.15	36.42 ± 20.74	26.69 ± 27.38	26.06 ± 25.25	27.54 ± 31.31	Two-way ANOVA	DF	1	1	1
								F-value	0.5387	0.3508	0.1990
								p-value	0.4670	0.5568	0.6578
n	20	9	11	26	15	11		Summary	n.s.	n.s.	n.s.
75 dB (mean ± SD)	44.28 ± 20.67	37.02 ± 21.59	50.23 ± 18.78	45.91 ± 24.01	46.32 ± 24.24	45.36 ± 24.86		DF	1	1	1
								F-value	0.1134	0.6043	1.0826
								p-value	0.7380	0.4413	0.3041
n	20	9	11	26	15	11		Summary	n.s.	n.s.	n.s.
80 dB (mean ± SD)	57.06 ± 16.50	50.64 ± 14.28	62.31 ± 16.94	52.96 ± 21.86	52.98 ± 24.00	52.93 ± 19.69		DF	1	1	1
								F-value	0.3399	0.7454	0.9761
								p-value	0.5630	0.3928	0.3288
n	20	9	11	26	15	11		Summary	n.s.	n.s.	n.s.
85 dB (mean ± SD)	68.24 ± 16.20	62.60 ± 13.50	72.85 ± 17.34	64.99 ± 18.97	63.40 ± 20.31	67.16 ± 17.70		DF	1	1	1
								F-value	0.2027	1.5469	0.3683
								p-value	0.6549	0.2205	0.5472
n	20	9	11	26	15	11		Summary	n.s.	n.s.	n.s.

Supplementary table S21 Monitoring of body weight in female mice. Group sizes, mean and standard deviation (SD) of the weight of female Wt and Orx-Bmal1$^{-/-}$ mice from the age of 3 weeks to 22 weeks.

Genotype	Sex	Females																			
	Age (weeks)	3	4	5	6	7	8	9	10	11	12	13	14	15	16	17	18	19	20	21	22
Wt	Weight (g) (mean ± SD)	11.3 ± 1.25	14.9 ± 1.23	15.7 ± 1.04	16.3 ± 1.35	17.5 ± 1.21	17.9 ± 1.34	18.6 ± 1.18	18.8 ± 1.09	19.4 ± 1.23	19.7 ± 1.11	20.0 ± 0.87	20.7 ± 1.03	21.2 ± 0.98	21.2 ± 1.07	21.4 ± 1.01	21.9 ± 1.00	21.9 ± 1.13	22.0 ± 1.08	22.8 ± 0.98	22.9 ± 0.95
	n	8	8	8	8	8	8	8	8	8	8	8	8	8	8	8	8	8	8	8	8
Orx-Bmal1$^{-/-}$	Weight (g) (mean ± SD)	11.9 ± 1.41	15.2 ± 1.15	15.9 ± 0.91	16.5 ± 0.98	17.4 ± 0.99	17.9 ± 1.18	18.2 ± 1.34	18.8 ± 1.39	19.2 ± 0.97	19.9 ± 1.18	20.2 ± 1.12	21.0 ± 1.25	21.2 ± 1.42	21.4 ± 1.38	21.4 ± 1.27	21.6 ± 1.16	22.1 ± 1.40	22.1 ± 1.24	22.5 ± 1.30	22.6 ± 1.26
	n	15	15	15	15	15	15	15	15	15	15	15	15	15	15	15	15	15	15	15	15

Supplementary table S22 Monitoring of body weight in male mice. Group sizes, mean and standard deviation (SD) of the weight of male Wt and Orx-Bmal1$^{-/-}$ mice from the age of 3 weeks to 22 weeks.

Genotype	Sex	Males																			
	Age (weeks)	3	4	5	6	7	8	9	10	11	12	13	14	15	16	17	18	19	20	21	22
Wt	Weight (g) (mean ± SD)	12.1 ± 1.66	16.3 ± 1.37	18.0 ± 1.17	19.1 ± 1.38	20.2 ± 1.45	21.2 ± 1.65	22.7 ± 1.42	23.6 ± 1.26	24.1 ± 1.56	24.1 ± 1.39	25.1 ± 1.17	25.7 ± 1.07	26.4 ± 1.20	27.2 ± 1.33	27.7 ± 1.15	28.1 ± 1.28	29.0 ± 1.49	28.9 ± 1.14	29.5 ± 1.27	29.8 ± 1.35
	n	9	9	9	9	9	9	9	9	9	9	9	9	9	9	9	9	9	9	9	9
Orx-Bmal1$^{-/-}$	Weight (g) (mean ± SD)	11.1 ± 0.94	16.2 ± 1.38	18.3 ± 1.15	20.3 ± 1.95	21.2 ± 1.65	22.1 ± 1.47	23.3 ± 1.66	24.0 ± 1.52	24.7 ± 1.42	24.6 ± 1.42	25.3 ± 1.17	26.0 ± 1.24	26.5 ± 1.16	27.2 ± 1.17	27.7 ± 1.39	27.9 ± 1.41	28.5 ± 1.44	29.1 ± 1.76	29.3 ± 1.61	29.7 ± 1.79
	n	11	11	11	11	11	11	11	11	11	11	11	11	11	11	11	11	11	11	11	11

Supplementary table S23 Monitoring of body weight. Repeated measures two-way ANOVA investigating the impact of age and genotype on weight in Wt and Orx-Bmal1$^{-/-}$. DF = degrees of freedom; n.s. = not significant; **p < 0.01, ***p < 0.001.

Parameter	Sex	Repeated measures two-way ANOVA	Source of variation		
			Genotype	Age	Genotype x Age
Weight	Females	DF	1	19	19
		F-value	0.024	532.344	1.044
		p-value	8.77e-01	9.39e-270	4.08e-01
		Summary	n.s.	***	n.s.
	Males	DF	1	19	19
		F-value	0.146	849.913	2.383
		p-value	7.07e-01	1.26e-274	1.00e-03
		Summary	n.s.	***	**

Supplementary table S24 Monitoring of body weight in male mice. Post-hoc pairwise t-test with bonferroni correction of the weight of male Wt and Orx-Bmal1$^{-/-}$ mice at different ages. n.s. = not significant.

Parameter	Age	Comparison males Wt vs Orx-Bmal1$^{-/-}$		
		p -value	Corrected p-value	Summary
Weight	3	0.0909	1	n.s.
	4	0.843	1	n.s.
	5	0.582	1	n.s.
	6	0.154	1	n.s.
	7	0.192	1	n.s.
	8	0.256	1	n.s.
	9	0.391	1	n.s.
	10	0.552	1	n.s.
	11	0.371	1	n.s.
	12	0.389	1	n.s.
	13	0.723	1	n.s.
	14	0.532	1	n.s.
	15	0.82	1	n.s.
	16	0.974	1	n.s.
	17	0.921	1	n.s.
	18	0.788	1	n.s.
	19	0.515	1	n.s.
	20	0.711	1	n.s.
	21	0.706	1	n.s.
	22	0.854	1	n.s.

Supplementary table S25 Metabolic cages. Group sizes, mean and standard deviation (SD) of water and food consumption, RER and activity during the day and during the night of Wt and Orx-Bmal1$^{-/-}$ mice of both sexes.

Parameter	Day						Night					
	Wt			Orx-Bmal1$^{-/-}$			Wt			Orx-Bmal1$^{-/-}$		
	All	Females	Males	All	Females	Males	All	Females	Males	All	Females	Males
Water Consumption (ml/BW (g)) (mean ± SD)	0.027 ± 0.013	0.032 ± 0.017	0.022 ± 0.008	0.033 ± 0.008	0.038 ± 0.007	0.029 ± 0.008	0.143 ± 0.030	0.165 ± 0.023	0.121 ± 0.018	0.144 ± 0.045	0.155 ± 0.026	0.133 ± 0.061
n	8	4	4	7	3	4	8	4	4	8	4	4
Food Consumption (g/BW (g)) (mean ± SD)	0.034 ± 0.01	0.036 ± 0.009	0.032 ± 0.012	0.036 ± 0.021	0.033 ± 0.029	0.039 ± 0.014	0.16 ± 0.049	0.202 ± 0.033	0.126 ± 0.026	0.19 ± 0.079	0.235 ± 0.075	0.154 ± 0.067
n	8	4	4	8	4	4	8	4	4	8	4	4
RER (mean ± SD)	0.823 ± 0.023	0.819 ± 0.029	0.827 ± 0.017	0.824 ± 0.030	0.820 ± 0.039	0.827 ± 0.025	0.944 ± 0.026	0.954 ± 0.033	0.934 ± 0.016	0.937 ± 0.018	0.935 ± 0.020	0.939 ± 0.019
n	8	4	4	8	4	4	8	4	4	8	4	4
Activity (beam breaks) (mean ± SD)	108577 ± 86271	100752 ± 80369	116402 ± 103651	62729 ± 33572	69058 ± 39480	54290 ± 29261	316117 ± 109511	410830 ± 49294	221405 ± 40391	329295 ± 125576	406739 ± 129772	251851 ± 62935
n	8	4	4	7	4	3	8	4	4	8	4	4

Supplementary table S26 Metabolic cages. Three-way ANOVA investigating the impact of genotype, sex and circadian phase on food and water consumption in Wt and Orx-Bmal1$^{-/-}$ mice of both sexes. DF = degrees of freedom; n.s. = not significant.; *p < 0.05, **p < 0.01, ***p < 0.001.

Parameter	Three-way ANOVA	Source of Variance						
		Genotype	Sex	Phase	Genotype x Sex	Genotype x Phase	Sex x Phase	Genotype x Sex x Phase
Food Consumption	d.f.	1	1	1	1	1	1	1
	F-value	1.2725	7.3097	101.4445	0.0064	1.0160	7.7279	0.0931
	p-value	0.2704	0.0124	4.272e-10	0.9368	0.3235	0.0104	0.7629
	Summary	n.s.	*	***	n.s.	n.s.	*	n.s.
Water Consumption	d.f.	1	1	1	1	1	1	1
	F-value	0.0989	4.8012	133.3632	0.3551	0.0713	1.5106	0.3043
	p-value	0.75598	0.03883	4.735e-11	0.55706	0.79177	0.23147	0.58654
	Summary	n.s.	*	***	n.s.	n.s.	n.s.	n.s.
RER	d.f.	1	1	1	1	1	1	1
	F-value	0.1209	0.0018	163.8080	0.3674	0.2012	0.6690	0.5078
	p-value	0.7311	0.9665	3.255e-12	0.5501	0.6578	0.4214	0.4830
	Summary	n.s.	n.s.	***	n.s.	n.s.	n.s.	n.s.
Activity	d.f.	1	1	1	1	1	1	1
	F-value	0.3087	10.4791	76.4805	0.0038	1.1527	10.0881	0.3513
	p-value	0.583872	0.003640	9e-09	0.951608	0.294125	0.004212	0.559149
	Summary	n.s.	**	***	n.s.	n.s.	**	n.s.

Supplementary table S27 Metabolic cages. Post-hoc pairwise t-test with bonferroni correction of the food consumption and activity of female and male mice independent of genotype. n.s. = not significant; *p < 0.05, ***p < 0.001.

Parameter	Phase	Post-hoc pairwise t-test with bonferroni correction females vs. males		
		p -value	Corrected p-value	Summary
Food Consumption	Day	0.8970	1	n.s.
	Night	0.0104	0.0208	*
Activity	Day	0.897000	1	n.s.
	Night	0.000369	0.000738	***

Supplementary table S28 Virus MOI test. Group sizes, mean and standard deviation (SD) of the amplitude of PER2::LUC oscillations in primary neurons infected with different MOIs of L31-2 or AAV mixture and of % cells infected with different MOIs of AAV. One-way ANOVA investigating the impact of MOI on these parameters. DF = degrees of freedom; n.s. = not significant; **p < 0.01.

Virus	Parameter	MOI						Source of variation
		500	1000	2000	CTL			MOI
L31-2	Amplitude (mean ± SD)	0.027 ± 0.006	0.049 ± 0.013	0.055 ± 0.015	0.185 ± 0.061	One-way ANOVA	DF	3
							F-value	17.337
							p-value	0.001275
	n	3	3	3	2		Summary	**
AAV	Amplitude (mean ± SD)	0.161 ± 0.006	0.163 ± 0.002	0.150 ± 0.003	0.192 ± 0.035		DF	3
							F-value	2.9926
							p-value	0.09559
	n	3	3	3	3		Summary	n.s.
AAV	Infected cells (%) (mean ± SD)	61.65 ± 8.58	63.49 ± 3.48	62.08 ± 4.32	N.A.		DF	1
							F-value	0.0011
							p-value	0.9741
	n	3	2	3	N.A.		Summary	n.s.

Supplementary table S29 Virus MOI test. Post-hoc pairwise t-test with bonferroni correction of the amplitude of PER2::LUC oscillations in primary neurons infected with different MOIs of L31-2. n.s. = not significant.

Virus	Parameter	Comparison				
		MOI	MOI	p -value	Corrected p-value	Summary
L31-2	Amplitude	1000	2000	0.93	1	n.s.
		1000	500	0.738	1	n.s.
		2000	500	0.805	1	n.s.
		1000	CTL	0.0313	0.188	n.s.
		2000	CTL	0.0262	0.157	n.s.
		500	CTL	0.0158	0.0949	n.s.

Supplementary table S30 Virus mediated Bmal1 KD. Group sizes, mean and standard deviation (SD) of the amplitude of PER2::LUC oscillations in primary neurons treated with different virus combinations between DIV 9 to 13 and DIV 14 to 18 and one-way ANOVA investigating the impact of treatment on this parameter. DF = degrees of freedom; n.s. = not significant; *p < 0.05.

DIV	Parameter	Treatment								Source of variation
		Bmal1 shRNA + Cre	*Bmal1* shRNA	Scrambled shRNA + Cre	Scrambled shRNA	Cre	Control			Treatment
9 to 13	Amplitude (mean ± SD)	0.096 ± 0.012	0.112 ± 0.007	0.113 ± 0.021	0.126 ± 0.058	0.121 ± 0.019	0.076 ± 0.025	One-way ANOVA	DF	5
									F-value	1.2195
									p-value	0.3581
	n	3	3	3	3	3	3		Summary	n.s.
14 to 18	Amplitude (mean ± SD)	0.081 ± 0.020	0.107 ± 0.068	0.109 ± 0.030	0.166 ± 0.144	0.199 ± 0.028	0.273 ± 0.043		DF	5
									F-value	3.697
									p-value	0.03297
	n	3	3	3	3	3	2		Summary	*

Supplementary table S31 Virus mediated Bmal1 knockdown. Post-hoc pairwise t-test with bonferroni correction of the amplitude of PER2::LUC oscillations between DIV 14 to 18 in primary neurons treated with different combinations of viruses. n.s. = not significant

DIV	Parameter	Comparison				
		Treatment	Treatment	p -value	Corrected p-value	Summary
14 to 18	Amplitude	*Bmal1* shRNA	*Bmal1* shRNA + Cre	0.599	1	n.s.
		Bmal1 shRNA	Cre	0.0791	1	n.s.
		Bmal1 shRNA + Cre	Cre	0.0308	0.462	n.s.
		Bmal1 shRNA	Control	0.00989	0.148	n.s.
		Bmal1 shRNA + Cre	Control	0.0042	0.063	n.s.
		Cre	Control	0.195	1	n.s.
		Bmal1 shRNA	Scrambled shRNA	0.241	1	n.s.
		Bmal1 shRNA + Cre	Scrambled shRNA	0.103	1	n.s.
		Cre	Scrambled shRNA	0.5	1	n.s.
		Control	Scrambled shRNA	0.0702	1	n.s.
		Bmal1 shRNA	Scrambled shRNA + Cre	0.967	1	n.s.
		Bmal1 shRNA + Cre	Scrambled shRNA + Cre	0.572	1	n.s.
		Cre	Scrambled shRNA + Cre	0.0849	1	n.s.
		Control	Scrambled shRNA + Cre	0.0106	0.159	n.s.
		Scrambled shRNA	Scrambled shRNA + Cre	0.257	1	n.s.

10. Acknowledgement

I would like to thank Dominic Landgraf for giving me the opportunity to work on this exciting project and for his supervision and guidance throughout the last years.

Further, I would like to thank my TAC members Charlotte Förster and Sergi Papiol for their input on my project, their advice and support.

The whole project was conducted at the department of molecular neurobiology (MNB) led by Moritz Rossner and I am thankful that I could be a part of this department and profit of its stimulating scientific environment.

Special thanks go to all members of the circadian biology group. In particular, I am very grateful for Muriel Frisch and Min Chen, who were the most amazing and supportive colleagues and helped out in so many ways, it would take another page to list all of it. I also want to thank Janina Heyke and Chris Tsatali, who joined me on my journey to learn about the ORX system and contributed to the experiments of the *Ppox* expression screen and the behavioral characterization.

All the mouse experiments would have not been possible without the MNB mouse unit team, especially Niels Jensen, Jessica Bly and Wilma Vogel, who provided the best care for the mice and helped out wherever they could.

In general, I would like to thank all my colleagues from the MNB for lots of scientific advice but also joyful moments. There are some people who need to be especially mentioned: Alexander Herholt, who designed the cloning strategy and together with Vivek Sahoo answered all of my questions on molecular biology. Sven Wichert, who solved all the IT problems. Nirmal Kannaiyan for his support in the *Ppox* expression study. Jan Wintgens, Sabrina Galinski and Nadia Gabellini who shared their knowledge on cell culture experiments. Beate Kauschat for her help with the virus generation and primary neuron preparation. Sylvia De Jonge, Stefanie Behrens and Karin Neumeir, for sharing their expertise on RNA isolation. Marius Stephan, who saved the day more than once. Florian Raabe and his scientific enthusiasm.

Finally, I am grateful for the support of my family and friends. Especially Dorothee Pöhlchen, who answered all kind of statistical questions.

11. Affidavit

Affidavit

Kling, Charlotte Maria

_____

Surname, first name

Nußbaumstraße 7

_____

Street

80336 Munich, Germany

_____

Zip code, town, country

I hereby declare, that the submitted thesis entitled:

The Role of Circadian Rhythms in Orexin Neurons of the Lateral Hypothalamus in the Regulation of Mood- and Anxiety-Related Behavior, and Metabolism in Mice

……

is my own work. I have only used the sources indicated and have not made unauthorised use of services of a third party. Where the work of others has been quoted or reproduced, the source is always given.

I further declare that the dissertation presented here has not been submitted in the same or similar form to any other institution for the purpose of obtaining an academic degree.

Munich, 25.03.2023 _____

place, date

Charlotte Maria Kling _____

Signature doctoral candidate

12. Confirmation of Congruency

LMU LUDWIG-MAXIMILIANS-UNIVERSITÄT MÜNCHEN | Promotionsbüro Medizinische Fakultät | MMRS

Confirmation of congruency between printed and electronic version of the doctoral thesis

Kling, Charlotte Maria

Surname, first name

Nußbaumstraße 7

Street

80336 Munich, Germany

Zip code, town, country

I hereby declare, that the submitted thesis entitled:

The Role of Circadian Rhythms in Orexin Neurons of the Lateral Hypothalamus in the Regulation of Mood- and Anxiety-Related Behavior, and Metabolism in Mice

……

is congruent with the printed version both in content and format.

Munich, 25.03.2023

place, date

Charlotte Maria Kling

Signature doctoral candidate